

Cover image: Karen Claesen

Cover design: Natacha Hoevenaegel, Nieuwe Mediadienst, UAntwerpen.

© 2022 Karen CLAESEN

Alle rechten voorbehouden. Niets uit deze uitgave mag worden vermenigvuldigd en/of openbaar gemaakt worden door middel van druk, fotokopie, microfilm, elektronisch of op welke andere wijze ook zonder voorafgaandelijke schriftelijke toestemming van de uitgever.

All rights reserved. No part of the publication may be reproduced in any form by print, photoprint, microfilm, electronic or any other means without written permission from the publisher



Faculteit Farmaceutische, Biomedische en Diergeneeskundige Wetenschappen
Departement Farmaceutische Wetenschappen

The carboxypeptidase U system in atherosclerosis

Insights in carboxypeptidase U mediated pleiotropic effects of statins

Het carboxypeptidase U systeem in atherosclerose

Inzichten in carboxypeptidase U gemedieerde pleiotrope effecten
van statines

Proefschrift voorgelegd tot het behalen van de graad van
doctor in de farmaceutische wetenschappen
aan de Universiteit Antwerpen te verdedigen door

Karen CLAESEN

Promotoren:

Prof. dr. Dirk Hendriks

Prof. dr. Ingrid De Meester

Antwerpen, 2022

Members of the jury

Internal doctoral committee

Prof. dr. Guido De Meyer (Chair)

Laboratory of Physiopharmacology – University of Antwerp

Prof. dr. Gilles De Keulenaer (Member)

Laboratory of Physiopharmacology – University of Antwerp

Prof. dr. Dirk Hendriks (Promotor)

Laboratory of Medical Biochemistry – University of Antwerp

Prof. dr. Ingrid De Meester (Co-promotor)

Laboratory of Medical Biochemistry – University of Antwerp

External members of the jury

Prof. dr. Joost Meijers

Department of Molecular Hematology, Sanquin Research,
Amsterdam, the Netherlands

Department of Experimental Vascular Medicine, Amsterdam University
Medical Centers, University of Amsterdam, Amsterdam, the Netherlands

Prof. dr. Nicola Mutch

School of Medicine, Institute of Medical Sciences,
University of Aberdeen, Aberdeen, United Kingdom

“Droom.
Durf.
Doe.”

- Phil Bosmans –

Table of contents

Table of contents.....	i
List of abbreviations	vii
List of amino acids	xv
1 Introduction to the CPU system	3
1.1 Discovery and nomenclature	3
1.2 CPU is a metalloproteinase.....	4
1.2.1 Classification according to catalytic mechanism.....	4
1.2.2 Classification according to structure.....	5
1.3 Molecular aspects.....	5
1.3.1 The <i>CPB2</i> gene and gene expression	5
1.3.2 Genetic polymorphisms	7
1.3.3 Non-genetic influences on plasma proCPU concentrations	7
1.4 Biochemical characteristics.....	8
1.4.1 Synthesis and distribution.....	8
1.4.2 Three-dimensional structure.....	11
1.5 Activation and inactivation	12
1.5.1 ProCPU activation and generation of CPU	12
1.5.2 Catalytic activity and specificity	14
1.5.3 CPU instability and inactivation	16
1.6 CPU at the interface between coagulation and fibrinolysis	17
1.6.1 Normal hemostasis.....	17
1.6.2 CPU: a potent antifibrinolytic enzyme	25
1.7 Measurement of proCPU, CPU and CPUi: methods, challenges and pitfalls...27	
1.7.1 ProCPU	28
1.7.2 CPU	30
1.7.3 Assessment of overall proCPU activation	36
1.7.4 Assessment of the CPU system by functional fibrinolysis assays	37

2	Pathophysiological role of the CPU system	43
2.1	The CPU system and the risk for cardiovascular disease and thrombotic disorders.....	43
2.1.1	Hyperlipidemia as a risk factor for atherosclerosis and cardiovascular disease	43
2.1.2	Risk factors and interventions at the individual level: focus on lipids and statin therapy	49
2.1.3	Plasma proCPU concentration and proCPU polymorphisms as risk factors?	54
2.1.4	Can proCPU, CPU or CPUi serve as diagnostic or prognostic biomarkers?	67
2.1.5	Potential benefit of the use of CPU inhibitors.....	71
2.2	A role for the CPU system in the regulation of other (patho)physiological processes.....	78
2.2.1	The anti-inflammatory role of the CPU system.....	78
2.2.2	CPU as a contributor to the hypofibrinolytic state in COVID-19 patients?	79
3	Objectives	83
4	Effect of statin therapy on the CPU system in patients with hyperlipidemia: a proof-of-concept observational study.....	93
4.1	Abstract.....	93
4.2	Introduction	94
4.3	Materials and methods	95
4.3.1	Study design	95
4.3.2	Sample collection	95
4.3.3	ProCPU measurement	96
4.3.4	Clot lysis assay	96
4.3.5	Lipid measurements	96
4.3.6	Other measurements	97
4.3.7	Statistical analysis.....	97
4.4	Results	97
4.4.1	Study population	97

4.4.2	Statin therapy downregulates proCPU levels	99
4.4.3	Downregulation of proCPU by statin therapy has a non-lipid related pleiotropic character	103
4.4.4	Plasma fibrinolysis potential improves under influence of statin therapy	104
4.5	Discussion	105
4.6	Conclusion.....	107
5	Pleiotropic effects of atorvastatin result in a downregulation of the CPU system in a mouse model of advanced atherosclerosis	111
5.1	Abstract.....	111
5.2	Introduction	112
5.3	Materials and methods.....	112
5.3.1	Animals and study protocol	112
5.3.2	Activity assay for the measurement of proCPU in plasma of mice.....	113
5.3.3	Measurement of total plasma cholesterol, CRP and blood immune cells.....	114
5.3.4	Statistical analysis	114
5.4	Results and discussion	114
5.4.1	Activity assay for the measurement of proCPU in mice	114
5.4.2	Total plasma cholesterol	117
5.4.3	ProCPU decrease in atorvastatin-treated mice on a western diet is cholesterol-independent.....	117
5.4.4	Inflammation and blood immune cells	119
5.5	Conclusion.....	121
6	ProCPU as a novel marker for identifying benefit from atorvastatin therapy	125
6.1	Abstract.....	125
6.2	Introduction	126
6.3	Materials and methods.....	127
6.3.1	Study design	127
6.3.2	Sample collection	128
6.3.3	ProCPU measurement and clot lysis assay.....	128

Table of contents

6.3.4	Lipid- and other measurements	128
6.3.5	Statistical analysis.....	129
6.4	Results and discussion.....	129
6.4.1	Study population	129
6.4.2	Atorvastatin normalizes high and marked interindividually variable plasma proCPU concentrations and fibrinolytic potential in hyperlipidemic individuals.....	132
6.4.3	ProCPU downregulation and increase in fibrinolytic rate by atorvastatin are dose-dependent.....	135
6.4.4	Addition of ezetimibe to atorvastatin therapy has no additional effect on proCPU concentrations or plasma fibrinolytic potential.....	136
6.5	Conclusions	137
7	ProCPU is expressed by (primary) human monocytes and macrophages and expression differs between states of differentiation and activation	141
7.1	Abstract	141
7.2	Introduction	142
7.3	Materials and methods	144
7.3.1	Cell culture.....	144
7.3.2	Conditioned media and cellular lysates	146
7.3.3	RNA isolation and cDNA synthesis for mRNA expression analysis.....	146
7.3.4	Validation of a quantitative reverse transcriptase-polymerase chain reaction (RT-qPCR) assay to study <i>CPB2</i> mRNA expression	147
7.3.5	<i>CPB2</i> mRNA expression in human monocyte and macrophage cell lines and primary cells.....	150
7.3.6	Western blot analysis	151
7.3.7	Immunocytochemistry	152
7.3.8	ProCPU measurement	152
7.3.9	Statistical analysis.....	153
7.4	Results	154
7.4.1	Validation of a quantitative reverse transcriptase-polymerase chain reaction (RT-qPCR) assay to study <i>CPB2</i> mRNA expression	154

7.4.2	<i>CPB2</i> mRNA is detected in (primary) human monocytes and macrophages	158
7.4.3	ProCPU and CPU protein are present in (primary) human monocyte and macrophage medium	161
7.4.4	Immunofluorescent staining shows proCPU/CPU inside (primary) human monocytes and macrophages	164
7.4.5	ProCPU concentration measured in medium of (primary) human monocytes and macrophages is related to their state of differentiation	165
7.5	Discussion	166
7.6	Conclusion.....	171
8	A new pedigree with thrombomodulin-associated coagulopathy in which delayed fibrinolysis is partially attenuated by co-inherited proCPU deficiency ...	177
8.1	Abstract.....	177
8.2	Introduction	178
8.3	Materials and methods.....	179
8.3.1	Study pedigree	179
8.3.2	DNA sequencing	179
8.3.3	ProCPU measurement.....	179
8.3.4	CPU generation during <i>in vitro</i> clot lysis	180
8.3.5	Other measurements	182
8.3.6	Statistical analysis	182
8.4	Results and discussion	182
8.4.1	Comparison of the time course of CPU generation in two <i>in vitro</i> clot lysis systems	182
8.4.2	Detection and annotation of the <i>THBD</i> and <i>CPB2</i> variants	187
8.4.3	Characteristics of the TM-AC cases.....	188
8.4.4	The <i>CPB2</i> p.Arg114* variant downregulates fibrinolysis	191
8.5	Conclusion.....	194
9	Activation of the CPU system in patients with SARS-CoV-2 infection could contribute to COVID-19 hypofibrinolytic state and disease severity prognosis ...	199
9.1	Abstract.....	199

Table of contents

9.2	Introduction	200
9.3	Materials and methods	201
9.3.1	Study design and participants	201
9.3.2	Sample collection and biochemical analysis	202
9.3.3	Statistical analysis.....	202
9.4	Results and discussion.....	202
9.4.1	Patient characteristics	202
9.4.2	ProCPU and CPU+CPUi antigen levels do not differ between COVID-19 exposed and non-exposed controls	204
9.4.3	ProCPU consumption with concomitant CPU generation in COVID-19 patients upon hospital admission	205
9.4.4	Time course of CPU-related parameters.....	206
9.4.5	CRP levels correlate with the decrease in proCPU levels early after disease onset.....	211
9.4.6	Baseline CPU+CPUi antigen levels correlate with disease severity and the duration of hospitalization.....	212
9.5	Conclusion	214
10	Conclusions and future perspectives.....	217
	References	225
	Summary.....	263
	Samenvatting.....	269
	Scientific curriculum vitae	275
	Bedankt!	283

List of abbreviations

5	5-HT	Serotonin
	ε-ACA	ε-aminocaproic acid
	ΔCLT	Reduction in clot lysis time after addition of CPU inhibitor
	ΔproCPU	Change in proCPU
A	aa	Amino acid
	AAFK	Anisylazoformyl-Lys
	AAFR	Anisylazoformyl-Arg
	ACDC	Aberdeen Cardiovascular & Diabetes Centre
	ACE	Angiotensin converting enzyme
	ADP	Adenosine diphosphate
	AIS	Acute ischemic stroke
	AMI	Acute myocardial infarction
	AP	Activation peptide
	APC	Activated protein C
	ApoE ^{-/-}	Apolipoprotein E-deficient mice
	ApoE ^{-/-} Fbn1 ^{C1039G+/-}	Apolipoprotein E-deficient mice with a heterozygous mutation in the fibrillin-1 gene
	ARDS	Acute respiratory distress syndrome
	ARPC1a	Actin related protein 2/3 complex subunit 1A
	ASCVD	Atherosclerotic cardiovascular disease
	ATIII	Antithrombin III
	AUC	Area under the curve
B	B2M	Beta-2-microglobulin
	BMI	Body mass index
	Bz-Gly-Arg	Benzoyl-glycine-arginine (hippuryl-L-arginine; Hip-Arg)
	Bz-Gly-Lys	Benzoyl-glycine-lysine (hippuryl-L-lysine; Hip-Lys)
	Bz- <i>o</i> -cyano-Phe	Benzoyl- <i>ortho</i> -cyano-phenylalanine

	Bz- <i>o</i> -cyano-Phe-Arg	Benzoyl- <i>ortho</i> -cyano-phenylalanyl-arginine
C	C/EBP	CCAAT/enhancer binding protein
	CAPD	Continuous ambulatory peritoneal dialysis
	CD71	Transferrin receptor
	CHRF	Human megakaryoblastic cell line
	CLA	Clot lysis assay
	CLA+TM	Clot lysis assay in the presence of thrombomodulin
	CLT	Clot lysis time
	CLT+TM	Clot lysis time in the presence of thrombomodulin
	CLT _{PTCI}	Clot lysis time in the presence of PTCI
	COVID-19	Coronavirus disease 2019
	CPB	Carboxypeptidase B
	CPB2	Carboxypeptidase B2
	CPN	Carboxypeptidase N
	CPR	Carboxypeptidase R
	CPU	Carboxypeptidase U
	CPUi	Inactivated carboxypeptidase U
	CRP	C-reactive protein
	CTPA	Computed tomography with pulmonary angiography
	CV	Coefficient of variation
	CVD	Cardiovascular disease
	CVT	Cerebral venous thrombosis
	CycA	Cyclophelin A pair 1
D	Dami	Human megakaryocytic cell line
	DAPI	4',6-diamino-2-phenylindole
	DM	Diabetes mellitus
	DMEM	Dulbecco's modified eagle medium
	DMSO	Dimethyl sulfoxide
	DPBS	Dulbecco's phosphate buffered saline

	DVT	Deep vein thrombosis
E	EC	Enzyme commission
	EDTA	Ethylenediaminetetraacetic acid
	ELISA	Enzyme-linked immunosorbent assay
	EMC7	ER membrane protein complex subunit 7
	ESC	European Society of Cardiology
F	FA-Ala-Arg	Furylacryloyl-Ala-Arg
	FA-Ala-Lys	Furylacryloyl-Ala-Lys
	FAM	6-carboxyfluorescein
	FCS	Fetal calf serum
	FDP	Fibrin degradation products
	FH	Familial hypercholesterolemia
	FITC	Fluorescein isothiocyanate
	fIIa	Coagulation factor IIa/Thrombin
G	gDNA	Genomic DNA
	GEMSA	Guanidinoethyl-mercapto-succinic acid
	GP	Glycoprotein
	GRE	Glucocorticoid response element
	GUS	Glucuronidase beta
H	h _{1st peak}	First CPU activity peak
	h _{2nd peak}	Second CPU activity peak
	HbA1c	Glycated hemoglobin A1
	HBSS	Hank's balanced salt solution
	HCAEC	Human coronary artery endothelial cells
	HDL-C	High-density lipoprotein cholesterol
	HEPES	4-(2-hydroxyethyl)-1-piperazineethanesulfonic acid
	HepG2	Human hepatocellular carcinoma cell line
	Hip-Arg	Hippuryl-L-arginine (Bz-Gly-Arg)
	Hip-Lys	Hippuryl-L-lysine (Bz-Gly-Lys)

List of abbreviations

	H _{max}	Height of the clot lysis curve
	HMG-CoA	3-hydroxy-3-methylglutaryl-coenzyme A
	HNF-1 α	Hepatocyte nuclear factor-1 α
	HPLC	High-performance liquid chromatography
	HPRT1	Hypoxanthine phosphoribosyl transferase
	HRP	Horseradish peroxidase
	HuR	Human antigen R
	HUVEC	Human umbilical vein endothelial cells
I	ICAM	Intracellular adhesion molecule
	ICU	Intensive care unit
	IDMS	Isotope diluted mass spectrometry
	IDT	Integrated DNA Technologies
	IHC	Immunohistochemistry
	IFN- γ	Interferon γ
	IL	Interleukin
	IMSEQ	Immune Repertoire Sequencing
	ISTH	International Society of Thrombosis and Haemostasis
	ITM	Institute of Tropical Medicine
	IV	Intravenous
K	kb	Kilo basepairs
	kDa	Kilo Dalton
	K _i	Inhibition constant
	K _m	Michaelis-Menten constant
L	LC	Liquid chromatography
	LCI	Leech carboxypeptidase inhibitor
	LDL-C	Low-density lipoprotein cholesterol
	LMW	Low molecular weight
	LOD	Limit of detection
	LOQ	Limit of quantification

	LPS	Lipopolysaccharide
M	M1-macrophage	IFN- γ /LPS-stimulated macrophage, classically activated macrophage
	M2-macrophage	IL-4-stimulated macrophage, alternatively activated macrophage
	mAb	Monoclonal antibody
	MACS	Magnetic-activated cell sorting
	MC	Metalloproteinases
	MCAO	Middle cerebral artery occlusion
	M-CSF	Macrophage colony-stimulating factor
	MedBio	Laboratory of Medical Biochemistry
	MEG-01	Human megakaryoblastic cell line
	MERGETPA	D,L-2-mercaptomethyl-3-guanidinoethylthiopropionic acid
	MS	Mass spectrometry
	MW	Molecular weight
N	N	Number
	N.A.	Not applicable
	NC-IUBMB	Nomenclature Committee of the International Union of Biochemistry and Molecular Biology
	ND	Normal diet
	NF	Normalization factor
	NF-Y	Nuclear factor Y
	NF- κ B	Nuclear factor κ B
	NK	Natural killer cell
	NKT	Natural killer T cell
	Non-HDL-C	Non-high-density lipoprotein cholesterol
	Non-ICU	Non-intensive care unit
	NS	Not significant

List of abbreviations

	NSTEMI	Non-ST-elevation myocardial infarction
	NPC1L1	Niemann-Pick C1-like protein 1
O	OD	Optical density
	OPN-Arg	Thrombin-cleaved osteopontin
	OxyHb	Oxyhemoglobin
P	PAI	Plasminogen activator inhibitor
	PBMC	Peripheral blood mononuclear cells
	PCR	Polymerase chain reaction
	PCSK9	Proprotein convertase subtilisin/kexin type 9
	PE	Pulmonary embolism
	PECAM	Platelet endothelial cell adhesion molecule
	PFA	Paraformaldehyde
	PGK-1	Phosphoglycerate kinase 1
	PLG	Plasminogen
	PMA	Phorbol 12-myristate 13-acetate
	PNP	Pooled normal plasma
	PPACK	D-phenylalanyl-L-propylarginylchloromethyl ketone
	PPAR α	Peroxisome proliferator-activated receptor α
	proCPU	Procarboxypeptidase U
	PSMB2	Proteasome 20S subunit beta 2
	PTCI	Potato tuber carboxypeptidase inhibitor
	PVDV	Polyvinylidene fluoride
R	RAT	Rapid antigen test
	RP-HPLC	Reversed-phase high-performance liquid chromatography
	RPMI	Roswell Park Memorial Institute
	RPS8	Ribosomal protein S8
	rtPA	Recombinant tissue-type plasminogen activator
S	SAHLSIS	Sahlgrenska Study on Ischemic Stroke Outcome

	SARS-CoV-2	Severe acute respiratory-syndrome coronavirus-2
	SCORE	Systemic coronary risk estimation
	SCORE-OP	Systemic coronary risk estimation – older person
	SD	Standard deviation
	SDF-1 α	Stromal cell-derived factor 1/C-X-C motif chemokine 12
	SDS-page	Sodium dodecyl sulphate polyacrylamide gel electrophoresis
	SEM	Standard error of the mean
	SI	International System of Units
	SNP	Single-nucleotide polymorphism
	SSC	Scientific and Standardization Committee
	STEMI	ST-elevation myocardial infarction
	sTM	Soluble thrombomodulin
T	T	Thrombin
	$t_{1/2}$	Half-life
	T1DM	Type 1 diabetes mellitus
	T2DM	Type 2 diabetes mellitus
	TAFI	Thrombin activatable fibrinolysis inhibitor (proCPU)
	TAFIa	Activated thrombin activatable fibrinolysis inhibitor (CPU)
	TAFIai	Inactivated thrombin activatable fibrinolysis inhibitor (CPUi)
	TBE	Tris/borate/EDTA buffer
	TBP	TATA box binding protein
	TBST	Tris-buffered saline and tween-20
	TC	Total cholesterol
	TCI	Tick carboxypeptidase inhibitor
	TF	Tissue factor
	TFPI	Tissue factor pathway inhibitor

List of abbreviations

	TG	Triglycerides
	<i>THBD</i>	Gene encoding thrombomodulin
	THP-1	Human monocyte cell line
	T _{lag}	Lag-time or time to clot initiation
	T _m	Melting temperature
	TM	Thrombomodulin
	TM-AC	Thrombomodulin-associated coagulopathy
	TNF- α	Tumor necrosis factor α
	tPA	Tissue-type plasminogen activator
	T-TM	Thrombin-thrombomodulin complex
	TTP	Tristetraprolin
	TXA2	Thromboxane A2
U	UAntwerp	University of Antwerp
	U/L	Units per liter
	uPA	Urokinase-type plasminogen activator
	UTR	Untranslated region
	UV/VIS	Ultraviolet/Visible
	UZA	University Hospital Antwerp
V	VCAM	Vascular adhesion molecule
	VFK-CK	d-Val-Phe-Lys chloromethyl ketone
	VTE	Venous thromboembolism
	VWF	Von Willebrand Factor
W	WBC	White blood cell
	WD	Western diet
	WD + atorvastatin	Western diet supplemented with atorvastatin
	WHO	World Health Organization
Y	YWHAZ	Tyrosine 3-monooxygenase/tryptophan 5-monooxygenase activation protein zeta
Z	ZNA	Ziekenhuis Netwerk Antwerpen

List of amino acids

A	Ala	Alanine
R	Arg	Arginine
N	Asn	Asparagine
D	Asp	Aspartic acid
C	Cys	Cysteine
Q	Gln	Glutamine
E	Glu	Glutamic acid
G	Gly	Glycine
H	His	Histidine
I	Ile	Isoleucine
L	Leu	Leucine
K	Lys	Lysine
M	Met	Methionine
F	Phe	Phenylalanine
P	Pro	Proline
S	Ser	Serine
T	Thr	Threonine
W	Trp	Tryptophan
Y	Tyr	Tyrosine
V	Val	Valine

Chapter 1

Introduction to the CPU system

Partly based on:

Mertens JC, **Claesen K**, Hendriks D. Carboxypeptidase U. Handbook of proteolytic enzymes, 4th Edition. (Handbook in preparation)

Claesen K, Mertens JC, Leenaerts D, Hendriks D. Carboxypeptidase U (CPU, TAF1a, CPB2) in Thromboembolic Disease: What Do We Know Three Decades after Its Discovery? *Int. J. Mol. Sci.* 2021, 22(2), 883.

1 Introduction to the CPU system

1.1 Discovery and nomenclature

Before the end of the 1980s, carboxypeptidase N (CPN) was the only known carboxypeptidase in human blood. In 1989 this changed when Hendriks *et al.* reported on the presence of an unstable arginine carboxypeptidase activity in fresh human serum [1,2]. This unknown carboxypeptidase was found to differ from CPN in terms of substrate specificity, esterase activity and pH optimum, but especially in terms of stability. CPN is stable for a longer time in plasma while the new enzyme quickly lost its activity after activation. This gave rise to the name carboxypeptidase U (CPU), where the “U” refers to its unstable character [1–3].

Shortly after, Campbell & co-workers independently reported the identification of an arginine-specific carboxypeptidase – carboxypeptidase R (CPR) – generated in blood during coagulation and inflammation [4]. In 1991, Eaton *et al.* were the first to suggest that CPU could play an important role in fibrinolysis. They discovered it as a novel plasminogen binding protein being present in plasma, with an amino acid sequence similar to pancreatic carboxypeptidase B and therefore named it plasma carboxypeptidase B (plasma CPB) [5]. The final link between coagulation and fibrinolysis was disclosed in 1995 by Bazjar *et al.* who identified a proenzyme that could be activated by thrombin and – upon activation – was the molecular link between the thrombin generation during the coagulation and the inhibition of fibrinolysis. This protein was accordingly named thrombin activatable fibrinolysis inhibitor (TAFI). The active enzyme was named TAFIa [6]. Subsequent amino-terminal sequencing revealed that CPU, TAFIa, CPR, and plasma CPB were identical [7]. Over the years, with additional roles being allocated to the *CPB2* gene product, additional names such as thrombin activatable carboxypeptidase B and carboxypeptidase B2 have been assigned to the enzyme, complicating literature searches even more [8,9]. Hitherto, a consensus on common nomenclature has not been reached, but since 2015 the fibrinolysis subcommittee of the Scientific and Standardization Committee (SSC) recommends that authors include the

official gene name, carboxypeptidase B2 (plasma), abbreviated as *CPB2* [Human] or *cpb2* [mouse] depending on the species, as a keyword (and MeSH term ‘carboxypeptidase B2’ where applicable) in all future publications. The adoption of this recommendation allows a more comprehensive literature search and will improve cross-referencing between publications [10]. Throughout this thesis, the terminology ‘procarboxypeptidase U (proCPU)’ will be used for the zymogen and ‘carboxypeptidase U (CPU)’ to refer to the enzyme.

1.2 CPU is a metallo-carboxypeptidase

1.2.1 Classification according to catalytic mechanism

The Nomenclature Committee of the International Union of Biochemistry and Molecular Biology (NC-IUBMB) uses the catalytic activity of an enzyme as the basis for its classification into classes, subclasses and sub-subclasses [11]. Since its catalytic activity comprises a specific property of a certain enzyme, it allows to distinguish one enzyme from another and is thus a good starting point for classification [11].

Following the NC-IUBMB classification, CPU is assigned the enzyme code EC 3.4.17.20, meaning that this enzyme catalyzes the hydrolysis (Enzyme Commission [EC] class 3) of C-terminal peptide bonds (EC 3.4; peptidases), releasing a single amino acid (EC 3.4.16-18; carboxypeptidases) [11]. According to their catalytic mechanism, the class of the carboxypeptidases is further subdivided into serine-type carboxypeptidases (EC 3.4.16), metallo-type carboxypeptidases (EC 3.4.17) and cysteine-type carboxypeptidases (EC 3.4.18). The former and latter respectively carry a serine or cysteine residue in their catalytic site, whereas metallo-carboxypeptidases carry a zinc atom that is important for their catalytic action. Finally, the last number of CPU’s enzyme code lists the carboxypeptidases according to the time of discovery (EC 3.4.17.20).

1.2.2 Classification according to structure

Alternatively, enzymes can be classified based on structural similarity as introduced by Rawlings and Barrett in 1993 [12]. In this classification system enzymes are classified into clans, families and subfamilies. A clan contains all peptidases that have evolved from a common ancestral gene, although comparison of their primary structures can no longer confirm their relationship. Within a clan, a further distinction into families is made based upon significant analogy in the amino acid sequence around the catalytic residues [13]. The catalytic type of a family is denoted by a single letter code (serine [S], threonine [T], cysteine [C], aspartic [A], metallo [M] or unknown [U]), followed by an arbitrarily assigned number [13]. The metallocarboxypeptidase family (clan MC, family M14) is further subdivided into two subfamilies, comprising on the one hand the carboxypeptidases which are synthesized as inactive zymogens and require proteolytic cleavage before they can exert enzymatic activity (subfamily A), and on the other hand carboxypeptidases that lack a pro-domain and are constitutively active (subfamily B). Consisting of two separate moieties: an activation peptide and a catalytic domain, CPU belongs to subfamily A (clan MC, family M14, subfamily A) [12,13].

1.3 Molecular aspects

1.3.1 The *CPB2* gene and gene expression

The human gene locus encoding proCPU, denoted the *CPB2* gene, is located on chromosome 13q14.11 (see also 1.1) [7]. The complete *CPB2* gene contains 11 exons and 10 introns and spans approximately 48 kb of genomic DNA [7,14].

Transcription of the *CPB2* gene in the liver is initiated from multiple sites in the 5'-flanking region, resulting in multiple *CPB2* transcripts with varying lengths [14]. Analysis of the 5'-flanking region of the *CPB2* gene revealed that liver-specific gene expression is regulated by several potential regulatory elements [15]. Boffa *et al.* identified a putative CCAAT/enhancer binding protein (C/EBP) binding site [16]. Mutations in this site that abolish the C/EBP binding were shown to decrease the proCPU promoter activity in

human hepatoma (HepG2) cells by approximately 80%. A second regulatory element of the *CPB2* gene transcription was reported in 2003, with the identification of a functional glucocorticoid response element (GRE) in the human proCPU promoter [17]. Mutations in the GRE markedly decreased the ability of the *CPB2* promoter to be activated by dexamethasone, a synthetic glucocorticoid. Treatment of HepG2 cells with dexamethasone resulted in a 2-fold increase of both proCPU mRNA levels and promoter activity [17]. More recently, Garand *et al.* identified ten potential binding sites for liver-expressed transcription factors within the proximal *CPB2* promoter [18]. These include the binding sites for transcription factors nuclear factor- κ B (NF- κ B) and hepatocyte nuclear factor-1 α (HNF-1 α), both of which have been identified to be important for basal *CPB2* promoter activity in hepatic cells [16–18].

As a result of post-transcriptional regulation of the *CPB2* transcript at three potential polyadenylation sites in the 3'-flanking region, *CPB2* mRNA transcripts containing 3'-untranslated regions (UTRs) of different lengths are generated [19]. The length of the 3'-end of the *CPB2* transcript was demonstrated to be related to the stability of the mRNA transcript: the longer the transcript, the lower its intrinsic stability and abundance [19,20]. Moreover, this difference in stability is also translated into the abundance of the *CPB2* transcripts, where a decreasing trend in abundance is seen from the shortest (most stable) to the longest (least stable) transcript [19]. By performing *in vitro* experiments using HepG2 cells, it was found that pro-inflammatory mediators (tumor necrosis factor [TNF]- α , interleukin [IL]-6, IL-1 β and lipopolysaccharide [LPS]) lead to the preferential formation of the longest transcript, resulting in a decrease in *CPB2* mRNA stability and proCPU protein expression. Stimulation of HepG2 cells with the anti-inflammatory cytokine IL-10 on the other hand increased *CPB2* mRNA stability and protein expression, whereas IL-13 – another inflammatory cytokine – did not affect proCPU protein expression in HepG2 cells [21]. The mechanism behind these observations was found to involve tristetraprolin (TTP; an mRNA decay-promoting factor) and human antigen R (HuR; an mRNA stabilizing factor), both RNA binding proteins [21,22]. In contrast, this same series of pro- and anti-inflammatory mediators had very different effects on *CPB2*

mRNA transcription and stability by THP-1 macrophages, with each mediator increasing proCPU expression [21].

1.3.2 Genetic polymorphisms

Hitherto, about 30 single nucleotide polymorphisms (SNPs) have been identified for the *CPB2* gene [23]. Most SNPs result in a silent mutation and thus do not affect the amino acid sequence and functionality of the protein formed. However, two SNPs in the coding region result in amino acid substitution, namely at position 147 (505A→G or Thr147Ala) and at position 325 (1040C→T or Thr325Ile) [24,25]. No functional differences are reported for the Ala¹⁴⁷ isoform, while the Ile³²⁵ variant gives rise to a significant change in thermal stability of the active enzyme CPU as the half-life increases from 7 to 15 min at 37 °C (Figure 1-1) [25–27]. Recently, a novel loss-of-function rare variant in *CPB2* has been described in several members of the same pedigree. This monoallelic variant resulted in premature truncation of the proCPU protein from Arg⁹² (340G→A), before the catalytic domain, thereby preventing functional proCPU expression from this allele resulting in a 2-fold reduction of circulating proCPU levels (see also Chapter 8) [28].

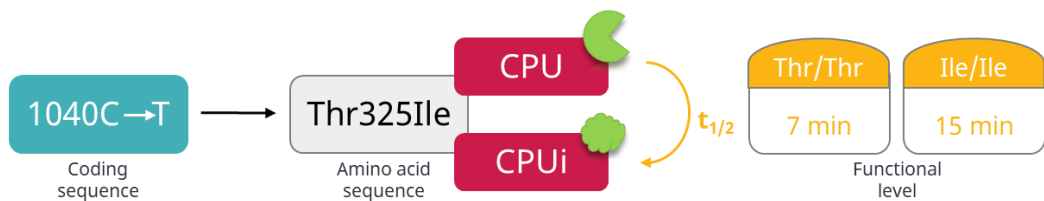


Figure 1-1. Schematic presentation of the single nucleotide polymorphism at position 325 of the coding sequence of *CPB2* (1040C→T or Thr325Ile). The Thr³²⁵ variant has a half-life of 8 minutes at 37 °C, while the Ile³²⁵ variant gives rise to a significant change in thermal stability of the active enzyme CPU with an increase of the half-life from 7 to 15 min at 37 °C.

1.3.3 Non-genetic influences on plasma proCPU concentrations

A considerable variation in plasma proCPU concentration is observed in the human population (range 75 – 275 nmol/L). However, only approximately 25% of this variation can be attributed to genetic factors (e.g. SNPs) [29]. Non-genetic factors are thus

important for the explanation of variation in plasma proCPU levels (e.g. influence of inflammation/interleukins, glucocorticoids, sex steroids... [see also 1.3.1]). Moreover, it appears that proCPU concentrations increase age-dependently in women (related to their hormonal status), but not in men [30–32]. Pregnancy is also known to elevate proCPU levels, returning to baseline after delivery [32–34].

Numerous disease states have been shown to be associated with changes in plasma proCPU concentration (extensively discussed in Chapter 2). However, the exact mechanism of these alterations remains to be elucidated.

1.4 Biochemical characteristics

1.4.1 Synthesis and distribution

1.4.1.1 General considerations

ProCPU is synthesized in the liver as a 423 amino acid-long prepropeptide, composed of a 22 amino acid signal peptide, a 92 amino acid activation peptide [AP] and a 309 amino acid catalytic domain (Figure 1-2) [5,35,36]. During translocation across the membrane, the N-terminal signal peptide is cleaved off and the glycosylated zymogen proCPU (molecular weight [MW] of 56 kDa on SDS-page) is released into the circulation [5,6,37–40]. Cleavage of the (N-terminal) AP (Phe¹-Arg⁹²; 20 kDa; heavily glycosylated) at Arg⁹² liberates the 36 kDa thermolabile catalytic unit, CPU (Ala⁹³-Val⁴⁰¹; 36 kDa) [41,42].

A second, non-hepatically-derived pool of proCPU was found in platelets and accounts for < 0.1% of blood-derived proCPU. It is synthesized by megakaryocytes and is released from the α -granules upon platelet activation [43,44]. Even though platelet-derived proCPU levels are low, an additive effect on fibrinolysis by boosting local proCPU concentrations was observed on top of the effect of proCPU in plasma [44,45]. ProCPU is also present in cerebrospinal- and amniotic fluid and *CPB2* mRNA has been detected in megakaryoblastic cell lines (CHRF, Dami and MEG-01), primary endothelial cells (both primary human coronary artery endothelial cells [HCAEC] and primary human umbilical vein endothelial cells [HUVEC]) and the human monocytic cell line THP-1 as well as in

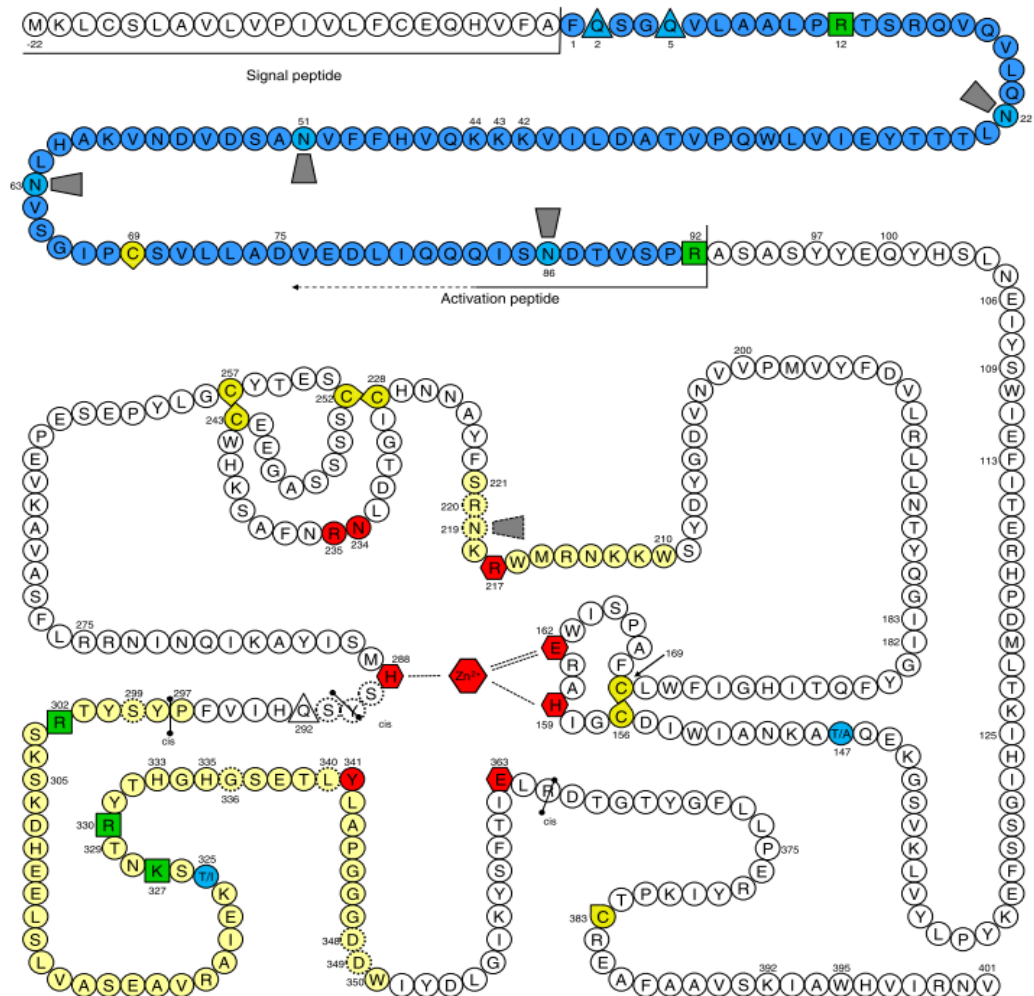


Figure 1-2. Two-dimensional representation of the amino acid sequence of proCPU. The activation peptide (Phe¹-Arg⁹²) is shown in blue; a glycosaminoglycan binding site (Trp²¹⁰-Ser²²¹) and the dynamic flap region (Phe²⁹⁷-Trp³⁵⁰) are shown in light yellow. Additionally, thrombin/plasmin cleavage sites (green squares), glutamines involved in factor XIIIa-mediated coupling to fibrin (triangles), cysteines (yellow droplets), glycans (grey trapezoids), polymorphisms (blue), residues involved in substrate hydrolysis (red hexagons), substrate specificity (red circles) and residues potentially involved in substrate binding (dashed line circles) are shown.

From: Plug T, Meijers JCM. Structure-function relationship in thrombin activatable fibrinolysis inhibitor. *J Thromb Haemost* 2016; 14: 633-44.

THP-1 cells differentiated into a macrophage-like phenotype [20,43,46–48]. A recent study showed a morphological association of (pro)CPU and plasminogen activator

inhibitor (PAI)-1 in advanced carotid plaques: (pro)CPU was found to be colocalized with macrophages and neovascular endothelium in these plaques [49]. Moreover, brain-derived, full-length *CPB2* transcripts and alternatively spliced *CPB2* transcripts without carboxypeptidase activity have been described [20,50].

A functional CPU system has also been described in several other mammalian species including rodents (rat, mouse, guinea pig), rabbits, dogs, and pigs. Nonetheless, marked differences in CPU activity and stability have been observed between several species [40,51,52]. Even though human, murine and rat proCPU have a very high amino acid sequence identity (rat to mouse 96% and mouse and rat to human 86%), the half-life at 37 °C of rat and murine CPU was found to be 3.5 min and 2.2 min respectively as compared to the human half-life of 7 to 15 min [51]. Furthermore, also the transcription regulation of the *CPB2* gene is different in rodents compared to humans (see also 1.3.1). There is a nuclear factor κB (NF-κB) binding site in the 5'-flanking region of the *cpb2* gene in mice, which is not conserved in the human promotor region, and rat and murine proCPU seem to be an acute phase protein while human proCPU is not [53,54]. On the other hand, the steroid-responsive elements that are present in the human promotor are absent in mice [55].

1.4.1.2 Interactions with other proteins

Studies suggest that proCPU circulates in plasma in a non-covalent complex with plasminogen [56,57]. ProCPU has a 10-fold higher binding affinity for Lys-plasminogen compared to Glu-plasminogen. The binding to plasminogen is most likely mediated by the glycosylated activation peptide of proCPU and the His³³³-Val⁴⁰¹ region [57,58]. The active enzyme CPU has a reduced ability to bind plasminogen due to the loss of the activation peptide. However, recent research has demonstrated that the CPU-plasminogen complex promotes the interaction of CPU with its substrate by 3-fold, increasing the catalytic efficiency of cleavage of lysine residues from partially degraded fibrin [59].

CPU was also shown to bind non-covalently to α 2-macroglobulin and pregnancy zone protein [60]. These interactions were suggested to function as an *in vivo* shuttle to modulate the clearance of CPU and inactivated CPU (CPUi; see also 1.5.3) from the circulation.

1.4.2 Three-dimensional structure

In 2008, Marx and colleagues first unraveled the crystal structure of recombinantly expressed proCPU (Figure 1-3) [61].

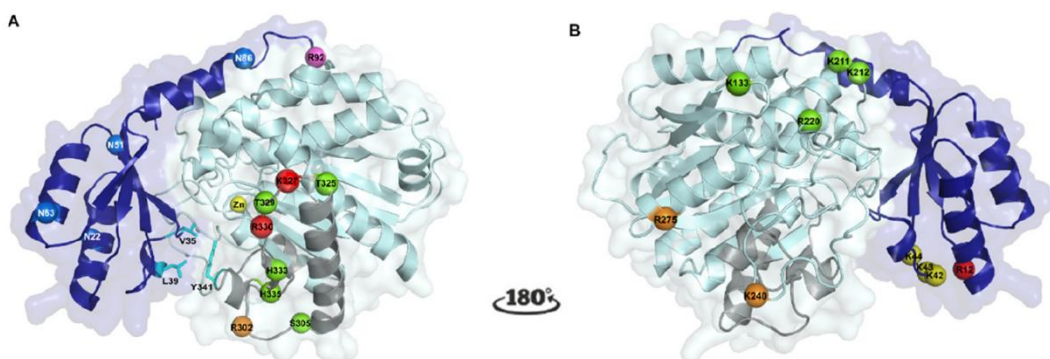


Figure 1-3. Crystal structure of human proCPU. A) Cartoon representation of proCPU. The activation peptide (AP) and the catalytic moiety are colored in dark and light blue respectively. The catalytic zinc-ion in the active center is shown as a yellow sphere. The four glycosylation sites in the AP (Asn²², Asn⁵¹, Asn⁶³, and Asn⁸⁶) are represented by blue spheres. ProCPU can be activated through cleavage at Arg⁹² (shown as a magenta sphere) by thrombin, plasmin, or the thrombin/thrombomodulin complex. Three putative thrombomodulin binding sites, Lys⁴²/Lys⁴³/Lys⁴⁴, Lys¹³³/Lys²¹¹/Lys²¹²/Arg²²⁰, and Lys²⁴⁰/Arg²⁷⁵, are indicated by yellow, green, and orange spheres, respectively. Upon the subsequent conformational change to inactivated CPU (CPUi), a cryptic cleavage site at Arg³⁰² (shown as an orange sphere) becomes exposed and can be cleaved by plasmin or thrombin. Two additional plasmin cleavage sites, Lys³²⁷ and Arg³³⁰, are indicated by red spheres. The dynamic flap (colored in gray), of which the mobility leads to conformational changes that disrupt the catalytic site to form CPUi, is stabilized by hydrophobic interactions between Val³⁵ and Leu³⁹ of the AP and Tyr³⁴¹ in the dynamic flap (shown as cyan sticks). **B) Cartoon representation of proCPU after rotating panel A 180 degrees along the y-axis.**

Adapted from: Sillen, M., Declerck, P.J. Thrombin Activatable Fibrinolysis Inhibitor (TAFI): An Updated Narrative Review. *Int. J. Mol. Sci.* 2021, 22, 3670.

The first 76 residues of the activation peptide (Phe¹-Val⁷⁶) fold into four β -strands and two α -helices that together form an open sandwich antiparallel α/β -fold. The latter is connected to the catalytic moiety through a partial α -helical linker region (Glu⁷⁷-Arg⁹²). Four N-linked glycosylation sites were identified within the activation peptide (Asn²², Asn⁵¹, Asn⁶³, and Asn⁸⁶) [36,61]. The catalytic domain itself has a globular shape, characterized by a typical α/β hydrolase fold – comprising an eight-strand mixed β -sheet flanked by nine α -helices – and carries the catalytic pocket containing a zinc ion coordinated by His¹⁵⁹, Glu¹⁶² and His²⁸⁸ [42,61,62].

1.5 Activation and inactivation

1.5.1 ProCPU activation and generation of CPU

As mentioned above, proteolytic cleavage of the Arg⁹²-Ala⁹³ bond is necessary to remove the activation peptide from the catalytic CPU moiety and make the active site accessible to substrates. This proteolytic cleavage can be mediated by different trypsin-like serine proteases, including thrombin and plasmin (Figure 1-3 and Figure 1-4) [5,57,63–66].

Thrombin itself is a weak activator of proCPU; however, in complex with either soluble or membrane-bound thrombomodulin (a transmembrane glycoprotein predominantly expressed on the luminal surface of endothelial cells that serves as a cofactor for thrombin; see also *infra*), the catalytic efficiency of thrombin-mediated proCPU activation is increased 1250-fold [5,63,67]. Besides the generation of the antifibrinolytic enzyme CPU, the thrombin-thrombomodulin complex also efficiently generates activated protein C. ProCPU and protein C bind to distinct thrombomodulin domains and therefore direct competition for the thrombin-thrombomodulin complex by proCPU and protein C was not expected [68]. This was confirmed by Wu *et al.* when endothelial cells (HUVECs) were used as the source of thrombomodulin [69]. Nonetheless, Kokame *et al.* demonstrated that there was a competition between the two substrates of thrombin-thrombomodulin when soluble thrombomodulin was used [70]. Importantly, active protein C can inhibit efficient thrombin formation and can thereby indirectly limit

proCPU activation by reducing the overall concentration of thrombin-thrombomodulin [71]. In other words: whereas massive coagulation is prevented through the activation of protein C by thrombin-thrombomodulin, generation of CPU by thrombin-thrombomodulin results in protection of the formed clot from premature lysis [72].

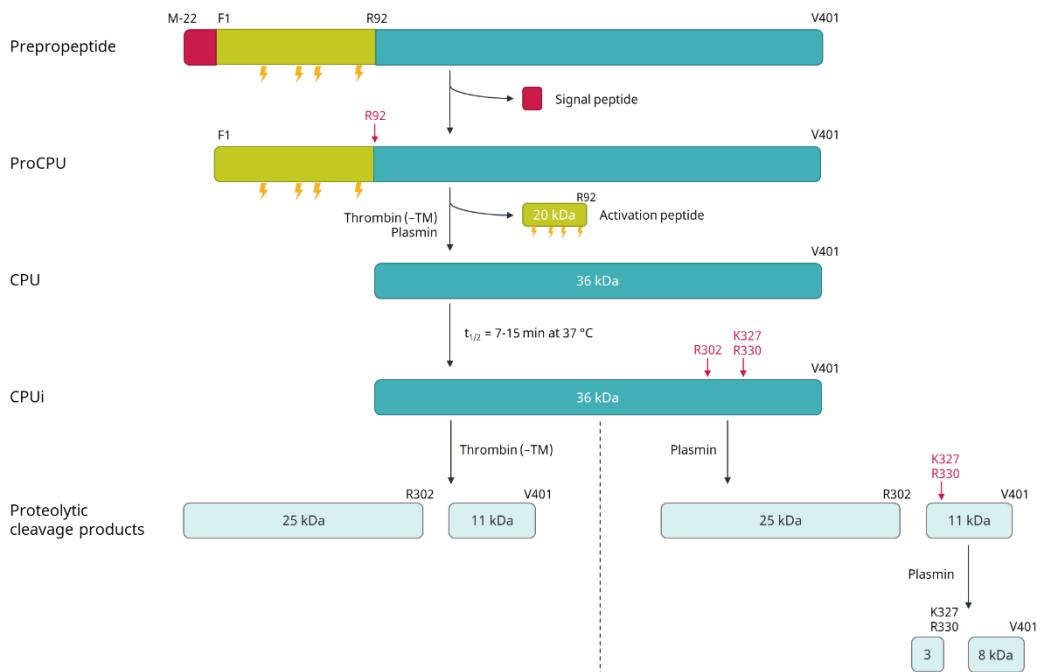


Figure 1-4. ProCPU activation and inactivation. ProCPU is synthesized in the liver as a prepropeptide. Upon secretion in the circulation, the signal peptide (pink) is cleaved off, releasing the 56 kDa zymogen proCPU that consists of a 20 kDa highly glycosylated (yellow) activation peptide (green) and a 36 kDa catalytic domain (blue). The zymogen is activated by plasmin, thrombin or the thrombin-thrombomodulin (TM) complex through cleavage at Arg⁹², thereby releasing the catalytic domain CPU. CPU is highly unstable. Thermal inactivation ($t_{1/2} = 7 - 15$ min at 37°C) is mediated through a conformational change. This conformational change makes the cryptic cleavage site Arg³⁰² accessible for thrombin and plasmin cleavage. Besides Arg³⁰², plasmin has two other cleavage sites: Lys³²⁷ and Arg³³⁰. Cleavage at these sites results in the formation of several proteolytic cleavage products (light blue).

Adapted from: Mertens J. The carboxypeptidase U system in acute ischemic stroke: translation from bench to bedside. Doctoral thesis. University of Antwerp. 2020. and Marx *et al.* Plasmin-mediated activation and inactivation of thrombin activatable fibrinolysis inhibitor. *Biochemistry*. 2002; 41: 6688–96.

Alternatively, proCPU can be activated by plasmin, which is a stronger activator than thrombin [64]. Even though the efficiency of plasmin-mediated proCPU activation is enhanced 20-fold by glycosaminoglycans such as heparin, the catalytic efficiency remains 10-fold lower than that of the thrombin-thrombomodulin complex [64]. Therefore, the thrombin-thrombomodulin complex was postulated to be the main physiological activator of proCPU, as was also suggested by an *in vivo* study using a monoclonal antibody (mAb) that selectively inhibits thrombin-thrombomodulin-mediated proCPU activation [73]. In *in vitro* settings, a biphasic proCPU activation pattern associated with consecutive activation by thrombin(-thrombomodulin) (during the coagulation) and plasmin (during the fibrinolytic phase) has been demonstrated (see also 1.6.2) [74]. The physiological relevance/importance of plasmin-mediated proCPU activation has been a matter of debate; however recent studies using mAbs that mainly impair plasmin-mediated proCPU activation revealed that plasmin contributes to proCPU activation both during clot formation and lysis *in vitro* [75], and showed that plasmin is a relevant physiological activator of proCPU *in vivo* as well [76].

1.5.2 Catalytic activity and specificity

As a metalloprotease, CPU carries a zinc atom in its catalytic site that is tetrahedrally coordinated by a water molecule, two histidines and one glutamate (Figure 1-5A) [77]. When a suitable substrate enters the catalytic groove, the zinc-coordinated water molecule – assisted by the general base glutamic acid – will perform a nucleophilic attack on the carbonyl group of the scissile peptide bond (Figure 1-5B). This results in the formation of a tetrahedral intermediate in which the negatively charged transition state is stabilized by the zinc ion and an arginine side chain (Arg²¹⁷ for CPU) (Figure 1-5C). Subsequently, glutamic acid donates a proton to the nitrogen atom of the C-terminal amino acid, this amino acid is then released and the enzyme returns to its free state (Figure 1-5D) [77,78].

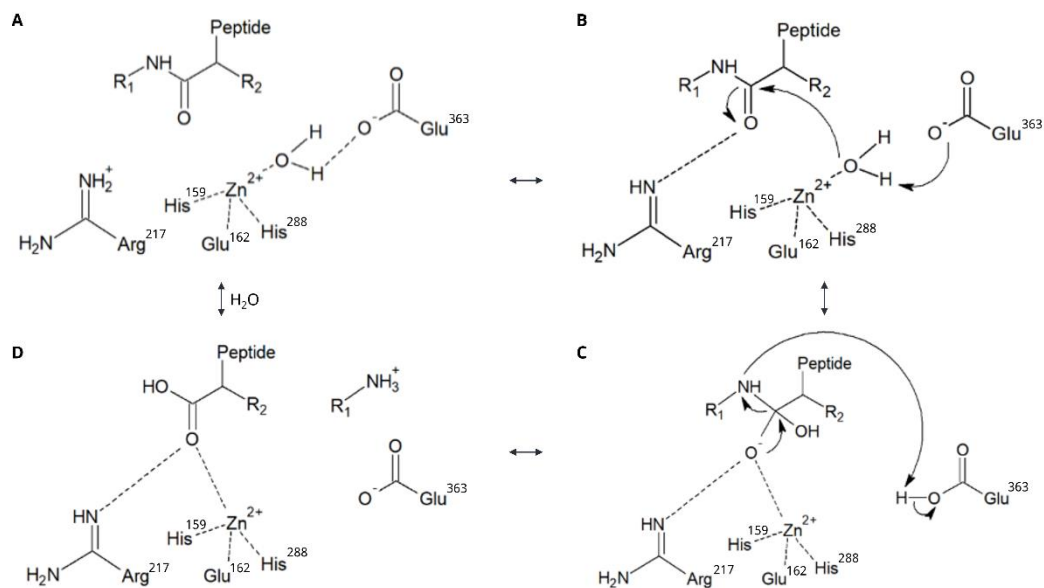


Figure 1-5. Catalytic mechanism of CPU. Schematic representation of the active site groove, with the catalytic zinc ion that is coordinated by a water molecule, glutamate (Glu¹⁶² in CPU) and two histidines (His¹⁵⁹ and His²⁸⁸ in CPU).

Adapted from: Wu *et al.* Catalysis of carboxypeptidase A: promoted-water vs nucleophilic pathways. *J Phys Chem B.* 2010; 114(28): 9259-9267.

The negative charge of Asp³⁴⁸, assisted by Gly³⁶³ and Ser²⁹⁹, creates a polar environment and mediates therein the substrate preference of CPU for basic amino acids such as arginine (Arg) and lysine (Lys). CPU removes a single C-terminal Arg/Lys from its substrates by cleaving peptide bonds between C-terminal Arg/Lys and any other amino acid, except for proline [5,12,13]. Throughout the years, the activity of CPU has been demonstrated on several synthetic peptides, with (synthetic) substrates containing an aromatic amino acid in the penultimate position being the most favorable [79]. Examples of synthetic substrates include hippuryl-L-Lys (Bz-Gly-Lys), hippuryl-L-Arg (Bz-Gly-Arg), furylacryloyl-Ala-Lys (FA-Ala-Lys), furylacryloyl-Ala-Arg (FA-Ala-Arg), anisylazofornyl-Lys (AAFk), anisylazofornyl-Arg (AAFR) [80,81]. Recently, a novel synthetic substrate (Bz-*o*-cyano-Phe-Arg) has been designed for application in activity-based assays with high enough specificity to measure CPU in the presence of high constitutive background

activities of CPN in plasma (see also 1.7.1) [81]. The pH optimum of CPU was found to be between pH 7.5 and 7.8 [2].

A range of endogenous CPU substrates has been discovered as well. Based on its catalytic efficiency, the primary physiological substrate of CPU is plasmin-degraded fibrin [59]. Other endogenous substrates of CPU include several enkephalins, bradykinin, complement-derived anaphylatoxins C3a and C5a, thrombin-cleaved osteopontin (OPN-Arg¹⁶⁸), chemerin, stromal cell-derived factor 1 α and vascular endothelial growth factor (see also 2.2.1) [82–87]. Compared with CPN, CPU has a 9-fold higher catalytic efficiency for bradykinin and C5a, and a 26-fold higher catalytic efficiency for OPN-Arg¹⁶⁸. C3a, on the other hand, is cleaved 3-fold less efficiently by CPU [83].

1.5.3 CPU instability and inactivation

As indicated by its name, CPU is characterized by a significant thermal instability, with a half-life at 37 °C varying between 7 min (Thr³²⁵) and 15 min (Ile³²⁵) depending on the Thr325Ile polymorphism (see also 1.3.2) [2,26,27]. At room temperature (20 °C) the half-life is prolonged to approximately 2 h, whereas CPU is highly stable at 0 °C [26,35,88,89]. Not only a decrease in temperature results in a significant increase in CPU stability, but also the presence of competitive inhibitors and an excess of substrate improves CPU stability [89,90]. The intrinsic thermal instability of CPU causes its action to be self-limiting and this mechanism of enzyme auto-regulation is controlled by a highly dynamic region (Phe²⁹⁷-Trp³⁵⁰) in the CPU structure [61,91]. The Ala⁷⁴-Arg⁹² segment of the activation peptide interacts with the dynamic flap, thereby stabilizing the catalytic moiety of the zymogen [92]. Upon proteolytic activation of proCPU, the stabilizing interaction between activation peptide and dynamic region is lost, the catalytic site becomes accessible for substrates and the dynamic region undergoes an irreversible conformational change, ultimately resulting in a disruption of the active site (formation of CPUi) [61,91]. Several stable CPU mutants have been described and were used to characterize the function, activation, and inactivation of CPU [92,93].

Besides activating proCPU, plasmin and thrombin are also involved in the proteolytic degradation of CPU/CPUi (Figure 1-4). In the presence of plasmin, enzymatic degradation of both CPU and CPUi is observed with cleavage of CPU/CPUi at Arg³⁰², a cryptic proteolytic cleavage site that becomes accessible after a conformational change of the dynamic flap [61,94]. Furthermore, also Lys³²⁷ and Arg³³⁰ have been identified as plasmin cleavage sites in CPU/CPUi, resulting in several possible peptide fragments that can be generated [94]. In the presence of thrombin on the other hand, proteolytic degradation mainly occurs after conformational inactivation (CPUi) and only cleavage at Arg³⁰² takes place [61,94].

1.6 CPU at the interface between coagulation and fibrinolysis

1.6.1 Normal hemostasis

Hemostasis is an essential physiological process that stops blood from flowing out of a damaged blood vessel while securing normal blood flow elsewhere in the body [95,96]. It is a complex and tightly regulated process that starts with the immediate vasoconstriction of the harmed vessels and the simultaneous formation of a platelet plug to mechanically block the vessel and stop blood loss (primary hemostasis; Figure 1-6) [95,97,98]. Subsequently, the coagulation cascade is activated, leading to the formation of a fibrin network that stabilizes the platelet plug (secondary hemostasis) [95,97,98]. Once vascular integrity is restored, the clot gradually dissolves through the cleavage of the fibrin network by plasmin (fibrinolysis) [97–99]. Disorders of hemostasis or unbalanced hemostasis may therefore lead to a tendency toward either bleeding complications or thrombosis [97–99].

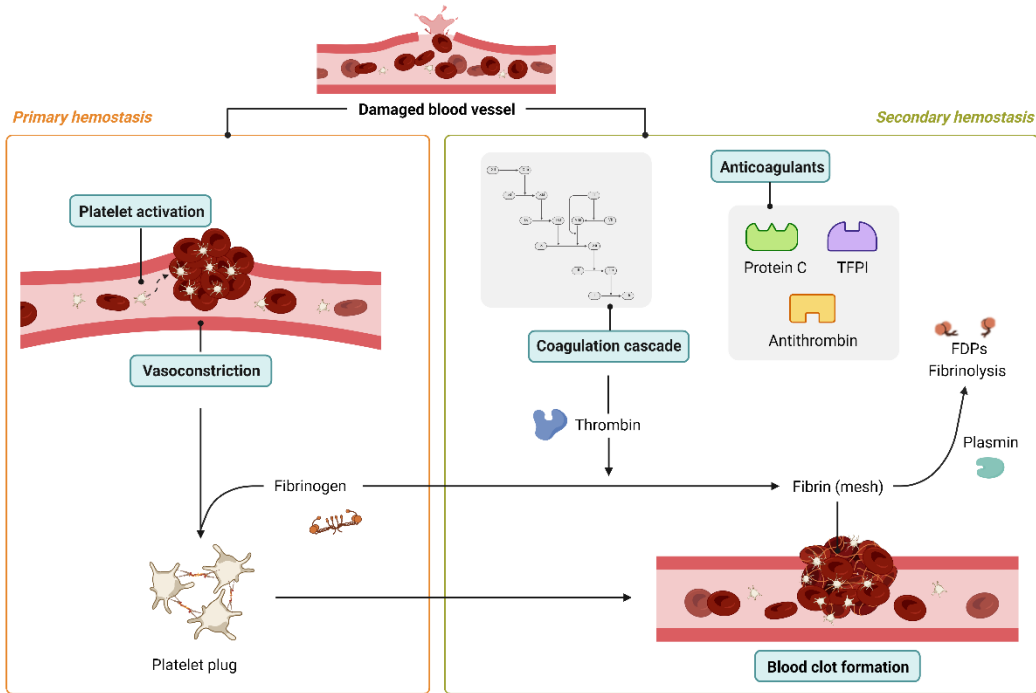


Figure 1-6. Visual depiction of hemostasis and the hemostatic response. FDP: fibrin degradation product; TFPI: tissue factor pathway inhibitor.

Adapted from: Arble E., Arnetz B.B. Anticoagulants and the hemostatic system: a primer for occupational stress researchers. *Int J Environ Res Public Health.* 2021; 18: 10626. *Created with:* BioRender.com.

1.6.1.1 Primary hemostasis

(a) Vascular endothelium and vasoconstriction

Under normal circumstances the vascular endothelium is a non-thrombogenic cellular monolayer, lining the inner surface of the blood vessels and allowing blood components to pass unhindered through the circulatory system [98,99]. In case of a vascular injury, endothelial cells become activated, resulting in the expression of adhesion receptors (e.g. intracellular adhesion molecule [ICAM] 1-3, vascular adhesion molecule [VCAM], and platelet endothelial cell adhesion molecule [PECAM]) on the endothelial membrane and the stimulation of exocytosis of Weibel-Palade bodies, containing von Willebrand factor (VWF) and P-selectin. In addition, the highly thrombogenic subendothelial matrix underlying the vascular endothelium becomes exposed, leading to the expression and

release of vasoactive peptides, collagen and tissue factor (TF) [98–101]. This switch to a prothrombotic and proinflammatory state sees the endothelium orchestrate vasoconstriction, platelet and leukocyte activation and adhesion, promotion of thrombin formation, coagulation and fibrin deposition at the vascular wall [99].

(b) Platelets

Shortly after damage to the vascular endothelium, platelets will begin to adhere to exposed subendothelial collagen and VWF through the action of the glycoprotein (GP) Ib/IX/V complex (Figure 1-7). As platelets adhere to the site of the injury, they become activated, causing them to i) undergo a change in shape that activates the GPIIb/IIIa receptor, ii) release platelet dense granule contents: e.g. adenosine diphosphate (ADP), serotonin (5-HT) and thromboxane A₂ (TXA₂), and iii) bind with other platelets via the GPIIb/IIIa receptor (platelet aggregation). ADP, 5-HT and TXA₂ will respectively attract additional platelets, promote vasoconstriction and stimulate platelet aggregation, vasoconstriction and degranulation [99,101,102]. Thus, more platelets will be attracted to the damaged area that, in turn, adhere to the already attached platelets, become activated and support a continuous cycle of platelet attraction and activation, ultimately promoting the formation and growth of a platelet plug/primary hemostatic plug [101].

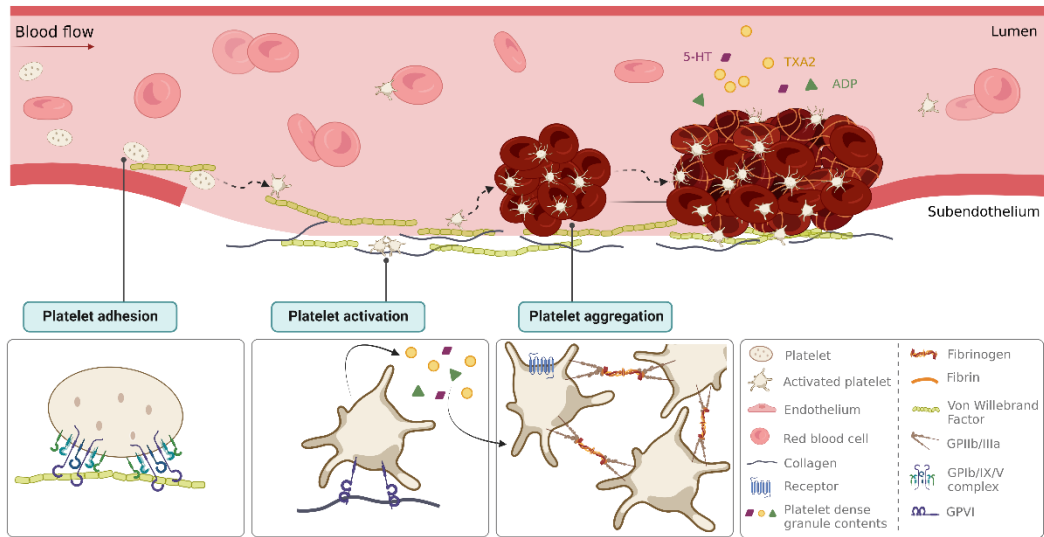


Figure 1-7. Primary hemostasis – Formation of a platelet plug. ADP: adenosine diphosphate; GP: glycoprotein; TXA2: thromboxane A2 (TXA2); 5-HT: serotonin.

Adapted from: McFadyen JD, Schaff M, Peter K. Current and future antiplatelet therapies: emphasis on preserving hemostasis. *Nat Rev Cardiol.* 2018; 15: 181-191 *and* Karampini E, Bierings R, Voorberg J. Orchestration of primary hemostasis by platelet and endothelial lysosome-related organelles. *Arterioscler Thromb Vasc Biol.* 2020; 40: 1441-1453 *and* Semple JW, Italiano JE, Freedman J. Platelets and the immune continuum. *Nat Rev Immunol.* 2011; 11: 264-274. *Created with:* BioRender.

1.6.1.2 Secondary hemostasis

The platelet plug formed as a primary hemostatic response is however ineffective in the long term unless the platelet plug is fortified with an insoluble fibrin network [97,101]. So while the platelet plug is forming, “secondary hemostasis” can begin. This process is defined by the coagulation cascade, a series of linked proteolytic reactions in which zymogens are converted into active serine proteases, and eventually leads to the formation of thrombin, which ultimately converts soluble fibrinogen into insoluble fibrin resulting in a cross-linked fibrin network [97,99,101].

Classically, the coagulation cascade is presented as two separate pathways that culminate in the common pathway: the TF pathway (or extrinsic pathway) and the contact activation pathway (or intrinsic pathway) [103]. This model is good for describing

the coagulation process *in vitro* (in the laboratory), where the intrinsic or extrinsic pathways can selectively be activated. However this separation is not entirely physiological correct [96,103,104]. The newer cell-based model of hemostasis, which gives a better description of the process of hemostasis as it occurs in the body and better reflects this process when compared to the cascade model, is therefore currently used. For the purpose of understanding, the process of coagulation is subdivided into three phases (initiation, amplification, and propagation) which are interwoven and overlap each other [96,103,104].

(a) Initiation phase

The initiation phase takes place when the circulating blood comes into contact with TF-bearing cells in the damaged endothelium (Figure 1-8). The potent procoagulant molecule TF is normally present in cells like smooth muscle cells and fibroblasts in the subendothelial layer of blood vessels and in a small amount in macrophages, endothelial cells and platelets circulating in the blood. It is hidden, membrane-bound and is expressed on the surface of these cells only after an injury [62,96,100,105]. By forming a tight complex with circulating coagulation factor VII (fVII), fVII becomes activated (fVIIa). In its turn the TF/fVIIa complex sets into motion a series of zymogen activation steps, resulting in the activation of factor IX (fIX) and factor X (fX) [96,99]. FXa can only activate small amounts of prothrombin into thrombin (fIIa) in the absence of its cofactor (fVa). Thrombin generation through this reaction is not robust and can be effectively terminated by tissue factor pathway inhibitor (TFPI) and antithrombin III (ATIII) present on normal endothelium (see 1.6.1.2(d)). However, this small amount of thrombin is sufficient to initiate the coagulation process and thus start the amplification phase [96,97,99,104].

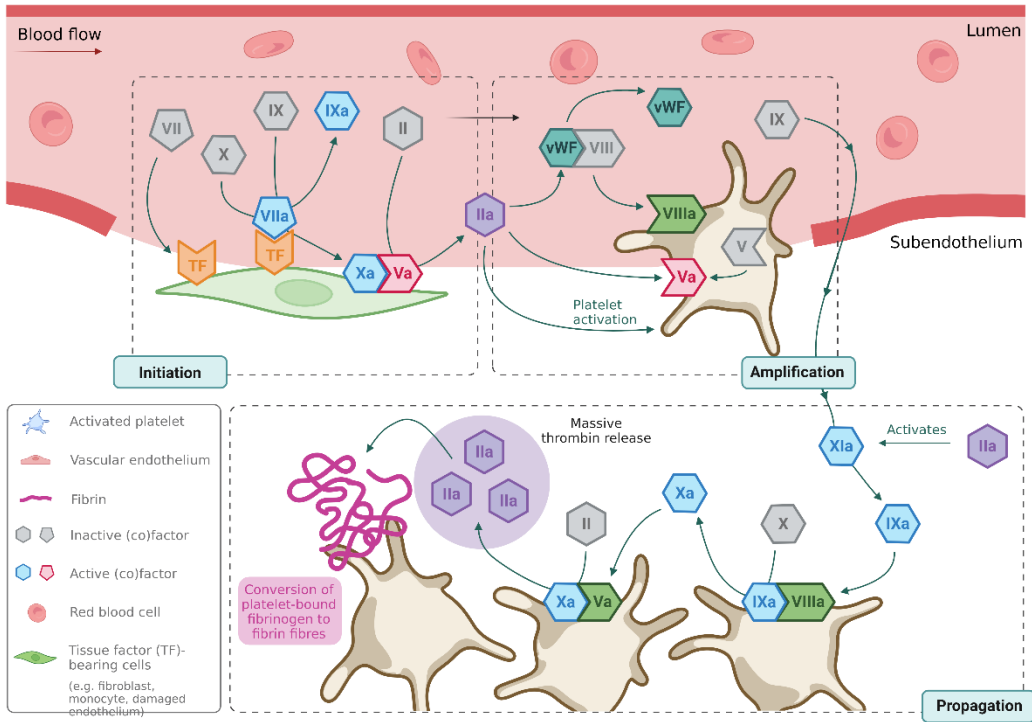


Figure 1-8. Secondary hemostasis – Cell-based model of clotting. Factor II: prothrombin; Factor IIa: thrombin; TF: tissue factor; VWF: von Willebrand factor.

Adapted from: Ward JPT, Linden RWA. Figure 10.2. In: *Physiology at a glance*. 4th ed. Wiley-Blackwell. 2017. 168 p. *Created with:* BioRender.com.

(b) Amplification phase

In the amplification phase, traces of thrombin fully activate platelets that have adhered to the site of injury (Figure 1-8). These activated platelets form a platelet aggregate and provide a surface for activation of other coagulant factors. At the same time, these thrombin traces proteolytically cleave fV released from the α -granules of activated platelets and activate fVIII bound to VWF on the platelet surface into fVa and fVIIIa respectively. In addition, thrombin converts fXI into fXIa, which promotes further fIXa generation [97,99,100,104,106].

(c) Propagation phase

Finally, during the propagation phase (Figure 1-8), thrombin is continuously generated on the surface of activated platelets by the action of two complexes: the prothrombinase complex (fVa/fXa) and the intrinsic tenase complex (fVIIIa/fIXa). The newly generated thrombin plays a key role in the eventual formation and stabilization of the fibrin clot by i) catalyzing the conversion of soluble fibrinogen into insoluble fibrin monomers that spontaneously polymerize into a structural meshwork, ii) by activating fXIII that subsequently stabilizes the fibrin clot by covalently cross-linking the fibrin strands, and iii) by activating proCPU to form a molecular link between coagulation and fibrinolysis. Taken together, the platelet aggregate and cross-linked fibrin form a stable clot, which seals off the site of injury and prevents excessive blood loss [97,99,100,106].

(d) Physiological limitation of the coagulation

Since the blood coagulation system is a potent and highly effective process, tight regulation of the blood coagulation system is essential to prevent unnecessary clot formation [100]. To do so, several anticoagulant mechanisms dampen the formation of thrombin and/or inactivate thrombin directly (Figure 1-6). The most important physiological anticoagulant is activated protein C. Together with its cofactor protein S, it inactivates fVa and fVIIIa. ATIII and TFPI are other important endogenous anticoagulant factors [97,99,100,106].

1.6.1.3 Fibrinolysis

To limit coagulation at the site of the injury and prevent vascular occlusion, the prothrombotic response is balanced by the fibrinolytic system. During fibrinolysis, the generation of plasmin from its inactive zymogen plasminogen by tissue-type (tPA) and urokinase-type (uPA) plasminogen activator is of central importance [98,107]. tPA, produced by vascular endothelial cells and released in response to thrombin and venous occlusion, is primarily involved in fibrin dissolution in the circulation [108–110]. uPA on the other hand, is expressed by many cell types (including renal epithelial cells,

inflammatory cells, and cancer cells), and is considered the major activator of fibrinolysis in the extravascular compartment [110–112]. uPA can activate plasminogen in solution, while tPA forms a ternary complex with plasminogen by both binding to fibrin at the clot surface. This interaction is of utmost importance as tPA-mediated plasminogen activation is two to three orders of magnitude higher in the presence of fibrin than in its absence. Next, the plasmin that is formed, cleaves fibrin, especially after internal lysine residues, generating partially degraded fibrin containing C-terminal lysines (Figure 1-9).

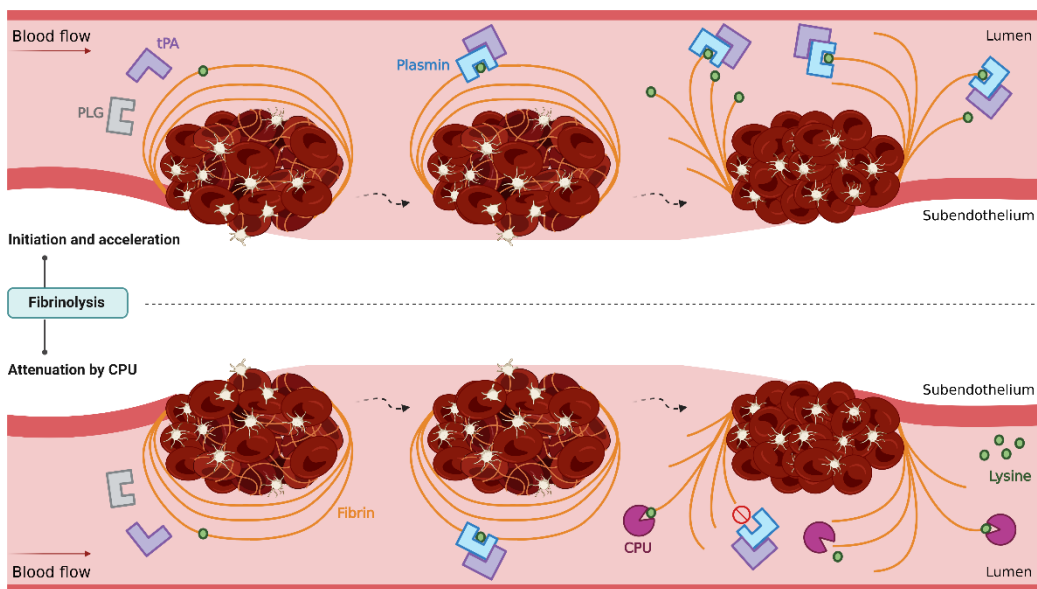


Figure 1-9. Fibrinolysis and mechanism of action by which CPU attenuates fibrinolysis. Upper panel: Plasminogen and tPA bind to fibrin, forming a ternary complex. Plasmin thus formed, initiates lysis by cleaving the fibrin fibers, in particular after lysine residues. The generated C-terminal lysine residues are high-affinity binding sites for plasminogen. Plasminogen binds to these lysines and the conformational change induced, provides a favorable substrate for further activation. This is known as the acceleration phase of fibrinolysis. **Lower panel:** CPU abrogates this feedback enhancement of plasminogen activation by cleaving these C-terminal lysine residues. CPU: carboxypeptidase U; tPA: tissue-type plasminogen activator.

Adapted from: Heylen E. Carboxypeptidase U: A new drug target for fibrinolytic therapy. Doctoral thesis. University of Antwerp. 2011.

These C-terminal lysine residues serve in turn as propagators of fibrinolysis by initiating a positive feedback mechanism: i) they serve as stronger binding sites for plasminogen,

promoting the binding of plasminogen and therefore also its activation by tPA [113]; ii) C-terminal lysine residues are essential for the decreased rate of plasmin inhibition, since plasmin bound to degraded fibrin and fibrin degradation products (FDPs), is protected from inactivation by α 2-antiplasmin [114].

To prevent hyperfibrinolysis, the action of plasmin is negatively modulated at several levels. Inhibition of fibrinolysis occurs i) at the level of the plasminogen activators by PAI-1 and PAI-2, ii) at the level of plasmin by α 2-antiplasmin, and finally iii) at the level of fibrin itself by means of the antifibrinolytic enzyme CPU [115,116].

1.6.2 CPU: a potent antifibrinolytic enzyme

CPU is present in the circulation as its inactive precursor proCPU and needs to be activated before it can exert an effect on fibrinolysis. Both thrombin(-thrombomodulin) and plasmin – the key enzymes of respectively coagulation and fibrinolysis – are able to convert the inactive zymogen into the active enzyme CPU, placing CPU at the nexus between coagulation and fibrinolysis [5,63]. Once activated, CPU cleaves off C-terminal lysine residues on partially degraded fibrin (Figure 1-9), thereby potentially attenuating fibrinolysis through i) loss of high-affinity binding sites for plasminogen, resulting in less incorporation in the clot and a deceleration of tPA-mediated plasminogen activation, ii) loss of protection of plasmin from inhibition by α 2-antiplasmin [117].

During *in vitro* clot lysis CPU generation follows a biphasic pattern and acts on fibrinolysis through a threshold-dependent mechanism [74,118]. A schematic representation of the biphasic pattern of CPU generation and the threshold principle is shown in Figure 1-10. Shortly after initiation of the coagulation, a first peak of CPU activity (pink curve) is generated through the action of thrombin(-thrombomodulin). Thereafter, the CPU activity declines rapidly as a result of the intrinsic instability of CPU, but propagation of fibrinolysis is prevented as long as the CPU activity remains above the threshold level. From the moment CPU activity drops under the critical threshold value, fibrinolysis (blue curve) accelerates and proceeds into its amplification/propagation phase. When

sufficient plasmin is generated during the fibrinolysis a second CPU activity peak will occur, formed by the action of plasmin [74].

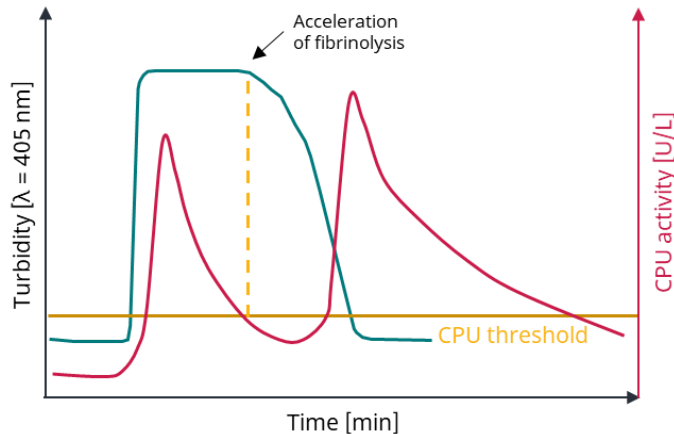


Figure 1-10. The biphasic pattern of CPU generation during *in vitro* clot lysis and the CPU threshold behavior. Shortly after initiation of coagulation, a first peak of CPU activity appears through the action of thrombin-(thrombomodulin). Afterward, CPU activity declines exponentially but propagation of fibrinolysis will be prevented as CPU acts on fibrinolysis via a threshold-dependent mechanism. As long as the CPU activity remains above the threshold value, fibrinolysis stays in its initial phase. The moment CPU activity drops under the critical threshold value, fibrinolysis is accelerated exponentially and proceeds into its amplification/propagation phase. When sufficient plasmin is generated a second CPU activity peak will occur, formed by the action of plasmin.

Adapted from: Leenaerts D. Towards improved understanding of the role of carboxypeptidase U in arterial thrombosis. Doctoral thesis. University of Antwerp. 2017.

CPU is a very potent antifibrinolytic enzyme and regulates tPA-dependent fibrinolysis at 1 nM, which is equivalent to only 1–2% of the circulating proCPU levels in plasma [63]. This suggests that even modest activation of proCPU can have a profound effect on the inhibition of fibrinolysis [59]. At the same time, this indicates that a slow and sustained rate of proCPU activation provides a more efficient regulation of fibrinolysis than an extensive but short-lived burst of CPU [62,118,119]. Importantly, the CPU threshold level is dictated by the plasmin concentration and thus the rate of plasminogen activation. The latter is determined by local plasminogen activator (tPA, uPA) and inhibitor (α 2-antiplasmin, PAI-1) concentrations. The time that the CPU activity remains above the

threshold is defined by the proCPU concentration, the extent of proCPU activation – and thus the concentrations of thrombin(-thrombomodulin) and plasmin – and the CPU half-life that is defined by the Thr325Ile polymorphism [118].

1.7 Measurement of proCPU, CPU and CPUi: methods, challenges and pitfalls

To date, a wide range of methods is available for the quantification of proCPU, CPU and CPUi, including immunological (antigen-based) methods, enzymological (activity-based) methods, and functional fibrinolytic assays (Figure 1-11). Each method has inherent advantages and shortcomings, so it is of utmost importance to carefully select an appropriate, well-characterized, and validated assay when investigating the (patho)physiological role of specific CPU forms (proCPU, CPU, and CPUi).

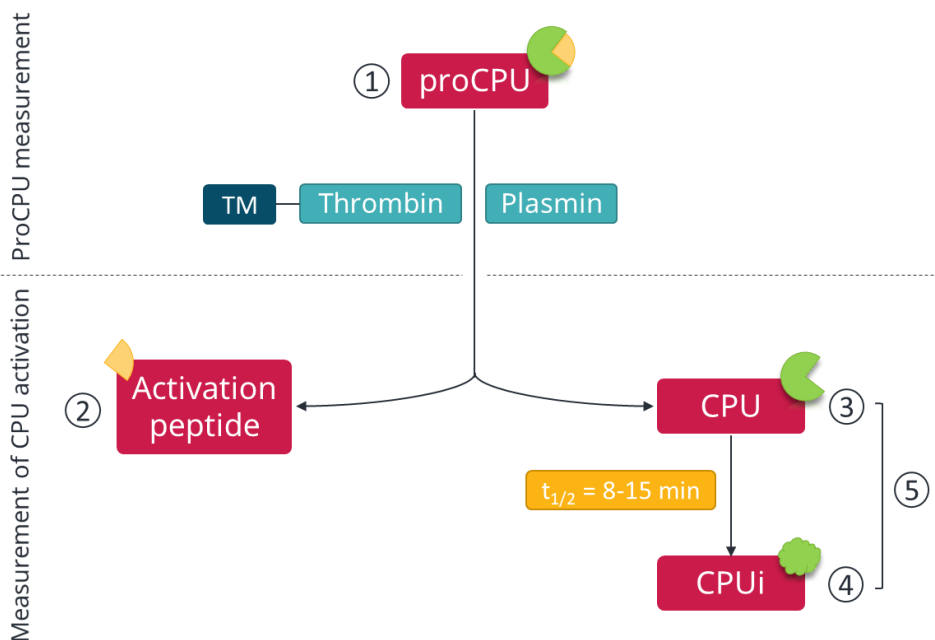


Figure 1-11. Measurement of different forms of the CPB2 gene product. The zymogen procarboxypeptidase U (proCPU; **1**) can be measured with antigen- or activity-based assays. Carboxypeptidase U (CPU) activation can also be determined. Upon activation with thrombin, the thrombin-thrombomodulin (TM) complex, or plasmin, the activation peptide (AP; **2**) is released and can be measured with an antigen-based assay. The active enzyme CPU can be directly measured by enzymatic assays (**3**). The active enzyme CPU is thermally inactivated into CPUi (**4**) which can be measured with antigen-based assays that detect both CPU and CPUi simultaneously (**5**).

1.7.1 ProCPU

Various in-house developed assays and commercially available quantification kits exist for the determination of proCPU in plasma (Table 1-1) [37–39,81,120]. Immunoassays (enzyme-linked immunosorbent assays, ELISAs) are relatively easy to perform, can be automated efficiently, do not require activation of the zymogen before measurement, and are not comprised by interference of plasma CPN [80]. A major challenge with this type of assay is cross-reactivity of the antibodies raised against proCPU with other components, such as CPU, CPUi, the released activation peptide of proCPU or other proteolytic fragments [120]. Also, depending on the antibodies used, ELISAs lack interspecies cross-reactivity which requires the necessity of species-specific antibody combinations and hampers flexibility towards animal studies [80,121]. Another issue is the unequal reactivity of certain ELISAs towards different proCPU isoforms of the Thr325Ile polymorphism, resulting in incorrect proCPU measurement [120,122,123]. In a comparative study by Heylen *et al.*, three commercially available antigen-based assays (Zymutest® TAFI, Visulize® TAFI and Immunoclone® TAFI) showed significantly lower reactivity towards the Ile³²⁵-isoform, giving rise to an overestimation of the variation between the different genotypes [124]. As these assays have been applied in clinical studies, the reported results need to be reinterpreted in this light [124]. Nevertheless, these three assays are still marketed today, without mentioning the difference in reactivity towards the Thr325Ile isoforms. Several other suppliers offer proCPU ELISA kits, but their ability to distinguish between proCPU, CPU, and CPUi, as well as their reactivity to the proCPU polymorphisms need to be validated before these kits can be reliably implemented in interventional and observational clinical trials.

Alternatively, activity-based enzymological methods can be implemented to quantify proCPU levels (Table 1-1). These methods require exogenous and quantitative activation of proCPU to CPU by thrombin-thrombomodulin, followed by quantification of the formed active CPU. The latter can be done by means of incubation with C-terminal Arg- or Lys-containing CPU-specific substrates. The released Arg/Lys or the other fragment

can thereafter be detected via different analytical approaches (high-performance liquid chromatography [HPLC], spectrophotometer or fluorimeter). Unfortunately, most of these substrates (e.g., Hip-Arg and AAFR) are not optimal for use in plasma or whole blood samples due to the interfering activity of endogenous CPN [35,125,126]. However, the more recently designed synthetic substrate N-benzoyl-*ortho*-cyano-phenylalanyl-arginine (Bz-*o*-cyano-Phe-Arg) has improved selectivity for CPU over CPN and allowed the development of an assay that does not suffer from interference by CPN [79,81]. Furthermore, proCPU itself has been described to show limited intrinsic enzymatic activity towards these small synthetic substrates, but this does not interfere with the above-described proCPU assays [127,128]. Other components are not detected in activity assays [127,128]. Another advantage of activity-based assays is that these assays are not hampered by different reactivity towards Thr325Ile isoforms, at least, when the proCPU activation is performed at 25 °C/room temperature. With activation at 37 °C, the difference in stability of the two isoforms can bias the results. Furthermore, a well-defined incubation interval to guarantee linear substrate conversion is important [129].

Recently, Wheeler and co-workers reported a quantitative isotope diluted mass spectrometry (IDMS) method for assigning an International System of Units (SI) value to proCPU in plasma, using an acetonitrile-assisted tryptic digestion and liquid chromatography (LC) separation followed by mass spectrometry (MS) analysis. Traceability is obtained by reference to calibrators that consist of proCPU-depleted plasma (blank) spiked with a defined amount of purified proCPU, value assigned by amino acid analysis. The calibrators are run alongside the samples, using the same preparation steps and conditions. Stable isotope-labeled proCPU is added as an internal standard to the samples and calibration standards to account for variations during the sample preparation process (e.g. losses during sample clean-up, incomplete digestion, variations in instrument performance...) [130]. This quantitative MS assay could be adopted as a suitable method to assign an SI value to a proCPU plasma reference preparation, but is probably too laborious for analyzing large quantities of samples.

Given the diversity of the available assays and the ensuing wide variation in estimates of plasma proCPU concentrations, proCPU research would benefit from international reference material. Therefore, the SSC fibrinolysis subcommittee of the International Society of Thrombosis and Haemostasis (ISTH) initiated an international collaborative study to generate the WHO 1st international reference standard for proCPU. The availability of this standard will be an aid for future assay development, allow a more straightforward comparison of study results, and will contribute to the reduction of the reported variability. The quantitative IDMS method established by Wheeler *et al.* can contribute to the introduction of such an SI-value assigned international reference material [130].

1.7.2 CPU

For a long time, measuring active CPU in the blood circulation and identifying pathological conditions in which CPU generation is enhanced, was not possible with the available methods. Activity-based and functional assays were not sensitive and selective enough to measure ultra-low levels of CPU in the presence of high concentrations of proCPU and CPN [80]. ELISAs at hand were unable to distinguish active CPU from CPUi. However, that changed with the advent of the in-house developed methods of Heylen *et al.* and Kim *et al.* (Table 1-1) [131,132]. In the former, the active enzyme is incubated with the substrate Bz-*o*-cyano-Phe-Arg at 25 °C, followed by UV-detection of the released Bz-*o*-cyano-Phe in a reversed-phase HPLC system [131]. Kim and co-workers on the other hand developed a functional assay in which plasmin-modified fibrin is covalently bound to a quencher molecule and mixed with fluorescein-labeled plasminogen and the plasma sample [132]. Given the fact that CPU cleaves off C-terminal lysine residues from partially degraded fibrin, the rate of fluorescence increase detected by a plate reader reflects the amount of CPU present in the sample. Both the direct enzymatic assay of Heylen *et al.* and the functional assay of Kim *et al.* allow highly sensitive quantification of CPU levels as low as 0.09 U/L (18 pM) and 12 pM respectively [131,132].

Table 1-1. Overview of in-house developed assays and commercially available quantification kits for the determination of different forms of the CPB2 gene product in human plasma.

Assay type	Interference or influence of					Additional information	Used in
	Thr325Ile	CPN	ProCPU	CPU	CPUI		
ProCPU measurement							
	Wang <i>et al.</i> 1994 [56]	No	Yes	-	Yes	No	Hip-Arg with detection by RP-HPLC
	Mosnier <i>et al.</i> 1998 [37]	No	Yes	-	Yes	No	Hip-Arg with colorimetric detection [133–135]
	Schatteman <i>et al.</i> 1999 [136]	No	Yes	-	Yes	No	Hip-Arg with detection by RP-HPLC [137–139]
	Schatteman <i>et al.</i> 2001 [140]	No	Yes	-	Yes	No	<i>p</i> -OH-Hip-Arg with colorimetric detection [141]
Activity *	Heylen <i>et al.</i> 2010 [81]	No	No	-	Yes	No	Bz- <i>o</i> -cyano-Phe-Arg with detection by RP-HPLC; Not very sensitive to the influence of hemolysis [142]
	STA-Stachrom® TAFI (Diagnostica Stago)	No	No	-	Yes	No	Azoformyl-AA2—AA1 (Patent: SERBIO PCT/FR 02/02376) with colorimetric detection [143]
	Actichrome® TAFI (American Diagnostica)	No	No	-	Yes	No	Chromogenic substrate with colorimetric detection; No longer marketed [144–150]
	Pefakit® TAFI (Pentapharm)	No	No	-	Yes	No	Synthetic substrate with colorimetric detection [151–159]

Assay type	Interference or influence of					Additional information	Used in
	Thr325Ile	CPN	ProCPU	CPU	CPUi		
ProCPU measurement (continued)							
ELISA	Mosnier <i>et al.</i> 1998 [37]	Unk.	No	-	Unk	Unk	Murine monoclonal capture and rabbit polyclonal detection antibody [160,161]
	van Tilburg <i>et al.</i> 2000 [30]	No	No	-	Yes	Yes	Electroimmunoassay [30,162–165]
	Strömqvist <i>et al.</i> 2001 [38]	Unk.	No	-	No	No	No reaction with plasma of other species (guinea pig, rat, dog, pig, hamster)
	Ceresa <i>et al.</i> 2006 [120]	No **	No	-	No	No	Monoclonal capture and detection antibody [163,164,166–168]
	VisuLize® TAFI (Affinity Biologicals)	Yes	No	-	Yes	Yes	Sheep polyclonal capture and detection antibody; Marketed by Milan Analytica [146–149,169–175]
	Imuclone® TAFI (American Diagnostica)	Yes	No	-	No	No	[176–180]
	Asserachrom® TAFI-1B1 (Diagnostica Stago)	No	No	-	No	No	Previously marketed by Kordia Laboratory Supplies; No longer marketed [24,48,157,181–187]
Zymutest® (Total) TAFI (Hyphen BioMed)	No	No	-	No	No	Previously marketed as Zymutest® proTAFI [144,188–191]	

Assay type		Interference or influence of					Additional information	Used in
		Thr325Ile	CPN	ProCPU	CPU	CPUi		
ProCPU measurement (continued)								
ELISA	Coalize® TAFI (Chromogenix)	Unk.	No	-	Unk	Unk	Monoclonal capture and polyclonal detection antibody	[145,192]
Isotope diluted mass spectrometry		No	No	-	No	No	IDMS method using an acetonitrile-assisted tryptic digestion and LC separation followed by MS analysis. Calibrators consisting of proCPU-depleted plasma (blank) spiked with a defined amount of purified proCPU (value assigned by amino acid analysis) run alongside the samples. Stable isotope-labeled proCPU is added as an internal standard to all samples and calibrators.	[130]
Activation peptide								
ELISA	Ceresa <i>et al.</i> 2006 [120]	No ***	No	No	Yes	No	Monoclonal capture and detection antibody; Measures both AP and CPU	[163,164,166,168]
Active CPU								
Activity	Hendriks <i>et al.</i> 1989 [2]	No	Yes	No	-	No	<i>p</i> -OH-Hip-Arg with colorimetric detection and Hip-Arg with detection by RP-HPLC	

Assay type	Interference or influence of					Additional information	Used in
	Thr325Ile	CPN	ProCPU	CPU	CPUi		
Active CPU (continued)							
Activity	Kim <i>et al.</i> 2008 [132]	No	No	No	-	No	Plasmin-modified fibrin is covalently bound to a quencher molecule and mixed with fluorescein-labeled plasminogen and the plasma sample. The rate of fluorescence increase detected by a plate reader reflects the amount of CPU present in the sample. High sensitive (LOD: 12 pM); Not affected by other hemostatic factors
	Heylen <i>et al.</i> 2010 [131]	No	No	No	-	No	Bz- <i>o</i> -cyano-Phe-Arg with detection by RP-HPLC; High sensitive (LOD: 18 pM); Highly sensitive to the influence of hemolysis [193–195]
ELISA	Zymutest® (Activatable) TAFI (Hyphen BioMed)	Yes				Previously marketed as Zymutest® TAFI	[159,196,197]
Active & inactive CPU ****							
ELISA	Asserachrom TAFIa/ai (Diagnostica Stago)	No	No	No	-	-	Combined measurement of CPU and CPUi; Not sensitive to the influence of hemolysis [143,168]
	Imubind® TAFIa/ai (Biomedica Diagnostics)	No	No	No	-	-	No longer marketed [198]

This is a non-exhaustive list of methods that are available for the measurement of different forms of the *CPB2* gene product. Methods used in clinical studies that are discussed in this thesis (or derivative methods) were included in this table. * Requires quantitative activation of proCPU before measurement. Consecutive measurements can reveal proCPU consumption (ongoing CPU activation). ** T12D11/T30E5. *** T12D11/T18A8. **** Reflects past or ongoing CPU generation over a longer period. AA: amino acid; AP: activation peptide; CPN: carboxypeptidase N; CPU: carboxypeptidase U (TAF1a, CPB2); CPUi: inactivated CPU; ELISA: enzyme-linked immunosorbent assay; IDMS: isotope diluted mass spectrometry; LOD: limit of detection; proCPU: procarboxypeptidase U (TAFI, proCPB2); LC: liquid chromatography; MS: mass spectrometry; RP-HPLC: reversed-phase high-performance liquid chromatography; TAFI: thrombin activatable fibrinolysis inhibitor (proCPU, proCPB2); Unk: unknown.

Although the recently developed methods allow the quantification of active CPU, measurement still is not straightforward. Several preanalytical and analytical difficulties need to be tackled. The first one is the sample collection. Blood sampling tubes intended for CPU measurement need to contain sodium citrate as an anticoagulant together with a thrombin- and/or plasmin inhibitor, such as chloromethyl ketones (e.g., D-phenylalanyl-L-propylarginylchloromethyl ketone [PPACK]) or d-Val-Phe-Lys chloromethyl ketone [VFK-CK]) and/or aprotinin, to avoid unwanted *ex vivo* activation of proCPU [199]. Following blood collection, samples should immediately be placed in iced water to minimize degradation of the intrinsically unstable CPU [131]. Moreover, centrifugation for isolation of plasma needs to be performed at 4 °C and long-term storage at – 80 °C is necessary. Additionally, hemolysis must be avoided as it was shown that this interferes with the measurement of CPU activity [200]. Furthermore, the short half-life of CPU at 37 °C also implies that the CPU activity measured in plasma is a snapshot that reflects only a limited timeframe. To accurately measure the influence of CPU activity on a pathologic state, multiple sample collections in the acute stage of a disease should be collected. Together, these preanalytical and analytical precautions require very strict procedures and make the organization of CPU assessment in clinical studies very demanding.

1.7.3 Assessment of overall proCPU activation

Another strategy is the assessment of the extent of proCPU activation by quantifying cleavage products, such as i) the amount of activation peptide or ii) the amount of active and inactive CPU (CPU+CPUi) (Table 1-1) [120]. Determination of these cleavage products provides insight into the *in vivo* activation of the proCPU pathway and thus past and ongoing CPU formation. Consecutive samplings allow to relatively assess the amount of CPU that has been generated between two specific time points and can provide complementary information to activity-based assays in patient populations where fibrinolysis is impaired [142,163,166,167,183]. Antibody pairs for application in sandwich-ELISAs have been developed and validated by Ceresa and co-workers [120]. A

first pair developed by this group allows the measurement of the amount of activation peptide that has been released through activation of proCPU (MA-T12D11/MA-T18A8-HRP). A second antibody pair measures the total amount of CPU+CPUi formed (MA-T30E5/MA-T17D7-HRP) [163,164,166,167,201]. Another assay that allows combined measurement of CPU and CPUi was published by Hulme *et al.* [202]. This assay was marketed as the Imubind® TAFIa/ai ELISA (US20060183172A1 and US7470519B2), but has been discontinued. At this moment, the only commercially available CPU+CPUi ELISA is the Asserachrom® TAFIa/ai ELISA (Diagnostica Stago, Asnières, France). The assay shows equal reactivity towards CPU and CPUi and is not affected by the Thr325Ile polymorphism.

1.7.4 Assessment of the CPU system by functional fibrinolysis assays

It is also possible to use indirect, functional fibrinolytic assays which measure the effect of CPU formation on the fibrinolytic rate. These methods often include experiments with and without the use of a CPU inhibitor, in order to selectively evaluate the contribution of CPU to fibrinolysis (Figure 1-12). Historically, turbidimetric measurements of clot formation and subsequent lysis in plasma-based systems were applied to functionally assess CPU formation in patients [203]. This type of assay is an interesting and valuable research tool in the characterization of the functional role of CPU and the development of CPU inhibitors, but has the downside that it is very sensitive to variations in plasma levels of other components of the fibrinolytic and coagulation system. Moreover, various plasma-based systems exist with small variations in the protocol, in terms of activator (Ca²⁺, TF, thrombin, thrombomodulin, phospholipids or combinations of the before mentioned) or tPA concentration, that result in high inter-laboratory variability as reported in an international study on the feasibility of a standardized clot lysis assay that was performed by the SSC fibrinolysis subcommittee of the ISTH [204]. Nevertheless, the in-house repeatability of the assays included in this study was shown to be excellent [204].

Moreover, combining a classic clot lysis experiment with the measurement of CPU activity on well-defined time points during this clot lysis assay offers a unique technique to determine an individual's endogenous CPU generation potential (Figure 1-12) [74,118,119,205]. It is an interesting tool to study mechanisms that influence CPU generation and may also be valuable to select individuals who would benefit from pharmacological CPU inhibition [205]. Additionally, Leenaerts *et al.* demonstrated that the effect of CPU on fibrinolysis can also be assessed in more complex systems. Viscoelastic methods such as thromboelastometry that are performed on whole blood showed a good response to the addition of thrombomodulin (CPU activation) and AZD9684 (CPU inhibition) [206]. In the same study, a complex model of arterial flow has also been assessed but showed substantial variability, thereby limiting its applicability for CPU assessment [206].

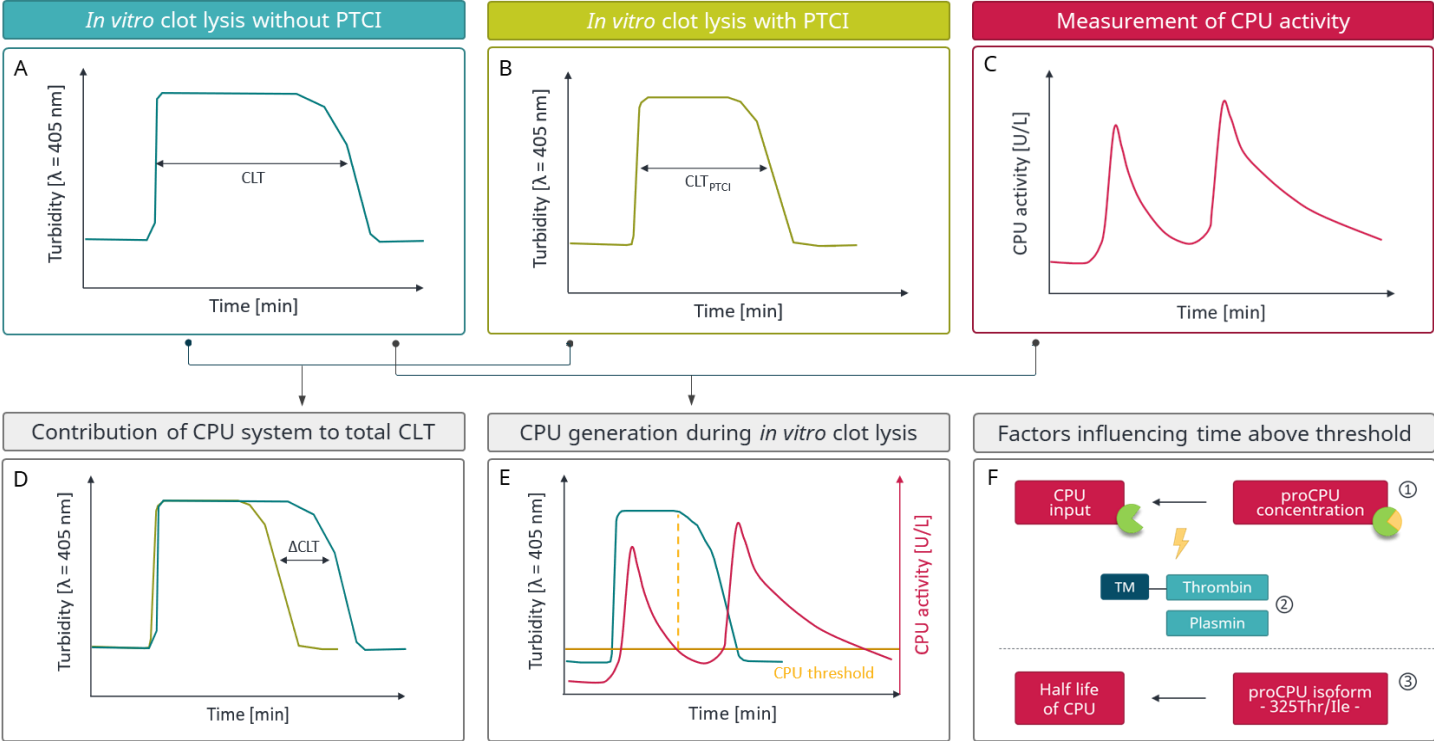


Figure 1-12. Functional assessment of CPU. The contribution of CPU to the total clot lysis time (Δ CLT; **D**) can be visualized by means of *in vitro* clot lysis experiments in the absence (**A**) or presence (**B**) of potato tuber carboxypeptidase inhibitor (PTCl) or a selective CPU inhibitor. During *in vitro* clot lysis, CPU is generated shortly after initiation of the coagulation – when proCPU is activated by thrombin(-thrombomodulin) – resulting in a first CPU activity peak (**D**) and halting fibrinolysis as long as the CPU level remains above a certain threshold value (**E**). This threshold concentration is dictated by steady-state plasmin concentrations, and thus dependent on tissue-type plasminogen activator (tPA) and plasmin inhibitor concentrations. Once CPU activity falls below this critical threshold value, fibrinolysis accelerates and the generated plasmin gives rise to the formation of a second CPU activity peak (**C,E**). The time that the CPU stays above the threshold (**F**) is defined by (1) the proCPU concentration, (2) the extent of proCPU activation – and thus the concentrations of thrombin(-thrombomodulin) – and (3) the CPU half-life, defined by the Thr325Ile polymorphism.

Chapter 2

Pathophysiological role of the CPU system

Partly based on:

Claesen K, Mertens JC, Leenaerts D, Hendriks D. Carboxypeptidase U (CPU, TAF1a, CPB2) in Thromboembolic Disease: What Do We Know Three Decades after Its Discovery? *Int. J. Mol. Sci.* 2021, 22(2), 883.

2 Pathophysiological role of the CPU system

2.1 The CPU system and the risk for cardiovascular disease and thrombotic disorders

2.1.1 Hyperlipidemia as a risk factor for atherosclerosis and cardiovascular disease

2.1.1.1 Atherosclerosis and atherosclerotic cardiovascular disease

Atherosclerosis is a chronic, progressive disease of the arterial wall in which lipid retention, oxidation and modification take place, provoking chronic inflammation and a build-up of scar tissue. Disease progression results in the formation of atherosclerotic plaques that narrow the arterial lumen, ultimately causing thrombosis or stenosis upon plaque rupture and leading to clinical events such as myocardial infarction and stroke (Figure 2-1) [207,208]. In the process of plaque progression, monocytes and macrophages play an important role. As oxidized low-density lipoprotein cholesterol (LDL-C) accumulates in the subendothelial space, recruitment of monocytes in the arterial wall is triggered. In the intima, the retained monocytes differentiate into macrophages, which scavenge lipoprotein particles, and eventually become foam cells. These macrophages and foam cells secrete inflammatory molecules that further promote lipoprotein retention, degrade the extracellular matrix and sustain inflammation, making the plaque unstable and enlarging the risk for plaque rupture [209].

Atherosclerotic cardiovascular disease (ASCVD) comprises a major burden of morbidity and remains a leading cause of mortality worldwide [210–212]. Over 17 million people died from ASCVD in 2015, representing 31% of all global deaths [210]. Since the 1950s advances in cardiovascular health have led to significant improvements in ASCVD outcomes. However, despite these improvements, tackling an unhealthy lifestyle and reducing risk factors (see *infra*) – both at population- and individual level – in order to prevent cardiovascular disease (CVD) events remains important [213].

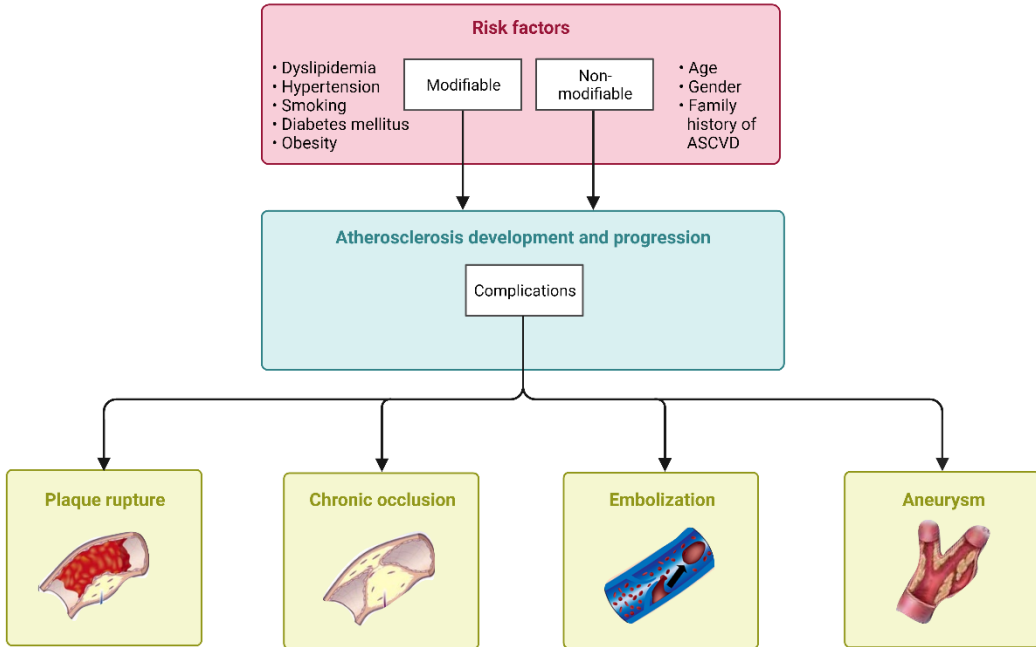


Figure 2-1. Risk factors and complications of atherosclerosis. ASCVD: Atherosclerotic cardiovascular disease.

Adapted from: Yelle D. Atherosclerosis. *McMasters Pathophysiology Review.* 2018. <http://www.pathophys.org/atherosclerosis>. *Created with:* BioRender.com.

2.1.1.2 Risk factors and cardiovascular disease risk classification

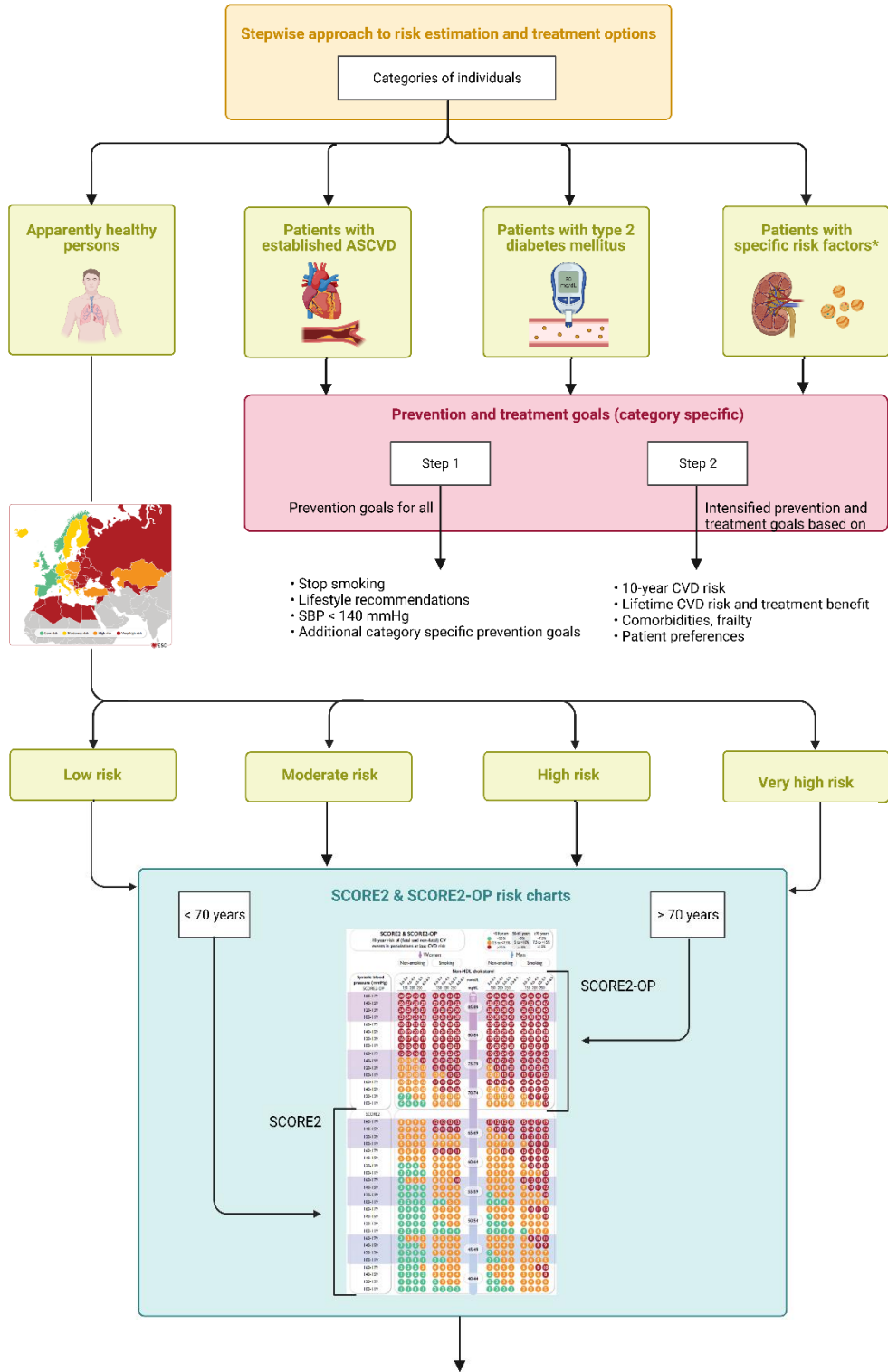
(a) Modifiable and non-modifiable cardiovascular risk factors

Epidemiological studies have identified a large number of risk factors for ASCVD. Some risk factors are genetically determined or non-modifiable (e.g. family history of ASCVD, age, sex), while others are environmental and thus modifiable by means of lifestyle changes and drug therapy (e.g. hyperlipidemia, hypertension, diabetes mellitus, obesity, smoking, physical inactivity, high alcohol use) (Figure 2-1). Important, exposure to risk factors has a cumulative effect throughout life [210,211].

(b) Cardiovascular disease risk classification – Systemic Coronary Risk Estimation (SCORE) algorithm

Subclinical atherosclerosis can start in childhood, and lifetime exposure to risk factors (see supra) augments CVD risk cumulatively [210]. Therefore, identifying patients who will benefit most from ASCVD risk factor treatment is central to ASCVD prevention efforts [211]. In Europe, the European Society of Cardiology (ESC) has developed an algorithm – the Systemic Coronary Risk Estimation (SCORE2) – to estimate a person’s 10-year risk of fatal and non-fatal CVD events (myocardial infarction, stroke). Depending on the presence of certain comorbidities and the medical history of the individual, as well as the country in which this person resides and his/her age, a certain SCORE table applies (Figure 2-2 and Figure 2-3). Within the appropriate SCORE table, this individual’s 10-year risk of fatal and non-fatal CVD events can be estimated by finding the cell nearest to the person’s sex, smoking status, blood pressure and non-high-density lipoprotein cholesterol (non-HDL-C). Of note, the most recent ESC guidelines recommend using non-HDL-C (calculated by subtracting high-density lipoprotein cholesterol [HDL-C] from total cholesterol [TC]) to estimate CVD risk rather than LDL-C. This is since non-HDL-C has the advantage that it does not require the triglyceride (TG) concentration to be < 400 mg/dL and it is more accurate in non-fasting setting and in patients with diabetes mellitus [211].

Based on the estimation of an individual’s lifetime CVD risk, the lifetime benefit from preventive interventions such as smoking cessation, lipid-lowering and blood pressure treatment can be estimated and decisions concerning initiating and intensifying risk factor treatment can be made [211]. For individuals with documented CVD or other high-risk conditions such as diabetes mellitus, familial hypercholesterolemia, or other genetic rare lipid or blood pressure disorders, and in pregnant women, the SCORE2 risk charts do not apply. ESC guidelines with category-specific treatment targets and prevention goals for LDL-C, blood pressure and/or glycemic control are available for these groups [211]. In the remainder of this thesis, the focus will be on lipids as a cardiovascular risk factor and lipid-lowering treatment.



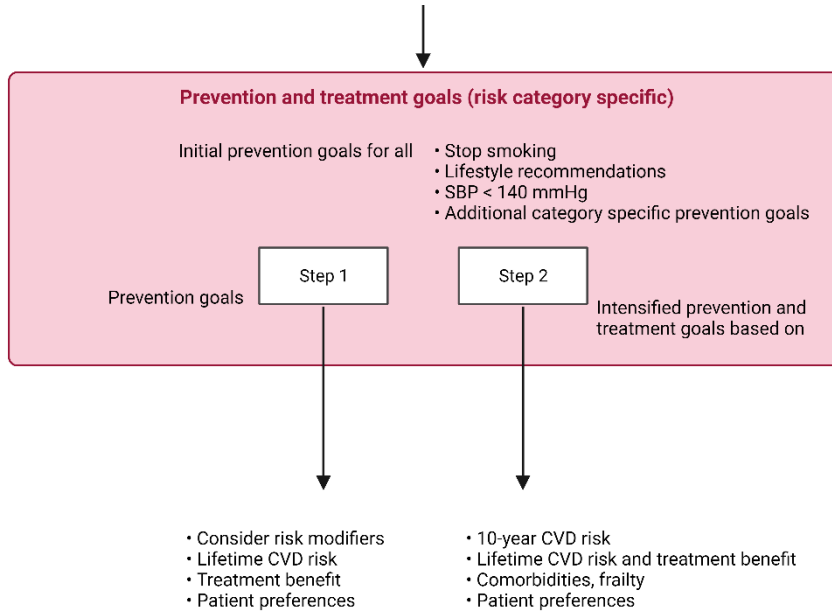


Figure 2-2. Flowchart of the stepwise approach to risk estimation and treatment options for different categories of individuals according to the ESC Guidelines on cardiovascular disease prevention in clinical practice. *Chronic kidney disease or familial hypercholesterolemia. ASCVD: Atherosclerotic cardiovascular disease; CVD: cardiovascular disease; ESC: European Society of Cardiology; SCORE2: Systemic Coronary Risk Estimation 2; SCORE2-OP: SCORE2-Older Persons; SBP: systolic blood pressure.

Adapted from: Visseren et al. 2021 ESC Guidelines on cardiovascular disease prevention in clinical practice. European Heart Journal (2021) 42, 3227-3337. Created with: BioRender.com.

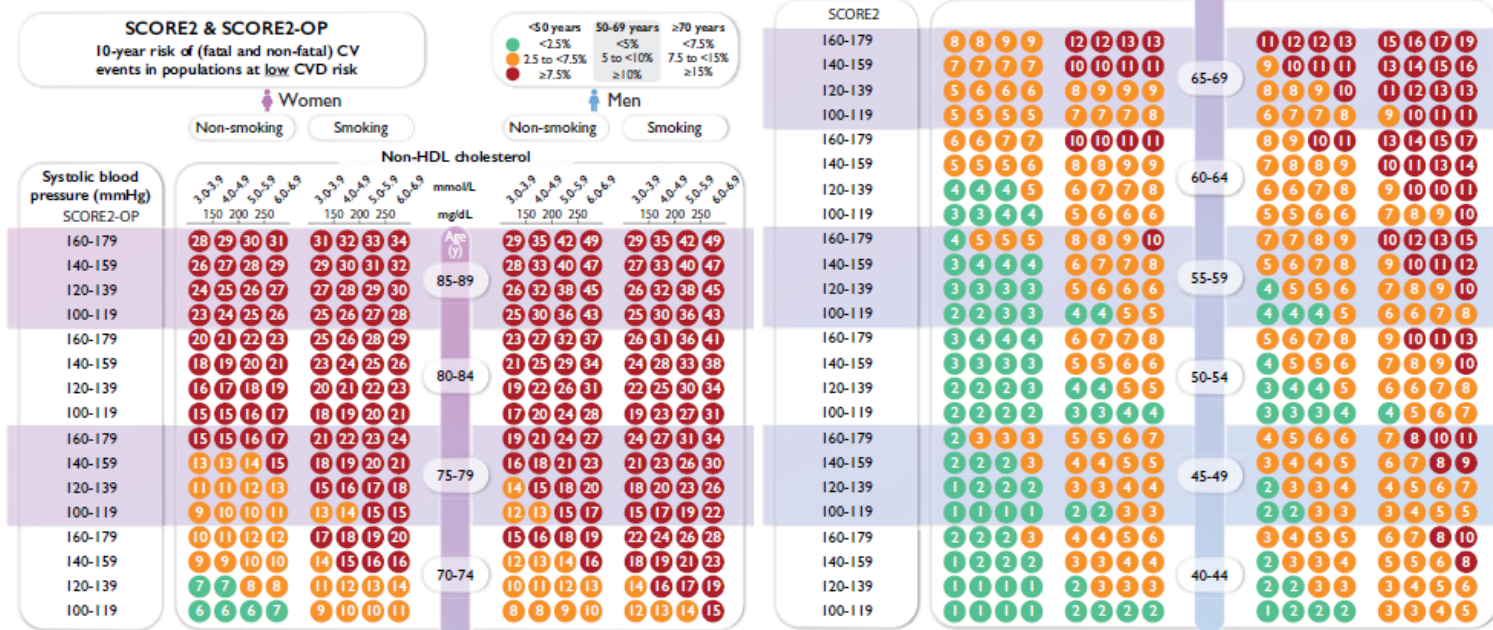


Figure 2-3. Example of a Systemic Coronary Risk Estimation 2 (SCORE2; right) and Systemic Coronary Risk Estimation 2-Older Persons (SCORE2-OP; left) risk charts for fatal and non-fatal (myocardial infarction, stroke) cardiovascular disease. CVD: cardiovascular disease; HDL-C: high-density lipoprotein cholesterol.

Adapted from: Visseren *et al.* 2021 ESC Guidelines on cardiovascular disease prevention in clinical practice. European Heart Journal (2021) 42, 3227-3337. *Created with:* BioRender.com.

2.1.2 Risk factors and interventions at the individual level: focus on lipids and statin therapy

Lipid abnormalities play a critical role in the development of atherosclerosis [214,215]. The exposure of an artery to high levels of LDL-C over the years and retention of LDL-C within the arterial wall remain the key events of atherosclerosis initiation and progression [210,211,214]. The causal role of LDL particles in the development of ASCVD is demonstrated beyond any doubt. Moreover, the results of a large number of clinical trials indicated that the relative reduction in CVD risk is proportional to the absolute reduction of LDL-C and lower levels of LDL-C achieved are associated with better clinical outcomes, with no evidence of a lower limit for LDL-C values [211,214]. The absolute benefit of lowering LDL-C depends on the absolute risk of ASCVD and the absolute reduction in LDL-C, so even a small absolute reduction in LDL-C may translate to significant absolute risk reduction in a high- or very-high-risk patient [211]. Furthermore, the HDL-C concentration is also of importance given its inverse relationship with the risk of atherosclerotic events [210,211]. Yet, clinical studies do not support a protective role for HDL-C against ASCVD event reduction from increasing HDL-C has not been established [210,211]. Thus, HDL-C may serve as a biomarker of risk, but today no evidence shows that HDL-C is a modifiable risk factor.

2.1.2.1 Low-density lipoprotein cholesterol goals

For LDL-C, the desired plasma concentration is different depending on the patient's comorbidities and medical history, as well as his/her estimated 10-year risk of fatal and non-fatal CVD events. LDL-C goals as proposed in the ESC 2021 Guidelines on CVD prevention in clinical practice are summarized in Table 2-1 [211].

2.1.2.2 Strategies to lower low-density lipoprotein cholesterol

Restoring (or improving) abnormal LDL-C levels contributes to slowing the formation and progression of atherosclerotic plaques. It also limits the consequences that

atherosclerosis can cause [216]. Thus, treating hyperlipidemia reduces cardiovascular morbidity, but above all it also has a beneficial effect on cardiovascular mortality [217].

Table 2-1. Low-density lipoprotein cholesterol goals.

Apparently healthy persons	
<i>Step 1</i>	50 – 69 year: LDL-C <100 mg/dL ≥ 70 year: LDL-C <100 mg/dL
<i>Step 2</i>	High-risk: < 70 mg/dL and ≥ 50% reduction Very-high-risk: < 55 mg/dL and ≥ 50% reduction
Patients with chronic kidney disease, familial hypercholesterolemia or type 2 diabetes mellitus*	
<i>Step 1</i>	LDL-C <100 mg/dL and ≥ 50% LDL-C reduction
<i>Step 2</i>	High-risk: < 70 mg/dL Very-high-risk: < 55 mg/dL
Patients with established atherosclerotic cardiovascular disease and/or type 2 diabetes mellitus patients with severe target organ damage	
<i>Step 1</i>	LDL-C <100 mg/dL and ≥ 50% LDL-C reduction
<i>Step 2</i>	< 55 mg/dL

Low-density lipoprotein cholesterol (LDL-C) goals follow a stepwise approach: in step 1 prevention goals are initiated, whereafter prevention and treatment goals are intensified in step 2. The stepwise approach has to be applied as a whole: after step1, considering proceeding to the intensified goals of step 2 is mandatory.

A first and important step in the treatment of hyperlipidemia is the implementation of lifestyle changes (healthier diet, weight loss, smoking cessation, more exercise...). However, this is not always enough to lower LDL-C levels sufficiently and when this is the case, different groups of drugs can be used (Figure 2-4) [218,219].

(a) Statins

Statins are the most prescribed cholesterol-lowering treatment [213,220,221]. By inhibiting the 3-hydroxy-3-methylglutaryl-coenzyme A (HMG-CoA) reductase enzyme, statins decrease cholesterol synthesis in the liver and stimulate upregulation of LDL-receptors on hepatocytes (Figure 2-4) [211]. As a result, the intracellular cholesterol

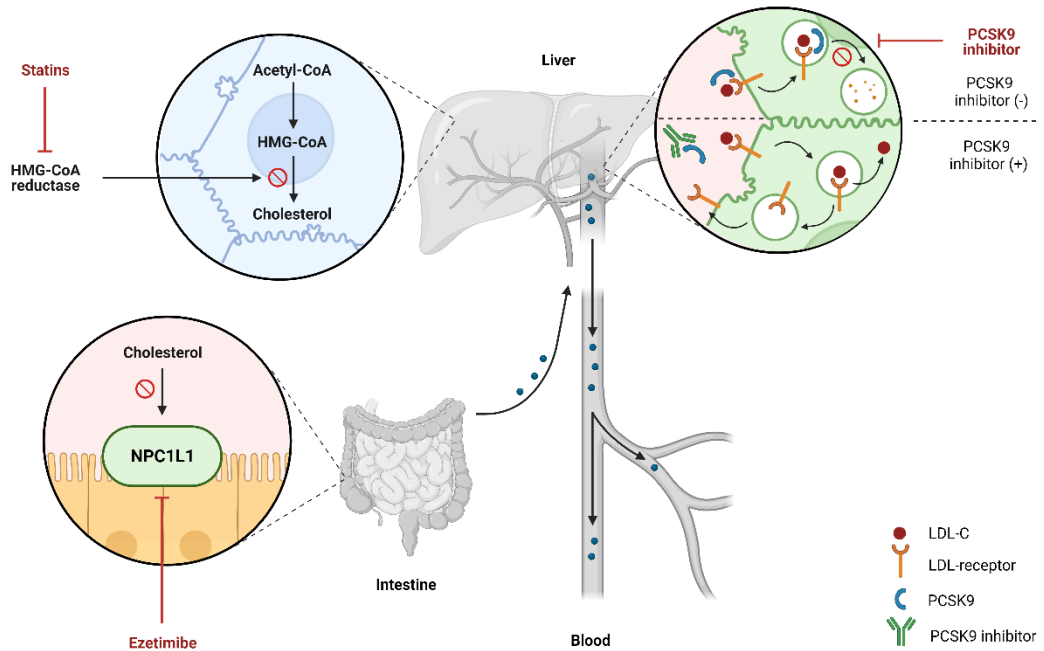


Figure 2-4. Pharmacologic approaches to lower low-density lipoprotein cholesterol (LDL-C). Statins inhibit the rate-limiting enzyme of cholesterol biosynthesis, HMG-CoA reductase, leading to decreased hepatic cholesterol production. Ezetimibe is an inhibitor of NPC1L1 which facilitates absorption of intestinal cholesterol and therefore selectively decreases dietary cholesterol uptake and hepatic cholesterol supply. The inhibition of cholesterol synthesis or intestinal absorption both lead to an upregulation of the LDL-receptor and subsequently, enhance LDL uptake and lower LDL-C serum concentrations. Therapeutic inhibition of PCSK9 also leads to a higher density of LDL receptors on the hepatocyte surface, not primarily through targeting cholesterol metabolism, but by affecting LDL receptor degradation and recycling pathways. Acetyl-CoA: acetyl-coenzyme A; HMG-CoA: 3-hydroxy-3-methylglutaryl-coenzyme A; LDL: low-density lipoprotein; PCSK9: proprotein convertase subtilisin/kexin type 9; NPC1L1: Niemann-Pick C1-like protein 1.

Adapted from: Ahn CH, Choi SH. *Diabetes Metab J.* 2015; 39(2):87-94 and Katzmann JL, Gouni-Berthold I, Laufs U. PCSK9 Inhibition: Insights From Clinical Trials and Future Prospects. *Front. Physiol.* 2020; 16(11):595819. *Created with:* BioRender.com.

concentration is reduced which leads to increased absorption of LDL-C from the blood into the liver and therefore decreases circulating LDL-C concentrations [211,219,221]. Moreover, statins exert various pleiotropic effects (including improving endothelial dysfunction and plaque stability, antithrombotic properties and reducing vascular

inflammation) that are independent of their lipid-lowering properties and associated with improved outcomes [222].

In Belgium, four different statins (atorvastatin, simvastatin, rosuvastatin and pravastatin) are available [213]. Atorvastatin and simvastatin are the most commonly prescribed with respectively over 570 000 and 520 000 users in 2019-2020 [223,224]. The extent to which a statin lowers LDL-C is dependent on its potency and dosing (Table 2-2) [225].

Table 2-2. Pharmacokinetic properties and lipid-lowering effect of statins marketed in Belgium in 2022.

	Atorvastatin	Simvastatin	Rosuvastatin	Pravastatin
Pharmacokinetic properties				
Prodrug	No	Yes	No	No
Half-life (hours)	14	3	29	1.3 – 2.7
Solubility	Lipophilic	Lipophilic	Hydrophilic	Hydrophilic
CYP substrate	CYP3A4	CYP3A4	CYP2C9	-
Bioavailability (%)	12	< 5	20	17
Renal excretion (%)	2	13	10	20
% Low-density lipoprotein cholesterol reduction				
27% ↓	-	10 mg	-	20 mg
34% ↓	10 mg	20 mg	-	40 mg
41% ↓	20mg	40 mg	-	80 mg
48% ↓	40 mg	80 mg	10 mg	-
54% ↓	80 mg	-	20 mg	-
60% ↓	-	-	40 mg	-

Adapted from: Van Matre ET, Sherman DS, Kiser TH. Management of intracerebral hemorrhage-use of statins. *Vasc Health Risk Manag.* 2016;12:153-61.

Besides the difference in magnitude of the LDL-C lowering effects, pleiotropic effects may differ from one statin to another as well as pharmacokinetic properties (Table 2-2) [225,226]. Adverse events have been associated with statin treatment. Muscle toxicity and effects on liver enzymes are well-acknowledged; the risk however is low. The risk of

myopathy can be minimized by identifying vulnerable patients and/or by avoiding statin interactions with specific drugs. Rhabdomyolysis, a severe form of muscle toxicity involving muscle breakdown which can cause renal failure and can be fatal, is extremely rare. Increased blood sugar and glycated hemoglobin A1c (HbA1c) levels (i.e. increased risk of type 2 diabetes mellitus [T2DM]) can also occur after treatment initiation and are dose-dependent, but the benefits of statins outweigh the risks for the majority of patients [211].

(b) Other low-density lipoprotein cholesterol-lowering therapies

(i) Cholesterol absorption inhibitors (ezetimibe)

Ezetimibe inhibits cholesterol absorption from the intestine by blocking the transport protein Niemann-Pick C1-like 1 (NPC1L1) in the brush border of enterocytes, without affecting the absorption of fat-soluble vitamins, TG or bile acids. Thereby it also indirectly augments the expression of liver LDL-receptors [211,221,227]. Studies showed that, when combining a statin with ezetimibe, an additional reduction in LDL-C of 15–20% can be achieved. In the treatment of hyperlipidemia, ezetimibe should be considered a second-line therapy, either on top of statins in patients who do not meet cholesterol goals on statin therapy alone or when a statin cannot be prescribed [211,227].

(ii) Proprotein convertase subtilisin/kexin type 9 inhibitors (PCSK9 inhibitors)

Proprotein convertase subtilisin/kexin type 9 (PCSK9) inhibitors are a new class of lipid-modulating agents and are currently reserved only for patients who are unable to reach treatment targets with maximum tolerable treatment with statins and other agents, but still have a very high risk of CVD and for patients with familial hypercholesterolemia (FH) [228,229]. These PCSK9 monoclonal antibodies lower LDL-C by binding to free plasma PCSK9, a liver-produced serine protease. In normal circumstances, PCSK9 binds to the LDL-receptor on the surface of hepatocytes, leading to the degradation of the LDL-receptor and subsequently to higher plasma LDL-C levels. By binding to PCSK9, PCSK9

antibodies promote the degradation of the enzyme and interfere with the binding of PCSK9 to the LDL-receptor. As a result, less free PCSK9 is available in plasma to bind to the LDL-receptor. This results in a higher fraction of LDL-receptor recycling towards the hepatocyte surface. As a direct consequence, the liver has the capacity to remove more LDL-C from the circulation, resulting in lower LDL-C plasma levels [211,230].

A very recent alternative to monoclonal antibodies for PCSK9 lowering are the PCSK9-small interfering RNA molecules (siRNA). These molecules interfere with PCSK9 by blocking its synthesis and offer a profound lowering of PCSK9 at a lower-dose frequency [231,232].

2.1.3 Plasma proCPU concentration and proCPU polymorphisms as risk factors?

Over the years, impaired fibrinolysis has gained attention as a predictor of increased cardiovascular risk [203,233,234]. Given the prominent bridging function of CPU in hemostasis, the question was raised whether increased plasma proCPU concentrations could be regarded as a risk factor for thromboembolic diseases. When a stimulus is present, the formation of CPU from its precursor proCPU will be directly proportional to the proCPU concentration [15,63,64]. In other words, we can hypothesize that a high proCPU concentration might tip the hemostatic balance to antifibrinolytic pathways, causing a predisposition towards a thrombotic tendency [63]. Furthermore, previous research has shown that SNPs in the *CPB2* gene contribute to plasma proCPU concentrations (see also 1.3.2), leading to the hypothesis that some of these proCPU variants might also contribute to a higher risk for thromboembolic diseases. Consequently, numerous studies aimed at evaluating the association between proCPU levels and thromboembolic diseases and investigating the role of *CPB2* SNPs as a risk factor. Concerning the latter, the focus here will be on the +1040C/T polymorphism (corresponding to a Thr to Ile substitution at position 325; Thr325Ile) as a potential cardiovascular risk factor.

2.1.3.1 Venous thrombosis

Studies investigating possible alterations of plasma proCPU levels in different venous thromboembolic diseases (VTE), including deep vein thrombosis (DVT) and pulmonary embolism (PE), are summarized in Table 2-3 [30,151,182,235,236]. Overall, these studies indicate that high plasma proCPU levels are associated with VTE and can be considered a mild risk factor (reviewed in [234] and [15]). However, as for the association between the Thr325Ile polymorphism and venous thrombosis risk, results have been inconclusive with some studies failing to detect any association and others that found clear correlations. Qian and co-workers performed a meta-analysis on 13 original studies and showed clear evidence that the +1040C/T polymorphism was associated with an increased risk of VTE (cerebral venous thrombosis [CVT], DVT, or PE) [237]. Considering some case-control studies were omitted while others were incorrectly included, a similar meta-analysis was carried out by Wang *et al.* taking into account these limitations. In line with the results of Qian *et al.*, the risk to develop venous thrombosis was significantly lower in carriers of the TT (Ile/Ile) genotype of the +1040C/T polymorphism compared to those with the C allele (CC [Thr/Thr] or CT [Thre/Ile] genotype). Subgroup analysis conducted based on ethnicity revealed similar results in different ethnic groups [238]. In accordance, the meta-analysis of Zwingerman and colleagues showed a decreased risk of VTE for the TT (Ile/Ile) genotype versus the CT (Thr/Ile) + CC (Thr/Thr) genotype in both the overall and European study population, although not significant in the overall study population [239].

In conclusion, there is a rationale that high proCPU levels carry a mild risk factor for the development of venous thrombosis. However, there is still a great need for more prospective studies examining the association between the Thr325Ile polymorphism and the risk for VTE before a more explicit conclusion can be drawn.

Table 2-3. Studies investigating the role of proCPU plasma concentrations and *CPB2* gene polymorphisms as risk factors for thromboembolic diseases.

Venous thrombosis		
Arauz <i>et al.</i> 2018 [240]	No risk association in CVT cases (N = 113) relative to controls (N = 131) for the +1040C/T polymorphism or in haplotype analysis of the <i>CPB2</i> gene.	PCR
Orikaza <i>et al.</i> 2014 [241]	The +1040C/T polymorphism significantly increased the risk of CVT (N = 72) compared to VTE cases (N = 128) and controls (N = 134).	PCR
Tokgoz <i>et al.</i> 2013 [242]	In 59 patients with CVT and 100 healthy control subjects, the association between the +1040C/T polymorphism and CVT was investigated. Frequencies of polymorphic genotype and allele were similar in patients and controls and were not significant for CVT.	PCR
Meltzer <i>et al.</i> 2010 [151]	In a study involving 770 patients from the MEGA study (first DVT of the leg or first PE) and 743 controls, high proCPU levels were shown to be an independent risk factor for VTE.	Activity assay (Pentapharm)
Meltzer <i>et al.</i> 2010 [235]	The +1040C/T polymorphism was associated with both proCPU levels and increased risk for recurrent VTE in 474 patients diagnosed with first DVT.	PCR + In-house developed activity assay [30]
Verdu <i>et al.</i> 2008 [181]	It was found that the Thr/Thr genotype of the Thr325Ile polymorphism was associated with an increased risk of VTE.	PCR + ELISA (Diagnostica Stago)
Folkeringa <i>et al.</i> 2008 [153]	In a large cohort of thrombophilic families, no correlation was observed between high proCPU levels and the risk of venous or arterial thromboembolism.	Activity assay (Pentapharm)
Verdu <i>et al.</i> 2006 [243]	High proCPU levels (> 90th percentile of the controls) increased the risk for future DVT 4-fold compared to patients with lower proCPU levels. 60 patients with previous DVT or PE and 62 controls were included in the study.	ELISA (Diagnostica Stago)
Martini <i>et al.</i> 2006 [165]	Thr325Ile polymorphism is associated with proCPU antigen levels in 471 patients with first DVT, but there was no association with increased risk for DVT.	PCR + In-house developed activity assay [30]
Zee <i>et al.</i> 2005 [244]	No evidence was provided for an association between six polymorphisms, including the +1040C/T polymorphism, in the <i>CPB2</i> gene and the risk for VTE.	PCR

Eichinger <i>et al.</i> 2004 [182]	Higher proCPU levels in patients with a previous first spontaneous VTE were associated with an almost 2-fold higher risk for VTE recurrence compared to patients with lower proCPU levels (N = 600 total study population).	ELISA (American Diagnostica)
Libourel <i>et al.</i> 2002 [236]	Symptomatic Factor V Leiden carriers (N = 17) had higher proCPU levels compared to asymptomatic carriers (N = 136). High levels of proCPU are a mild risk factor for VTE.	In-house developed activity assay [136]
Franco <i>et al.</i> 2001 [135]	A tendency towards protection against DVT was observed for several <i>CPB2</i> gene polymorphisms, that paralleled the lower proCPU levels detected in carriers of these polymorphisms (N = 388) compared to controls (N = 388).	PCR + In-house developed ELISA [37]
Van Tilburg <i>et al.</i> 2000 [30]	ProCPU levels were similar in patients with a first episode of DVT (N = 474) compared to controls (N = 474). Although, there were more DVT patients than controls with high proCPU levels and high proCPU levels were associated with an increased risk for thrombosis.	In-house developed activity assay [30]
Arterial thrombosis and coronary artery disease		
Isordia-Salas <i>et al.</i> 2019 [245]	Thr325Ile polymorphism in the <i>CPB2</i> gene was associated with an increased risk for STEMI (N = 244), but not for IIS (N = 250). Genotype and allele distribution were similar in IIS patients and controls (N = 244).	PCR
Rattanawan <i>et al.</i> 2018 [246]	The +1040C/T polymorphism was not associated with the severity of coronary artery stenosis.	PCR
Khalifa <i>et al.</i> 2012 [198]	ProCPU levels were not correlated with the pre-disposition of in-stent restenosis following coronary stenting in 37 patients with CAD.	CPU+CPUi ELISA (American Diagnostica)
Jood <i>et al.</i> 2012 [166]	No association between intact proCPU antigen and survival rate, nor reoccurrence of vascular events (recurrent stroke, transient ischemic attack or coronary event; N = 37) in ischemic stroke survivors (N = 517). Blood was collected 3 months after the index event. Two years after inclusion the survival rates and vascular events were assessed.	In-house developed ELISA [120]

De Bruijne <i>et al.</i> 2011 [164]	Increased levels of intact proCPU antigen are associated with an increased risk of premature peripheral arterial disease. Functional proCPU was not significantly higher in patients (N = 47) compared to controls (N = 141). Blood samples were collected 1–3 months after the event.	In-house developed ELISA [120] + In-house developed activity assay [247]
Kamal <i>et al.</i> 2011 [248]	Homozygous and heterozygous carriers of Ile ³²⁵ were more frequent in patients with AMI (N = 46) than in controls (N = 54).	PCR
Kozian <i>et al.</i> 2010 [25]	Homozygosity for the Ile ³²⁵ allele of the Thr325Ile polymorphism was associated with the incidence of stroke and the age at onset of first stroke (N = 3300).	PCR
Tassies <i>et al.</i> 2009 [24]	ProCPU polymorphism Thr325Ile is related to the type of acute coronary syndrome (N = 248; total cohort). Homozygous Ile ³²⁵ genotypes are less prevalent in patients with STEMI compared to NSTEMI patients.	ELISA (Diagnostica Stago) + Activity assay (American Diagnostica)
De Bruijne <i>et al.</i> 2009 [163]	In young patients with arterial thrombosis (N = 327), the distribution of the Thr325Ile SNP was compared to healthy controls (N = 332). In homozygous carriers of the Ile ³²⁵ allele lower proCPU levels were observed together with a decreased risk of arterial thrombosis compared to homozygous carriers of the Thr ³²⁵ allele. In the same population total proCPU levels and proCPU activity levels did not differ from controls. Blood samples were collected 1–3 months after the event.	In-house developed ELISA [120] + In-house developed activity assay [247]
Tregouet <i>et al.</i> 2009 [183]	In a prospective study on patients with angiographically proven coronary artery disease none of the selected CPB2 gene polymorphisms, including Thr325Ile, was associated with the occurrence of cardiovascular events (N = 1668). In the same study, the total proCPU antigen was associated with an increased risk of future cardiovascular death.	PCR + ELISA (Diagnostica Stago)
Meltzer <i>et al.</i> 2009 [152]	The +1040C/T SNP was not associated with myocardial infarction in men (N = 554) versus controls (N = 643). Also, patients with proCPU levels in the first quartile (lowest levels) display an increased risk of a first myocardial infarction compared to patients with proCPU levels in the fourth quartile. The time between blood sampling after the infarct ranged from 88 days to 5.8 years with a median of 2.6 years.	PCR + Activity assay (Pentapharm)

Biswas <i>et al.</i> 2008 [184]	No association was detected between 16 SNPs (of which the Thr325Ile polymorphism was one) and the risk of cardio-embolic stroke (N = 120). Also, significantly higher proCPU antigen levels were observed in patients with acute onset non-cardioembolic stroke (N = 120) compared to normal individuals (N = 120). Blood samples were collected within 10 days of the stroke and at 3-month follow-up.	ELISA (Diagnostica Stago)
Ladenvall <i>et al.</i> 2007 [167]	No association was detected between 11 SNPs (including Thr325Ile SNP) and overall ischemic stroke risk (N = 600). In addition, increased levels of intact proCPU are found in ischemic stroke patients compared to controls (N = 600). An independent association was found with large vessel disease, cryptogenic stroke and acute-phase small vessel disease subtypes. Increased proCPU levels do not reflect an acute phase response. Blood sampling was conducted within 10 days of the stroke and at 3-month follow-up.	PCR + In-house developed ELISA [120]
Fernandez-Cadenas <i>et al.</i> 2007 [249]	Ile/Ile homozygosity for the Thr325Ile polymorphism was associated with lower rates of recanalization after rtPA infusion in ischemic stroke patients (N = 139).	PCR
Cruden <i>et al.</i> 2006 [144]	Plasma proCPU does not predict reperfusion in patients receiving thrombolytic therapy for acute STEMI (N = 110). Blood was collected prior to administration of thrombolytic therapy.	ELISA (Hyphen Biomed) + Activity assay (American Diagnostica)
Schroeder <i>et al.</i> 2006 [154]	Re-evaluation of the study in 2002 which was compromised by genotype-dependent artifacts. Significant associations between proCPU activity and cardiovascular risk factors as well as with coronary artery disease were found. ProCPU activity was higher in coronary artery disease patients (N = 338) than in controls (N = 158). Blood samples were collected during angiography.	Activity assay (Pentapharm)
Morange <i>et al.</i> 2005 [185]	No clear relation between coronary heart disease and six proCPU gene polymorphism was found (including Thr325Ile). A total of 248 cases and 493 controls were used. And no significant association between proCPU levels and angina pectoris or hard coronary events was present after re-analysis of the PRIME data with an ELISA which was shown to be insensitive to proCPU genotype.	PCR + ELISA (Diagnostica Stago)

Leebeek <i>et al.</i> 2005 [250]	The proCPU genotype does not seem to predict the risk of ischemic stroke. No difference was found between patients (N = 124) and controls (N = 125) with respect to the distribution of the +1040C/T polymorphism. Also, increased proCPU levels, resulting in decreased fibrinolysis, are associated with an increased risk of first ischemic stroke (ischemic stroke N = 124 vs. controls N = 125). As demonstrated by the persisting elevated proCPU levels three months after the stroke, the increase in functional proCPU levels is not caused by an acute phase reaction. Blood collection between 7 and 14 days after the stroke, second blood collection in a subgroup (N = 36) three months after the stroke.	PCR + In-house developed functional TAFI clot lysis assay [247]
Lisowski <i>et al.</i> 2005 [146]	ProCPU levels were significantly higher 7 days after elective CABG in 45 stable angina pectoris patients with confirmed CAD compared to controls (N = 33).	ELISA (Affinity Biologicals) + Activity assay (American Diagnostica)
Kim <i>et al.</i> 2005 [189]	No difference was seen in proCPU levels in acute ischemic stroke patients with (N = 30) or without successful recanalization (N = 13). Blood samples were collected on admission.	ELISA (Hyphen Biomed)
Santamaria <i>et al.</i> 2004 [251]	ProCPU levels tended to be higher in patients with acute CAD (N = 174) than in controls (N = 211). Blood samples were collected at least six months after the acute episode.	In-house developed activity assay [37]
Segev <i>et al.</i> 2004 [177]	It was shown that the proCPU antigen level is strongly determined by the Thr325Ile polymorphism in patients with stable angina pectoris (N = 159). The T/T genotype was the least prevalent and associated with the lowest proCPU levels and the lowest rate of angiographic restenosis in this population.	PCR + ELISA (American Diagnostica)
Akatsu <i>et al.</i> 2004 [252]	In 253 patients with confirmed neuropathology that died during hospitalization, no statistical correlation between the Thr325Ile polymorphisms and risk for cerebral infarction was found.	PCR
Morange <i>et al.</i> 2003 [188] <i>Re-evaluated in 2005</i>	In France, proCPU levels were significantly higher in men who subsequently developed angina pectoris (N = 81) than in their controls (N = 81), whereas no difference was observed between cases (N = 62) and controls (N = 124) in Northern Ireland.	PCR + ELISA (Hyphen Biomed)

Brouwers <i>et al.</i> 2003 [170]	No significant association between the Thr325Ile polymorphism was found in non-refractory patients (N = 133) compared to refractory patients (N = 76) with unstable angina pectoris. Higher proCPU levels in patients with non-refractory unstable angina pectoris (N = 133) than in refractory patients (N = 76). Blood samples were obtained on admission.	PCR + ELISA (Affinity Biologicals)
Zorio <i>et al.</i> 2003 [145]	No difference according to the Thr325Ile polymorphism between young patients with myocardial infarction (N = 127) and controls (N = 99). Patients had higher plasma proCPU activity levels, but lower proCPU antigen in comparison to controls. Blood sample was collected at least 3 months after the myocardial infarction.	PCR + ELISA (Chromogenix) + Activity assay (American Diagnostica)
Lau <i>et al.</i> 2003 [176]	Higher preprocedural proCPU plasma levels in patients with restenosis. ProCPU plasma levels correlated with 6-month % diameter stenosis after percutaneous coronary intervention (N = 159).	ELISA (American Diagnostica)
Juhan-Vague <i>et al.</i> 2003 [172]	No difference in proCPU plasma concentration in men who subsequently suffered from myocardial infarction or coronary death (N = 159) when compared with their controls (N = 317). Prospective study.	ELISA (Milan Analytica)
Santamaria <i>et al.</i> 2003 [134]	Higher proCPU plasma levels in ischemic stroke patients (N = 114) than in healthy controls (N = 150). Blood samples were collected at least one month after the acute thrombotic episode	In-house developed activity assay [37]
Juhan-Vague <i>et al.</i> 2002 [173]	Patients who suffered from AMI (N = 598) showed lower plasma proCPU antigen values versus controls (N = 653). Blood samples were collected 3–5 months after myocardial infarction.	PCR + ELISA (Milan Analytica)
Morange <i>et al.</i> 2002 [253]	The Thr325Ile polymorphism does not influence the risk of MI in white male patients younger than 60 years who survived a first MI (N = 533) and male controls of the same age (N = 575).	PCR
Schroeder <i>et al.</i> 2002 [171] <i>Re-evaluated in 2006</i>	Higher proCPU antigen levels in coronary artery disease patients (N = 362) compared to controls with angiographically verified normal coronary vessels (N = 134). The difference was more prominent in intracoronary than in venous blood samples. Blood samples were collected during angiography.	ELISA (Milan Analytica)

Silveira <i>et al.</i> 2000 [137]	Higher proCPU plasma concentration in men requiring coronary artery bypass grafting because of stable angina pectoris (N = 110) than in controls (N = 56). Blood samples were collected preoperatively.	In-house developed activity assay [136]
--------------------------------------	---	---

Table based upon earlier overviews published by Leurs *et al.* [254] and Heylen *et al.* [124], complemented with additional and new reports. Meta-analyses were not included, but are discussed in paragraphs 2.1.3.1 and 2.1.3.2. AMI: acute myocardial infarction; CAD: coronary artery disease; CVT: cerebral venous thrombosis; DVT: deep vein thrombosis; ELISA: enzyme-linked immunosorbent assay; IIS: idiopathic ischemic stroke; NSTEMI: non-ST-elevation myocardial infarction; PCR: polymerase chain reaction; proCPU: procarboxypeptidase U (TAFI, proCPB2); rtPA: recombinant tissue-type plasminogen activator; SNP: single nucleotide polymorphism; STEMI: ST-elevation myocardial infarction; VTE: venous thromboembolism.

2.1.3.2 Arterial thrombosis

In addition to studies investigating the role of proCPU in VTE, even more studies were published on the association between proCPU concentrations or genotype and arterial thrombosis. Table 2-3 is based upon earlier overviews published by Leurs *et al.* and Heylen *et al.*, complemented with additional and new reports, and provides an overview of studies investigating proCPU in arterial thrombosis [41,254]. New reports include the 10-year follow-up of the SAHLSIS study. In the first SAHLSIS follow-up by Jood *et al.* in 2012, levels of CPU activation peptide measured in 517 ischemic stroke survivors three months after the index event predicted future death and reoccurrence of vascular events (recurrent stroke, transient ischemic attack or coronary event; N = 37) in the first two years [166]. However, at 10-year follow-up, this association could not be confirmed [201]. Furthermore, proCPU antigen levels were not a predictor of future death or reoccurrence of vascular events in any of the SAHLSIS follow-up studies [166,201]. De Bruijne *et al.* described an association between proCPU antigen levels and an increased risk of premature peripheral arterial disease [164].

In the last decade, some groups also looked into the association of the +1040C/T polymorphism with increased risk for arterial thrombosis. Rattanawan and co-workers selected a total of 327 patients that were scheduled for an elective coronary angiography and found that the +1040C/T polymorphism was not associated with more severe coronary stenosis [246]. Another study reported that the Thr325Ile polymorphism was associated with an increased risk for ST-elevation myocardial infarction (STEMI) but not for idiopathic ischemic stroke in young individuals [245]. A meta-analysis conducted by Shi and colleagues showed that the Thr325Ile variant had no significant influence on the susceptibility to CVD. Moreover, sub-analysis based on ethnicity did not show an association between the polymorphism and CVD as well. However, sub-analysis did reveal that TT (Ile/Ile) genotype carriers had a 25% higher risk of coronary heart disease than those with a CT (Thr/Ile) or CC (Thr/Thr) genotype [255]. In contrast, the results of the meta-analysis of Wang *et al.* supported the independent association of the +1040C/T

polymorphism with the extent and severity of cardiovascular and cerebrovascular diseases, especially among Asian populations and more for the development of cardiovascular, than cerebrovascular diseases [256]. However, it is of note that one of the included studies investigated the association between certain *CPB2* SNPs and CVT risk, whereas all other studies focused on arterial thrombosis or coronary artery disease.

Overall, several studies in which proCPU concentrations were measured before or ample time after the acute phase of arterial thrombosis, indicated that high proCPU levels are associated with a thrombotic tendency, whereas other prospective and retrospective studies were not able to demonstrate an association or even found that high proCPU levels are protective. As a result, data are inconclusive and no consensus was reached so far with regard to proCPU levels and arterial thrombosis. Nevertheless, it must be emphasized that alongside differences in population, risk factors, or definition of control groups, another reason for these discrepancies between results originates from the variety of proCPU assays that were used, which might provide different results depending on the assay type and properties. On the other hand, these conflicting data can also indicate that variations in the proCPU plasma concentration might simply be too small to be regarded as an important risk factor in arterial thrombosis. As a result, measurement of proCPU levels in non-acute settings might not be the most appropriate marker for the investigation of the contribution of the CPU pathway to the development and outcome of thrombotic events. Moreover, the contribution of the Thr325Ile polymorphism seems also limited with regard to the risk for arterial thrombosis.

2.1.3.3 Cardiovascular risk factors

Besides evaluating correlations of proCPU levels and genotypes with risk for thromboembolic diseases, there has also been interest in potential associations of proCPU levels with certain cardiovascular risk factors (hypertension, diabetes mellitus, smoking, hyperlipidemia) and whether proCPU levels could be affected by lifestyle modifications or certain pharmacological treatments.

(a) Hyperlipidemia

In a study by Puccetti and co-workers significantly higher proCPU levels were found in hypercholesterolemic patients, but not in patients with hypertriglyceridemia, isolated low HDL-C or mixed hyperlipoproteinemia compared to controls [138]. In accordance, Santamaria and colleagues described lower proCPU levels in non-hypercholesterolemic individuals, although only in women irrespective of their age [251]. Further, Aso *et al.* showed that LDL-C was an independent determinant of plasma proCPU levels in 105 patients with T2DM. In addition, subgroup analysis revealed significantly higher plasma proCPU levels in two subgroups: hypercholesterolemic diabetic patients with or without metabolic syndrome [202]. In another study, proCPU levels were reported to be significantly higher in dyslipidemic versus normolipidemic subjects [257]. Likewise, significantly higher proCPU levels were seen in 44 hypercholesterolemic patients compared to 40 controls. Treatment of these hypercholesterolemic patients with atorvastatin resulted in a significant decrease in proCPU levels [196]. Decreased proCPU levels were also observed in seven CAPD (continuous ambulatory peritoneal dialysis) patients after six months of simvastatin therapy, as well as in 35 hyperlipidemic patients treated with simvastatin for eight weeks and in another study in which 126 patients with previous VTE received rosuvastatin for 28 days [155,174,179]. In a population of kidney transplant patients, proCPU levels were higher in 12 hyperlipidemic kidney transplant patients than in the normolipidemic subgroup (N = 31). Three months of fluvastatin daily significantly decreased proCPU levels in the hyperlipidemic subpopulation [174]. Furthermore, it was reported that fenofibrate also reduced proCPU levels in patients with metabolic syndrome and dyslipidemia [180]. The effect of hyperlipidemia on proCPU biology was further explored in Chapter 4 of this thesis.

(b) Hypertension

In this regard, Malyszko *et al.* investigated the effect of hypertension on proCPU levels in a population of renal transplant patients with normal blood pressure or with unregulated blood pressure despite treatment with an angiotensin converting enzyme

(ACE)-inhibitor, beta-blocker or calcium channel blocker. They found that proCPU levels were elevated in the hypertensive cohort and correlated with diastolic blood pressure in these patients [147]. Higher proCPU levels in 58 hypertensive patients compared to 27 controls, were also reported by Ozkan and colleagues [178]. The administration of amlodipine in 31 of these hypertensive patients led to a significant decrease of 7% in proCPU levels after the first month of therapy compared to the initial value, whereas proCPU levels did not change in 27 patients receiving ramipril [178]. In addition, no significant change in proCPU levels was observed in 12 patients with uncontrolled hypertension under an adequate dose of an ACE inhibitor before and after the addition of an angiotensin-receptor blocker to their regimen [258]. Further, both proCPU antigen and activity levels were higher in hypertensive patients treated with enalapril compared to untreated and betaxolol-treated individuals [148].

(c) Diabetes mellitus

A third cardiovascular risk factor that has been studied with regard to its effect on plasma proCPU concentrations is diabetes mellitus. For this risk factor, plasma proCPU levels were reported to be comparable between type 1 diabetes mellitus (T1DM) patients and healthy subjects [149,156]. Likewise, Verkleij and coworkers found similar proCPU levels in T2DM patients compared to non-diabetic controls, whereas a tendency of increased plasma proCPU levels in T2DM patients was observed in other studies [48,161,186,187,196]. Additionally, Hori *et al.* found higher proCPU levels in obese versus non-obese T2DM patients, whereas Yano and coworkers observed in their population lower levels of plasma proCPU in T2DM patients without microalbuminuria compared to those with microalbuminuria [48,186]. Moreover, both Kitagawa *et al.* and Rigla *et al.* showed that plasma proCPU levels correlated with HbA1c levels in untreated T2DM patients [187,196]. In contrast, Verkleij and colleagues reported similar proCPU levels in both tightly (HbA1c < 6%) and poorly (HbA1c > 9%) regulated T2DM patients [160].

Altogether, the literature currently available designates high proCPU levels to appear together with hyperlipidemia, hypertension and hyperglycemia. Interestingly, several studies indicated that normalizing these parameters by pharmacological intervention reduced proCPU levels, whereas others – especially those that investigated the effect of antihypertensive treatment on circulating proCPU levels – presented opposing results.

2.1.4 Can proCPU, CPU or CPUi serve as diagnostic or prognostic biomarkers?

Throughout the years, research groups also investigated different forms of the *CPB2* gene product (proCPU, CPU and CPUi) in the acute phase of thromboembolic diseases, thereby aiming to elucidate the *in vivo* role of CPU and the value of different CPU forms (proCPU, CPU and CPUi) as potential diagnostic markers. These studies should be clearly distinguished from prospective and retrospective studies that review the contribution of the CPU pathway to the development and outcome of thrombotic events.

2.1.4.1 Venous thrombosis

To the best of our knowledge, the role of proCPU and CPU during the acute phase of VTE has only been studied once. In this study, Schroeder *et al.* measured proCPU antigen levels in 120 patients with suspected PE in blood collected one hour after admission at the hospital [175]. Results showed that proCPU levels were alike in both patients diagnosed with acute PE and those with suspected, yet excluded PE. Concomitant DVT in patients with acute PE did also not influence proCPU levels. However, there was a significant increase in proCPU levels in patients with the highest occlusion rates (95 – 100%) compared to those with non-massive PE, which correlated inversely with D-dimer levels. Although the presence of acute PE is not associated with an increase in proCPU antigen levels, the severity of PE might be [175]. The mechanism leading to higher proCPU levels in patients with high occlusion rates however remains unclear.

2.1.4.2 Arterial thrombosis

Montaner *et al.* and Rooth *et al.* found elevated proCPU antigen levels in ischemic stroke patients within the first 24 h after onset of the symptoms [169,190]. Ribo and co-workers measured proCPU plasma concentrations in patients with acute proximal middle cerebral artery occlusion (MCAO) on admission and before recombinant tPA (rtPA) administration. Results showed that proCPU levels did not differ between patients that recanalized after one hour of rtPA infusion (N = 25) and patients without recanalization (N = 19) [197]. In contrast, during therapeutic thrombolysis of patients with acute ischemic stroke (AIS), a 15 – 20% decrease in proCPU levels was found by Willemse *et al.*, along with a very significant increase of CPU activity in plasma of these patients after thrombolysis with rtPA (N = 4) [199]. In a follow-up study, Brouns *et al.* could not detect basal CPU activity of patients with AIS at admission (N = 12), but demonstrated that during thrombolytic therapy, the CPU activity increased and relatively high levels of CPU (4.5 – 10 U/L) were generated in the circulation. In addition, the extent of proCPU activation during thrombolytic therapy was inversely related to efficacy and safety [139]. The decrease in proCPU levels and corresponding CPU generation was observed in rtPA-treated patients in multiple studies, with larger proCPU consumption being associated with a poor outcome [143,150]. In non-thrombolysed patients, significant plasma proCPU activation (reflecting fibrinolytic activity and/or activation of the coagulation cascade) in the first 72 h after ischemic stroke onset was observed [141]. In the same study cohort, increased proCPU levels were measured in cerebrospinal fluid (CSF) of stroke patients [142]. More pronounced plasma proCPU consumption and increased proCPU levels in CSF have been associated with blood-barrier dysfunction, stroke progression and poor outcome [141,142]. Alessi *et al.* demonstrated that stroke patients at admission had higher CPU+CPUi levels compared to control subjects and that CPU+CPUi levels were associated with stroke severity in non-thrombolysed patients [143]. However, it was not reported whether precautions were taken during sample collection to avoid *ex vivo* proCPU activation in this study (Table 2-4) [143,199].

Table 2-4. Studies investigating the role of CPU and/or CPUi as diagnostic or prognostic biomarkers for thromboembolic diseases during the acute phase.

Arterial Thrombosis and Coronary Artery Disease (CAD)		
Mertens <i>et al.</i> 2021 [259]	<p>CPU activity and CPU+CPUi levels were measured in AIS patients with cerebral artery occlusion receiving rtPA (N = 20) or rtPa + EVT (N = 16) at admission and throughout the first 24 h. Additional <i>in situ</i> blood samples were collected in the rtPA + EVT cohort proximal from the thrombus. CPU activity and CPU+CPUi levels increased upon rtPA administration and reached peak values at the end of thrombolysis (1 h). High inter-individual variability was observed in both groups. CPU activity decreased rapidly within 3 h, while CPU+CPUi levels were still elevated at 7 h. CPU activity or CPU+CPUi levels were similar in <i>in situ</i> and peripheral samples. No correlation between CPU or CPU+CPUi and NIHSS or thrombus localization was found.</p> <p><i>Blood was collected in prechilled tubes containing sodium citrate, PPACK and aprotinin. Samples were immediately placed on ice after collection.</i></p>	In-house developed activity assay [131] + CPU+CPUi ELISA (Diagnostica Stago)
Alessi <i>et al.</i> 2016 [143]	<p>CPU+CPUi levels were monitored in 109 patients with ischemic stroke, with 41 receiving rtPA. Blood samples were collected post-admission/ post-thrombolysis up to day 90 at eight different time points. AIS patients had higher levels of CPU+CPUi at admission in comparison with the control population. In thrombolysed patients, an increase in CPU+CPUi was observed at the end of thrombolytic therapy, which lasted up to 4 h. In the non-thrombolysed group, CPU+CPUi levels did not differ over time. Both in thrombolysed and non-thrombolysed patients, higher CPU+CPUi levels were associated with more severe stroke and unfavorable outcome.</p> <p><i>No details available on sample collection and the use of inhibitors to prevent ex vivo proCPU activation.</i></p>	CPU+CPUi ELISA (Diagnostica Stago)
Leenaerts <i>et al.</i> 2015 [193]	<p>During the acute phase of myocardial infarction, CPU activity levels are higher in patients with AMI (N = 45) than in controls (N = 42). No association was found between CPU activity and AMI type (NSTEMI vs. STEMI). Intracoronary samples contained higher CPU levels than peripheral samples, indicating increased local CPU generation. Blood samples were collected at the start of coronary catheterization.</p> <p><i>Blood was collected in prechilled tubes containing sodium citrate, PPACK and aprotinin. Samples were immediately placed on ice after collection.</i></p>	In-house developed activity assay [131]

Brouns <i>et al.</i> 2009 [139]	In patients with ischemic stroke receiving thrombolytic therapy (N = 12), the amount of CPU generated was associated with the evolution of the neurological deficit as well as with achieved recanalization. Blood samples were taken at 6 – 9 different time points before, during and after thrombolytic therapy. <i>Blood was collected in prechilled tubes containing sodium citrate, PPACK and aprotinin. Samples were immediately placed on ice after collection.</i>	In-house developed activity assay [260]
Willemse <i>et al.</i> 2008 [199]	CPU activity is induced during therapeutic thrombolysis of patients with acute ischemic stroke (N = 8). Blood samples were collected at 6 - 9 time points before, during and after thrombolysis. <i>Blood was collected in prechilled tubes containing sodium citrate, PPACK and aprotinin. Samples were immediately placed on ice after collection.</i>	In-house developed activity assay [260]

AIS: acute ischemic stroke; AMI: acute myocardial infarction; CAD: coronary artery disease; CPU: carboxypeptidase U; CPUi: inactivated CPU; ELISA: enzyme-linked immunosorbent assay; EVT: endovascular thrombectomy; NSTEMI: non-ST-elevation myocardial infarction; PCR: polymerase chain reaction; proCPU: procarboxypeptidase U (TAFI, proCPB2); rtPA: recombinant tissue-type plasminogen activator; STEMI: ST-elevation myocardial infarction.

Similar to the findings of Brouns *et al.* in AIS, in the hyperacute phase of myocardial infarction, Pang and co-workers found significantly lower proCPU levels in 211 patients with acute coronary syndrome (ACS) compared to 211 controls [261]. Likewise, Leenaerts *et al.* detected lower proCPU levels in acute myocardial infarction patients compared to controls, indicating ongoing activation of proCPU which was confirmed by CPU activity levels that were higher in patients than in controls. In the same study, increased intra-arterial CPU activity was found near the occlusion site, demonstrating local CPU generation [193]. In contrast, Skeppholm *et al.* presented higher proCPU levels in ACS patients in the acute phase of the disease with the Asserachrom TAFI-1B1 ELISA, while no differences in proCPU levels (neither activity nor antigen) were found in ACS patients in the study of Cellai *et al.* [157,192]. Shantsila and colleagues measured increased proCPU antigen levels in STEMI patients during the subacute phase of the myocardial infarction, reaching a maximum seven days after admission, while proCPU antigen levels in NSTEMI (non-ST-elevation myocardial infarction) patients were higher at admission followed by a gradual decrease over time [191].

The somewhat contradictory proCPU results make it apparent that this parameter – when used as a single denominator – might not be the most appropriate marker for the exploration of the exact role of CPU during the acute phase of thromboembolic diseases. In contrast, the repeated observation of ongoing proCPU activation simultaneous with marked increases in CPU activity during the acute stage points out that quantification of the extent of proCPU activation, via measurement of the released activation peptide or formation of CPU – most likely – is a more reliable and precise marker and will provide a better picture of the *in vivo* role of proCPU, CPU and CPUi in these diseases.

2.1.5 Potential benefit of the use of CPU inhibitors

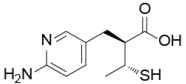
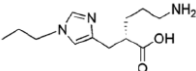
So far, no physiological inhibitors of CPU have been described, but several small molecule, peptide, antibody, and nanobody inhibitors were developed. CPU activity is inhibited by non-specific inhibitors of the metallopeptidase activity such as the zinc-

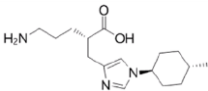
chelating agent EDTA (ethylenediaminetetraacetic acid) and agents that reduce the disulfide bridges in the active site of CPU such as 2-mercaptoethanol and dithiothreitol [2,5,56]. The organic arginine analogs MERGETPA (D,L-2-mercaptomethyl-3-guanidinoethylthiopropionic acid) and GEMSA (guanidinoethyl-mercapto-succinic acid) and the lysine analog ϵ -aminocaproic acid (ϵ -ACA) inhibit several carboxypeptidases including CPU, but they are not selective for CPU over CPN [35,56,262]. Several natural carboxypeptidase inhibitors were discovered, but only potato tuber carboxypeptidase inhibitor (PTCI), leech carboxypeptidase inhibitor (LCI), and tick carboxypeptidase inhibitor (TCI) have been characterized as competitive inhibitors of CPU with a K_i (inhibition constant) in the nanomolar range [263–266]. PTCI reversibly inhibits several carboxypeptidases from subfamily A and B, including CPU, but not CPN [263]. As CPU and CPN have several substrates in common, this selectivity is of utmost importance for the clinical application of CPU inhibitors.

Several pharmaceutical companies patented a range of low molecular weight (LMW) inhibitors of CPU. Of these drug candidates, so far six LMW compounds reached the clinical development phase: AZD9684 from AstraZeneca (Cambridge, United Kingdom), UK-396082 from Pfizer (New York, USA), SAR104772 and SAR126119 from Sanofi (Paris, France), DS-1040 from Daiichi Sankyo (Tokyo, Japan), and S62798 from Servier (Paris, France) (Table 2-5).

Even though these LMW inhibitors showed an excellent safety profile and selectivity towards CPU, further development was often discontinued for various reasons, including the lack of oral bioavailability of the compound, the absence of superiority versus standard treatment or the challenging clinical trial set-up in complex acute pathologies such as stroke.

Table 2-5. Overview of the low molecular weight CPU inhibitors that have reached the clinical development phase.

Company	Lead Compound	Chemical Structure	Highest Development Status Reported	Clinical Trial Setting and Results	Pharmacokinetics	Reference
AstraZeneca	AZD9684		Phase II completed	<p>Thrombosis and pulmonary embolism</p> <ul style="list-style-type: none"> Improved resolution rate of pulmonary emboli Clear stimulation of endogenous fibrinolysis in patients with acute symptomatic embolism Development halted Still used as a research tool 	<ul style="list-style-type: none"> Good oral bioavailability Short half-life 	[270–275]
Pfizer	UK-396082		Phase I completed	<ul style="list-style-type: none"> Development halted Still used as a research tool 	<ul style="list-style-type: none"> Half-life of 4h after IV administration Good bioavailability after oral dosing 	[62,168,276–278]
Sanofi	SAR104772 SAR126119	Unknown	Phase I completed Phase II initiated in 2012	<ul style="list-style-type: none"> No data available 	<ul style="list-style-type: none"> No data available 	[279–283]

Company	Lead Compound	Chemical Structure	Highest Development Status Reported	Clinical Trial Setting and Results	Pharmacokinetics	Reference
Daiichi Sankyo	DS-1040		Phase Ib/II completed	<p>Acute ischemic stroke and acute submassive pulmonary embolism</p> <ul style="list-style-type: none"> High selectivity for CPU over CPN (510 000-fold) 10-fold more potent than PTCI Well tolerated by young and elderly healthy volunteers Dose-dependent decrease in CPU activity Single-dose is well tolerated in Japanese patients with AIS undergoing thrombectomy Development halted 	<ul style="list-style-type: none"> Half-life of 1.5 days after IV and oral administration 80% and 10% respectively recovered unchanged in urine after IV and oral administration 	[158,159,284,285]
Servier	S62798	Unknown	Phase I completed	<ul style="list-style-type: none"> Rapid and dose-dependent inhibition of CPU in three different pharmacodynamic assays All doses well-tolerated Development halted 	<ul style="list-style-type: none"> Favorable safety profile and linear pharmacokinetics 	[195,286]

In the last 15 years, also several novel antibodies and nanobodies have been developed to target human, rat, or murine CPU [75,267–269]. Direct CPU inhibition was obtained through mAbs or nanobodies that block the catalytic site or that destabilize CPU [267]. Besides these highly specific, direct inhibitors of active CPU, molecules that selectively impair the activation of proCPU by either thrombin-thrombomodulin or plasmin have also been characterized [75,267,269]. These antibodies and nanobodies accelerated *in vitro* clot lysis and have been extensively used as profibrinolytic tools and to further unravel (patho)physiologic activation and inactivation of proCPU [76,268,287]. Noteworthy, some antibodies and nanobodies have been reported to stimulate the intrinsic carboxypeptidase activity of proCPU in *in vitro* clot lysis models which was explained by the translocation of the activation peptide, making the catalytic cleft accessible for larger substrates such as C-terminal lysines residues on partially degraded fibrin [75,76,287–290]. Wyseure *et al.* fused a mAb directed against CPU with a mAb raised against PAI-1 into a bispecific diabody (Db-TCK26D6 33H1F7) that showed promising thromboprophylactic effects in a mouse model of venous thromboembolism. Also in two stroke models, a transient MCAO model and a thrombin-induced MCAO model, the diabody reduced lesion volume markedly. Its effect even exceeded the effect of 10 mg/kg rtPA in the thrombin-induced MCAO model. In the transient MCAO model, fibrin(ogen) deposition was also reduced which was associated with improved neurologic and motor outcome [291]. The diabody was recently patented [292].

Noteworthy, some competitive LMW inhibitors and nanobodies exhibit an ambiguous activity in *in vitro* clot lysis experiments. As expected, at high concentrations these inhibitors enhance fibrinolysis, but paradoxically, at very low concentrations, a small prolongation of the clot lysis time (CLT) can be observed [89,90,268]. The observed prolongation of the CLT is attributed to the appearance of two CPU pools when proCPU is activated in the presence of low concentrations of a CPU inhibitor: one pool of “circulating” free CPU and one inhibitor-bound pool. Free CPU is susceptible to rapid inactivation due to its intrinsic thermal instability, whereas inhibitor-bound CPU is

stabilized by most inhibitors and thus protected from decay [89,90]. The two pools are in constant equilibrium and when free CPU is inactivated, the free CPU pool is replenished by CPU that is released from the CPU-inhibitor complex [89,90]. This phenomenon only occurs when not all circulating CPU is bound to the inhibitor, thus when the CPU concentration is high relative to the inhibitor concentration.

Overall, the currently evaluated inhibitors show an excellent safety profile in terms of possible bleeding complications and issues with selectivity towards CPN seem to be overcome. Furthermore, some of the LMW compounds display excellent oral bioavailability were others, as well as antibodies, can only be administered intravenously (IV). In acute settings such as AIS, an IV compound is preferred over oral administration given the fact that the latter results in a slower increase of plasma levels and is not possible in unconscious patients or patients facing difficulties with swallowing. However, in the setting of the prevention of recurrent stroke, or even in primary prevention, an orally administered compound is desirable. Although, if the terminal half-life of the inhibitor allows a less intense dosing regimen, a subcutaneous, intramuscular, or even an IV administered compound may be considered as well. As for antibody inhibitors, other major drawbacks are the risk of immunogenicity and the significantly higher production time and cost compared to LMW inhibitors [293]. Moreover, questions have also been raised about the ability of mAbs to penetrate a clot, as antibodies are significantly larger than LMW inhibitors, which might limit their applications in this context *in vivo*. In this point of view, nanobodies – the smallest naturally-occurring antigen-binding antibody fragments – are of particular interest. Nanobodies are ten times smaller than conventional mAbs and display increased clot penetration in an *in vitro* clot lysis model as demonstrated by Buelens and colleagues [269]. Furthermore, nanobodies combine several advantages of LMW compounds and mAbs such as high solubility, stability, low immunogenicity, and high affinity toward their targets, but they are still costly and time-consuming to manufacture [268,293]. A major drawback of the inhibitory nanobodies is the lack of species cross-reactivity between nanobodies raised

against mouse and rat or human (pro)CPU which might hamper the translation from animal models to patients.

The ability of CPU to counteract efficient plasmin formation makes its inhibition an appealing strategy for the treatment of venous and arterial thrombotic disorders. *In vitro* evidence for the importance of the CPU pathway is provided by studies in which it is shown that the rate of fibrinolysis is significantly enhanced when either CPU is inhibited or proCPU is depleted [37,63,89]. In addition, *in vivo* evidence of the potential of a CPU inhibitor to improve endogenous fibrinolysis and thrombolysis in either the presence or absence of exogenous rtPA has been evaluated in several animal models over the years. However, these studies in animal models showed somewhat contradictory results [62,266,285,294]. Despite these inconclusive results of CPU inhibition in various animal models, the first-in-man trials and phase II trial of DS-1040 and AZD9684 respectively showed increased D-dimer levels in several patients which points towards stimulation of endogenous fibrinolysis [205,243,295]. As for the approach of using CPU inhibition as an adjuvant to tPA-mediated thrombolysis, reviews by Willemse *et al.* and Foley *et al.* on this topic suggest that CPU deficiency/inhibition may improve the thrombolytic efficacy of tPA [201,234,296,297]. CPU inhibition alone or in combination with PAI-1 inhibition or rtPA administration was – depending on the LMW inhibitor, antibody or nanobody used – successful in the reduction of infarct size, increasing the reperfusion rate or decreasing fibrin(ogen) depositions in the brain of infarcted mice [282,290,291]. This was in contrast with the findings in several knockout models where *cpb2* knockout mice did not show significant differences in infarct volume, functional outcome, or fibrin(ogen) in a transient MCAO model [298,299]. Bleeding complications related to CPU inhibition have neither been reported in *cpb2* knockout mice nor after administration of CPU inhibitors. Westbury *et al.* recently showed that hemostasis was not significantly impacted in individuals with a partial proCPU deficiency (see Chapter 8), which underscores the potential of pharmacological inhibition of CPU for the treatment of thromboembolic diseases and encourages that this therapeutic strategy will unlikely

result in bleeding complications [28,300]. However, data need to be interpreted with caution as only limited activation of proCPU (1 – 2%) can be enough to exert its antifibrinolytic effects.

For both approaches – CPU inhibitor alone and combined administration with tPA – it is important to bear in mind that the type of inhibitor and thrombosis model, but also interspecies differences and the timing of inhibitor administration (before or after thrombus induction) are determinants of the *in vivo* profibrinolytic efficiency of a CPU inhibitor. Moreover, whether or not an apparent effect of a CPU inhibitor alone can be observed also depends on the magnitude of the thrombotic stimulus that was applied [301].

2.2 A role for the CPU system in the regulation of other (patho)physiological processes

2.2.1 The anti-inflammatory role of the CPU system

A role for the CPU system in various aspects of inflammation has also been suggested [302]. Several inflammatory proteins, including bradykinin, the complement factors C3a and C5a, thrombin-cleaved osteopontin and plasmin-cleaved chemerin have been recognized as *in vitro* and *in vivo* CPU substrates [82–84,87,302]. Because bradykinin has vasodilating properties, CPU may also have a function in blood pressure regulation; however, the physiological relevance of this link is not completely understood as several studies reported conflicting data (see also 2.1.3.3(b)) [83,303,304]. Moreover, CPU attenuates the formation of plasmin and it has also been reported that C-terminal Lys and Arg from cellular plasminogen receptors are also substrates of CPU, therefore suggesting a role for CPU in cellular processes involving wound healing, cell migration, and angiogenesis, which also contributes to its anti-inflammatory activity [305–307].

The exact role of the CPU system in inflammatory diseases seems to be very complex and the effects of CPU on pathophysiology depend on which of the CPU substrates is

primarily involved and what the effect of that mediator is on the outcome [302]. Moreover, all the potential effects of CPU in the regulation of inflammation must be considered in the context of the requirement for activation, the duration of the efficacy due to its short half-life, and in light of the presence of CPN in plasma. Nevertheless, in recent years, evidence from *cpb2* knockout mice demonstrates that CPU plays an important role in the clearance of active inflammatory mediators. These data are very intriguing and call for further exploration, but caution must be taken when translating the conclusions from mouse to human. As mentioned before, the murine and human CPU system display significant differences in regulation and stability, and this might suggest a different role of the proCPU pathway in inflammation [17,20,21,54].

2.2.2 CPU as a contributor to the hypofibrinolytic state in COVID-19 patients?

Starting end 2019, the world has been confronted with an outbreak of a new coronavirus called SARS-CoV-2 (severe acute respiratory-syndrome coronavirus-2) that causes the disease COVID-19 (coronavirus disease 2019) and poses a global health emergency [308]. Infection with SARS-CoV-2 primarily affects the respiratory system, with no or minimal symptoms in the majority of patients. In severe cases, patients present with hypoxemic respiratory failure that can rapidly evolve into severe acute respiratory distress syndrome (ARDS), sepsis and/or multiorgan failure [309–312]. Aside from respiratory failure, systemic thromboembolic complications are frequent in COVID-19 patients and the result of a dysregulation of the hemostatic balance, tipping it towards an overall hypercoagulable and hypofibrinolytic state [309,313–316]. Since CPU counteracts the progression of fibrinolysis, the question arises whether CPU may play a role in the hypofibrinolytic state observed in SARS-CoV-2 infected patients and thus may contribute to the high prothrombotic status in these patients. This hypothesis was explored in Chapter 9 of this thesis.

Chapter 3

Objectives

3 Objectives

The overall objective of this doctoral research was to **contribute to a better understanding of the clinical context and expression of CPU, mainly related to hyperlipidemia & atherosclerosis**. A schematic overview of the outline of this doctoral thesis can be found in Figure 3-1.

Chapter 1 provides a general introduction to the CPU system, focusing on the characteristics of CPU and the methods available for measuring proCPU, CPU and CPUi. The current literature on the pathophysiological role of the CPU system is summarized in **Chapter 2**.

Part I – Hyperlipidemia & atherosclerosis

Objective 1. Evaluation of the influence of statin therapy on proCPU biology

Sub-objective 1a. Evaluate the effect of statin therapy on proCPU biology in hyperlipidemic patients

Statins are the cornerstone of lipid-lowering therapy and widely used in primary and secondary prevention of CVD [217,229]. Over the years, it has been proposed that the beneficial effects of statins on morbidity and mortality cannot solely be attributed to their lipid-lowering properties [317,318]. There is considerable evidence of cholesterol-independent effects (so-called “pleiotropic effects”), including profibrinolytic properties [222,319]. As discussed in Chapter 2 of this thesis, a number of research groups have investigated the effect of different statins on circulating proCPU levels, showing the potential of statins to downregulate proCPU levels, thereby positively affecting fibrinolysis. Nonetheless, drawbacks in the study design (e.g. lack of a control group, very specific patient populations) and/or the analytical methods used in these studies, raised questions about the validity of the results. Given the methodological drawbacks in the majority of the previous studies, we initiated a proof-of-concept observational study to explore the influence of statin therapy on proCPU biology in a limited number of statin-

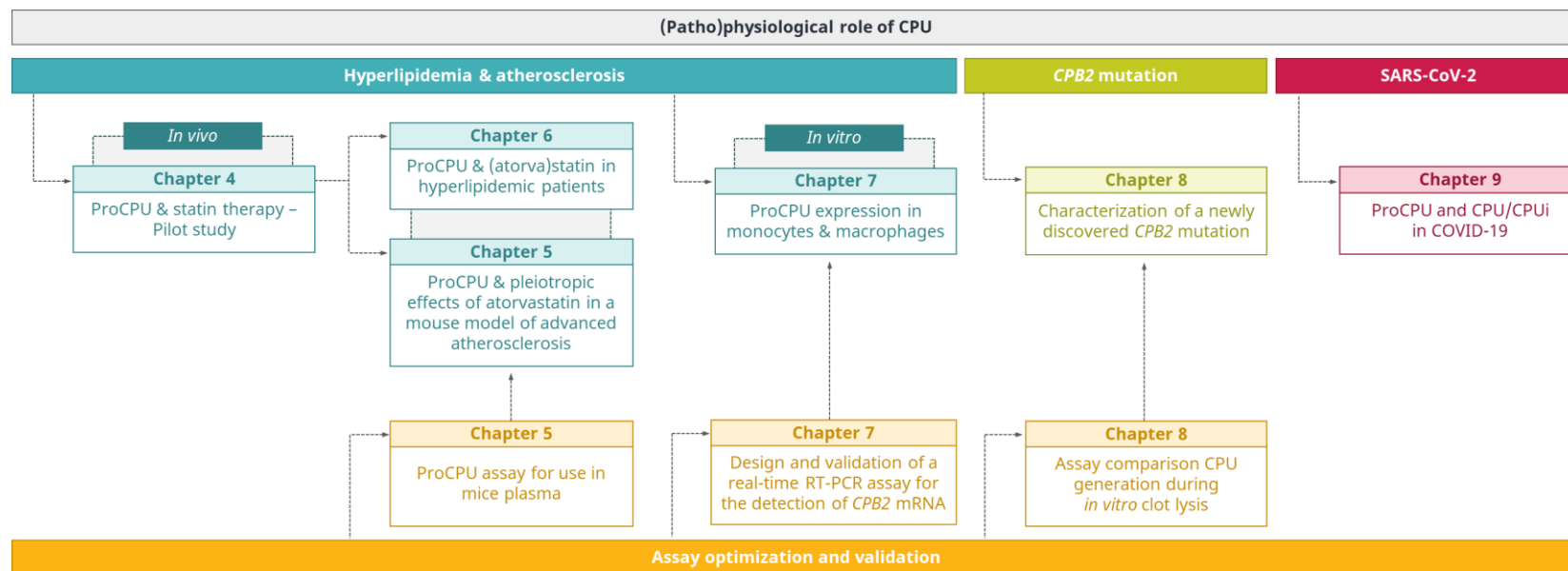


Figure 3-1. Overview of the different aspects covered in this doctoral thesis. COVID-19: coronavirus disease 2019; (pro)CPU: (pro)carboxypeptidase U; SARS-CoV-2: severe acute respiratory-syndrome coronavirus-2; RT-qPCR: reverse-transcriptase quantitative polymerase chain reaction.

treated patients with hyperlipidemia to search for possible effects and associations that can be further elaborated on in a subsequent larger study (Chapter 6), with the ultimate goal of further elucidating the effect of this treatment on fibrinolysis. The results of this study are described in **Chapter 4**.

The pilot study provided valuable information on the effect of statin therapy on the proCPU system in hyperlipidemic patients. However, important questions remained and there was a need to re-evaluate the observations from the pilot study in a larger cohort to solidify these findings.

Sub-objective 1b. Study the nature (lipid- or non-lipid-related) of the downregulation of the CPU system by statin therapy

One of the remaining questions was the nature of the effect of the HMG-CoA reductase inhibitors on the CPU system (lipid- or non-lipid related). Since it is challenging to discriminate between lipid- and non-lipid related pleiotropic effects in humans, we opted to investigate this in apolipoprotein E-deficient mice with a heterozygous mutation in the fibrillin-1 gene (ApoE^{-/-}Fbn1^{C1039G^{+/-}}). Statins do not predominantly lower cholesterol in these mice [320], allowing us to study the cholesterol-independent effects of statins more straightforwardly. We adapted our in-house human proCPU assay and validated it to be applicable in mice plasma samples. The assay optimization and the results of proCPU measurement in atorvastatin-treated ApoE^{-/-} Fbn1^{C1039G^{+/-}} mice are described in **Chapter 5**.

Sub-objective 1c. Further explore the clinical relevance of the proCPU downregulation by statin therapy and unravel whether this effect is dose-dependent

Starting from the main observations of the pilot study, a larger clinical study was set up (**Chapter 6**) to further examine the clinical relevance of the observations made in the pilot study and the hypothesis that it might be valuable to include proCPU measurement in risk assessment for starting statin therapy. Moreover, in this larger cohort study we also aimed to answer the question whether additional reductions in proCPU levels can

be obtained when administering a higher statin dose (e.g., atorvastatin 40 or 80 mg instead of atorvastatin 20 mg in the pilot study) and what this could mean in terms of additional health benefit for the patient.

Objective 2. Study of the expression of proCPU in human monocytes and macrophages

Recently, *CPB2* mRNA was detected in peripheral blood mononuclear cells (PBMCs) and it was hypothesized that the *CPB2* transcripts were derived from *CPB2* gene expression by monocytes and macrophages in this cell fraction [46]. Since both CPU and monocytes & macrophages are involved in inflammation and thrombus formation, we were interested in studying the expression of proCPU (on mRNA, protein and activity level) in (primary) human monocytes and different subsets of (primary) human macrophages (**Chapter 7**) [321]. This will provide more insight into human monocytes and monocyte-derived-macrophages as potential sources of proCPU within atherosclerotic plaques and extra-vascular inflammatory sites.

Part II

During the conduct of this PhD research, some very interesting CPU-related research questions/opportunities came into the spotlight that we were eager to explore further and which lead to two additional objectives. Specifically, it concerned the discovery of a new mutation in the *CPB2* gene and the study of the CPU system in the context of COVID-19.

Objective 3. Functional characterization of a new mutation in the *THBD* and *CPB2* gene

Recently a new mutation in the *CPB2* gene of proCPU was discovered; the first known case of a genetic proCPU deficiency described in humans. The case was particularly interesting because of the co-inheritance of a new mutation in the *THBD* gene of thrombomodulin, which – in complex with thrombin – is one of the activators of proCPU.

We collaborated on the functional characterization of these novel *THBD* and *CPB2* mutations (**Chapter 8**).

An important element of the characterization of the influence of these mutations on fibrinolysis – and the CPU system in particular – is the measurement of the time course of CPU generation during *in vitro* clot lysis. Given only limited amounts of plasma samples were available and preliminary *in vitro* clot lysis experiments were performed with the Aberdeen Cardiovascular & Diabetes Centre *in vitro* clot lysis assay, CPU generation was implemented in this *in vitro* clot lysis assay. Prior to measurement of the patient samples, the robustness of the CPU generation assay was established by comparing the time course of CPU generation to this in our in-house *in vitro* clot lysis assay for which the CPU generation assay was originally developed and validated (**Chapter 8**).

Objective 4. Exploration of the effect of SARS-CoV-2 infection on the CPU system

During this doctoral research, the world was confronted with an outbreak of a new coronavirus: SARS-CoV-2 [308]. Infection with SARS-CoV-2 primarily affects the respiratory system, but it soon became clear that systemic thrombotic complications were also frequent in COVID-19 patients [309–316]. In this context several markers of coagulation and fibrinolysis have been studied extensively, showing a dysregulated hemostatic balance with an overall hypercoagulable and hypofibrinolytic state. However, little is known about the effect of SARS-CoV-2 infection on CPU. Through its action of cleaving off C-terminal lysines from partially degraded fibrin, CPU counteracts the progression of fibrinolysis. As a result, the question arose whether CPU may play a role in the hypofibrinolytic state observed in SARS-CoV-2 infected patients and thus may contribute to the high prothrombotic status in these patients. This hypothesis was further explored in **Chapter 9** of this thesis.

PART I

Hyperlipidemia & atherosclerosis

Chapter 4

Effect of statin therapy on the CPU system in patients with hyperlipidemia: a proof-of-concept observational study

Based on:

Claesen K, Mertens JC, Basir S, De Belder S, Maes J, Bosmans J, Stoffelen H, De Meester I, Hendriks D. Effect of statin therapy on the carboxypeptidase U (CPU, TAF1a, CPB2) system in patients with hyperlipidemia: a proof-of-concept observational study. *Clinical Therapeutics*. 2021; 43(5): 908-16.

4 Effect of statin therapy on the CPU system in patients with hyperlipidemia: a proof-of-concept observational study

4.1 Abstract

Background

Statins are commonly used in patients with hyperlipidemia to lower their cholesterol levels and reduce their cardiovascular risk. There is also considerable evidence that statins possess a range of cholesterol-independent effects, including profibrinolytic properties. This pilot study aimed to explore the influence of statins on proCPU biology and to search for possible effects and associations that can be followed up in a larger study.

Methods

Blood was collected from 16 patients with hyperlipidemia, before and after 3 months of statin therapy (simvastatin 20 mg or atorvastatin 20 mg). Fifteen age-matched normolipidemic persons served as control subjects. Lipid parameters and markers of inflammation and fibrinolysis (proCPU levels and clot lysis times) were determined in all samples.

Results

Mean proCPU levels were significantly higher in patients with hyperlipidemia compared to control subjects (1186 ± 189 U/L vs 1061 ± 60 U/L). Treatment of these patients with a statin led to a significant average decrease of 11.6% in proCPU levels and brought the proCPU concentration to the same level as in the control subjects. On a functional level, enhancement in plasma fibrinolytic potential was observed in the statin group, with the largest improvement in fibrinolysis seen in patients with the highest baseline proCPU levels and largest proCPU decrease upon statin treatment.

Conclusions

Increased proCPU levels are present in patients with hyperlipidemia. Statin treatment significantly decreased proCPU levels and improved plasma fibrinolysis in these patients. Moreover, our study indicates that patients with high baseline proCPU levels are likely to benefit most from statin therapy. The latter should be examined further in a large cohort.

4.2 Introduction

Statins are the cornerstone of lipid-lowering therapy and are widely used in primary and secondary prevention of CVD [217,229]. Over the years, it has been established that the beneficial effects of statins on morbidity and mortality cannot solely be attributed to their lipid-lowering properties [317,318]. There is considerable evidence of cholesterol-independent effects (so-called “pleiotropic effects”), including profibrinolytic properties (e.g., influence on TF, platelet aggregation, and fibrinolysis) [222,319].

The antifibrinolytic enzyme CPU is present in the circulation as its inactive precursor proCPU. Upon activation by thrombin(-thrombomodulin) or plasmin, the zymogen is converted into the active enzyme [3,91]. Once activated, the enzyme potently attenuates fibrinolysis by cleaving C-terminal lysines on partially degraded fibrin, thereby interfering with efficient plasminogen activation [41].

The effect of different statins on circulating proCPU levels has been studied, showing the potential of statins to modulate the CPU system, thereby positively affecting fibrinolysis [147,155,174,179,322]. A number of these studies, however, have methodologic drawbacks.

The present proof-of-concept observational study aimed to explore the influence of statin therapy on proCPU biology in a limited number of statin-treated patients with hyperlipidemia to search for possible effects and associations that can be followed up in a subsequent larger study, with the ultimate goal of further elucidating the effect of this

treatment on fibrinolysis. Participants' proCPU levels, as well as their plasma fibrinolytic potential, were assessed before and after 3 months of therapy. In addition, the potential relationship between lipid parameters and markers of fibrinolysis and inflammation was studied.

4.3 Materials and methods

4.3.1 Study design

Patients with hyperlipidemia (TC \geq 190 mg/dL or LDL-C \geq 115 mg/dL) with a 10-year risk of fatal CVD of \geq 5% (calculated with the SCORE chart) were enrolled and allocated to receive simvastatin 20 mg or atorvastatin 20 mg by the collaborating general practitioners [229]. Age-matched normolipidemic subjects, presenting at the general practitioner for a routine physical examination or renewal of chronic prescription drugs, were recruited as control subjects. Exclusion criteria for both groups were the clinical history of cardiovascular events, (chronic) liver disease, pregnancy, a glomerular filtration rate $<$ 30 mL/min, the use of anticoagulant or lipid-lowering drugs, and initiation of a new medication (other than statin therapy) during the course of the study.

The study was approved by the local ethics committee (B300201837918), and all participants gave written informed consent before enrolment.

4.3.2 Sample collection

Blood samples were collected from individuals with hyperlipidemia at the time of inclusion (baseline) and after 3 months of statin therapy. In control subjects, two blood collections were performed 3 months apart. Participants' blood was drawn in a fasting state between 8 and 10 am. Blood intended for proCPU determination, clot lysis experiments, measurement of soluble thrombomodulin (sTM), and high-sensitivity C-reactive protein (CRP) was drawn in 3.2% trisodium citrate tubes (9:1 v/v; BD Vacutainer, USA). Serum separator tubes (BD Vacutainer) were used for the determination of a lipid panel. After collection, one tube of citrated whole blood was kept apart for the isolation

of genomic DNA. All other tubes were centrifuged at $2000 \times g$ for 15 min at $4\text{ }^{\circ}\text{C}$, aliquoted, and stored at $-80\text{ }^{\circ}\text{C}$ in our biobank (BE71030031000) until further analysis [323].

4.3.3 ProCPU measurement

Plasma was diluted 40-fold in 4-2-hydroxyethyl-1-piperazineethanesulfonic acid (HEPES, 20 mmol/L, pH 7.4; Merck, Germany), after which proCPU was activated with human thrombin (Merck, Germany), rabbit-lung thrombomodulin (Sekisui Diagnostics, USA), and CaCl_2 (Merck, Germany) (final concentrations of 4 nM, 16 nM, and 50 mM, respectively). Subsequently, the active CPU was incubated with the in-house substrate Bz-*o*-cyano-Phe-Arg and the formed product was quantified by RP-HPLC [81].

4.3.4 Clot lysis assay

In vitro clot lysis was assessed by mixing citrated plasma with tPA (final concentration 40 ng/mL) alone or tPA in combination with PTCl (final concentration 75 $\mu\text{g}/\text{mL}$; Merck, Germany). Coagulation was initiated by addition of CaCl_2 (final concentration 12.5 mM), and turbidity was measured spectrophotometrically every 30 seconds at 405 nm and $37\text{ }^{\circ}\text{C}$ (VersaMax, Molecular Devices, USA) [194,205]. The clot lysis time (CLT; the time between half-maximal turbidity during coagulation and fibrinolysis) and ΔCLT (the absolute reduction in CLT after addition of PTCl) were calculated [205].

4.3.5 Lipid measurements

TC, HDL-C, and TG were measured using a Siemens Healthineers Atellica CH Analyzer (Siemens Healthcare Diagnostics, Canada). LDL-C levels were calculated based on the Friedewald formula.

4.3.6 Other measurements

High-sensitivity CRP and sTM antigen levels were measured by ELISA according to the manufacturer's instructions (Human CRP ELISA Kit and Thrombomodulin Human ELISA kit, respectively; Abcam, United Kingdom). Oxyhemoglobin (oxyHb) levels were determined to exclude the potential influence of hemolysis on the proCPU and clot lysis assays [200]. Detection of the Thr325Ile proCPU polymorphism was performed according to Zorio *et al.* [145].

4.3.7 Statistical analysis

Results are expressed as mean \pm standard deviation (SD). GraphPad Prism version 9.3.1 (GraphPad Software, Inc., USA) was used for statistical analysis and data plotting. Continuous variables were evaluated with a Mann-Whitney U test (unpaired data) or a Wilcoxon matched-pairs signed-rank test (paired data). A χ^2 test was used for categorical data. Spearman correlation coefficients were computed to assess the following associations: change in proCPU (Δ proCPU) – baseline proCPU levels, Δ proCPU – Δ LDL-C, Δ proCPU – Δ CRP, and baseline Δ CLT – change in Δ CLT. Results with p -values < 0.05 were considered statistically significant.

4.4 Results

4.4.1 Study population

Sixteen statin-treated patients with hyperlipidemia (participation rate was 89%) and 15 normolipidemic control subjects were included in the study between November 2018 and May 2020. Baseline characteristics of the study population are summarized in Table 4-1. Sex ($p = 0.04$), systolic blood pressure ($p = 0.001$), and the use of antihypertensive and antiaggregant drugs (both $p = 0.04$) differed significantly between both groups. All other characteristics were balanced.

Table 4-1. Baseline characteristics of patients eligible for statin therapy and controls.

	Controls	Statin patients	<i>p</i> -value
Demographics			
Number – N	15	16	
Age – years (range)	66 (53 – 80)	69 (49 – 80)	0.32†
Male sex – N (%)	8 (53)	3 (19)	0.04‡
BMI – kg/m ² (mean ± SD)	24.4 ± 3.6	27.8 ± 5.3	0.09†
Smoking – N (%)	5 (33)	4 (25)	0.62‡
Genotype *			0.66‡
Ile/Ile – N (%)	1 (7)	1 (6)	
Thr/Ile – N (%)	10 (67)	7 (44)	
Thr/Thr – N (%)	4 (27)	8 (50)	
Blood pressure			
Systolic – mmHg (mean ± SD)	129 ± 10	141 ± 8	0.001†
Diastolic – mmHg (mean ± SD)	79 ± 6	83 ± 7	0.21†
Medication use			
Antihypertensive – N (%)	5 (33)	13 (81)	0.04‡
Antiaggregant – N (%)	0 (0)	6 (38)	0.04‡
Antidiabetic – N (%)	0 (0)	1 (6)	0.37‡
Antidepressant – N (%)	1 (7)	2 (13)	0.71‡
Statin therapy			
Simvastatin 20 mg – N (%)	-	5 (31)	-
Atorvastatin 20 mg – N (%)	-	11 (69)	-

Results are given as a number (N) with percentage in parentheses or as mean ± standard deviation (SD). A Mann-Whitney U-test † or a Chi-square test ‡ were used to test for statistically significant between-group differences. * Single nucleotide polymorphism +1040C/T, corresponding to a Thr/Ile substitution at position 325 of proCPU. BMI: body mass index.

Lipid profiles of statin-treated patients and control subjects are shown in Table 4-2. At the time of inclusion, TC and LDL-C levels were significantly higher in the statin group (both, $p = 0.002$). After 3 months of statin therapy, both parameters were significantly reduced (both $p < 0.001$) and were even lower compared with levels in the control subjects (although not statistically significant for TC), indicating good therapy adherence.

4.4.2 Statin therapy downregulates proCPU levels

Mean baseline proCPU levels were significantly higher in statin-eligible patients compared with control subjects (1186 ± 189 U/L vs 1061 ± 60 U/L; $p = 0.04$) (Figure 4-1A and Table 4-2). Statin therapy in these patients led to a significant decrease of 138 U/L (11.6%; $p = 0.002$) in plasma proCPU levels after 3 months compared with baseline, whereas proCPU levels remained the same in control subjects. At the end of the study, proCPU levels no longer differed between statin-treated patients and control subjects ($p = 0.18$).

A positive correlation was observed between baseline proCPU levels and the decrease in proCPU under the influence of statin treatment (Δ proCPU) ($r = 0.88$; $p < 0.001$) (Figure 4-1E). Both baseline proCPU levels and the decrease in proCPU exhibited high interindividual variation. Three subpopulations were identified: i) a cohort with baseline proCPU levels (1063 ± 47 U/L) similar to those of the control subjects (1061 ± 46 U/L) and no proCPU decrease under the influence of a statin ($p = 0.63$); ii) a second cohort with baseline proCPU levels (1104 ± 56 U/L) similar to those of the control subjects and a 5% to 10% decrease in proCPU levels after statin use ($p = 0.06$); and iii) a cohort in which baseline proCPU levels were 20% higher (1316 ± 225 U/L) and in which statin treatment resulted in an approximately 20% decrease after 3 months ($p = 0.02$) (Figure 4-1C).

Table 4-2. Biochemical and hemostatic parameters of statin patients and controls at inclusion (baseline) and after three months.

		N	Baseline (mean ± SD)	After three months (mean ± SD)	Mean change	p-value†
Lipid parameters						
TC (mg/dL)	Statin patients	16	239 ± 37	172 ± 27	-67	< 0.001
	Controls	15	188 ± 25	180 ± 23	-8	0.50
	p-value ‡		0.002	0.48		
LDL-C (mg/dL)	Statin patients	16	147 ± 32	82 ± 28	-65	< 0.001
	Controls	15	115 ± 29	123 ± 29	+8	0.63
	p-value ‡		0.002	0.01		
HDL-C (mg/dL)	Statin patients	16	66 ± 17	72 ± 14	+6	0.09
	Controls	15	50 ± 7	47 ± 8	-3	0.25
	p-value ‡		0.44	0.002		
TG (mg/dL)	Statin patients	16	135 ± 66	96 ± 40	-39	0.02
	Controls	15	114 ± 16	90 ± 24	-24	0.13
	p-value ‡		0.66	0.83		
Markers of fibrinolysis and inflammation						
ProCPU (U/L)	Statin patients	16	1186 ± 189	1048 ± 124	-138	0.002
	Controls	12	1061 ± 60	1066 ± 44	+5	> 0.99
	p-value ‡		0.04	0.18		

Effect of statin therapy on the CPU system in hyperlipidemic patients: a pilot study

		N	Baseline (mean ± SD)	After three months (mean ± SD)	Mean change	p-value[†]
Markers of fibrinolysis and inflammation (continued)						
CLT (min)	Statin patients	15	68.7 ± 27.4	65.5 ± 23.1	-3.2	0.03
	Controls	11	65.4 ± 10.7	66.8 ± 22.0	+1.4	0.87
	<i>p</i> -value [‡]		0.34	0.75		
CLT_{PTCI} (min)	Statin patients	15	42.7 ± 15.9	42.4 ± 11.6	-0.3	0.76
	Controls	11	39.5 ± 8.2	39.7 ± 13.2	+0.2	> 0.99
	<i>p</i> -value [‡]		0.63	0.95		
ΔCLT (min)	Statin patients	15	26.1 ± 12.4	23.1 ± 14.3	-3.0	0.001
	Controls	11	25.9 ± 13.4	27.1 ± 15.6	+1.2	0.74
	<i>p</i> -value [‡]		0.37	0.01		
sTM (ng/mL)	Statin patients	16	3.1 ± 1.2	3.0 ± 0.8	-0.1	0.75
	Controls	12	3.3 ± 0.2	3.1 ± 0.4	-0.2	0.13
	<i>p</i> -value [‡]		0.38	0.74		
hsCRP (mg/L)	Statin patients	16	6.3 ± 1.5	3.3 ± 5.4	-0.30	< 0.001
	Controls	12	1.9 ± 2.9	2.0 ± 1.0	+0.01	0.81
	<i>p</i> -value [‡]		0.04	0.84		

Results are presented as mean ± standard deviation (SD). [†] Wilcoxon Matched-Pairs Signed Rank test. [‡] Mann-Whitney test. N, number; TC, total cholesterol; LDL-C, low-density lipoprotein cholesterol; HDL-C, high-density lipoprotein cholesterol; TG, triglycerides; ProCPU, procarboxypeptidase U (TAFI, proCPB2); CLT, clot lysis time; CLT_{PTCI}, CLT in the presence of potato-tuber carboxypeptidase inhibitor (PTCI); ΔCLT; absolute reduction in CLT after addition of PTCI; sTM, soluble thrombomodulin; hsCRP, high-sensitive C-reactive protein.

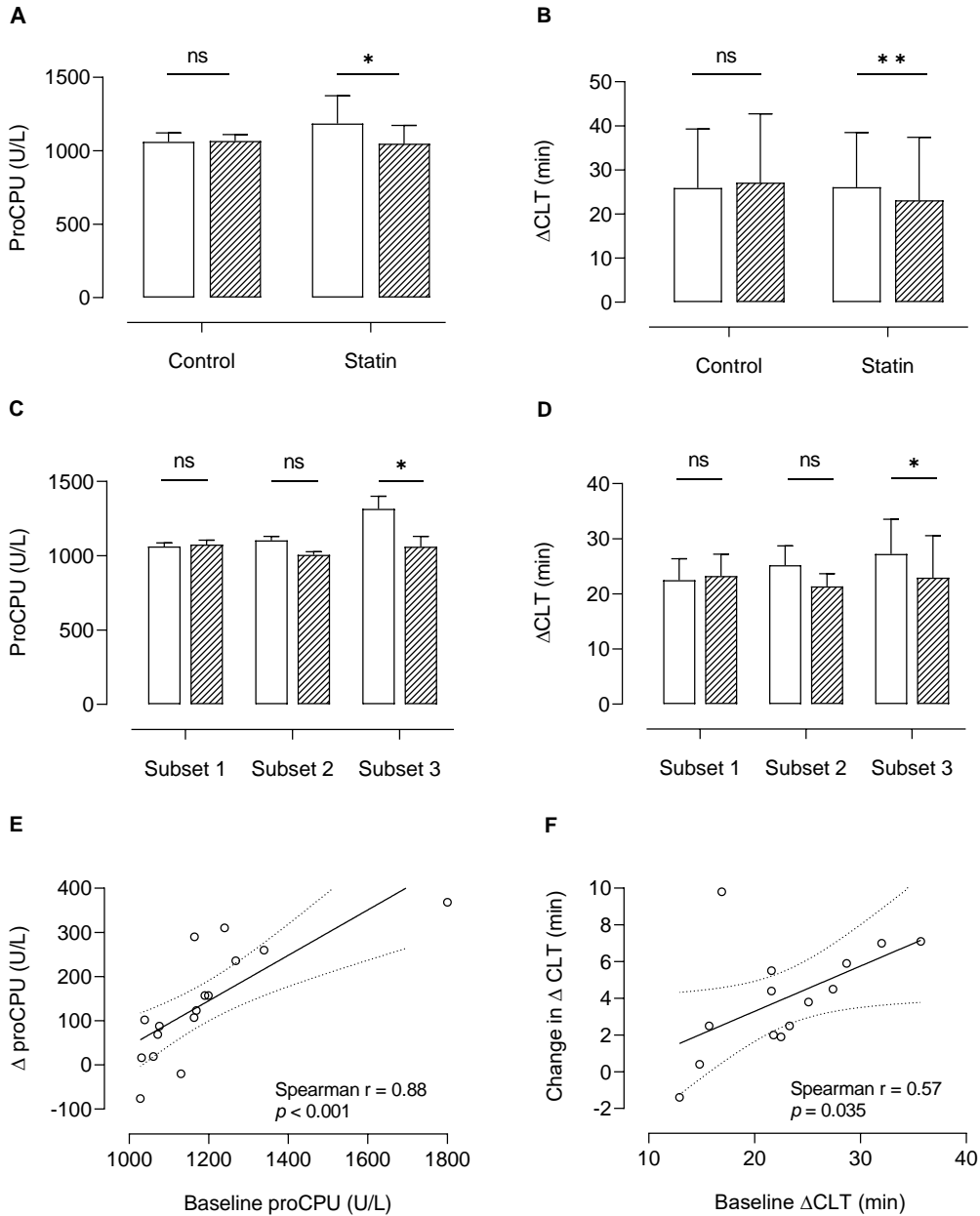


Figure 4-1. ProCPU levels and ΔCLT in statin-treated patients and control subjects. A) Bar graph showing plasma proCPU levels in control subjects (N = 12) and statin-treated patients (N = 16) at baseline (white) and after 3 months (black stripes). B) Bar graph showing ΔCLT (actual contribution of the CPU system to the total clot lysis time) in control subjects (N = 11) and statin-treated patients (N = 16) at baseline (white) and after 3 months (black stripes). C) Bar graph showing plasma proCPU levels at baseline (white) and after 3 months (black stripes) in 3 subsets of statin patients. Subset 1: patients with baseline proCPU levels similar to those of control

subjects and no proCPU decrease under influence of a statin (N = 4). Subset 2: patients with baseline proCPU levels similar to those of control subjects and a 5% to 10% decrease in proCPU levels after 3 months of statin use (N = 5). Subset 3: patients in whom baseline proCPU levels were 20% higher and in which statin treatment resulted in an approximately 20% decrease after 3 months (N = 7). **D) Bar graph showing Δ CLT at baseline (white) and after 3 months (black stripes) in 3 subsets of statin patients.** Subset definitions are shown in panel C. **E) Correlation between baseline proCPU levels and the decrease in proCPU (Δ proCPU) in statin-treated individuals (N = 16).** **F) Correlation between baseline Δ CLT and the change in Δ CLT in statin-treated individuals (N = 16).** Data are presented as mean \pm SD in panels A, B, C and D. Wilcoxon matched-pairs signed-rank test, * $p < 0.05$, ** $p < 0.01$. NS = not significant. Spearman correlation coefficient r was determined, and the best-fit line (solid line) with 95% confidence bands was plotted (dashed lines) in panels E and F.

4.4.3 Downregulation of proCPU by statin therapy has a non-lipid related pleiotropic character

To evaluate the nature of the effect of statins on the CPU system, the correlation between the difference in proCPU levels and the decrease in LDL-C levels was investigated. No association was observed between these parameters ($r = 0.26$; $p = 0.32$) (Figure 4-2A).

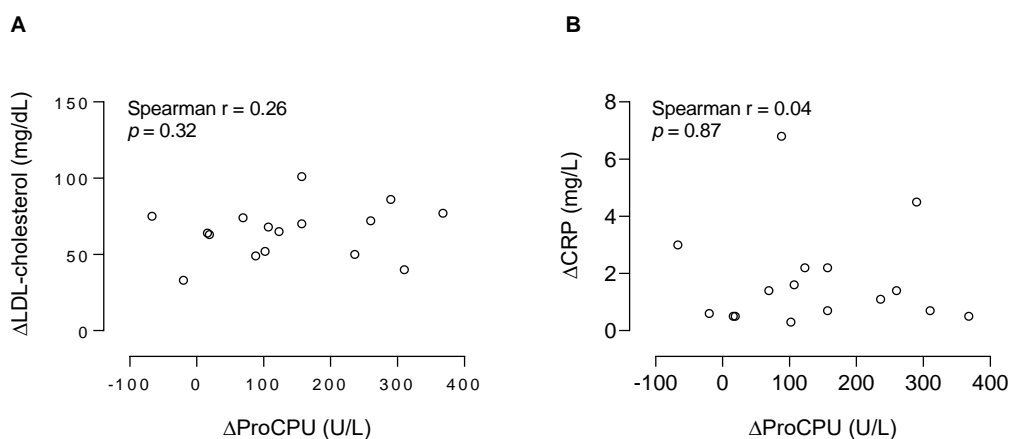


Figure 4-2. Correlation of proCPU levels with LDL-cholesterol and CRP in statin-treated patients. **A)** Correlation between the decrease in proCPU (Δ proCPU) and the decrease in low-density lipoprotein cholesterol (Δ LDL-cholesterol) in statin-treated individuals (N = 16). **B)** Correlation between Δ proCPU and the change in C-reactive protein levels (Δ CRP) in statin-treated individuals (N = 16). Spearman correlation coefficient r was determined.

Plasma CRP was significantly increased in patients with hyperlipidemia ($p = 0.04$) and decreased by statin therapy (48%; $p < 0.001$), while unchanged in the control population (Table 4-2). No association was found between the statin-induced reduction in both CRP and proCPU levels ($r = 0.04$; $p = 0.87$) (Figure 4-2B).

4.4.4 Plasma fibrinolysis potential improves under influence of statin therapy

Participants' CLTs were measured as an indicator of their plasma fibrinolytic potential. CLTs at inclusion tended to be higher in statin-treated patients compared with control subjects (68.7 ± 27.4 min vs 65.4 ± 10.7 min; $p = 0.34$). Furthermore, the CLT did not change in control subjects during follow-up (mean change 1.4 min; $p = 0.87$), whereas this parameter was significantly lowered in statin-treated patients (mean change -3.2 min; $p = 0.03$) (Table 4-2).

The addition of the carboxypeptidase inhibitor PTCl resulted in similar CLTs (presented as CLT_{PTCl} in Table 4-2) in patients and control subjects at both time points. The ΔCLT was shortened by 3.0 min ($p = 0.001$) under the influence of statin therapy, whereas the ΔCLT was not significantly changed over time in control subjects (1.2 min; $p = 0.74$) (Figure 4-1B and Table 4-2).

A correlation was observed between the baseline ΔCLT and the change in ΔCLT after 3 months of statin treatment ($r = 0.57$; $p = 0.035$) (Figure 4-1F). Moreover, the mean change in ΔCLT corresponded with the observed decrease in proCPU levels in the earlier described subpopulations, with the largest improvement in fibrinolysis seen in the subpopulation with the highest baseline proCPU levels and largest proCPU decrease upon statin treatment (Figure 4-1D and Figure 4-3).

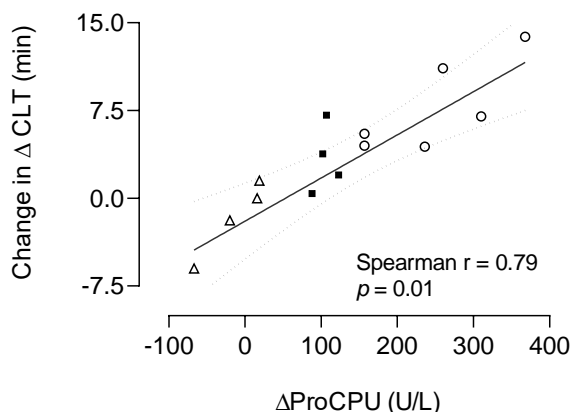


Figure 4-3. Correlation between the change in proCPU levels (Δ proCPU) and the change in Δ CLT (actual contribution of the CPU system to the total clot lysis time) in statin-treated individuals. Each symbol represents a different subset: Open triangle = subset 1 (N = 4); black square = subset 2 (N = 4); open dot = subset 3 (N = 6). Spearman correlation coefficient r was determined, and the best-fit line (solid line) with 95% confidence bands was plotted (dashed lines).

sTM levels were the same in control subjects and statin-treated patients at both the time of inclusion (3.3 ± 0.2 ng/mL and 3.1 ± 1.2 ng/mL, respectively; $p = 0.38$) and 3 months later (3.1 ± 0.4 ng/mL and 3.0 ± 0.8 ng/mL; $p = 0.74$) (Table 4-2).

4.5 Discussion

The finding of increased proCPU levels in patients with hyperlipidemia (compared with age-matched control subjects) is similar to previously reported results [155,179,322]. Moreover, a proCPU decrease after statin treatment has also been described previously. However, this study is the first to identify subpopulations based on the high interindividual variation observed in both baseline proCPU levels and the decrease in proCPU. An improvement in fibrinolysis is to be expected, at least in the subpopulation in which baseline proCPU levels were 20% higher and in which statin treatment resulted in approximately 20% decrease after 3 months. As a result, these individuals with high proCPU concentrations are likely to benefit most from statin therapy [183].

The nature of the effect of the HMG-CoA reductase inhibitors on the CPU system (lipid- or non-lipid-related) was further investigated. The lack of an association between the

difference in proCPU levels and the decrease in LDL-C levels suggests that statins downregulate plasma proCPU concentrations in a non-lipid related manner. In agreement with previous research, an increase in plasma CRP levels was observed in patients with hyperlipidemia as well as a decrease of this parameter under the influence of statin treatment [324]. The reduction in CRP during statin therapy is described as being independent of the magnitude of the LDL-C reduction and is considered indirect proof of the presence of pleiotropic effects of statins [324,325]. In this light, the correlation between the statin-induced reduction in both CRP and proCPU levels was investigated. Because no association was found, the mechanism underlying the reduction of both these parameters seems to be different.

Measurement of the participants' CLTs showed that statin administration improved the fibrinolytic potential in the statin cohort. A profibrinolytic effect of statins was also observed in 126 patients with prior VTE receiving rosuvastatin [155]. In the same study, the fibrinolytic potential was reported to be unchanged during follow-up in 121 non-rosuvastatin users.

Moreover, the observation that the CLT_{PTCI} was similar in both groups at both time points is an indication that the *in vitro* fibrinolytic capacity excluding the CPU system was not significantly affected by hyperlipidemia or by statin therapy. However, when evaluating the actual contribution of the CPU system to the total CLT (ΔCLT), a mean change over time of -3.0 min was observed for statin-treated patients. Based on the CPU threshold mechanism, the mean reduction of 138 U/L in proCPU levels under the influence of statin therapy theoretically corresponds to a reduction in the ΔCLT of approximately 2.7 min [118]. This finding is in line with the observed change in the ΔCLT .

Furthermore, the fact that the largest improvement in fibrinolysis was seen in those statin-treated patients with the highest baseline proCPU levels and the largest proCPU decrease indicates that the profibrinolytic effect seen in statin users can, at least partly, be explained by the downregulation of plasma proCPU concentrations. Although the

clinical relevance (reduction in morbidity and mortality) of the observed phenomenon is not yet clear, these observations highlight that individuals with high proCPU concentrations are especially likely to benefit from statin therapy.

Traces of sTM prolong fibrinolysis as a result of their ability to increase the catalytic efficiency of proCPU activation 1250-fold [41]. Increased sTM levels can therefore result in prolonged CLTs. In the present study, sTM levels were equal in control subjects and statin-treated patients at both time points. This is a strong indicator that the difference in CLT during follow-up is the result of lower proCPU levels and cannot be attributed to alterations in proCPU activation.

Our study confirms recently published data [155]; it additionally focuses on all details of the proCPU/CPU system and has a longer follow-up time. Furthermore, particular attention was paid to the selection of the proCPU assay: proCPU measurements were performed with a thoroughly validated activity-based assay that allows selective measurement of proCPU and is not accompanied by important limitations, including unequal reactivity toward different isoforms of the proCPU Thr325Ile polymorphism [81,136,326]. Due to the small sample size and the statin and control populations not being matched on sex, the results serve as pilot data that need to be explored in a large cohort. In addition, further research is needed to more accurately determine the target proCPU level to obtain a beneficial effect of statin therapy, as well as to unravel whether the proCPU downregulation under the influence of statin therapy is a class-mediated effect and if the effect is dose-dependent.

4.6 Conclusion

This pilot study found that increased proCPU levels are present in patients with hyperlipidemia. Treatment of these patients with a statin led to a significant average decrease of 11.6% in proCPU levels and brought the proCPU concentration to the same level as in control subjects. On a functional level, improvement in plasma fibrinolysis (as

measured by the change in ΔCLT) was observed in the statin group, which could be linked to the observed proCPU decrease. Moreover, the largest improvement in fibrinolysis was seen in patients with the highest baseline proCPU levels. The latter should be examined further in a large cohort not only to identify the clinical relevance of this observation but also as it offers the hypothesis that it might be valuable to include proCPU measurement in the risk assessment for starting statin therapy.

Chapter 5

Pleiotropic effects of atorvastatin result in a downregulation of the CPU system in a mouse model of advanced atherosclerosis

Based on:

Claesen K, Roth L, Mertens JC, Hermans K, Sim Y, Hendriks D. Pleiotropic Effects of Atorvastatin Result in a Downregulation of the Carboxypeptidase U System (CPU, TAF1a, CPB2) in a Mouse Model of Advanced Atherosclerosis. *Pharmaceutics*. 2021; 13(10):1731.

5 Pleiotropic effects of atorvastatin result in a downregulation of the CPU system in a mouse model of advanced atherosclerosis

5.1 Abstract

Background

Statins lower proCPU. However, it is challenging to prove whether this is a lipid or non-lipid related pleiotropic effect since statin treatment decreases cholesterol levels in humans. In apolipoprotein E-deficient mice with a heterozygous mutation in the fibrillin-1 gene (ApoE^{-/-} Fbn1^{C1039G+/-}), a model of advanced atherosclerosis, statins do not lower cholesterol. Consequently, studying the cholesterol-independent effects of statins can be achieved more straightforwardly in these mice.

Methods

Female ApoE^{-/-} Fbn1^{C1039G+/-} mice were fed a Western diet (WD). At week 10 of WD, mice were divided into a WD group (receiving WD only) and a WD + atorvastatin group (receiving 10 mg/kg/day atorvastatin + WD) group. After 15 weeks, blood was collected from the retro-orbital plexus, and the mice were sacrificed. Total plasma cholesterol and CRP were measured with commercially available kits. Plasma proCPU levels were determined with an activity-based assay.

Results

Total plasma cholesterol levels were not significantly different between both groups, while proCPU levels were significantly lower in the WD + atorvastatin group. Interestingly proCPU levels correlated with CRP and circulating monocytes.

Conclusion

In conclusion, our results confirm that atorvastatin downregulates proCPU levels in ApoE^{-/-} Fbn1^{C1039G+/-} mice on a WD, and evidence was provided that this downregulation is a pleiotropic effect of atorvastatin treatment.

5.2 Introduction

The zymogen proCPU circulates in plasma and is converted into the active enzyme CPU by thrombin(-thrombomodulin) or plasmin [3,41]. CPU potently attenuates fibrinolysis through the cleavage of C-terminal lysines on partially degraded fibrin, thereby interfering with efficient plasminogen activation [41]. Lowering proCPU levels will improve the fibrinolytic capacity and is therefore expected to be beneficial in individuals at high risk for thromboembolic diseases. Furthermore, CPU has been shown to modulate inflammation through the cleavage of proinflammatory mediators (e.g., C3a, C5a, bradykinin) [84,254]. Statins (inhibitors of HMG-CoA reductase) exert cardiovascular protective effects that are independent of the lowering of LDL-C, including profibrinolytic effects such as the reduction of proCPU levels in hyperlipidemic patients [222,317,322,327]. However, it is challenging to prove whether this is a lipid or a non-lipid-related pleiotropic effect, since lowering cholesterol is inherent to statin treatment in humans. In ApoE^{-/-} Fbn1^{C1039G^{+/-}} on a WD – a model of advanced atherosclerosis – statins do not significantly lower cholesterol [320,328]. Therefore, this model was used in the current study to investigate the effect of atorvastatin treatment on proCPU biology in a cholesterol-independent setting.

5.3 Materials and methods

This research is a *post-hoc* analysis within the study of Roth *et al.* on the cholesterol-independent effects of atorvastatin on the prevention of cardiovascular morbidity and mortality in a mouse model of atherosclerotic plaque rupture [320].

5.3.1 Animals and study protocol

Female ApoE^{-/-} Fbn1^{C1039G^{+/-}} mice were housed in a temperature-controlled room with a 12 h light/dark cycle and had free access to water and food. At an age of 6 weeks, all mice were fed a WD (4021.90, AB Diets, the Netherlands) for 10 weeks; then, the ApoE^{-/-} Fbn1^{C1039G^{+/-}} mice were randomly divided into two groups. A WD was continued in both

groups for another 15 weeks, but only in one group was the diet supplemented with atorvastatin (10 mg/kg/day, Pfizer, USA). Groups are referred to as mice on WD (N = 21) and atorvastatin-treated mice (N = 20), respectively.

On the 25th week from the initiation of WD, mice were anesthetized by an intraperitoneal injection of ketamine (100 mg/kg) and xylazine (10 mg/kg) for blood sampling. Blood was collected via the retro-orbital plexus into tubes containing EDTA (final concentration 5 mM) and kept on ice. Afterward, samples were centrifuged for 15 min at $2000 \times g$ at 4 °C, then aliquoted and stored at -80 °C until further analysis. Subsequently, mice were sacrificed with sodium pentobarbital (250 mg/kg, i.p).

Cases of sudden death during the experiment were documented. All animal procedures were approved by the ethics committee of the University of Antwerp (UAntwerp; EC nr. 2014-15; 01/04/2014) and complied with the guidelines from Directive 2010/63/EU of the European Parliament on the protection of animals used for scientific purposes.

5.3.2 Activity assay for the measurement of proCPU in plasma of mice

To accurately determine the proCPU concentration in mouse plasma samples, preanalytical and analytical variables (including the thrombin-thrombomodulin concentration, preincubation time, preincubation temperature and substrate concentration) of an in-house, activity-based human proCPU assay were optimized. EDTA plasma from female ApoE^{-/-} mice on a normal diet (N = 6) and the following reagents were used for the optimization: rabbit-lung thrombomodulin (Seikisui Diagnostics, USA), Bz-o-cyano-Phe-Arg (Laboratory of Medicinal Chemistry, University of Antwerp, Belgium), HEPES, human thrombin, PPACK and CaCl₂ (all from Merck, Germany) [81]. The within and between-run imprecision of the adapted assay was determined, and the cut-off oxyHb level – resulting in a 10% reduction of the proCPU concentration – was defined according to Mertens *et al.* using hemolysate obtained by the lysis of red blood cells from ApoE^{-/-} mice on a normal diet (N = 6) [200].

Subsequently, plasma proCPU levels of ApoE^{-/-} Fbn1^{C1039G^{+/-}} mice on WD and WD + atorvastatin therapy were measured with the newly validated assay. The method described by Kahn *et al.* was used to determine cell-free oxyHb levels in all samples [329].

5.3.3 Measurement of total plasma cholesterol, CRP and blood immune cells

Total plasma cholesterol and CRP were measured with commercially available ELISA kits (Total cholesterol, Randox, UK and MCRP00, R&D systems, USA respectively).

Red blood cells in EDTA whole blood were lysed (red blood cell lysing buffer Hybri-Max, Sigma, USA), followed by the labeling of the remaining leukocytes (monocytes, neutrophils and dendritic, natural killer [NK], natural killer T [NKT] and T cells). Next, labeled leukocytes were analyzed by flow cytometry as described previously [320].

5.3.4 Statistical analysis

All data were expressed as mean \pm SD. Statistical analysis and data plotting were performed using GraphPad Prism version 9.3.1 (GraphPad Software, Inc., USA). Statistical tests are specified in the figure legends. Results were considered significant at $p < 0.05$.

5.4 Results and discussion

5.4.1 Activity assay for the measurement of proCPU in mice

Our in-house assay for proCPU measurement in human citrated plasma was adapted for use in mice EDTA plasma [81]. The quantitative activation of proCPU in mice samples was found to be optimal when plasma was diluted 10-times in HEPES (20 mmol/L, pH 7.4) followed by incubation with 8 nM purified human thrombin, 16 nM rabbit-lung thrombomodulin and 50 mM CaCl₂ for 25 min at 10 °C (Figure 5-1).

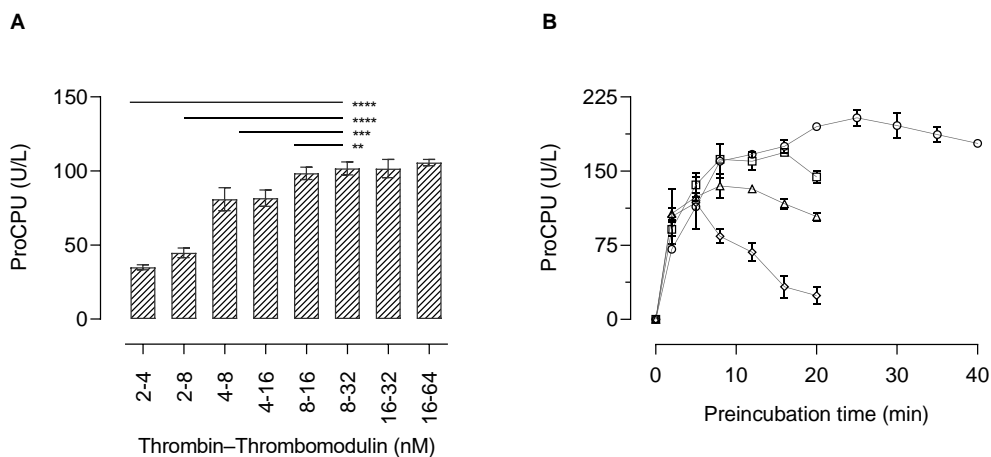


Figure 5-1. A) Optimization of thrombin and thrombomodulin concentration. Plasma samples were activated with 50 mM CaCl_2 and different concentrations of human thrombin and rabbit-lung thrombomodulin in different ratios. Samples were diluted 10-fold in 20mM HEPES (4-(2-hydroxyethyl)-1-piperazineethanesulfonic acid) prior to activation. After 10 min of preincubation with the thrombin–thrombomodulin mixture at 25 °C, CPU activity was quantified. Data represent mean \pm SD (N = 3). A Kruskal-Wallis test with Dunn’s multiple comparison test was used to test for statistical significance between all groups. The significance levels of **, ***, **** correspond to p -values of <0.01, <0.001 and <0.0001, respectively. **B) Effect of preincubation temperature and time interval on proCPU activation.** Plasma samples were diluted 10-fold in 20 mM HEPES. Preincubation with 8 nM human thrombin and 16 nM rabbit-lung thrombomodulin was performed at 10 °C (dots), 15 °C (squares), 20 °C (triangles) and 25 °C (diamonds). At different time points, the reaction was stopped with PPACK (D-Phenylalanyl-L-prolyl-L-arginine chloromethyl ketone). CPU activity was determined by adding Bz-*o*-cyano-Phe-Arg (900 μM), and the formation of Bz-*o*-cyano-Phe was measured by reversed-phase high-performance liquid chromatography (RP-HPLC). Data are presented as mean \pm SD (N = 2).

To determine proCPU activity, the generated active CPU was incubated for 15 min at 25 °C with the specific and selective substrate Bz-*o*-cyano-Phe-Arg (900 μM final concentration) (Figure 5-2). Subsequently, the formed product was quantified by RP-HPLC as previously described [81]. For this assay, 1 unit of enzyme activity was defined as the amount of enzyme required to hydrolyze 1 μmol of substrate per minute at 25 °C under the conditions described.

The modified assay proved to be precise (within-run CV = 2.3%, between-run CV = 4.9%) and oxyHb levels up to 6.5 g/L are allowable (Figure 5-3).

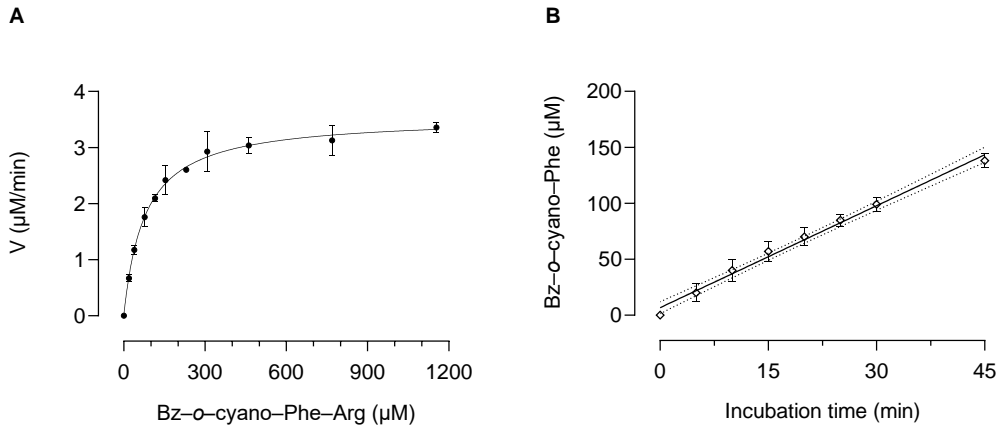


Figure 5-2. A) Michaelis–Menten curve of Bz-*o*-cyano-Phe-Arg cleavage by CPU in mouse plasma. ProCPU in pooled mouse plasma was quantitatively activated. The activation was stopped with PPACK followed by incubation with different concentrations of Bz-*o*-cyano-Phe-Arg (0 – 1150 μM). The initial velocities of product formation were plotted against the different substrate concentrations. A K_m value of $89 \pm 4 \mu\text{M}$ was obtained. Data are presented as mean \pm SD (N = 4). **B) Linearity of substrate conversion.** ProCPU in pooled mouse plasma was activated with thrombin–thrombomodulin followed by incubation with 900 μM of Bz-*o*-cyano-Phe-Arg at 25 °C for different periods of time. The formation of the reaction product Bz-*o*-cyano-Phe was plotted against the incubation time. Data represent mean \pm SD, N = 2. The linear regression curve and its 95% CI (dotted lines) are displayed in black. Linear substrate conversion was achieved up to 45 min.

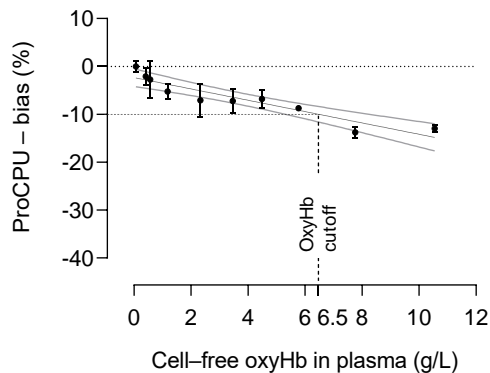


Figure 5-3. Influence of hemolysis on proCPU levels. Different concentrations of oxyhemoglobin (oxyHb; final concentration 0 – 10.5 g/L) (hemolysate) were spiked in mouse plasma and proCPU levels were measured. The bias in the proCPU concentration – compared to the nonhemolytic reference level (black dotted line) – was plotted for each oxyHb concentration. Data are presented as mean \pm SD (N = 3). The linear regression curve (black line) and its 95% CI (grey lines) are displayed. The cut-off oxyHb level (black dashed lines) – resulting in a 10% reduction of the baseline proCPU concentration – was 6.5 g/L.

5.4.2 Total plasma cholesterol

TC was measured in plasma of ApoE^{-/-} Fbn1^{C1039G^{+/-}} mice that were fed a WD (N = 12) or a WD combined with atorvastatin (WD + atorvastatin; 10 mg/kg/day; N = 17). Results confirmed that atorvastatin did not significantly reduce TC in these mice ($p = 0.19$; Figure 5-4A).

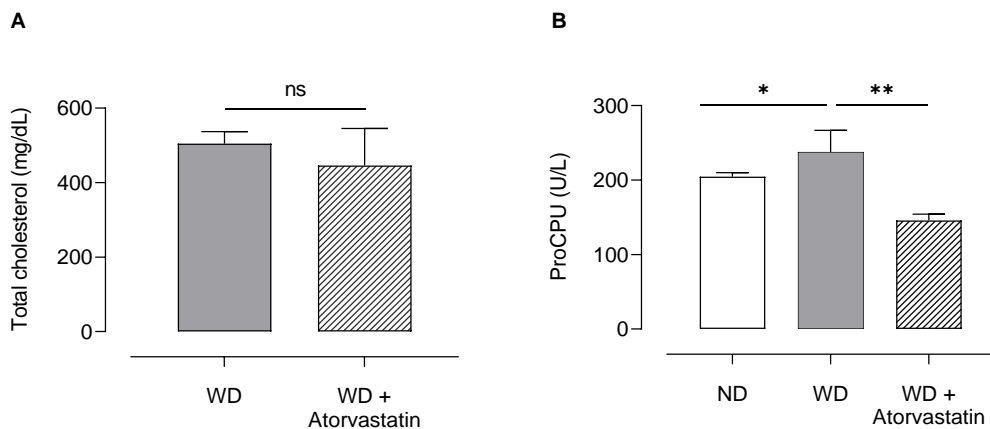


Figure 5-4. A) Bar graph showing total plasma cholesterol levels in ApoE^{-/-} Fbn1^{C1039G^{+/-}} mice on a Western diet (WD) (N = 12) or WD supplemented with atorvastatin (WD + atorvastatin) (N = 17). Data are presented as mean \pm SD. A Mann–Whitney U test was used to test for statistical significance between both groups; $p > 0.05$. **B)** Bar graph showing plasma proCPU levels in the WD group (N = 12), WD + atorvastatin group (N = 15) and in ApoE^{-/-} mice on a normal diet (N = 6). Data are presented as mean \pm SD. A Mann–Whitney U test was used to test for statistical significance; * $p < 0.05$, ** $p < 0.01$.

5.4.3 ProCPU decrease in atorvastatin-treated mice on a western diet is cholesterol-independent

After adapting our in-house activity-based proCPU assay for use in mouse EDTA plasma, plasma proCPU levels were determined, and the effect of atorvastatin on proCPU biology in a cholesterol-independent setting was evaluated. ProCPU levels were found to be significantly lower in mice receiving WD + atorvastatin compared to mice on control WD (159 ± 63 U/L [range 97–227 U/L] vs. 238 ± 101 U/L [range 123–455 U/L]; $p = 0.004$; Figure 5-4B). Similar to observations made in humans, atorvastatin reduced proCPU levels in ApoE^{-/-} Fbn1^{C1039G^{+/-}} mice fed a WD, resulting in plasma proCPU concentrations

similar to those found in ApoE^{-/-} mice on a normal diet (178 ± 32 U/L [range 165–210 U/L]; $p = 0.24$; $N = 6$) [327]. The study design did not allow us to determine the change in proCPU levels before and after treatment with atorvastatin in individual mice. Therefore, it was not possible to establish whether the largest proCPU decrease is seen in mice with the highest baseline proCPU levels – something that was perceived in humans receiving statin therapy [327].

In addition, no correlation was observed between plasma proCPU and TC in the WD group (Figure 5-5A). In this model, the downregulation of proCPU levels is thus a cholesterol-independent, pleiotropic effect of atorvastatin treatment. A possible mechanism for this downregulation is related to peroxisome proliferator-activated receptor α (PPAR α). PPAR α participates in the regulation of various aspects of lipid metabolism in the liver, finally resulting in hypolipidemic effects [330,331]. Kilicarslan *et al.* described that fenofibrate, a PPAR α agonist, decreased proCPU levels in patients with metabolic syndrome, suggesting that agonists of PPAR α possess anti-thrombotic properties through the decrease of circulating proCPU levels on top of their role as anti-lipidemic agents [180]. Moreover, Masuda *et al.* reported on the downregulation of the *CPB2* gene expression and decreases in both *CPB2* mRNA and proCPU antigen levels in HepG2 cells, mediated by the PPAR α signaling pathway upon treatment with the PPAR α agonist WY14643 [332]. Since it has been described that statins increase PPAR α expression (although they are not direct ligands for PPAR α), the hypothesis that statin therapy could increase PPAR α expression – which in turn could lead to reduced *CPB2* gene expression and thus lower plasma proCPU levels – seems plausible but was not further explored in the current work [222,333–335].

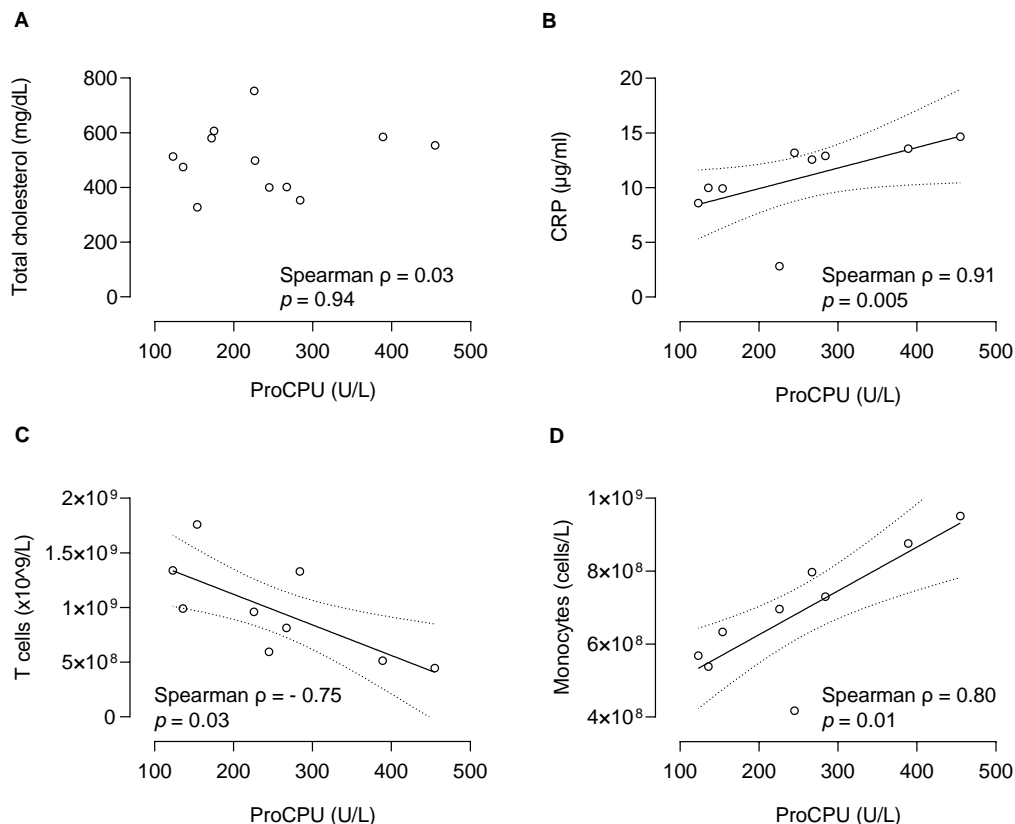


Figure 5-5. Relation between plasma proCPU levels and total plasma cholesterol (A), C-reactive protein (CRP; B), circulating T cells (C) and circulating monocytes (D). Spearman correlation coefficient r was determined for all correlations. In case of a significant correlation ($p < 0.05$), linear regression analysis was performed, and the best-fit line (solid line) with 95% confidence bands was plotted (dashed lines).

5.4.4 Inflammation and blood immune cells

Alongside TC and proCPU levels, plasma CRP and circulating blood immune cells were also measured, revealing that atorvastatin significantly improved the inflammatory blood profile in ApoE^{-/-} Fbn1^{C1039G^{+/-}} mice with significant reductions in plasma CRP ($p = 0.001$) and circulating monocytes ($p < 0.01$; Table 5-1). T cells were significantly increased ($p = 0.01$; Table 5-1). Possible correlations between these parameters and proCPU concentrations were investigated in the WD-fed mice. A clear positive association was found between plasma proCPU and CRP ($r = 0.91$, $p = 0.005$; Figure 5-5B), while a negative association was observed between circulating T cells and plasma proCPU ($r =$

-0.75, $p = 0.03$; Figure 5-5C). Moreover, proCPU levels also correlated with circulating monocytes ($r = 0.80$, $p = 0.01$), meaning that higher proCPU levels occur together with high amounts of these immune cells (Figure 5-5D). Besides liver-derived proCPU, the existence of extra-hepatic proCPU in megakaryocytic and monocytic cell lines (cell lysates and conditioned media) has been reported [46,71]. Lin and co-workers also suggested that these cells may be a source of proCPU within atherosclerotic plaques as well as in other extravascular sites during inflammation [46,49]. Hence, monocyte-derived proCPU could contribute to the increase in plasma proCPU concentration in WD mice, although presumably only to a limited extent since the liver remains the main source of circulation proCPU [326]. Interestingly, it was demonstrated that inflammatory cytokines (both pro and anti-inflammatory), which are abundantly present and upregulated in atherosclerosis, increase proCPU secretion in monocytes [21,46]. Consequently, the reduction of inflammatory cytokines and circulating monocytes induced by atorvastatin therapy could (partly) be attributed to the decrease in proCPU levels that is also seen with this therapy.

Table 5-1. Inflammation and blood immune cells.

Parameter		WD	WD + atorvastatin	<i>p</i> -value
CRP	($\mu\text{g/mL}$)	10.9 \pm 3.6	7.4 \pm 2.6	0.001
Leukocytes	($10^9/\text{L}$)	5.20 [4.13 – 8.08]	6.50 [5.13 – 7.53]	0.35
Monocytes	($10^9/\text{L}$)	0.63 [0.55 – 0.84]	0.29 [0.19 – 0.43]	0.01
Neutrophils	($10^9/\text{L}$)	1.87 [1.08 – 2.94]	2.44 [1.42 – 3.04]	0.08
Dendritic cells	($10^9/\text{L}$)	0.039 [0.016 – 0.13]	0.083 [0.060 – 0.11]	0.16
T cells	($10^9/\text{L}$)	0.81 [0.48 – 1.37]	1.26 [1.01 – 1.93]	0.01
NK cells	($10^9/\text{L}$)	0.47 [0.31 – 0.67]	0.45 [0.36 – 0.63]	0.93
NKT cells	($10^9/\text{L}$)	0.039 [0.034 – 0.10]	0.057 [0.042 – 0.91]	0.49

Data are expressed as median with interquartile range. CRP: c-reactive protein; NK cells: natural killer cells; NKT cells: natural killer T cells; WD: ApoE^{-/-} Fbn1^{C1039G^{+/+}} on a western diet (N = 9–12); WD + atorvastatin: ApoE^{-/-} Fbn1^{C1039G^{+/+}} receiving a Western diet supplemented with atorvastatin (10 mg/kg/day) (N = 15–17). A Mann-Whitney U test was used to test for statistical significance.

The importance of the correlation between proCPU and circulating T cells is not clear; in particular, because — to the best of our knowledge — *CPB2* expression and regulation have not yet been studied in T cells, complicating the correct interpretation of these results.

5.5 Conclusion

In conclusion, our results confirm that atorvastatin downregulates proCPU levels in ApoE^{-/-} Fbn1^{C1039G^{+/-}} mice on a WD, in line with the observations in humans. As a result, this therapy improves fibrinolytic capacity in addition to its lipid-lowering properties. Evidence is provided that this downregulation is a pleiotropic effect of statin treatment. Furthermore, this report is to our knowledge the first to describe a correlation between plasma proCPU levels and certain circulating immune cells. Elucidating the role of these immune cells in the atorvastatin-induced downregulation of the CPU system and looking into the involvement of the PPAR α pathway will provide valuable information to help unravel the molecular mechanism by which atorvastatin modulates plasma proCPU levels.

Chapter 6

ProCPU as a novel marker for identifying benefit from atorvastatin therapy

Based on:

Claesen K, Sim Y, De Belder S, van den Keybus T, Van Edom G, Stoffelen H, De Keulenaer G, Bosmans J, Bringmans T, De Meester I, Hendriks D. Procarboxypeptidase U (proCPU, TAFI, CPB2) as a novel marker for identifying benefit from atorvastatin therapy. Manuscript submitted.

6 ProCPU as a novel marker for identifying benefit from atorvastatin therapy

6.1 Abstract

Background

Statins efficiently lower cholesterol and also exert pleiotropic effects that extend beyond lipid-lowering [222,336]. In a recent pilot study, valuable information on the CPU system in hyperlipidemia and the effect of statin therapy was collected. It was shown that proCPU levels are increased in hyperlipidemic patients. Statin treatment significantly decreased proCPU levels and improved plasma fibrinolysis. Furthermore, it was suggested that patients with high baseline proCPU levels are most likely to benefit from statin therapy [327].

Aims

We aimed to further substantiate the hypothesis that including proCPU measurement in the risk assessment for statin therapy may be valuable. Additionally, we investigated whether the proCPU lowering effect of statin therapy is dose-dependent.

Methods

Blood was collected from 141 individuals treated with different dosages of atorvastatin (10 – 80 mg), 38 normolipidemic- and 37 hyperlipidemic controls. Lipid parameters and markers of fibrinolysis (proCPU levels and CLT) were determined and compared between the groups.

Results

Pilot study results of high proCPU levels in hyperlipidemic patients and the proCPU reducing effect of atorvastatin were confirmed. Accordingly, an improvement in plasma fibrinolytic potential (as measured by Δ CLT; actual contribution of the CPU system to the total CLT) was seen under influence of atorvastatin. High interindividual variation in

proCPU levels was observed in the hyperlipidemic cohort, with up to 80% higher proCPU levels compared to normolipidemic controls. Furthermore, proCPU concentration and the dosage of atorvastatin were inversely correlated.

Conclusion

The current results support the hypothesis that measurement of proCPU or Δ CLT in risk assessment might be valuable additional parameters for starting statin therapy, in particular for those patients where there are doubts about starting statin therapy based on conventional risk factors.

6.2 Introduction

Statins effectively lower cholesterol by inhibiting the HMG-CoA reductase enzyme [211,336]. Moreover, the clinical benefits of this therapy extend beyond lipid-lowering effects with various pleiotropic effects evidenced in experimental and clinical studies, including enhanced stability of atherosclerotic plaques, profibrinolytic properties and decreased vascular inflammation [222,336].

CPU provides a molecular link between coagulation and fibrinolysis. By cleaving C-terminal lysines from partially degraded fibrin it counteracts efficient plasminogen activation, thereby attenuating the fibrinolytic rate [2,115]. CPU circulates in plasma as the zymogen proCPU. Several studies have been conducted, evaluating the potential association of proCPU levels with cardiovascular risk factors and whether proCPU levels can be affected by lifestyle modifications or certain pharmacological treatments [326]. A limited number of studies currently available point to an association between high proCPU levels and hyperlipidemia. Treatment of hyperlipidemic individuals with statin therapy normalized their proCPU levels and on a functional level a resulting improvement of the fibrinolytic rate was observed [155,174,179,327]. Our recent pilot study revealed that the statin-dependent decline in plasma proCPU concentrations is highly different interindividually with the largest improvement in fibrinolytic rate seen

in patients with the highest pre-treatment proCPU levels [327]. Evidence that the proCPU downregulation in response to statins is a pleiotropic effect of this therapy was also provided in a murine model of atherosclerosis [337]. In the present study, our first goal was to further substantiate the hypothesis that including proCPU measurement in risk assessment for statin therapy might be valuable. The second aim was to explore whether additional reductions in proCPU levels can be obtained when increasing the statin dose.

6.3 Materials and methods

6.3.1 Study design

Patients (≥ 18 years of age) currently treated with atorvastatin (10 mg or more daily) for hyperlipidemia, as well as age- and sex-matched healthy controls (no hyperlipidemia) and patients with untreated hyperlipidemia were recruited by the collaborating general practitioners' office (Epione, Edegem) and cardiologists of the Antwerp University Hospital (UZA) and ZNA Middelheim Hospital. Starting from the results of our earlier pilot study, a sample size of 32 participants per group was estimated to achieve an overall study power of 90% with a significance level of 0.05, for detecting a true difference in mean proCPU levels of 125 U/L between two study groups [327,338].

All individuals included presented at the general practitioner or cardiology department for routine physical examination or renewal of chronic prescription drugs and had no history of acute CVD in the previous month nor a recent COVID-19 infection (defined as a positive SARS-CoV-2 polymerase chain reaction- [PCR] or rapid antigen test [RAT] < 2 months before inclusion) [339]. Other exclusion criteria for all groups were (chronic) liver disease, pregnancy, glomerular filtration rate < 30 mL/min and the use of lipid-lowering drugs (other than atorvastatin for the statin-treated group, except for ezetimibe in a limited number of atorvastatin-treated patients). Inclusion criteria were TC ≥ 190 mg/dL and LDL-C ≥ 115 mg/dL for the hyperlipidemic controls and TC ≤ 190 mg/dL and LDL-C ≤ 115 mg/dL for the normolipidemic controls [229].

The study was approved by the institutional Ethics Committee UZA/UAntwerp (B3002021000051), and written informed consent was obtained from all participants before inclusion.

6.3.2 Sample collection

A citrated blood sample (3.2% trisodium citrate tube, 9:1 v/v; BD Vacutainer, USA) and a serum sample (serum separator tube; BD Vacutainer, USA) were collected from all participants. The blood samples were centrifugation (15 min at 2000 x *g* and 4 °C), aliquoted and stored at -80 °C in the local biobank (BE71030031000) until use. Citrated plasma samples were used to determine proCPU levels and clot lysis times. Serum samples were used to determine lipid parameters. A small amount of citrated whole blood was kept apart for the determination of the proCPU Thr325Ile polymorphism.

6.3.3 ProCPU measurement and clot lysis assay

Plasma proCPU levels were measured using an in-house developed method as previously described [81]. *In vitro* clot lysis was performed in the presence and absence of PTCl following the protocol of Leenaerts *et al.* [206]. The clot lysis time (CLT; the time between half-maximal turbidity during coagulation and fibrinolysis) was calculated automatically [205]. The total contribution of the CPU system to plasma clot lysis, expressed as Δ CLT (the absolute reduction in CLT after addition of PTCl) was determined as well [205].

6.3.4 Lipid- and other measurements

TC, HDL-C, and TG were measured on a Siemens Healthineers Atellica CH Analyzer (Siemens Healthcare Diagnostics, Canada). LDL-C and non-HDL-C levels were calculated using the Friedewald formula or by subtracting HDL-C from TC respectively.

OxyHb levels were assessed and severely hemolytic samples were excluded as severe hemolysis interferes with CPU-related assays [200]. The Thr325Ile proCPU polymorphism was determined according to Zorio *et al.* [145].

6.3.5 Statistical analysis

Results are expressed as mean \pm SD. GraphPad Prism version 9.3.1 (GraphPad Software, La Jolla, California) was used for statistical analysis and data plotting. A One-Way Anova with Tukey multiple comparison tests was used to compare continuous variables (unpaired data). Categorical data were evaluated with a χ^2 test. Pearson correlation coefficients were computed to assess the association between proCPU – LDL-C and proCPU – Δ CLT. Results with a p -value < 0.05 were considered statistically significant.

6.4 Results and discussion

6.4.1 Study population

Between March and December 2021, 226 individuals were included in the study (Table 6-1). Thirty-eight individuals formed the normolipidemic control group and 37 the hyperlipidemic control group. The group of atorvastatin-treated patients consisted of 141 individuals, divided into subgroups of approximately 35 patients each based on the dose of atorvastatin used (10 – 80 mg). Atorvastatin users were more likely to be on antihypertensive ($p < 0.001$), antiaggregant ($p < 0.001$) and anticoagulant ($p = 0.002$) drugs than non-users (normolipidemic and hyperlipidemic) (Table 6-1). Other characteristics were similar in all study (sub)groups.

Lipid profiles obtained from atorvastatin-treated patients and control subjects are shown in Table 6-1. TC, LDL-C and non-HDL levels were significantly higher in hyperlipidemic patients compared to the normolipidemic control group and all atorvastatin subgroups (all $p < 0.0001$). As expected, treatment with a higher dose of atorvastatin resulted in lower TC, LDL-C and non-HDL-C concentrations, suggesting good therapy adherence.

Table 6-1. Baseline characteristics, biochemical- and CPU-related parameters of normolipidemic controls, hyperlipidemic controls and atorvastatin-treated patients (with or without ezetimibe).

	Normolipidemic controls	Hyperlipidemic controls	Atorvastatin-treated patients					Atorvastatin + ezetimibe*	p-value
			All	10 mg	20 mg	40 mg	80 mg		
Demographics									
Number – N	38	37	141	34	35	35	37	10	
Age – years (range)	65 (42 – 88)	62 (43 – 80)	68 (42 – 92)	68 (49 – 92)	70 (53 – 85)	66 (42 – 89)	66 (47 – 83)	63 (47 – 83)	0.13†
Male sex – N (%)	26 (68)	23 (62)	91 (65)	21 (68)	22 (63)	23 (66)	25 (68)	7 (70)	0.96‡
BMI – kg/m ² (mean ± SD)	26.9 ± 4.4	26.9 ± 4.3	27.7 ± 4.6	26.9 ± 4.2	26.9 ± 4.5	28.5 ± 4.8	28.6 ± 4.8	27.1 ± 4.4	0.39†
Smoking – N (%)	5 (13)	5 (14)	11 (8)	4 (13)	0 (0)	3 (9)	4 (11)	2 (20)	0.51‡
Genotype *									
Ile/Ile – N (%)	3 (8)	5 (13)	14 (10)	5 (15)	1 (3)	4 (11)	4 (11)	1 (10)	0.46‡
Thr/Ile – N (%)	23 (60)	15 (41)	69 (49)	18 (53)	14 (40)	18 (51)	19 (51)	6 (60)	
Thr/Thr – N (%)	12 (32)	17 (46)	58 (41)	11 (32)	20 (57)	13 (37)	14 (38)	3 (30)	
Blood pressure									
Systolic – mmHg (mean ± SD)	132 ± 17	139 ± 16	136 ± 16	138 ± 19	134 ± 12	137 ± 17	133 ± 15	130 ± 13	0.38†
Diastolic – mmHg (mean ± SD)	78 ± 14	82 ± 8	77 ± 9	75 ± 10	78 ± 9	79 ± 10	77 ± 7	80 ± 8	0.15†
Medication use (N (%))									
Antihypertensive	24 (65)	18 (51)	118 (87)	25 (81)	29 (83)	33 (97)	31 (86)	10 (100)	<0.001‡
Antiaggregant	8 (22)	6 (17)	86 (64)	17 (57)	17 (49)	22 (65)	30 (83)	9 (90)	<0.001‡
Anticoagulant	3 (8)	2 (6)	38 (29)	6 (20)	6 (17)	14 (42)	12 (34)	3 (30)	0.002‡
Antidiabetic	3 (8)	1 (3)	26 (19)	5 (16)	4 (11)	7 (21)	10 (28)	4 (40)	0.06‡
Antidepressant	2 (6)	2 (6)	14 (10)	3 (10)	7 (20)	1 (3)	3 (8)	1 (10)	0.20‡

	Normolipidemic controls	Hyperlipidemic controls	Atorvastatin-treated patients					Atorvastatin + ezetimibe*	p-value
			All	10 mg	20 mg	40 mg	80 mg		
Lipid parameters (mean ± SD)									
TC – mg/dL	166 ± 28	243 ± 41	152 ± 38	167 ± 36	161 ± 31	149 ± 35	133 ± 38	120 ± 19	<0.0001†
LDL-C – mg/dL	92 ± 20	153 ± 34	76 ± 28	90 ± 29	80 ± 28	72 ± 20	66 ± 31	54 ± 22	<0.0001†
HDL-C – mg/dL	49 ± 11	66 ± 22	52 ± 18	53 ± 21	60 ± 22	49 ± 15	47 ± 12	52 ± 18	<0.0001†
Non-HDL-C – mg/dL	117 ± 27	179 ± 45	98 ± 31	111 ± 29	103 ± 29	94 ± 25	86 ± 34	74 ± 14	<0.0001†
TG – mg/dL	112 ± 48	137 ± 45	122 ± 57	142 ± 77	120 ± 61	136 ± 73	108 ± 62	118 ± 56	0.037†
Markers of fibrinolysis and inflammation (mean ± SD)									
ProCPU – U/L	992 ± 136	1154 ± 187	943 ± 127	1002 ± 127	956 ± 109	924 ± 118	891 ± 131	905 ± 135	<0.0001†
CLT – min	58.3 ± 19.6	74.3 ± 37.2	62.7 ± 17.2	65.7 ± 20	61.6 ± 16.5	59.6 ± 17.0	57.7 ± 10.4	58.1 ± 8.9	0.009†
CLT _{PTCI} – min	38.9 ± 15.4	51.9 ± 14.0	40.0 ± 9.3	42.2 ± 10.2	39.2 ± 9.4	39.7 ± 15.2	39.0 ± 7.3	39.1 ± 8.9	<0.001†
ΔCLT – min	19.4 ± 6.0	24.5 ± 9.3	20.6 ± 10.4	22.4 ± 11.9	21.3 ± 9.4	19.9 ± 12.4	18.7 ± 5.6	19.0 ± 4.1	0.036†

Results are given as number (N) with percentage in parentheses or as mean with standard deviation (SD). A One-Way Anova[†] or a Chi-square test[‡] were used to test for statistical significant between-group differences. * Single nucleotide polymorphism +1040C/T, corresponding to a Thr/Ile substitution at position 325 of proCPU. BMI: body mass index, CLT: clot lysis time; ΔCLT: absolute reduction in CLT after addition of potato tuber carboxypeptidase inhibitor, CLT_{PTCI}: clot lysis time in the presence of potato tuber carboxypeptidase inhibitor, HDL-C: high-density lipoprotein cholesterol, LDL-C: low-density lipoprotein cholesterol, proCPU: procarboxypeptidase U, TC: total cholesterol, TG: triglycerides.

6.4.2 Atorvastatin normalizes high and marked interindividually variable plasma proCPU concentrations and fibrinolytic potential in hyperlipidemic individuals

Plasma proCPU concentrations were significantly higher in hyperlipidemic patients compared to normolipidemic controls (1154 ± 187 vs 992 ± 136 U/L; $p < 0.0001$) (Table 6-1 and Figure 6-1A), which is consistent with our pilot study results [327]. Atorvastatin treatment reduced plasma proCPU levels, resulting in proCPU concentrations that were significantly lower compared to hyperlipidemic controls (943 ± 127 ; $p < 0.0001$), but similar compared to normolipidemic controls (992 ± 136 ; $p = 0.54$). ProCPU results translate on a functional level into a shorter Δ CLT (actual contribution of the CPU system to the total CLT) in atorvastatin-treated patients compared to hyperlipidemic individuals, while similar to normolipidemic controls (Figure 6-1D). Atorvastatin treatment thus clearly improves the fibrinolytic rate (as measured by the Δ CLT) as a result of the downregulation of plasma proCPU concentrations.

High interindividual variation in proCPU was observed in the hyperlipidemic group (Figure 6-1B) and three subpopulations were identified: a cohort with proCPU levels (984 ± 39 U/L) similar to those of the normolipidemic subjects (992 ± 136 U/L; $p = 0.95$); a second cohort with 15% higher proCPU levels (1143 ± 37 U/L); and a third cohort in which proCPU levels were over 1300 U/L and up to 80% higher in comparison to the normolipidemic cohort. Δ CLT of the hyperlipidemic cohort also showed large interindividual differences (Figure 6-1E) that corresponded with the variation in proCPU concentrations (Figure 6-2B). The observation of subpopulations based on high interindividual variation in proCPU levels of hyperlipidemic individuals was first described in our pilot study and related with the decrease in proCPU levels under statin treatment [327]. The study design here did not allow us to investigate the individual decrease in proCPU levels and correlate it with untreated proCPU levels. Nevertheless, also in this population, the largest proCPU downregulation with consequent improvement in fibrinolysis and thus the largest benefit from atorvastatin is expected in individuals with the highest proCPU levels [155,327]. Interestingly, individuals with the

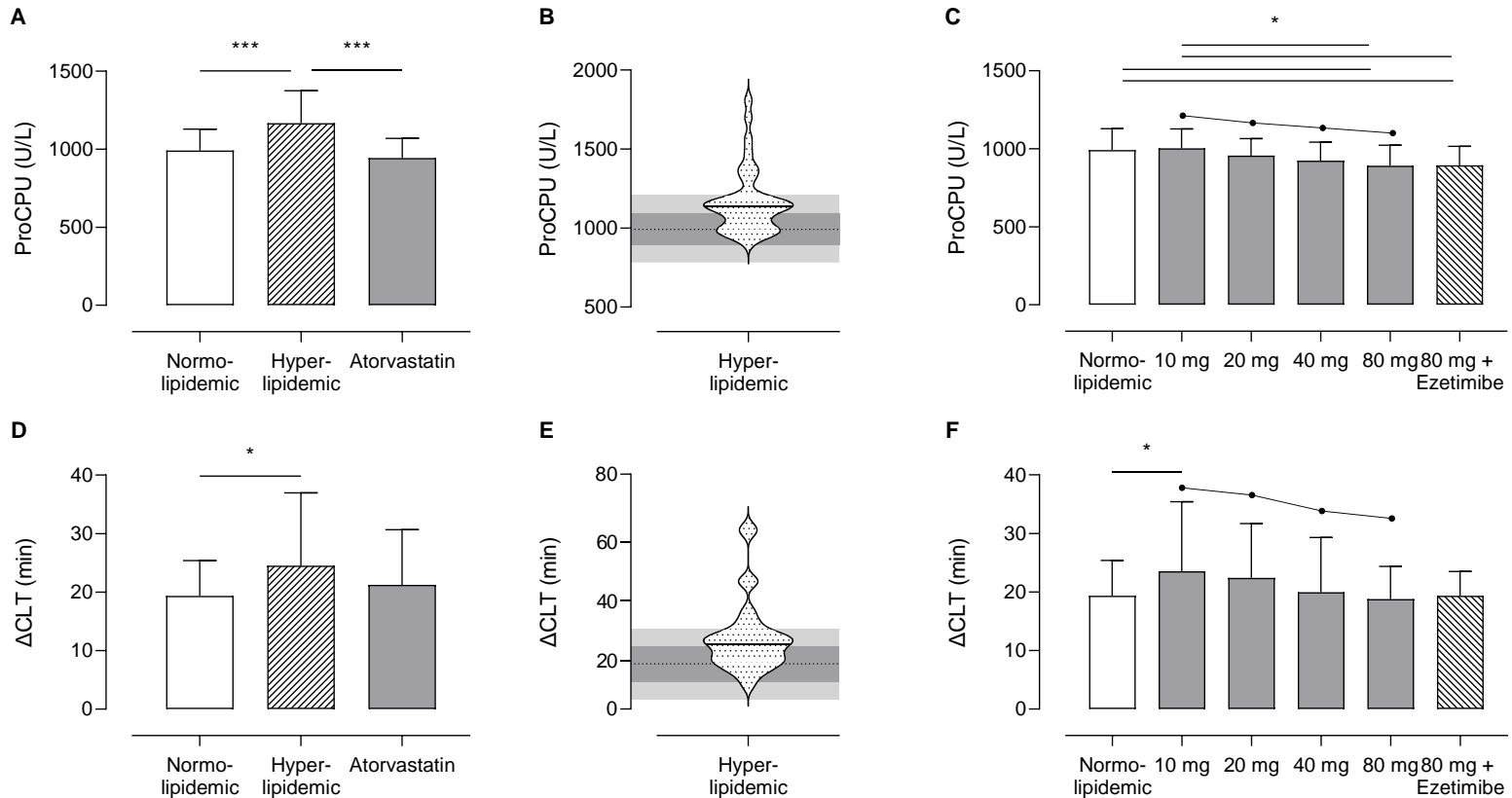


Figure 6-1. A) Bar graph showing plasma proCPU levels in normolipidemic controls (N = 38; white), hyperlipidemic controls (N = 37; black stripes) and in atorvastatin-treated patients (N = 141; grey). B) Violin plot of proCPU levels in hyperlipidemic subjects (N = 37). Subset 1: patients with proCPU levels similar to those of normolipidemic subjects (proCPU hyperlipidemic group < mean proCPU + 1*SD of the normolipidemic group; N = 15). Subset 2: patients with ~15% higher proCPU levels compared to normolipidemic controls (proCPU hyperlipidemic group between mean proCPU + 1*SD and mean

proCPU + 2*SD of the normolipidemic group; N = 14). Subset 3: patients in which proCPU levels were over 1300 U/L and up to 80% higher in comparison to the normolipidemic cohort (proCPU hyperlipidemic group > mean proCPU + 2*SD of the normolipidemic group; N = 8). **C) Bar graph showing proCPU levels in normolipidemic controls (N = 38; white), patients treated with different dosages of atorvastatin (grey: 10 mg (N = 34), 20 mg (N = 35), 40 mg (N = 35) and 80 mg (N = 37)) and patients treated with a combination of atorvastatin 80 mg and ezetimibe 10 mg (N = 10; black stripes).** **D) Bar graph showing Δ CLT (actual contribution of the CPU system to the total clot lysis time (CLT)) in normolipidemic controls (N = 38; white), hyperlipidemic controls (N = 37; black stripes) and atorvastatin-treated patients (N = 141; grey).** **E) Violin plot of Δ CLT in hyperlipidemic subjects (N = 37).** Subset definitions are shown in panel B. Subset 1: N = 5; Subset 2: N = 5; Subset 3: N = 27. **F) Bar graph showing Δ CLT in normolipidemic controls (N = 38; white), patients treated with different dosages of atorvastatin (grey: 10 mg (N = 34), 20 mg (N = 35), 40 mg (N = 35) and 80 mg (N = 37)) and patients treated with a combination of 80 mg atorvastatin and 10 mg ezetimibe (N = 10; black stripes).** Data are presented as mean \pm SD in panels A, C, D, and F and a one-way anova with Tukey multiple comparison test was performed. * $p < 0.05$, *** $p < 0.001$. The horizontal dotted line in panels B and E represents the mean proCPU level or Δ CLT of the normolipidemic controls with the corresponding confidence interval (1*SD: dark grey area; 2*SD: light grey area).

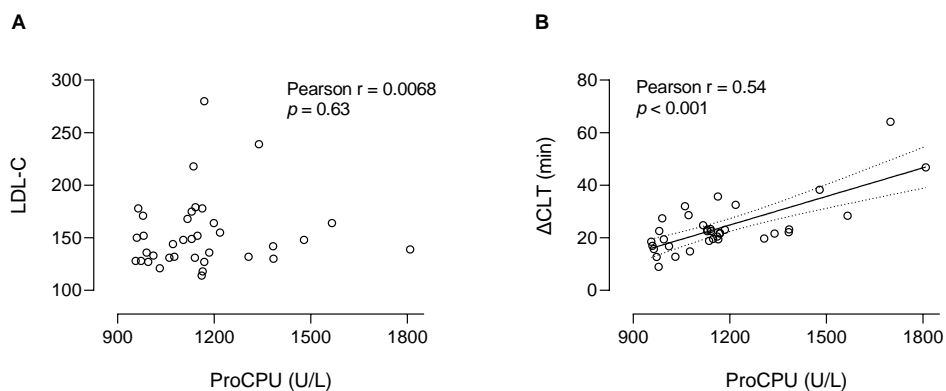


Figure 6-2. Correlation between plasma proCPU levels and low-density lipoprotein cholesterol (LDL-C; A) or Δ CLT (actual contribution of the CPU system to the total clot lysis time [CLT]; B) Pearson correlation coefficient r was determined for all correlations. In case of a significant correlation ($p < 0.05$), linear regression analysis was performed, and the best-fit line (solid line) with 95% confidence bands was plotted (dashed lines).

highest proCPU levels do not necessarily have the highest cholesterol levels (Figure 6-2A). This observation supports the hypothesis that including plasma proCPU and/or Δ CLT measurements in risk assessment for starting statin therapy may be valuable, especially in those cases where conventional risk factors place patients at moderate risk [340,341]. In these cases proCPU and/or Δ CLT measurement (alone or in combination with other cardiovascular biomarkers e.g. CRP) may help to reclassify moderate-risk individuals as high or low risk, thus guiding statin therapy

6.4.3 ProCPU downregulation and increase in fibrinolytic rate by atorvastatin are dose-dependent

The group of atorvastatin-treated patients was divided into subgroups based on the dose of atorvastatin they received. Figure 6-1C clearly shows that lower proCPU levels were measured in patients who received a higher dose of atorvastatin, confirming a clear correlation between the dose of atorvastatin and the magnitude of proCPU lowering. When comparing 10 mg to 20mg, 20 mg to 40 mg or 40 to 80 mg atorvastatin, each time 3-5% (32 – 46 U/L) lower proCPU concentrations were observed with the highest dose

of atorvastatin; and a 11.1% (111 U/L; $p = 0.01$) lower proCPU concentration was measured in the highest (80 mg) vs the lowest (10 mg) atorvastatin dosage group. Based on these results, an improvement in the fibrinolytic rate is expected when increasing the statin dose. The dose-dependent reduction in Δ CLT confirmed this (Figure 6-1F).

At present, LDL-C is the key measure of the success/efficacy of lipid-lowering treatments [340]. However, there may also be a role for proCPU determination in this setting: when there is doubt about choosing moderate- or high-intensity statin therapy or intensifying the treatment based on cardiovascular risk classification and/or LDL-C parameters, proCPU measurement may aid in choosing the intensity of atorvastatin therapy.

6.4.4 Addition of ezetimibe to atorvastatin therapy has no additional effect on proCPU concentrations or plasma fibrinolytic potential

A previous study in mice evidenced that the proCPU downregulation by statin therapy is a pleiotropic effect of this treatment, rather than the result of the lipid-lowering effect [327,337]. The mouse model used in that study has the advantage that statins do not lower cholesterol levels. In contrast, in humans, it is challenging to study the nature (lipid or non-lipid related) of the proCPU downregulation since statin therapy uniformly reduces cholesterol levels in humans. The lack of an association between the change in proCPU levels and the change in LDL-C levels in the initial pilot study was however a first indication that statins also downregulate plasma proCPU concentrations in a non-lipid-related manner in humans. To gather more evidence on the pleiotropic character of statin therapy in humans, a small group of patients ($N = 10$; Table 6-1) treated with atorvastatin 80 mg in combination with ezetimibe 10 mg was included here. Comparison of proCPU and Δ CLT values between this atorvastatin/ezetimibe group and patients treated with monotherapy atorvastatin 80 mg showed that addition of ezetimibe further reduced cholesterol levels while proCPU and Δ CLT values were equal in both groups ($p > 0.99$ for both) (Figure 6-1C and F). Ezetimibe is an inhibitor of intestinal cholesterol absorption that is used alone or in combination with statins, but has no or negligible

pleiotropic effects [342–347]. Our observation on proCPU and Δ CLT values further supports the pleiotropic character of the effect of atorvastatin on proCPU biology in humans.

With this study the understanding of the proCPU system in hyperlipidemia and the effect of statin therapy on this system was extended. An important next step in positioning proCPU as a marker for identifying the benefit of atorvastatin treatment will be to prospectively study the value of proCPU screening to help optimize statin therapy in cardiovascular risk prevention and determine how the observed proCPU decrease translates into effects on morbidity and mortality. In addition, it will be interesting to repeat this study with other statins as well to be able to determine whether these effects on the proCPU system are class-mediated.

6.5 Conclusions

This study clearly shows that plasma proCPU concentrations and its expected effect on the fibrinolytic rate (as measured by Δ CLT) are increased in hyperlipidemic patients and that these effects can be normalized (and even further reduced versus normolipidemic patients) by treatment with atorvastatin. The proCPU downregulation and the improvement of the plasma fibrinolytic potential are dose-dependent. The current results support the hypothesis that including measurement of proCPU and/or Δ CLT in risk assessment for starting statin therapy might be valuable, in particular for those patients where there are doubts about starting statin therapy based on conventional risk factors or for choosing the proper dosing of atorvastatin.

Chapter 7

ProCPU is expressed by (primary) human monocytes and macrophages and expression differs between states of differentiation and activation

Based on:

Claesen K, De Loose J, Van Wielendaele P, De bruyne E, Sim Y, Thys S, Pintelon I, De Meester I, Hendriks D. Procarboxypeptidase U (proCPU, TAFI, CPB2) is expressed by (primary) human monocytes and macrophages and expression differs between states of differentiation and activation. Manuscript submitted.

7 ProCPU is expressed by (primary) human monocytes and macrophages and expression differs between states of differentiation and activation

7.1 Abstract

Background

CPU is a potent attenuator of fibrinolysis that is mainly synthesized by the liver as its inactive precursor proCPU. Besides its antifibrinolytic properties, evidence exists that CPU can modulate inflammation, thereby regulating communication between coagulation and inflammation.

Monocytes and macrophages play a central role in inflammation and interact with coagulation mechanisms resulting in thrombus formation. Numerous macrophage subtypes have been identified, with pro-inflammatory interferon (IFN)- γ /LPS-stimulated and anti-inflammatory IL-4-stimulated macrophages representing the opposite sites of the macrophage spectrum.

Aims

The involvement of both CPU and monocytes/macrophages in inflammation and thrombus formation [348], and a recent hypothesis that proCPU is expressed in monocytes and macrophages [46], prompted us to investigate (primary) human monocytes and different (primary) human macrophages as a potential source of proCPU.

Methods

CPB2 mRNA expression and the presence of proCPU/CPU protein were studied in the human monocytic cell line THP-1, PMA-stimulated THP-1 cells (macrophage-like phenotype) and primary human monocytes, M-CSF-, IFN- γ /LPS- and IL-4-stimulated macrophages by quantitative reverse-transcriptase polymerase chain reaction (RT-qPCR), Western blotting, enzyme activity measurements and immunocytochemistry.

Results

CPB2 mRNA is expressed by THP-1 and PMA-stimulated THP-1 cells, as well as by primary monocytes and macrophages. On a protein level, proCPU was detected in cellular lysate and medium of THP-1, PMA-stimulated THP-1 cells and primary monocytes, M-CSF-, M1- and M2-macrophages. Moreover, CPU was detected in cell medium of all investigated cell types and it was demonstrated that proCPU can be activated into functionally active CPU in the *in vitro* cell culture environment. Comparison of both relative *CPB2* mRNA expression and proCPU concentrations in the cell medium between the different cell types provided evidence that *CPB2* mRNA expression and proCPU secretion in monocytes and macrophages is related to the degree to which these cells are differentiated.

Conclusions

Our results indicate that primary monocytes and macrophages express proCPU. This sheds new light on monocytes and macrophages as local proCPU sources within atherosclerotic plaques and extravascular inflammatory sites.

7.2 Introduction

Monocytes and macrophages play a central role in the inflammatory response in atherosclerosis and at extravascular inflammatory sites [209,321,349]. In addition, these cells can interact with blood coagulation mechanisms, activating the coagulation system and leading to thrombus formation or extravascular fibrin deposition [348,350]. Numerous macrophage subtypes have been identified, with IFN- γ /LPS- and IL-4-stimulated macrophages representing the opposite sites of the macrophage spectrum [209,351–354]. IFN- γ /LPS-stimulated macrophages, also known as M1- or classically activated macrophages, are important producers of pro-inflammatory cytokines. IL-4-stimulated macrophages also called M2- or alternatively activated macrophages, are producers of anti-inflammatory cytokines. In relation to plaque morphology, IFN- γ /LPS-

stimulated macrophages are associated with symptomatic and unstable plaques, whereas IL-4-stimulated macrophages are particularly abundant in stable zones of the plaque and asymptomatic lesions [209,355,356].

The intrinsically unstable CPU is primarily seen as a potent attenuator of fibrinolysis through its action of cleaving C-terminal lysines on partially degraded fibrin. Yet, there is increasing evidence that the function of CPU is not restricted to fibrinolysis, but that it also plays a role as a modulator of inflammation. The mechanism is most likely two-fold, with the two effects not being mutually exclusive. Firstly, CPU can act as a direct modulator of inflammatory mediators by removing their C-terminal arginine or lysine, thereby inactivating them [83,302]. In this context, several inflammatory proteins, including bradykinin, the complement factors C3a and C5a, thrombin-cleaved osteopontin and plasmin-cleaved chemerin have been recognized as *in vitro* and *in vivo* CPU substrates [82–84,87,302]. Secondly, CPU's activity results in reduced plasmin generation and induces changes downstream of the latter enzyme, e.g. reduced cleavage of either fibrin or non-fibrin substrates such as matrix metalloproteases [83,302].

CPU is present in the circulation as its zymogen proCPU and can be activated by thrombin(-thrombomodulin) or plasmin. Plasma proCPU mainly originates from transcription of the *CPB2* gene in the liver. However, over the years several studies identified other cell types as (potential) additional proCPU sources. A first non-hepatically derived pool of proCPU was found in platelets and accounts for <0.1% of blood-derived proCPU. It is synthesized by megakaryocytes and is released from the α -granules upon platelet activation [43]. *CPB2* mRNA was also detected in megakaryocytic cell lines (CHRF, Dami and MEG-01), primary endothelial cells (both HCAEC and HUVEC) and the human monocytic cell line THP-1 as well as in THP-1 cells differentiated into a macrophage-like phenotype and in primary human PBMCs [20,43,46–48]. In the promonocytic cell line U937 *CPB2* mRNA expression increased after treatment with dexamethasone or M-CSF [357]. ProCPU protein was detected in the lysate of

differentiated and undifferentiated Dami and MEG-01 cells and the conditioned media of differentiated Dami and PMA-stimulated THP-1 cells [46]. In addition, Rylander *et al.* recently demonstrated that (pro)CPU is present in advanced carotid plaques, with the highest levels found in the vulnerable part of the plaque, colocalized with macrophages/foam cells and neovascular endothelium [49].

CPB2 mRNA was recently detected in PBMCs and it was hypothesized that the *CPB2* transcripts were derived from *CPB2* gene expression by monocytes and macrophages present in this cell fraction [46]. Since monocytes and macrophages provide a potential link between inflammation and thrombus formation [321], and the CPU system also plays a role in both systems, this was an interesting hypothesis. Therefore, we investigated the expression of proCPU (on mRNA, protein and activity level) in (primary) human monocytes and different (primary) human macrophage subsets to gain more insight into these cells as potential sources of proCPU within atherosclerotic plaques and extravascular inflammatory sites.

7.3 Materials and methods

7.3.1 Cell culture

7.3.1.1 Cell lines

The human hepatocellular carcinoma cell line HepG2 (Sigma-Aldrich, USA) was grown in Dulbecco's Modified Eagle Medium (DMEM) supplemented with 10% fetal calf serum (FCS), 100 U/mL penicillin and 100 µg/mL streptomycin (Gibco, Belgium). THP-1 cells (human acute monocytic leukemia; ATCC, USA) were grown in Roswell Park Memorial Institute (RPMI) 1640 medium supplemented as described for HepG2 cells. Part of the THP-1 cells was differentiated into a macrophage-like phenotype by addition of 0.2 µM phorbol 12-myristate 13-acetate (PMA; Sigma-Aldrich, USA) to the medium for 72 h. All cells were incubated at 37 °C under 95% air/5% CO₂ atmosphere. Medium was replaced every 2 – 3 days. Passage numbers 2 – 5 were used for HepG2 and 2 – 8 for THP-1 cells.

7.3.1.2 Primary cells

(a) Isolation of human CD14⁺ cells

Human PBMCs were isolated from buffy coats of anonymous clinically healthy blood donors (Blood Transfusion Centre, Red Cross, Mechelen, Belgium) by Ficoll-Paque Premium gradient centrifugation. Ethical approval for the buffy coats and processes used in this study was given by the Ethics Committee UZA/UAntwerp (B300201939437) and all donors (N = 17) gave their written informed consent. Briefly, a 40 mL buffy coat was diluted in Dulbecco's phosphate buffered saline (DPBS, 1:1, vol/vol) and carefully layered on top of Ficoll-Paque Premium solution (GE Healthcare, UK). A centrifugation step was carried out (40 min, 400 x *g*, no brakes) whereafter PBMCs were collected from the interface and subsequently washed two times with DPBS. Monocytes (CD14⁺ cells) were enriched from the freshly isolated mononuclear cell fraction via CD14⁺ positive magnetic selection using CD14 microbeads (20 µL of microbeads per 10⁷ total PBMCs; Miltenyi Biotec GmbH, Germany) following the manufacturer's protocol. MACS-purified CD14⁺ monocytes were then seeded at a density of 2 x 10⁶ cells/mL in RPMI 1640 (Gibco, Belgium) supplemented with 10% FCS, 100 U/mL penicillin and 100 µg/mL streptomycin and placed in a humidified incubator with 5% CO₂ at 37 °C. Monocytes were either harvested after 24 h of culturing or differentiated into macrophages immediately after seeding.

(b) Human monocyte-to-macrophage differentiation and activation

For human monocyte-to-macrophage differentiation, freshly isolated human CD14⁺ monocytes were seeded at a density of 2 x 10⁶ cells/mL in complete RPMI 1640 medium supplemented with 20 ng/mL recombinant human macrophage colony-stimulating factor (rhM-CSF, Immunotools, Germany) [358]. After 5 days of incubation, macrophages were harvested or further polarized by 2 days of incubation with 20 ng/mL rhM-CSF in combination with either 100 U/mL IFN-γ (Immunotools, Germany) and 20 ng/mL LPS (Immunotools, Germany) to obtain classically activated (M1) macrophages or 20 ng/mL IL-4 (Immunotools, Germany) for alternatively activated (M2) macrophages [358,359]. To

confirm appropriate macrophage polarization by these stimulation protocols, medium was aspirated 8 and 24 h after the start of the polarization [359]. TNF- α levels were determined in the 8 h aspirate and IL-6, IL-1 β and IL-10 levels in the 24 h aspirate using respective ELISAs (hTNF- α ELISA, hIL-6 ELISA, hIL-1 β ELISA and hIL-10 ELISA; Immunotools, Germany). All ELISAs were performed according to the manufacturer's instructions with the modification that standards were diluted in complete growth medium.

7.3.2 Conditioned media and cellular lysates

Conditioned medium of the different cell types was obtained by replacing complete medium by 5% of the respective complete medium and 95% Hank's Balanced Salt Solution (HBSS, Gibco, Belgium) 24 h before harvesting. After 24 h, the conditioned medium was collected and stored at -80 °C until further analysis. Cellular lysates were prepared by washing 2×10^6 cells twice with DPBS and suspending these cells in 50 μ L of the appropriate lysis buffer: lysis buffer for proCPU measurement (1% octylglucoside, 10 mM EDTA, 70 μ g/mL aprotinin, 50 mM Tris-HCl pH 8.3) or lysis buffer for Western blot analysis (1% Triton X-100, 150 mM NaCl, Complete Protease Inhibitor Cocktail [Roche Diagnostics, Belgium], 50 mM Tris pH 7.6). After 1 hour on ice with frequent agitation, the samples were centrifuged at 12 000 $\times g$ for 10 min at 4 °C and the cellular lysate was collected. Conditioned media and cellular lysates were stored at -80 °C and later used for proCPU measurement or Western blot analysis. The protein content of the conditioned media and cellular lysates was determined according to the Bradford method using bovine serum albumin (Sigma-Aldrich, USA) as a standard [360].

7.3.3 RNA isolation and cDNA synthesis for mRNA expression analysis

Total RNA was isolated from 2×10^6 cells using the SV Total RNA Isolation System kit (Promega, USA) following the manufacturer's instructions. RNA quality and concentration were assessed by measuring the absorbance at 230, 260 and 280 nm using a UV-visible spectrophotometer (Nanodrop 2000, Thermo Fisher Scientific, USA). Next,

first-strand cDNA was synthesized starting from 2 µg of extracted total RNA and using the Omniscript® Reverse Transcription Kit (Qiagen, Germany) according to the standard protocol.

7.3.4 Validation of a quantitative reverse transcriptase-polymerase chain reaction (RT-qPCR) assay to study *CPB2* mRNA expression

7.3.4.1 Primer selection for reference genes and the target gene *CPB2*

A pool of twelve candidate reference genes was chosen based on their common use as endogenous reference genes in human gene expression studies. Primers were designed based on sequences from existing literature and the PrimerBank database (Massachusetts General Hospital) [361–363]. All primer pairs were designed for the primers to be located on different exons or for one of the primers to be situated on an exon-exon junction. This to ensure the specific amplification of cDNA and not genomic DNA (gDNA). *In-silico* specificity analysis using the primer-BLAST tool was conducted to verify the specificity of the selected primers. Primers were synthesized by Integrated DNA Technologies (IDT, USA). The sequences, length of products, predicted melting temperature (T_m) and source sequences are listed in Table 7-1.

A primer/probe set for the gene of interest (*CPB2*) was selected from literature (Table 7-2) [19,46] and purchased from IDT. The probe was labeled with FAM (6-carboxyfluorescein) as the reporter dye at the 5'-end, an internal ZEN™ quencher and with a second quencher at the 3'-end (ABkFQ). These primers and probe were also designed to minimize the signal generated from possible contaminating gDNA.

7.3.4.2 Quantitative reverse transcriptase-polymerase chain reaction (RT-qPCR) analysis

RT-PCR amplification reactions were performed using the CFX Connect™ Real-Time PCR System (Bio-Rad, USA). The reaction mixture (20 µL) contained 10 µL 2X SSoAdvanced™ Universal SYBR® Green supermix (Bio-Rad, USA), 1 µL (250 nM, 300 nM or 500 nM

Table 7-1. Candidate reference genes and corresponding primer pairs evaluated in this study.

Gene	PrimerBank accession	Primer sequence forward/reverse (5' to 3')	Amplicon size (bp)	Predicted Tm (°C)	
<i>ARPC1a</i>	Actin related protein 2/3 complex subunit 1A	300360514c1	ATTGCCCTCAGTCCCAATAATCA CAAGTGACAATGCGGTCCG	143	81.0
<i>B2M</i>	Beta-2-microglobulin	37704380c1	CGCTACTCTCTTTTCTGG ATTTGACTTTCCATTCTCTGC	111	81.0
<i>CD71</i>	Transferrin receptor	332309170c3	ATCGGTTGGTGCCACTGAATGG ACAACAGTGGGCTGGCAGAAAC	131	79.0
<i>CycA</i>	Cyclophelin A pair 1	45439319c1	GGCAAATGCTGGACCCAACACA TGCTGGTCTTGCCATTCTGGA	161	81.5
<i>EMC7</i>	ER membrane protein complex subunit 7	14211875a1	CTTCAGGACTGGATCTCGG CGGGATCAAATCTGTAAGCTGGA	151	80.0
<i>GUS</i>	Glucuronidase beta	268834191c3	CTCATTTGGAATTTTGCCGAT CCGAGTGAAGATCCCCTTTTTA	81	80.0
<i>HPRT1</i>	Hypoxanthine phosphoribosyl transferase	164518913c1	CCTGGCGTCGTGATTAGTGAT AGACGTTCACTCTGTCCATAA	131	79.5
<i>PGK-1</i>	Phosphoglycerate kinase 1	183603937c2	GAACAAGGTTAAAGCCGAGCC GTGGCAGATTGACTCTACCA	137	83.5
<i>PSMB2</i>	Proteasome 20S subunit beta 2	315139005c1	ATCCTCGACCGATACTACACAC GAACACTGAAGTTGGCAGAT	118	83.0
<i>RPS8</i>	Ribosomal protein S8	4506742c1	GCTCAGAGTGTTGTAICTCGTAAA AGCACGATGCAATTCTTACC	106	81.0
<i>TBP</i>	TATA box binding protein	285026518c3	GAGCCAAGAGTGAAGAACAGTC GCTCCCCACCATATTCTGAATCT	116	78.0
<i>YWHAZ</i>	Tyrosine 3-monooxygenase/ tryptophan 5-monooxygenase activation protein zeta	208973243c2	TGTAGGAGCCCGTAGGTCATC GTGAAGCATTGGGGATCAAGA	179	79.0

Bp: base pairs; conc: concentration of forward and reverse primer used for validation of the primer pair; Tm: melting temperature.

Table 7-2. Sequences of the primers and probe for detection of the *CPB2* gene by RT-qPCR.

Primer	Primer sequence (5' to 3')	Amplicon size (bp)	Conc (nM)
Forward	TGCATCGGAACAGACCTGAA	65	500
Reverse	CTGGATGCACCTTCCTCACA		500
Probe	6FAM-TTGCTTCCA-ZEN-AACTG-AbkFQ		200

6FAM: 6-carboxyfluorescein (5'-end reporter dye); AbkFQ: nonfluorescent quencher (3'-end nonfluorescent quencher); bp: base pairs; conc: concentration of forward and reverse primer used for validation of the primerpair; RT-qPCR: quantitative reverse transcriptase-polymerase chain reaction; ZEN: internal quencher.

depending on the primer set; Table 7-3) of each primer, 5 μ L cDNA and 3 μ L nuclease-free water as recommended in the manufacturer's instructions. For amplification of *CPB2*, the 2X SSoAdvanced™ Universal SYBR® Green supermix and 2 μ L nuclease-free water were substituted by an equal volume of 2X SSoAdvanced™ Universal probes supermix (Bio-Rad, USA) and probe (200 nM; IDT, USA). All samples were run in triplicate and each run included a no-template control (nuclease-free water instead of sample) for the genes included in the run. Thermocycling conditions used were as follows: one cycle of 95 °C for 30 s, followed by 40 cycles of denaturation at 96 °C for 15 s and annealing and extension with fluorescent plate read at 60 °C for 40 s. Afterward, a melt curve was obtained by melting the amplicon from 60 to 95 °C to check for primer dimers. Data, including individual quantification cycle (Cq) values for each gene, were acquired using the CFX Manager software.

7.3.4.3 Primer specificity and PCR amplification efficiency of the selected primer pairs
To validate that accurate template quantification is achieved with the selected primer pairs, primer specificity (verification that each reaction amplifies the correct target) and PCR amplification efficiency were determined. The specificity of each primer pair was evaluated by melt curve analysis, agarose gel electrophoresis on the RT-qPCR products and sequencing of purified RT-qPCR products. For agarose gel electrophoresis, PCR products were loaded onto a 2% agarose gel with TBE buffer, ran for 75 min at 100 V

(Mini Sub-Cell GT Cell and PowerPac Basic Power Supply, Bio-Rad, USA) and stained with Gel Red (Sigma-Aldrich, USA). Visualization was performed on an OptiGo Gel Imaging System (Isogen Life Sciences, The Netherlands) with UV-light. The amplification efficiency of each primer pair was determined using a relative standard curve constructed by performing RT-qPCR on each gene using a 5-fold serial dilution series of template cDNA from HepG2 cells. Individual Cq values were plotted against the logarithm of the dilution factor whereafter PCR amplification efficiencies (E) were calculated from the slope of the respective relative standard curve by the formula $E(\%) = 10^{-1/\text{slope}-1} * 100$ and R^2 values were obtained from the lines of best fit.

7.3.4.4 Gene stability analysis and reference gene selection

To accurately perform relative quantification, normalization of the gene expression is required to correct for non-specific experimental variations [364]. Therefore, the expression stability of the candidate reference genes in the different cell types (HepG2, THP-1, PMA-stimulated THP-1 cells, primary human monocytes, primary human M-CSF macrophages, primary human IFN- γ /LPS-stimulated [M1]- and IL-4-stimulated [M2] macrophages) was evaluated by RT-qPCR. Cq values for all samples were calculated. The stability of the reference genes was determined, the optimal combination of reference genes for normalization was selected and normalization factors (NFs) of the selected reference genes were calculated using the geNorm algorithm of the qbase+ software (Biogazelle, Ghent, Belgium) [364,365].

7.3.5 *CPB2* mRNA expression in human monocyte and macrophage cell lines and primary cells

Cq values of the gene of interest, *CPB2*, were determined by RT-qPCR for HepG2, THP-1, PMA-stimulated THP-1 cells, primary human monocytes, primary M-CSF macrophages, primary INF γ /LPS-stimulated- (M1) and IL-4-stimulated (M2) macrophages. Using the NFs of the selected reference genes, the relative *CPB2* mRNA expression was calculated for each cell type and eventually compared between all cell types [364].

7.3.6 Western blot analysis

Purified proCPU was obtained from human plasma as previously described [66]. Prior to Western blot analysis, conditioned medium of at least four independent experiments/donors was pooled for each cell type and concentrated 20-fold using 10K centrifugal filter devices (Amicon® Ultra-0.5, Merck Millipore, Germany). All samples were then diluted in 4X sample buffer (0.5 M Tris pH 6.8, glycerol, 10% sodium dodecylsulphate [SDS], mercaptoethanol, bromophenol blue) and boiled for 5 min before loading onto a 10% SDS-page gel. To obtain active CPU as a control, purified proCPU was activated at 25 °C with thrombin-thrombomodulin (4 nM and 16 nM respectively) in the presence of 50 mM CaCl₂. The reaction was stopped after 20 min by adding 4X sample buffer and immediately boiling the samples. Electrophoresis was performed at a constant voltage of 180 V for 60 min in the Mini Protean III system (Bio-Rad, USA). Equal amounts of protein were loaded for each sample. After SDS-page, the proteins were transferred onto a 0.45 µm nitrocellulose membrane by electroblotting in 25 mM Tris buffer pH 8.3 with 0.192 M glycine and 20% methanol using the Mini Trans-blot Cell Assembly (Bio-Rad, USA) for 1 h at 250 mA. Blocking of non-specific binding sites was achieved by placing the membrane in blocking buffer (5% BSA in washing buffer [0.05 M Tris, 0.15 M NaCl, 0.15% Tween 20, pH 7.4]) for 1 h at room temperature. Membranes were incubated overnight with primary antibodies diluted in blocking buffer: polyclonal sheep anti-human proCPU antibody (PATAFI-S, Prolytix, USA; 1:1500) or polyclonal rabbit anti-human proCPU/CPU antibody (CP17, Agrisera, Sweden; 1:1500). Subsequently, secondary antibodies diluted in blocking buffer were added for 2 h at room temperature: goat anti-sheep horseradish peroxidase (HRP) (31480, ThermoFisher, USA; 1:5000) and goat anti-rabbit HRP (65-6120, Invitrogen, USA; 1:5000) were used. Between the different incubations, membranes were washed 6 x 5 min with washing buffer. Chemiluminescent detection was performed using the SuperSignal West Femto substrate kit (ThermoFisher Scientific, USA). The protein bands were visualized on a Chemidoc MP system with Image Lab software (Bio-Rad, USA). Precision Plus Protein Dual Color Standards (Bio-Rad, USA) were used for MW estimation.

7.3.7 Immunocytochemistry

HepG2, THP-1 and CD14+ cells were seeded in Nunc™ Lab-Tek™ II CC2™ Chamber Slides at a density of 0.25 – 1 x 10⁵ cells per well (depending on the cell type) and incubated at 37 °C. Cell culturing and differentiation protocols were identical as described above. At the end of the respective culturing or differentiation protocol, the cells were washed with HBSS (Gibco, Belgium) and fixed with 4% paraformaldehyde (PFA) for 30 min at room temperature. A washing step with DPBS was then performed. Hereafter, the cells were permeabilized with 0.1% Triton X-100 in blocking buffer (2% bovine serum albumin, 5% normal goat serum in DPBS) for 10 min, followed by a subsequent blocking step in blocking buffer for 30 min at room temperature. Next, the cells were incubated overnight at 4 °C with primary antibodies against proCPU/CPU (CP17, Agrisera, Sweden; 1:100) diluted in blocking buffer. After washing in DPBS, the cells were incubated with secondary antibodies for 1 h at room temperature protected from light. The secondary antibody FITC-labeled goat anti-rabbit IgG (554020, BD Biosciences, Belgium; 1:200 in blocking buffer) was used to visualize the primary antibody against proCPU/CPU. The slides were covered with a cover glass using Vectashield antifade mounting medium with DAPI (Vector Laboratories, USA) and visualized on an inverted Leica TCS SP8 confocal laser scanning microscope. The staining was checked for autofluorescence and non-specific binding of the secondary antibody. Normal rabbit IgG (Invitrogen, USA) was used as isotype control.

7.3.8 ProCPU measurement

ProCPU concentrations were measured in both the conditioned media and cellular lysate using a previously described, in-house enzymatic assay [81] with the modification that the conditioned media samples were not diluted and the cellular lysates were concentrated three- to four-fold before proCPU measurement using a 10K centrifugal filter devices (Amicon® Ultra-0.5, Merck Millipore, Germany). Samples were then incubated with AZD9684 (a potent and selective small-molecule CPU inhibitor that was a kind gift from AstraZeneca (Mölnådal, Sweden); final concentration 5 µM) or an equal

volume of HEPES (4-2-hydroxyethyl-1-piperazineethansulphonic acid (Merck, Germany); 20 mmol/L; pH 7.4) for 5 min [31,32]. Hereafter a mixture of human thrombin (Merck, Germany), rabbit-lung thrombomodulin (Seikisui Diagnostics, USA) and CaCl₂ (Merck, Germany) (final concentrations 4 nM, 16 nM and 50 mM respectively) was added to quantitatively convert proCPU into the active enzyme. Subsequently, the active CPU was incubated with the selective and specific substrate Bz-*o*-cyano-Phe-Arg (Laboratory of Medicinal Chemistry, University of Antwerp, Belgium), followed by quantification of the formed product by high-performance liquid chromatography. The enzymatic activity measured in the presence of AZD9684 was then subtracted from the enzymatic activity in the absence of AZD9684 to obtain the actual proCPU concentration and to exclude that the measured activity originated from other basis carboxypeptidases or other enzymes that could be present in the samples. Enzyme activity is expressed as units per liter (U/L) for the conditioned media or units per gram (U/g) protein for the cellular lysates. One unit defines the amount of enzyme that hydrolyzes 1 μmole of substrate per minute under the reaction conditions described [81].

7.3.9 Statistical analysis

Statistics were performed using IBM SPSS Statistics 27 and figures were compiled in GraphPad Prism 9.3.1 (GraphPad Software, Inc., USA). The specific statistical tests used in this study are mentioned in the legends underneath the figures. Data are presented as mean ± standard error of the mean (SEM). Results were considered significant if the *p*-value was < 0.05.

7.4 Results

7.4.1 Validation of a quantitative reverse transcriptase-polymerase chain reaction (RT-qPCR) assay to study *CPB2* mRNA expression

7.4.1.1 Primer specificity, efficiency and expression profiling of candidate reference genes

A total of twelve candidate reference genes were targeted to select suitable internal controls for gene expression studies using RT-qPCR. The specificity of the primer pairs was confirmed via agarose gel electrophoresis, melt curve analysis and Sanger sequencing.

Single sharp bands at the expected MW were present on the agarose gel for the amplicons of all reference genes, except for *PSMB2*, *RPS8* and *PGK-1* (Figure 7-1). For the latter, a diminished band appeared on the gel underneath the main band. This is suspicious for the presence of various DNA sequences (e.g. primer dimers or non-specific amplification products). Therefore, the specificity of these three reference genes was analyzed more closely using Sanger sequencing and melt curve analysis.

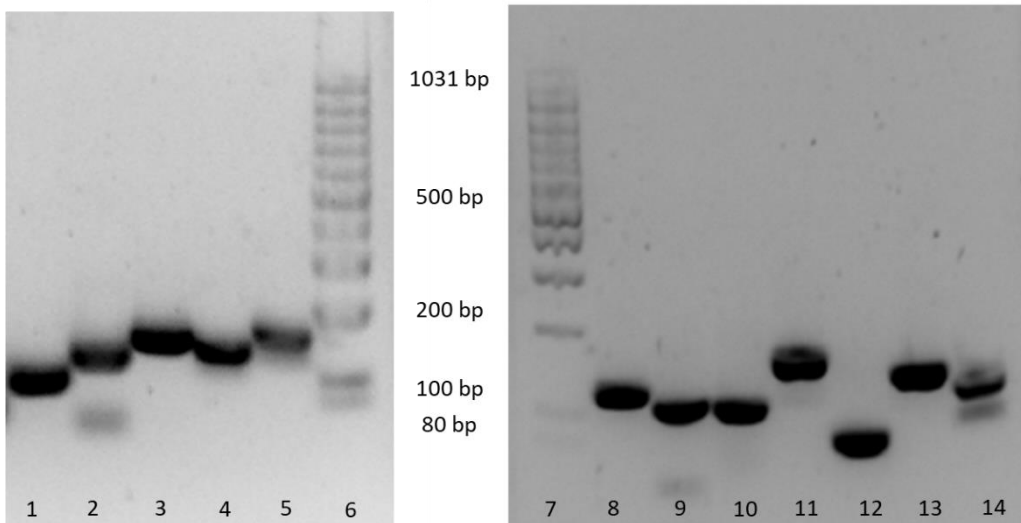


Figure 7-1. Specificity of primers. Agarose gel electrophoresis showing amplification specificity of the candidate reference genes. Lane 1: B2M; lane 2: *PSMB2*; lane 3: *ARCP1a*; lane 4: *CD71*; lane 5: *CycA*; lane 6-7: low range DNA ladder; lane 8: *HPRT1*; lane 9: *RPS8*; lane 10: *TBP*; lane 11: *YWHAZ*; lane 12: *GUS*; lane 13: *EMC7*; lane 14: *PGK-1*. Bp: base pairs.

Sanger sequencing is a PCR-based sequencing method that allows to unambiguously verify the identity of the amplified PCR products by determining the actual nucleotide sequence of the fragments after purification from the qPCR reactions. Sequencing of the primer pairs PSMB2, RPS8 and PGK-1 was successful with a pairwise identity between 96.9-100.0%, confirming amplification of the correct sequence (data not shown). In addition, the melt curves of these three genes, and also those of the other candidate reference genes, showed a single peak. The presence of this single peak in the melt curve indicates that the primers amplified specific products (Figure 7-2).

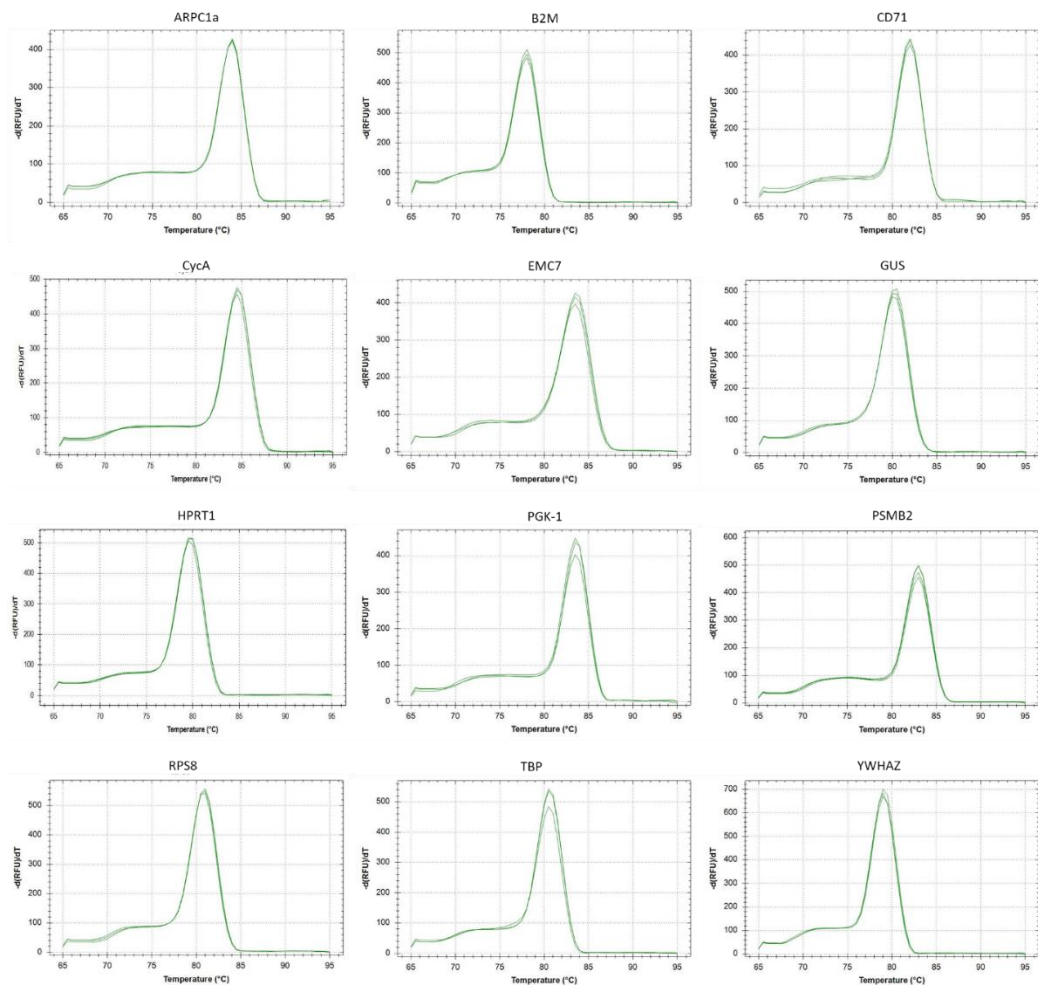


Figure 7-2. Specificity of RT-qPCR amplification. Melt curves of the 12 candidate reference genes with single peak after RT-qPCR reactions. RFU: relative fluorescence units, RT-qPCR: quantitative reverse transcriptase-polymerase chain reaction.

Next, the amplification efficiency of the primers was determined and ranged from 91.2 to 134.7%. R^2 was > 0.93 for all primers (Table 7-3). Only those primer pairs with an amplification efficiency between 90 – 110 % and an $R^2 > 0.98$ were retained as candidate reference genes. As a result HPRT1 (efficiency = 134.7% and $R^2 = 0.931$) and PGK-1 (efficiency = 131.2% and $R^2 = 0.97$) were henceforth excluded as potential reference genes.

Table 7-3. Candidate reference genes and corresponding primer pairs evaluated in this study.

Gene	Primer concentration	Range of Cq values	Efficiency (%)	Slope	Y-intercept	R^2
<i>ARPC1a</i>	250 nM	27.19 – 32.85	91.2	-3.6	44.5	0.999
<i>B2M</i>	250 nM	19.57 – 28.59	109.0	-3.1	40.2	0.991
<i>CD71</i>	200 nM	22.60 – 32.04	98.3	-3.4	42.9	0.996
<i>CycA</i>	200 nM	24.26 – 33.48	93.3	-3.5	38.9	0.998
<i>EMC7</i>	250 nM	29.16 – 36.65	92.1	-3.5	43.9	0.998
<i>GUS</i>	250 nM	29.10 – 36.85	102.2	-3.3	42.0	0.996
<i>HPRT1</i>	250 nM	23.13 – 33.17	134.7	-2.7	40.0	0.931
<i>PGK-1</i>	250 nM	19.51 – 30.16	131.2	-2.7	36.5	0.972
<i>PSMB2</i>	250 nM	27.52 – 33.15	97.4	-3.4	40.7	0.994
<i>RPS8</i>	250 nM	23.56 – 33.65	95.9	-3.4	37.0	0.995
<i>TBP</i>	200 nM	27.18 – 33.99	98.5	-3.4	43.5	0.996
<i>YWHAZ</i>	250 nM	19.26 – 32.07	103.0	-3.3	39.1	0.993
<i>CPB2</i>	500 nM	19.19 – 30.75	100.1	-3.3	39.1	0.999

Cq: quantification cycle.

The Cq values obtained by RT-qPCR were used to provide an overview of the expression levels of the candidate reference genes across all the samples. The mean Cq values of all primer pairs for the different samples ranged from 19.57 to 36.85, which is acceptable for reliable RT-qPCR quantification. ARPC1a showed the least variation in its transcript level with a coefficient of variation (CV) of 7.3%, across all samples and TBP showed the second least variation in gene expression with a CV of 7.8%, followed by EMC7 (CV =

8.69%). B2M was the most variable reference gene (CV = 18.4%) followed by RPS8 (CV = 17.7%) (Figure 7-3).

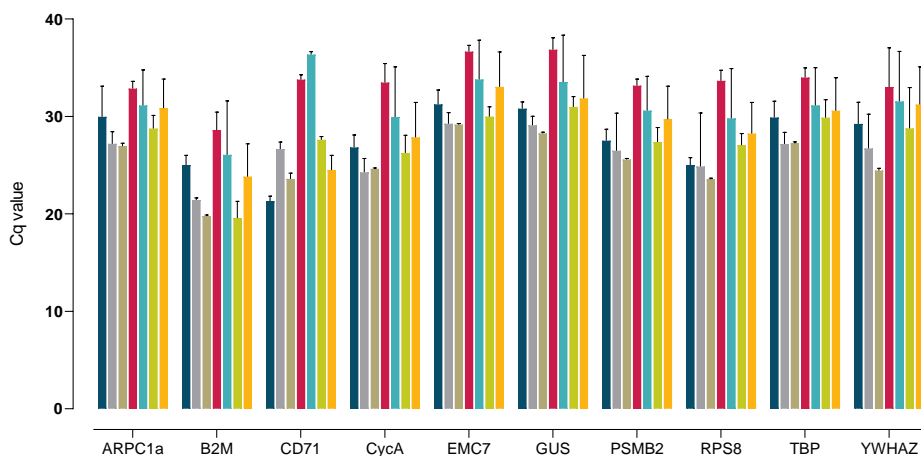


Figure 7-3. Expression profiles of candidate reference genes across all the experimental samples. The expression profiles of 12 candidate reference genes in absolute quantification cycle (Cq) values over different samples including from left to right HepG2 (dark blue), THP-1 (grey), PMA-stimulated THP-1 cells (brown), primary human monocytes (pink), primary human M-CSF macrophages (light blue), primary human IFN- γ /LPS stimulated macrophages (green) and primary human IL-4-stimulated macrophages (yellow).

7.4.1.2 Analysis of expression stability and determination of the optimal number of reference genes

Using qbase+ software, the mean expression stability of the candidate reference genes was defined by allocating a so-called M-value to each gene in a pool of potential internal control genes. An M-value is the mean pairwise variation between an individual gene and the other putative reference genes tested [364,365]. Genes with the lowest M-values have the most stable expression. GeNorm analysis revealed that the most stably expressed gene was TBP with an M-value of 0.465, followed by EMC7 (M = 0.505) and ARPC1a (M = 0.550). B2M was the least stable gene for RT-qPCR normalization (Figure 7-4A).

The optimal number of reference genes required for accurate normalization to obtain precise RT-qPCR results was also determined by pairwise variation (V_n/V_{n+1}) using geNorm [366]. According to Vandesompele *et al.*, a cutoff value of $V_n/V_{n+1} < 0.15$ suggests that the addition of another reference gene would have no significant contribution to normalization in RT-qPCR analysis [364,365]. As shown in Figure 7-4B, the V2/3 pairwise variation (0.199) was higher than 0.15, while the V3/4 variation was 0.147. Therefore, the combination of three genes (ARPC1a, EMC7 and TBP) is good enough to perform accurate RT-qPCR normalization.

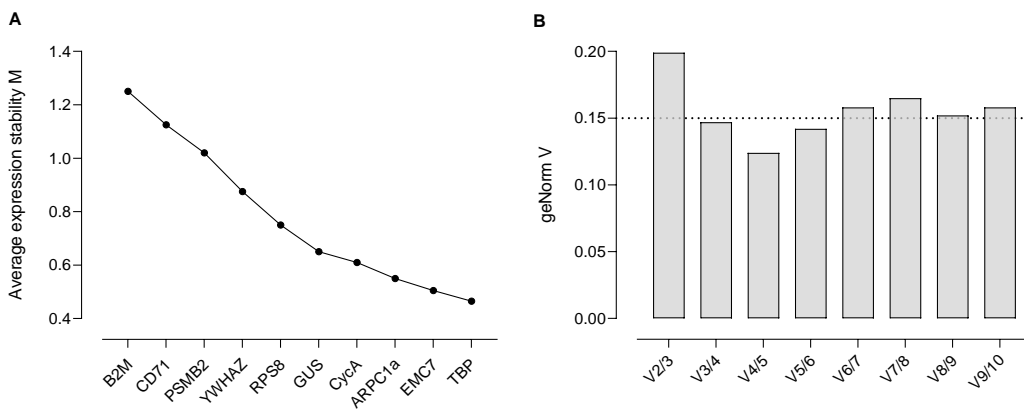


Figure 7-4. A) Average expression stability values of remaining potential internal control genes. Average expression stability values (M) during stepwise exclusion of the least stable internal control genes by geNorm application. The highest M values corresponded to the least stable gene, B2M; while the lowest M values corresponded to the most stable gene, TBP. **B) Determination of the optimal number of internal genes for accurate normalization.** The pairwise variation ($V = V_n/V_{n+1}$) was calculated by geNorm to determine the optimal number of reference genes required for RT-qPCR normalization. Values under 0.15 indicate that no additional genes are required for the normalization. Here the optimal number of reference genes is three.

7.4.2 CPB2 mRNA is detected in (primary) human monocytes and macrophages

Using the validated RT-qPCR assay, *CPB2* mRNA expression was studied in human monocyte and macrophage cell lines and primary cells and displayed relative to the expression of the reference genes selected for accurate normalization (ARPC1a, EMC7 and TBP; Figure 7-4B). The human hepatocellular carcinoma cell line HepG2 was used as

a positive control given hepatocytes are the primary source of proCPU protein in plasma. RT-qPCR results showed that *CPB2* mRNA was present in all cell types studied here, with the highest expression detected in HepG2 cells (Figure 7-5). When comparing the *CPB2* mRNA abundance in the monocytic cell line THP-1 with primary human monocytes, the expression of *CPB2* transcripts was significantly lower in THP-1 cells compared to its

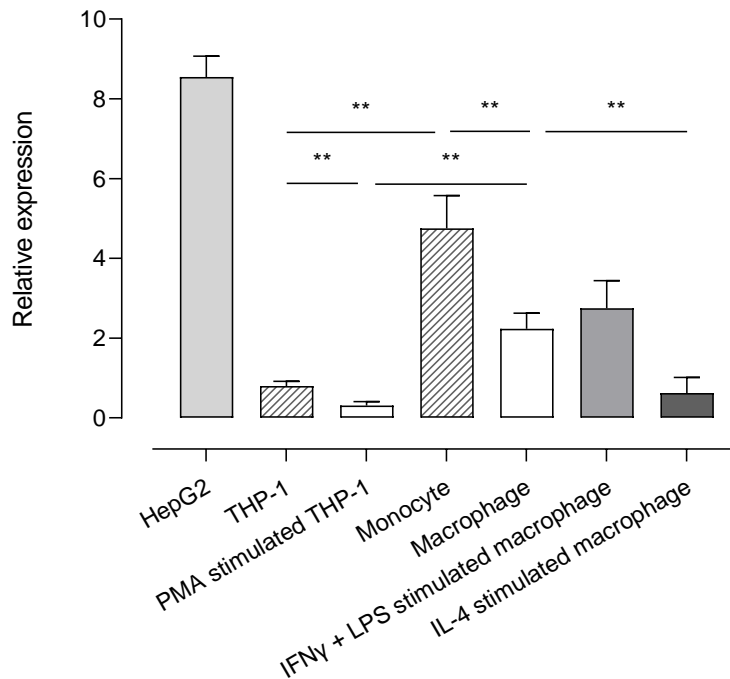


Figure 7-5. Relative expression of *CPB2* mRNA in various cell types. The abundance of *CPB2* mRNA in HepG2, THP-1, PMA-stimulated THP-1 cells (macrophage-like phenotype), primary human monocytes, primary human M-CSF primed macrophages, IFN- γ /LPS-stimulated macrophages (M1 macrophage, classically activated) and IL-4-stimulated macrophages (M2 macrophage, alternatively activated) was analysed by quantitative reverse-transcriptase polymerase chain reaction (RT-qPCR). *CPB2* mRNA expression was displayed relative to a set of stable reference genes (ARCP1a, EMC7 and TBP). Data present the mean of 5 – 7 biological replicats measured in triplicate. Error bars represent the standard error of the mean (SEM). A Kruskal-Wallis test with Dunn’s multiple comparison test was used to test for statistical significance between all groups of monocytes/macrophages. Statistically significant differences are indicated with an asterisk (** $p < 0.01$).

primary cell counterpart. Although the magnitude of relative *CPB2* mRNA expression is different between primary monocytes and THP-1 cells, a clear and significant decrease in *CPB2* mRNA expression is observed for both cell types when differentiating these cells into macrophages with M-CSF or the phorbol ester PMA respectively. The magnitude of the decrease in *CPB2* mRNA abundance was similar: 61% decrease in case of PMA stimulation of THP-1 cells versus 54% decrease in primary monocyte-to-macrophage differentiation. Furthermore, activation of primary M-CSF macrophages into either classically activated macrophages (M1-macrophage; LPS/INF- γ) or alternatively activated macrophages (M2-macrophage; IL-4) resulted in differential *CPB2* gene expression: classical macrophage activation gave rise to a slightly, but not significantly higher *CPB2* mRNA abundance compared to M-CSF primed macrophages, whereas alternative activation significantly lowered expression of *CPB2* transcripts.

Appropriate macrophage activation was confirmed beforehand by measuring the concentration of different cytokines (TNF α , IL-6, IL-1 β and IL-10) in the supernatant of unstimulated and stimulated macrophages by use of ELISA and comparing the concentration of these cytokines in all groups. Stimulation of primary M-CSF primed macrophages with a combination of IFN- γ and LPS resulted in a significant increase in pro-inflammatory TNF α , IL-6 and IL-1 β secretion (Figure 7-6). A clear decrease in pro-inflammatory cytokine production (TNF α , IL-6 and IL-1 β) and a substantial increase in the concentration of the anti-inflammatory cytokine IL-10 confirmed successful differentiation of primary M-CSF primed macrophages into an anti-inflammatory subtype after IL-4-stimulation.

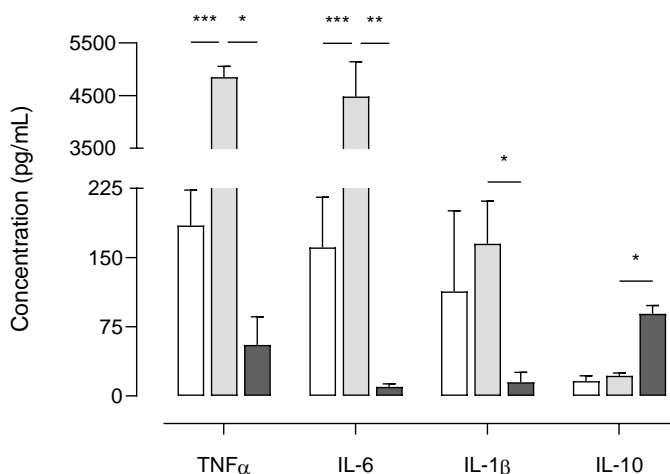


Figure 7-6. Appropriate stimulation of primary human M-CSF macrophages with IFN- γ /LPS or IL-4 was confirmed by ELISA. TNF α (8h after activation), IL-6, IL-1 β and IL-10 (all 24h after activation) levels were determined in the medium of primary human M-CSF primed macrophages (white), primary human IFN- γ /LPS-stimulated macrophages (light grey) and primary human IL-4-stimulated macrophages (dark grey). Results are presented as mean \pm SEM (N = 4 – 6). *p*-values were calculated by performing a Kruskal-Wallis test with Dunn's multiple comparison test; * *p* < 0.05, ** *p* < 0.01 and *** *p* < 0.001.

7.4.3 ProCPU and CPU protein are present in (primary) human monocyte and macrophage medium

The presence of proCPU protein in concentrated conditioned medium and cell lysate of human monocytes and macrophages was studied by Western blotting using two different polyclonal proCPU/CPU antibodies. ProCPU purified from plasma as well as CPU obtained after activating purified proCPU by addition of thrombin-thrombomodulin were included as positive controls. Both antibodies against proCPU/CPU reacted with purified proCPU and CPU at a MW around 58 kDa and 35 kDa respectively, corresponding with previously reported data on human proCPU/CPU (Figure 7-7). Using the sheep polyclonal proCPU antibody (PATAFI-S, Prolytix), a similar proCPU immunoreactive band was detected in all concentrated conditioned media samples, though the apparent MW was slightly lower compared to purified proCPU (Figure 7-7A). With this antibody, no CPU band was observed in the media samples. The second Western blot showed a 35

kDa CPU band for all conditioned media, but this polyclonal antibody (CP17, Agrisera) did not react with proCPU in any of the media samples (Figure 7-7B).

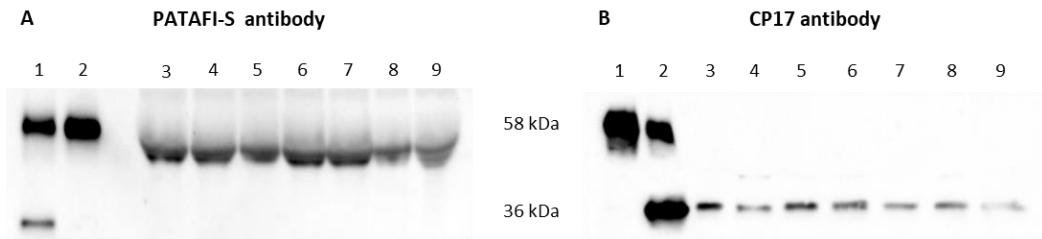


Figure 7-7. Detection of human proCPU and CPU protein in concentrated conditioned media of various cell types. A) Western blot using a polyclonal sheep anti-human proCPU antibody (PATAFI-S, Prolytix). Lane 1: Mixture of purified plasma proCPU (58 kDa) and CPU (35 kDa) as control, Lane 2: Purified plasma proCPU as control, Lane 3-9: concentrated conditioned media HepG2 (lane 3), THP-1 (lane 4), PMA-stimulated THP-1 (lane 5), primary human monocytes (lane 6), primary human M-CSF macrophage (lane 7), primary human IFN- γ /LPS-stimulated macrophage (lane 8), primary human IL-4-stimulated macrophage (lane 9). **B) Western blot using a polyclonal rabbit anti-human proCPU/CPU antibody (CP17, Agrisera).** Lane 1: Purified plasma proCPU as control, Lane 2: Mixture of purified plasma proCPU (58 kDa) and CPU (35 kDa) as control, Lane 3-9: concentrated conditioned media: HepG2 (lane 3), THP-1 (lane 4), PMA-stimulated THP-1 (lane 5), primary human monocytes (lane 6), primary human M-CSF macrophage (lane 7), primary human IFN- γ /LPS-stimulated macrophage (lane 8), primary human IL-4-stimulated macrophage (lane 9).

An additional Western blot experiment was performed to gain more insight into the reactivity of both polyclonal antibodies against proCPU and CPU (Figure 7-8). PATAFI-S was found to better recognize proCPU, while CP17 showed higher affinity towards CPU. Lysate from all cell types, including HepG2, was also subjected to Western blot analysis. Despite all our efforts neither proCPU, nor CPU could be detected by Western blotting in any of the cell lysates using either proCPU/CPU antibody (data not shown).

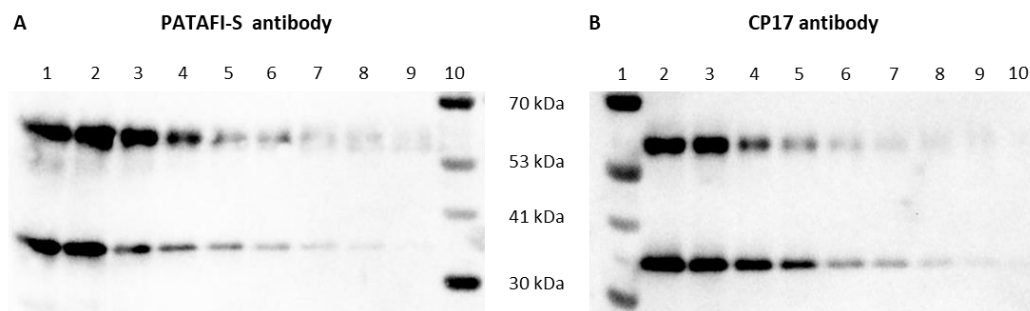


Figure 7-8. Reactivity of a polyclonal sheep anti-human proCPU antibody (PATAFI-S; A) and a polyclonal rabbit anti-human proCPU/CPU antibody (CP17; B) towards proCPU and CPU. A serial dilution of a mixture of purified plasma proCPU (58 kDa) and CPU (36 kDa) was prepared and subjected to SDS-page and Western blotting (PATAFI: lane 1 – 9; CP17: lane 2 – 10) to get insight into the reactivity of both polyclonal antibodies against proCPU and/or CPU. Prestained Protein Ladder – Broad molecular weight is present in lane 10 for PATAFI and lane 1 for CP17 both Western blots.

In order to identify that the 35 kDa protein band detected in the conditioned media with the CP17 antibody is truly CPU and to substantiate that proCPU can be activated into functionally active CPU in the *in vitro* cell environment, HepG2, THP-1 and PMA-stimulated THP-1 cells were cultured in the presence of 1 mM Bz-*o*-cyano-Phe-Arg, a specific CPU substrate. At different time points, medium was collected and subjected to RP-HPLC following an in-house protocol of HPLC-assisted CPU activity measurement to investigate whether the substrate had been cleaved in the cellular environment [131]. As shown in Figure 7-9, the cleaved substrate (Bz-*o*-cyano-Phe) was detected in the medium of all tested cell types.

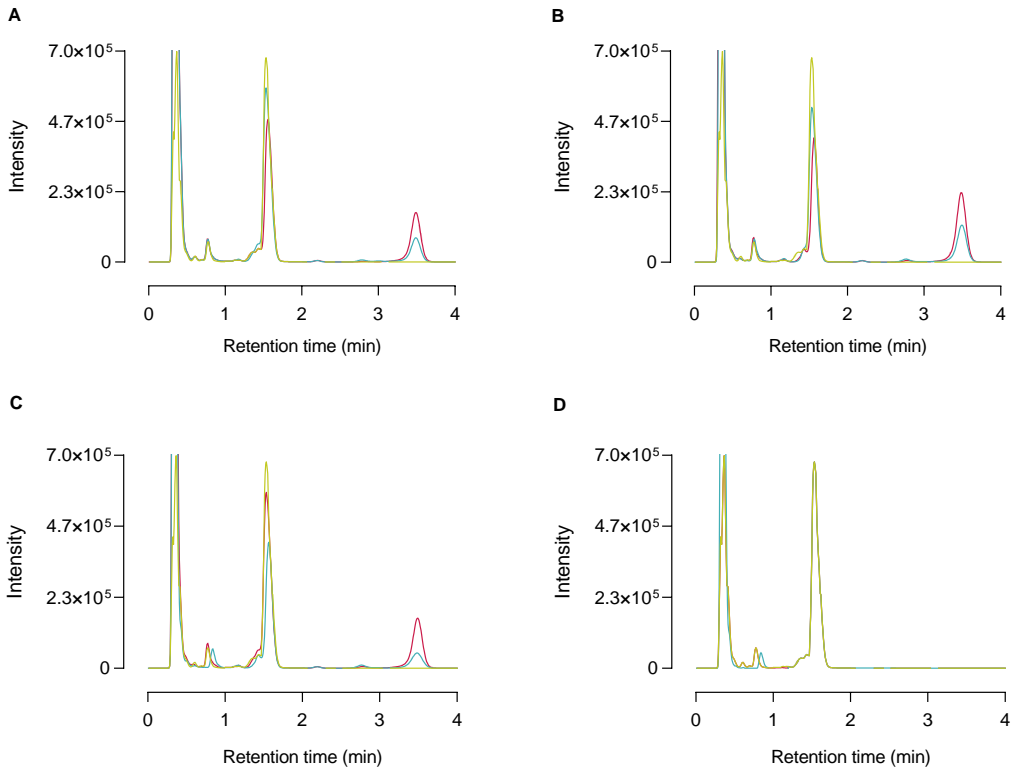


Figure 7-9. High-performance liquid chromatography (HPLC) chromatogram of medium samples from cleavage of the selective CPU substrate Bz-*o*-cyano-Phe-Arg (final concentration 1 mM) by HepG2 (A), THP-1 (B), PMA-stimulated THP-1 cells (C) or in the absence of any cells (blanc; D). 0 h (green curve), 24 h (blue curve) and 72 h (red curve) after incubation with the substrate, cell medium was collected and analyzed by reversed-phase HPLC. The retention time of Bz-*o*-cyano-Phe-Arg (substrate) and Bz-*o*-cyano-Phe (cleaved substrate) is ± 1.53 min and ± 3.49 min respectively.

7.4.4 Immunofluorescent staining shows proCPU/CPU inside (primary) human monocytes and macrophages

Since we did not succeed to detect proCPU/CPU protein in the cellular lysates of any of the cell types, not even in the lysate of HepG2 cells, we tried immunocytochemistry to investigate the presence of proCPU/CPU inside the different cell types. Immunofluorescent staining with a polyclonal rabbit anti-human proCPU/CPU antibody confirmed the presence of proCPU/CPU in all cell types (Figure 7-10). In general, proCPU/CPU staining was diffuse and distributed throughout the cytoplasm with no

granular intracellular staining pattern. All staining controls were negative (Figure 7-10H-J).

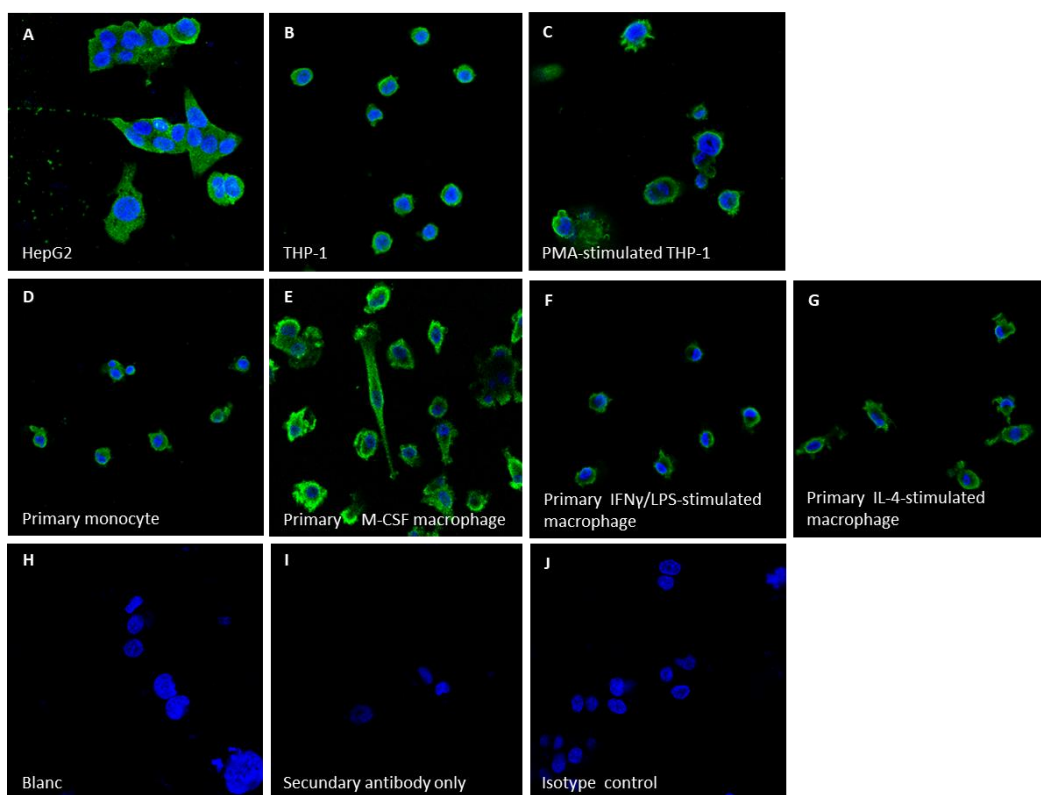


Figure 7-10. Staining of proCPU/CPU in HepG2 (A), THP-1 (B), PMA-stimulated THP-1 cells (C), primary human monocytes (D), primary human M-CSF macrophages (E), primary human IFN- γ /LPS-stimulated macrophages (F) and primary human IL-4-stimulated macrophages (G). Cells were fixed with 4% PFA, permeabilised with 0.1% Triton X-100 and stained for proCPU/CPU (green; CP17, polyclonal rabbit anti-human proCPU/CPU antibody) and DAPI (nuclear marker, blue). Staining controls (H: blanc; I: secondary antibody only; J: isotype control: normal rabbit IgG [Invitrogen, USA]) were all negative. Representative images of three independent experiments. (bar = 20 μ m)

7.4.5 ProCPU concentration measured in medium of (primary) human monocytes and macrophages is related to their state of differentiation

Figure 7-11 shows the results on proCPU concentration in concentrated conditioned medium and lysates of monocytes and macrophages. ProCPU was measured in

conditioned medium samples, with the highest levels seen in HepG2 medium. ProCPU concentration was similar in medium of THP-1 cells and primary human monocytes and significantly higher compared to the concentration in medium of PMA-stimulated THP-1 cells and primary human M-CSF primed macrophages respectively. Moreover, a slight but non-significant increase in proCPU concentration was observed after stimulation of the primary human M-CSF primed macrophages with IFN- γ and LPS, whereas IL-4 stimulation led to a further significant decrease in proCPU activity. In the cell lysates, proCPU concentration was similar in all studied cell types.

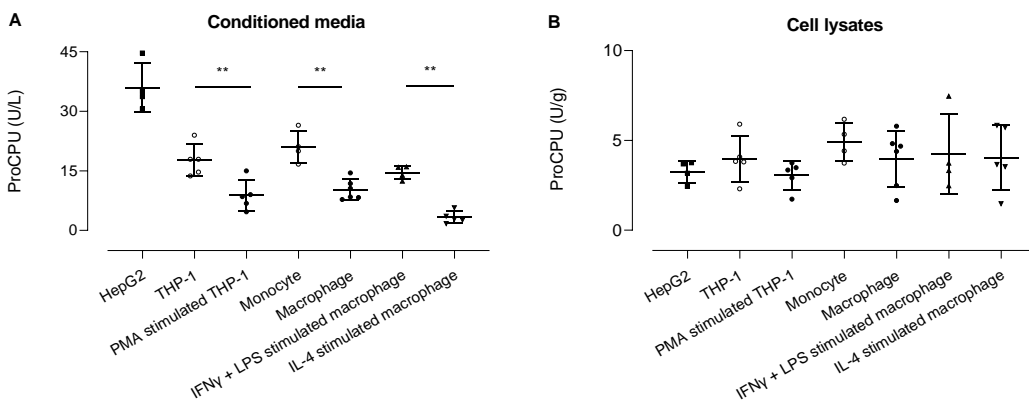


Figure 7-11. ProCPU activity levels measured in A) concentrated conditioned media (U/L) and B) concentrated cell lysates (U/g) of various cell types. Results are reported as mean \pm SEM (N = 4-6; for primary cells each data point represents the result from an independent experiment with cells obtained from another donor for each experiment). A Kruskal-Wallis test with Dunn's multiple comparison test was used to test for statistical significance between all groups; ** $p < 0.01$.

7.5 Discussion

The involvement of both CPU and monocytes/macrophages in inflammation and thrombus formation [321], and the hypothesis of Lin *et al.* that monocytes and macrophages are responsible for the *CPB2* mRNA expression of PBMCs [46], prompted us to investigate the expression of proCPU in (primary) human monocytes and different (primary) human macrophage subsets to gain more insight into these cells as potential sources of proCPU within atherosclerotic plaques and extravascular inflammatory sites.

For this research, we used the human monocytic cell line THP-1 and primary human monocytes and macrophages. The THP-1 cell line has been extensively used to study monocyte/macrophage function and biology, but suffers from the disadvantage that THP-1 cells differ genetically and phenotypically from primary monocytes. Primary cells, such as PBMC-derived monocytes, mimic the *in vivo* human physiology more closely, making it often a more relevant cell culture model [367,368]. Therefore, we here included primary human monocytes and macrophages derived from these monocytes.

After successfully validating primers for RT-qPCR, selecting a set of reference genes to accurately perform RT-qPCR normalization of *CPB2* mRNA expression and confirming appropriate activation of primary resting M-CSF macrophages with IFN- γ /LPS or IL-4, relative *CPB2* mRNA expression was determined in human monocyte- and macrophage cell lines and primary cells by RT-qPCR. Primary human monocytes displayed considerable *CPB2* mRNA expression while the expression decreased substantially after differentiating these cells into resting macrophages by addition of M-CSF. Similar results were obtained in the THP-1 monocytic cell line and PMA-stimulated THP-1 cells where *CPB2* mRNA expression reduced after differentiation of the THP-1 cells into a macrophage-like phenotype. This is in line with the observations of Lin *et al.*, although based on their results we expected *CPB2* mRNA expression to be of similar magnitude in primary human monocytes and THP-1 cells, but this was not the case [46]. The abundance of *CPB2* transcripts was higher in primary cells. The higher expression observed here might be because *CPB2* mRNA expression was studied specifically in monocytes and not in the whole PBMC fraction (of which monocytes make up 10-30%) as Lin *et al.* did. Also, as mentioned earlier, cell lines and primary cells may genetically differ and this might account (in part) for the difference in *CPB2* mRNA expression observed between THP-1 cells and primary human monocytes. Moreover, it is difficult to quantitatively compare the RT-qPCR results obtained in this study and those of Lin *et al.* because here the *CPB2* mRNA expression was expressed relative to a pool of reference genes, while Lin and co-workers made use of RNA standards for absolute

quantification. Nevertheless, a clear trend between expression of *CPB2* transcripts and the state of differentiation was observed for both the monocytic cell line and primary monocytes and macrophages.

Macrophages display remarkable plasticity and can change their physiology in response to environmental cues [369]. As a result, numerous macrophage subtypes with distinct functions have been identified [209,351–354,370]. In this context, we were also interested whether the *CPB2* mRNA expression is different between resting M-CSF macrophages and so-called M1- and M2-macrophages, representing the opposite sites of the diverse macrophage spectrum. Primary M-CSF primed macrophages incubated in the presence of IFN- γ /LPS develop into pro-inflammatory macrophages (M1, classically activated), while IL-4 differentiates monocytes into anti-inflammatory macrophages (M2, alternatively activated). Interestingly, activation of primary human M-CSF macrophages resulted in differential *CPB2* mRNA expression: classical macrophage activation gave rise to a slightly, but not significantly higher *CPB2* mRNA abundance compared to M-CSF primed macrophages, whereas alternative activation significantly lowered expression of *CPB2* transcripts. These observations further support that the expression of *CPB2* mRNA in monocytes and (activated) macrophages is related to the degree to which these cells are differentiated and/or activated.

At protein level we were not able to detect proCPU or CPU protein with Western blot analysis in the cellular lysate of any of the investigated cell types, not even in HepG2 cells. However, immunocytochemistry results clearly demonstrated the presence of proCPU/CPU in HepG2 cells, but also in human monocyte- and macrophage cell lines and primary cells. In addition, using a sensitive proCPU assay, a comparable amount of proCPU was found in all cells, indicating that proCPU present in monocytes and macrophages may boost local proCPU concentrations and have an additive effect on fibrinolysis driven by plasma proCPU. Together with the results of the mRNA analysis, these findings support the hypothesis of Lin *et al.* that proCPU is expressed in monocytes and macrophages [46]. The presence of proCPU in macrophages of atherosclerotic

plaques, as detected by Rylander and co-workers, thus cannot solely be attributed to phagocytosis of environmental proCPU by these macrophages [49].

In concentrated conditioned medium of all studied cell types, proCPU protein was detected using a polyclonal sheep anti-human proCPU antibody (PATAFI-S). Notably, the protein band appeared at a slightly different MW compared to plasma purified proCPU (58 kDa). This small difference is probably caused by differences in posttranslational modification. Differences herein have previously been reported for platelet-derived proCPU and recombinant proCPU produced in insect cells, indicating that one or more glycosylation sites of proCPU are susceptible to variation in glycosylation [43,371]. With this antibody, no CPU was detected in the concentrated conditioned medium samples. In an attempt to detect proCPU or CPU protein in the cellular lysate samples, Western blotting was repeated on those samples using a second proCPU/CPU antibody and the same was done for the conditioned medium samples. To our surprise, this polyclonal rabbit anti-human proCPU/CPU antibody (CP17) visualized a protein band at a MW of around 35 kDa in all samples, exactly at the same level as the protein band of purified CPU. Unexpectedly, no 58 kDa proCPU band was detected on Western blot in any of the media samples using the CP17 antibody. A similar finding with the CP17 antibody was reported by Rylander *et al.* who suggested that denaturation with SDS may affect proCPU more than CPU, making proCPU more rigid and less detectable with the CP17 antibody. Comparing the reactivity of both the PATAFI-S and CP17 antibody towards purified plasma proCPU and CPU on Western blot, the PATAFI-S antibody seems to have a higher affinity towards proCPU, while CP17 better reacts with CPU. A hypothesis is that the level of CPU in the conditioned media is too low to be detected with the PATAFI-S antibody, while proCPU is above the limit of detection for this antibody and vice versa for the CP17 antibody.

By incubating HepG2, THP-1 and PMA-stimulated THP-1 cells with a specific CPU substrate and detecting cleaved substrate in the cell environment, it was demonstrated that proCPU can be activated into functionally active CPU in the *in vitro* cell culture

environment. This confirmed that it was truly CPU that was detected on the CP17 Western blot.

In addition to Western blotting, proCPU was also measured in the concentrated conditioned media using an in-house enzymatic assay. In accordance with the results of the mRNA analysis, a decrease in proCPU concentration in the cell medium was found upon monocyte-to-macrophage differentiation and this phenomenon was seen in the monocytic cell line as well as in primary cells. In contrast to *CPB2* mRNA expression, proCPU levels in medium of THP-1 cells and primary human monocytes were very similar. A discrepancy between mRNA and protein abundance as observed for the THP-1/PMA-stimulated THP-1 cells is however frequently seen and a theoretical understanding mostly remains elusive [362]. Aside from this, it is becoming increasingly clear that – even though their proCPU levels are lower compared to plasma proCPU concentrations – monocytes and macrophages may provide a local source of proCPU and boost proCPU concentrations resulting in an additive effect on fibrinolysis driven by plasma proCPU [44,45]. The downregulation of proCPU levels in the cell medium during monocyte-to-macrophage differentiation suggests a more pronounced role for this enzyme in monocytes as compared to macrophages. However, the exact role and significance of these cells as local proCPU sources is not clear at this time.

Incubation of primary M-CSF primed macrophages with IFN- γ /LPS had little influence on proCPU levels, while alternative macrophage activation with IL-4 caused a further downregulation of proCPU levels. The significance of the differential expression of *CPB2* mRNA and secretion of proCPU protein by classically and alternatively activated macrophages is also still an open question. In the setting of atherosclerosis, IFN- γ /LPS-stimulated macrophages are associated with symptomatic and unstable plaques, whereas IL-4-stimulated macrophages are particularly abundant in stable zones of the plaque and asymptomatic lesions [49,209,355,356]. In addition, it was recently shown that proCPU/CPU is present in considerable amounts in carotid plaques, with the highest levels corresponding to the vulnerable part of the plaque, adjacent to an area with high

macrophage/foam cell content and substantial neovascularization [49]. Based on this, we can speculate that there might be a need for plaque stabilizing mechanisms in unstable, M1-rich plaques. Since CPU limits plasmin generation, thereby preventing fragmentation of the fibrin network (fibrinolysis), counteracting destabilizing effects in this environment and contributing to keeping the plaque intact, it seems plausible that the presence of higher proCPU concentrations in this environment (through proCPU expression by IFN- γ /LPS-stimulated macrophages) is one such mechanism. Following this hypothesis, it seems logical that proCPU expression is the lowest in IL-4-stimulated macrophages. This type of macrophage is predominantly present in the stable environment of the plaque, where there is little or no need for additional plaque stabilizing mechanisms.

7.6 Conclusion

In this study, we confirmed the expression of *CPB2* mRNA by THP-1 and PMA-stimulated THP-1 cells and showed that *CPB2* mRNA is expressed in primary human monocytes isolated from PBMCs and macrophages derived from these monocytes. On a protein level, proCPU was detected in lysate and conditioned medium of HepG2, THP-1, PMA-stimulated THP-1 cells, primary human monocytes, primary human M-CSF macrophages, primary human IFN- γ /LPS-stimulated macrophages and primary human IL-4-stimulated macrophages. Moreover, CPU was detected in the conditioned media of all investigated cell types and it was demonstrated that proCPU can be activated into functionally active CPU in the *in vitro* cell culture environment. Comparison of both relative *CPB2* mRNA expression and proCPU concentrations in the cell medium between the different cell types provided evidence that *CPB2* mRNA expression and proCPU secretion in monocytes and (activated) macrophages are related to the degree to which these cells are differentiated and activated. This sheds new light on monocytes and macrophages as local proCPU sources within atherosclerotic plaques and extravascular inflammatory sites and the potential role of the proCPU system as a modulator of inflammation in these environments.

PART II

Chapter 8

A new pedigree with thrombomodulin-associated coagulopathy in which delayed fibrinolysis is partially attenuated by co-inherited proCPU deficiency

Partly based on:

Westbury SK, Whyte CS, Stephens J, Downes K, Turro E, **Claesen K**, Mertens JC, Hendriks D, Latif A, Leishman EK, NIHR BioResource, Mutch NJ, Tait RC, Mumford AD. A new pedigree with thrombomodulin-associated coagulopathy in which delayed fibrinolysis is partially attenuated by co-inherited TAFI deficiency. *J Thromb Haemost.* 2020;18:2209–2214.

8 A new pedigree with thrombomodulin-associated coagulopathy in which delayed fibrinolysis is partially attenuated by co-inherited proCPU deficiency

8.1 Abstract

Background

Thrombomodulin-associated coagulopathy (TM-AC) is a rare bleeding disorder in which a single reported p.Cys537* variant in the thrombomodulin gene *THBD* causes high plasma thrombomodulin levels. High thrombomodulin levels attenuate thrombin generation and delay fibrinolysis.

Aims

This research aimed to unreport the characteristics of a pedigree with a novel *THBD* variant causing TM-AC, and co-inherited deficiency of proCPU.

Methods

Identification of pathogenic variants in hemostasis genes by Sanger sequencing and case recall for deep phenotyping.

Results

Pedigree members with a previously reported *THBD* variant predicting p.Pro496Argfs*10 and chain truncation in the thrombomodulin transmembrane domain had abnormal bleeding and greatly increased plasma thrombomodulin levels. Affected cases had attenuated thrombin generation (through the protein C pathway) and delayed fibrinolysis (through the CPU pathway) similar to previous reported TM-AC cases with *THBD* p.Cys537*. Coincidentally, some pedigree members also harboured a stop-gain variant in *CPB2* encoding proCPU. This reduced plasma proCPU levels but was asymptomatic. Pedigree members with TM-AC caused by the p.Pro496Argfs*10 *THBD*

variant and also proCPU deficiency had a partially attenuated delay in fibrinolysis, but no change in the defective thrombin generation.

Conclusions

These data extend the reported genetic repertoire of TM-AC and establish a common molecular pathogenesis arising from high plasma levels of thrombomodulin extracellular domain. The data further confirm that the delay in fibrinolysis associated with TM-AC is directly linked to increased proCPU activation. The combination of the rare variants in the pedigree members provides a unique genetic model to develop understanding of the thrombin-thrombomodulin system and its regulation of proCPU.

8.2 Introduction

The transmembrane protein thrombomodulin critically regulates blood coagulation by localizing thrombin to the vascular endothelial surface enabling the activation of several key substrates. The targets of the thrombin-thrombomodulin complex include protein C, which after conversion to activated protein C (APC) limits further thrombin generation by inactivating coagulation factors Va and VIIIa (see also 1.6.1.2(d)) [372]. Thrombomodulin also acts as a cofactor in thrombin-mediated activation of proCPU to the active enzyme CPU. CPU attenuates the binding of tPA and plasminogen to fibrin by cleaving carboxyterminal lysines from partially degraded fibrin, thereby downregulating fibrinolysis [91].

The physiological importance of thrombomodulin is illustrated by the newly-recognized autosomal dominant bleeding disorder TM-AC, which to date has been associated with a single p.Cys537* variant in the thrombomodulin gene *THBD* [373–376]. This truncation variant results in excessive shedding of large quantities of the functionally active thrombomodulin extracellular domain into plasma. This results in a significant bleeding diathesis because the high thrombomodulin levels promote excessive generation of APC which suppresses normal thrombin generation [373–376]. TM-AC is also associated with

delayed fibrinolysis that can be corrected by inhibition of CPU, suggesting that the surplus thrombomodulin in plasma stimulates thrombin-mediated proCPU activation [373].

Here we report on a TM-AC pedigree with abnormal bleeding associated with a previously unreported *THBD* variant. We also describe how some pedigree members also harbour an independently inherited loss-of-function rare variant in *CPB2* resulting in a reduction in proCPU levels and CPU generation and causing amelioration of the delayed fibrinolysis associated with TM-AC.

8.3 Materials and methods

8.3.1 Study pedigree

The study pedigree was identified in a systematic inspection of genotypes in the National Institute for Health Research BioResource – Rare Diseases, which included a collection of 1472 index cases with unexplained bleeding or platelet disorders enrolled between 2012 and 2016. Informed consent for enrolment and recall for extended phenotyping was in accordance with the Declaration of Helsinki (UK Research Ethics Committee approval 13/EE/0325).

8.3.2 DNA sequencing

Procedures for collection of standardized phenotype terms, whole genome sequencing and variant calling were as previously reported [377]. DNA sequencing for co-segregation analysis was performed using Sanger sequencing and the ThromboGenomics platform [378].

8.3.3 ProCPU measurement

Plasma was diluted 40 times in HEPES (20 mmol/L; pH 7.4) and proCPU was activated with human thrombin (4 nmol/L), thrombomodulin (16 nmol/L), and CaCl₂ (50 mmol/L),

after which the generated active CPU was measured with the substrate Bz-*o*-cyano-Phe-Arg and the formed product quantified by HPLC [81].

8.3.4 CPU generation during *in vitro* clot lysis

To functionally characterize the influence of the new *THBD* and *CPB2* mutation on clot formation and lysis, CPU generation during *in vitro* clot lysis was assessed in plasma of the pedigree members. Prior to these measurements, the CPU generation assay was implemented to be used in the *in vitro* clot lysis assay (CLA) of the Aberdeen Cardiovascular & Diabetes Centre (ACDC); and clot lysis- and CPU generation profiles and parameters were compared to those obtained in our in-house *in vitro* CLA for which the CPU generation assay was originally developed and validated.

8.3.4.1 Sample collection for assay comparison

For comparison of CPU generation in the two *in vitro* clot lysis systems, blood from twenty healthy adult volunteers in a fasting state was collected between 8 and 10 am in sodium citrate vacutainer tubes (3.2%; 9:1 v/v; Greiner Bio-One). Blood samples were centrifuged for 15 min at 2000 x *g* and 4 °C. Thereafter the collected plasma was pooled to obtain pooled normal citrated plasma (PNP). Samples were aliquoted before storage at -80 °C. Ethical approval was obtained from the Medical Ethics Committee UZA/UA (B300201214328). All study participants gave written informed consent before enrolment.

8.3.4.2 *In vitro* clot lysis assay of the Aberdeen Cardiovascular & Diabetes Centre

In vitro clot lysis was performed according to a previously published protocol [379]. In a 96-well microtiter plate (Nunc, Denmark) 15 µL plasma (final concentration 30%) was mixed with 4 µL phospholipids (final concentration 16 µM; Rossix, Sweden) in Tris-buffered saline with Tween 20 (TBST), 4 µL tPA in TBST (final concentration 300 pM; Genentech, USA) and 17 µL TBST. Subsequently, 10 µL of a thrombin-CaCl₂ mixture (final

concentrations respectively 0.1 U/L and 10.6 mM) was added to initiate coagulation. The microtiter plate was then shaken for 10 s and a transparent cover was applied to avoid evaporation during the experiment. Finally, the microtiter plate was placed in the spectrophotometer and optical density was measured every 30 s at 405 nm and 37 °C (Versamax, SoftMax Pro v7, Molecular Devices, USA).

Additionally, *in vitro* clot lysis was measured in the presence of PTCl and/or thrombomodulin. To do so, the volume of TBST was substituted by PTCl (final concentration 75 µg/mL) and/or thrombomodulin (final concentration 500 ng/mL).

8.3.4.3 *In vitro* clot lysis assay of the Laboratory of Medical Biochemistry

In a 96-well microtiter plate, 80 µL citrated plasma was mixed with 20 µL tPA in HEPES 20 mM, 0.01% Tween 20 pH 7.4 (final concentration 40 ng/mL). Subsequently, 35 µL 0.9% (m/v) NaCl and 5 µL HEPES 20 mM pH 7.4 were added to this mixture. Coagulation was initiated by adding 20 µL 100 mM CaCl₂ in 20 mM HEPES pH 7.4 (37 °C, final CaCl₂ concentration 12.5 mM). The microtiter plate was shaken for 10 s, a transparent cover was applied and optical density was registered with a spectrophotometer every 30 s at 405 nm and 37 °C (Versamax, SoftMax Pro v5, Molecular Devices, USA).

In vitro clot lysis was also measured in the presence of PTCl and/or thrombomodulin by substituting the volume of HEPES 20 mM pH 7.4 by PTCl (final concentration 75 µg/mL) and/or thrombomodulin (final concentration 500 ng/mL).

8.3.4.4 CPU generation

For both *in vitro* clot lysis protocols, an identical *in vitro* clot lysis experiment was carried out simultaneously in a second microtiter plate placed on a calibrated plate heater. At well-defined time points, 12 µL of sample was aspirated and transferred to a prechilled tube containing aprotinin/PPACK (final concentrations respectively 130 µg/mL and 5 µM) to avoid ongoing proCPU activation. The sample was then immediately placed on iced

water (4 °C). Afterward, CPU activity was determined with our previously published RP-HPLC-based method [131].

8.3.5 Other measurements

Thrombin generation and measurement of sTM were performed as described previously [81,122,373]. Thrombin generation was initiated with 1 pM TF in the presence of 4 μM phospholipids.

8.3.6 Statistical analysis

Clot lysis- and CPU generation profiles and parameters were calculated using a Matlab algorithm [205]. Results are given as mean ± SD. Statistical tests and data plotting were performed with Graphpad Prism version 9.3.1 (GraphPad Software, Inc. La Jolla, USA). Statistical tests are specified in the figure legends. Results with $p < 0.05$ were considered statistically significant.

8.4 Results and discussion

8.4.1 Comparison of the time course of CPU generation in two *in vitro* clot lysis systems

An important element of the characterization of the influence of the newly discovered *THBD* and *CPB2* gene mutation on fibrinolysis – and the CPU system in particular – is the measurement of the time course of CPU generation during *in vitro* clot lysis. Given only limited amounts of plasma samples were available and preliminary *in vitro* clot lysis experiments were performed with the Aberdeen Cardiovascular & Diabetes Centre (ACDC) CLA, CPU generation was implemented in this *in vitro* CLA. Prior to measurement of the patient samples, the robustness of the CPU generation assay was established by comparing the time course of CPU generation to our in-house *in vitro* CLA for which the CPU generation assay was originally developed and validated. This comparison was particularly interesting as both assays differ in terms of the activator used to initiate

coagulation, the concentration of reagents and dilution of plasma, with the ACDC CLA mimicking more closely the physiological situation (Table 8-1).

Table 8-1. Comparison of the *in vitro* clot lysis protocols of the Laboratory of Medical Biochemistry and Aberdeen Cardiovascular & Diabetes Centre.

Reagent	Laboratory of Medical Biochemistry	Aberdeen Cardiovascular & Diabetes Centre
Activator	Recalcification	Recalcification, thrombin, phospholipids
tPA concentration (final)	700 pM	300 pM
Plasma dilution	50%	30%

8.4.1.1 Standard *in vitro* clot lysis assay

As shown in Table 8-2, the standard CLT (without PTCl and thrombomodulin) was 60.2 ± 0.7 min in the ACDC CLA and 49.3 ± 1.3 min in our MedBio CLA. The CLT is thus noticeably longer in the ACDC CLA, which can be explained by the significantly lower tPA concentration used in this *in vitro* clot lysis system (300 pM vs 700 pM tPA in the MedBio CLA). Addition of PTCl to the clot lysis experiment shortened the CLT by 29% in the ACDC CLA, compared to 34% in the MedBio CLA (Figure 8-1). For T_{lag} (lag-time or time to clot initiation) and H_{max} (height of the clot lysis curve), two additional parameters that define the clot lysis profile, a substantial difference between both assays was also noticed. In the ACDC CLA, the T_{lag} was – as expected – significantly shorter (1.0 ± 0.1 vs 6.5 ± 1.1 min) and the first CPU activity peak appeared faster as a result of the addition of phospholipids and thrombin. H_{max} in the MedBio CLA was almost double compared to the ACDC CLA. This is the result of the higher final plasma concentration (50% in the MedBio CLA vs 30% in the ACDC CLA). This difference in final plasma concentration did also influence the height of the first and second CPU activity peaks ($h_{1st\ peak}$ and $h_{2nd\ peak}$), resulting in both peaks being lower in the ACDC CLA (about 2-times for the first peak) versus the MedBio CLA.

Table 8-2. Overview of clot lysis- and CPU generation parameters using the *in vitro* clot lysis protocol of the Laboratory of Medical Biochemistry or the Aberdeen Cardiovascular & Diabetes Centre (N = 2).

	Standard CLA		CLA in the presence of 500 ng/mL thrombomodulin	
	Medical Biochemistry	Aberdeen Cardiovascular & Diabetes Centre	Medical Biochemistry	Aberdeen Cardiovascular & Diabetes Centre
Clot lysis parameters				
T _{lag} (min)	6.5 ± 1.1	1.0 ± 0.0	8.5 ± 1.1	1.5 ± 0.0
CLT (min)	49.3 ± 1.3	60.2 ± 0.7	78.2 ± 0.4	99.4 ± 0.5
CLT with PTCl (min)	32.4 ± 0.6	42.9 ± 0.3	34.1 ± 1.0	41.6 ± 0.9
ΔCLT (min)	16.9 ± 0.6	17.3 ± 0.5	44.1 ± 1.3	57.8 ± 0.7
H _{max} (OD 405 nm)	0.61 ± 0.04	0.34 ± 0.01	0.67 ± 0.03	0.34 ± 0.02
CPU generation parameters				
h _{1st peak} (U/L)	7.7 ± 0.2	3.5 ± 0.2	144 ± 7	278 ± 13
AUC _{1st peak} (U/L.min)	189 ± 1	72 ± 8	3410 ± 141	2883 ± 553
t _{1/2 1st peak} (min)	12.4 ± 0.5	9.9 ± 1.4	11.9 ± 0.1	9.2 ± 0.3
h _{2nd peak} (U/L)	8.1 ± 0.1	2.1 ± 0.1	4.3 ± 0.4	0.0 ± 0.4
AUC _{2nd peak} (U/L.min)	498 ± 15	126 ± 4	267 ± 6	N.A.
t _{1/2 2nd peak} (min)	33.3 ± 0.7	25.1 ± 2.1	29.0 ± 0.6	N.A.

Data are reported as mean ± standard deviation (SD). AUC_{peak}: area under the curve of the first/second CPU activity peak; CLT (min): clot lysis time, time interval between half maximal turbidity during coagulation and fibrinolysis; ΔCLT (min): absolute reduction in clot lysis time after addition of the CPU inhibitor PTCl; H_{max}: height of the clot lysis curve, maximum increase in turbidity from the baseline of the curve, h_{peak}: maximum height of the first/second CPU activity peak; N.A.: not applicable; PTCl: potato tuber carboxypeptidase inhibitor; t_{1/2} observed half-life of the first/second CPU activity peak; T_{lag} (min): lag-time or time to clot initiation.

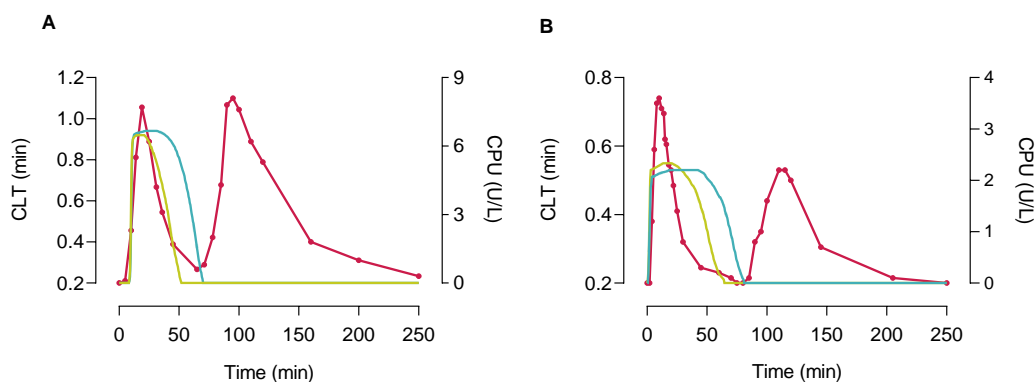


Figure 8-1. CPU generation- and clot lysis profile using the *in vitro* clot lysis protocol of the **Laboratory of Medical Biochemistry (A)** or the **Aberdeen Cardiovascular & Diabetes Centre (B)**. Green curve: clot lysis profile in the absence of potato tuber carboxypeptidase U (PTCl); blue curve: clot lysis profile in the presence of PTCl; pink curve: CPU generation profile.

8.4.1.2 *In vitro* clot lysis assay in the presence of 500 ng/mL thrombomodulin

Addition of thrombomodulin (CLA+TM) lead to significantly more CPU generation (20-times more in the MedBio CLA and 80-times more in the ACDC CLA) and thus caused a delay in fibrinolysis, resulting in a significantly prolonged CLT in both *in vitro* clot lysis systems: 78.2 ± 0.4 min and 99.4 ± 0.5 min in the MedBio and ACDC CLA+TM respectively (Table 8-2). In accordance with the results of the standard CLA, the CLT was longer in the ACDC CLA+TM compared to the MedBio CLA+TM (Table 8-2 and Figure 8-2). Furthermore, the CLT is the same for CLA+TM with PTCl and standard CLA with PTCl, both for the ACDC and MedBio CLA. This implicates full inhibition of the CPU activity in both systems in all tested conditions. When looking at the CPU activity peaks, a high first CPU activity peak and a small second peak were present in the MedBio CLA+TM. In the ACDC CLA+TM, the first CPU activity peak was about 2-times higher compared to the MedBio CLA+TM and no second peak was observed, indicating almost complete activation of proCPU into CPU by thrombin(-thrombomodulin). Most likely the difference in activator used to initiate coagulation is the basis for the difference in peak height between both systems. Based on the height of the first CPU activity peak in the ACDC CLA+TM, the CLT is expected to be about 5 half-lives longer than the normal CLA. The results are consistent with this theoretical assumption.

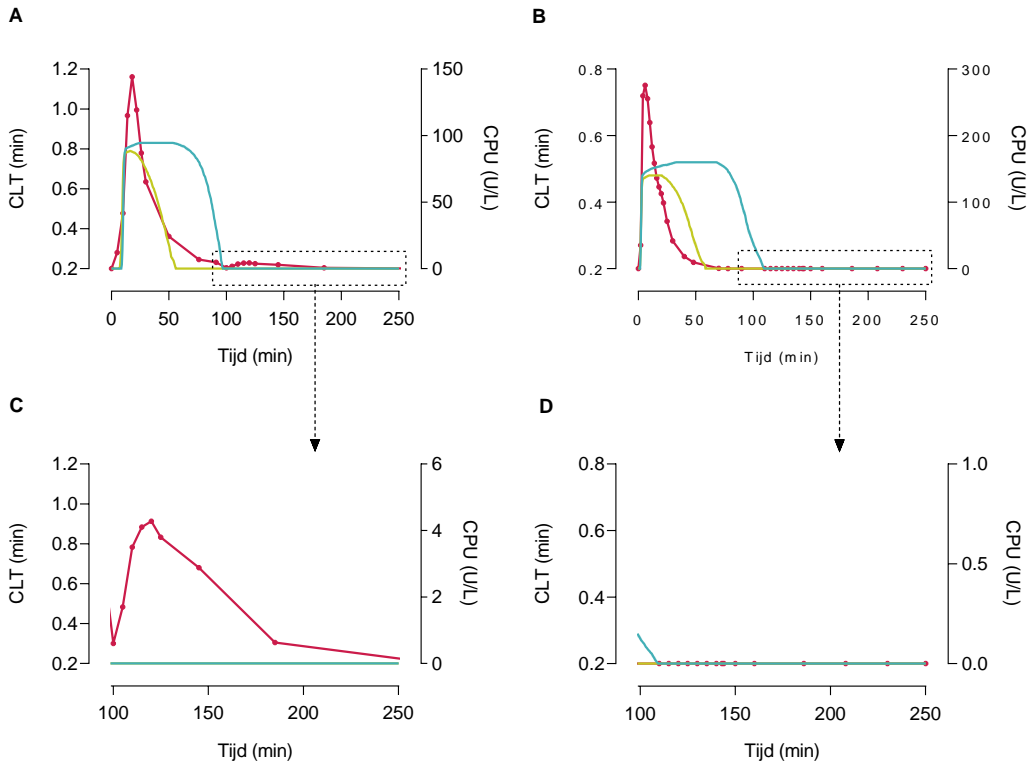


Figure 8-2. CPU generation- and clot lysis profile using the *in vitro* clot lysis protocol of the **Laboratory of Medical Biochemistry (A)** or the **Aberdeen Cardiovascular & Diabetes Centre (B)** in the presence of 500 ng/mL thrombomodulin. Zoom on the second CPU activity peak: MedBio CLA (C) or ACDC (D). Green curve: clot lysis profile in the absence of potato tuber carboxypeptidase U (PTCl); blue curve: clot lysis profile in the presence of PTCl; pink curve: CPU generation profile.

The results of the comparison of CPU generation in these two *in vitro* clot lysis systems showed that the time course of CPU activity generation can be studied in an *in vitro* clot lysis system that mimics the physiological situation through the addition of thrombin and phospholipids. Furthermore, the CPU generation assay is adaptable and sensitive to different experimental conditions. Measurement of CPU generation in plasma of the pedigree members was then performed using the ACDC *in vitro* CLA.

8.4.2 Detection and annotation of the *THBD* and *CPB2* variants

Within the study collection, there was a single index case (II.2, Figure 8-3) with a previously unreported high-impact *THBD* variant, similar to the variant in previously reported pedigrees with TM-AC [373–376].

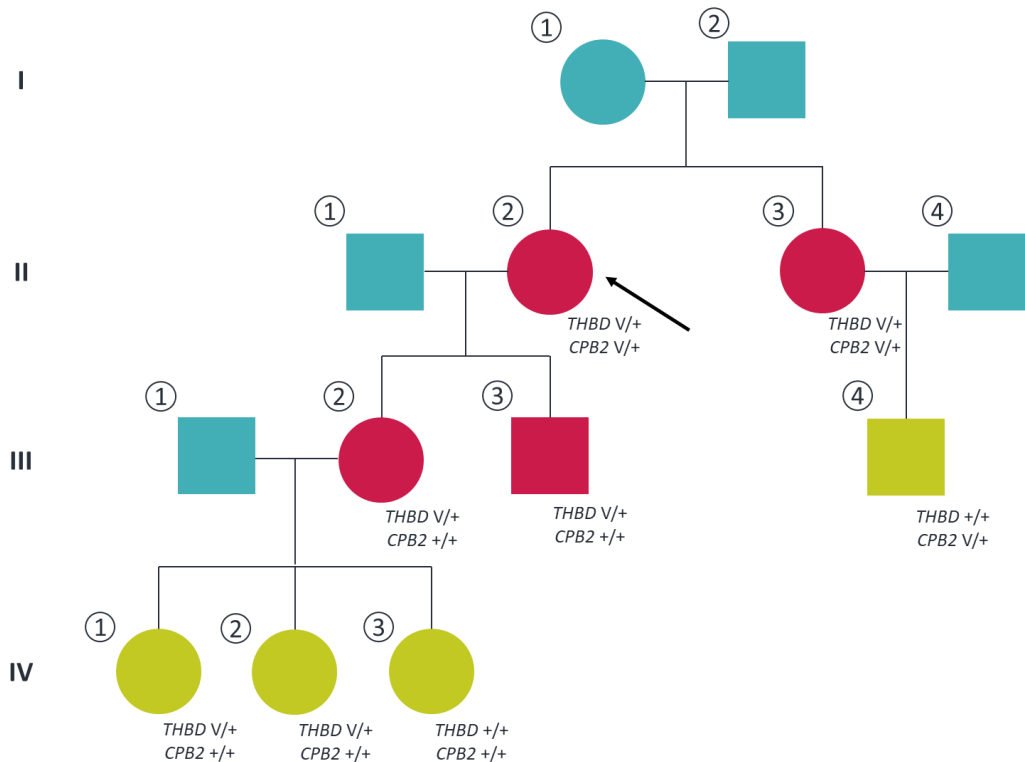


Figure 8-3. Pedigree of the thrombomodulin-associated coagulopathy cases. Pedigree showing the index case (→), indicating the genotype of the individuals for both the *THBD* and *CPB2* variants. The red symbols indicate cases with abnormal bleeding symptoms. The green symbols indicate pedigree members without bleeding symptoms, and the blue symbols indicate pedigree members unavailable for evaluation. V, variant allele; +, wild type allele.

This was a monoallelic single nucleotide deletion annotated as *THBD* c.1487delC, p.Pro496Argfs*10 relative to canonical transcript ENST00000377103.2. This predicted frameshift from codon 496 and a stop gain at codon 505 will result in the loss of the final 11 residues of the thrombomodulin extracellular domain, as well as the transmembrane

domain and the intracellular domain (UniProtKB P07204; Figure 8-4). Inspection of the coding regions of genes encoding known interactors of thrombomodulin within the fibrinolysis pathway revealed that case II.2 also harboured a monoallelic variant in *CPB2*, encoding proCPU, annotated as c.340G>A; p.Arg114* relative to the canonical transcript ENST00000181383.10, which was absent in reference datasets [349,377]. This variant predicts premature truncation of the proCPU protein from residue 114, before the catalytic domain (residues 115-423) [91], thereby preventing functional proCPU expression from this allele (Figure 8-4). The *THBD* variant p.Pro496Argfs*10 was identified in five further pedigree members (II.3, III.2, III.3, IV.1 and IV.2, Figure 8-3). Only case II.3 also harboured *CPB2* p.Arg114*. A single pedigree member (III.4) harboured *CPB2* p.Arg114* but not *THBD* p.Pro496Argfs*10 (Figure 8-3).

8.4.3 Characteristics of the TM-AC cases

The adult cases with *THBD* p.Pro496Argfs*10 (II.2, II.3, III.2, and III.3) all reported bleeding (median ISTH bleeding score 6 versus 0 in the unaffected adult pedigree member; Table 8-3), predominantly after dental procedures and trauma similar to previously reported TM-AC pedigrees [373–376], but also after childbirth. Abnormal bleeding was not reported for the two cases in generation IV who were all aged 14 years or younger at enrolment and who had not undergone invasive dental or surgical procedures. Coinheritance of *CPB2* p.Arg114* (cases II.2 and II.3) had no discernible effect on the frequency or severity of bleeding. Plasma coagulation times, clotting factor levels, and platelet function testing in the *THBD* p.Pro496Argfs*10 cases were normal (data not shown). Consistent with previous reports of TM-AC, plasma thrombomodulin levels were increased by at least two orders of magnitude in all pedigree members with *THBD* p.Pro496Argfs*10 (Table 8-3). Plasma proCPU levels were almost two-fold lower in the three cases harboring *CPB2* p.Arg114* compared to cases without this genotype (542 ± 81 versus 1025 ± 113 U/L; Table 8-3), consistent with absent expression of the *CPB2* allele harboring the p.Arg114* variant.

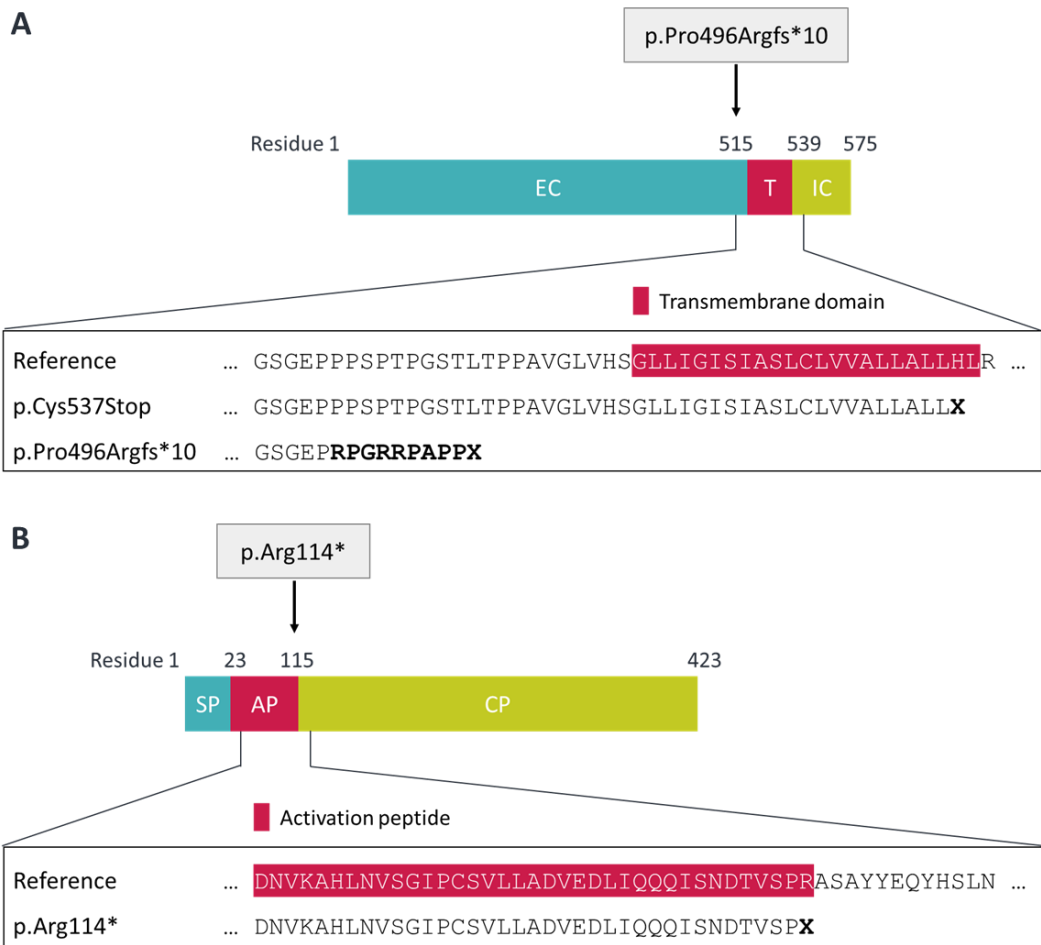


Figure 8-4. Schematic diagram of the *THBD* and *CPB2* variant. A) Schematic diagram of the mature thrombomodulin protein showing the position and amino acid sequence impact of the novel p.Pro496Argfs*10 in relation to the previously described variant associated with thrombomodulin-associated coagulopathy. EC, extracellular domain; T, transmembrane domain; IC, intracellular domain. **B)** Schematic diagram of the proCPU protein indicating the position of the novel p.Arg114* variant. SP, signal peptide; AP, activation peptide; CP carboxypeptidase domain.

Table 8-3. Clinical and laboratory characteristics of pedigree members showing *THBD* and *CPB2* genotypes.

	Age (years)	Bleeding symptoms	ISTH bleeding score	ETP (nM . min)	Peak thrombin (nM)	Plasma TM (ng/mL)	Plasma proCPU (U/L)	<i>THBD</i>	<i>CPB2</i>
Control	-	-	-	1497	143	2.9 - 7.6	667 - 1309	-	-
II.2	64	PPH, dental cutaneous	9	170	31	400	447	V/+	V/+
II.3	60	Dental*	4	NT	NT	364	704	V/+	V/+
III.2	42	PPH, dental	6	82	13	640	912	V/+	+/+
III.3	40	Dental, trauma	6	83	12	514	1138	V/+	+/+
III.4	20	None	0	NT	NT	2.6	475	+/+	V/+
IV.1	14	None	0	NT	NT	598	NT	V/+	+/+
IV.2	11	None	0	NT	NT	698	NT	V/+	+/+
IV.3	8	None	0	NT	NT	2.64	NT	+/+	+/+

Bleeding symptoms were enumerated using the International Society on Thrombosis and Haemostasis (ISTH) bleeding assessment tool [380]. ETP: endogenous thrombin potential; TM: thrombomodulin; proCPU: procarboxypeptidase U; PPH: post-partum hemorrhage; V: variant allele; +: wild type allele; NT: not tested. *Indicates abnormal dental bleeding despite pro-hemostatic measures including antifibrinolytic and plasma treatment. Control ranges are shown in square brackets.

To investigate potential interactions between the *THBD* and *CPB2* genotypes, we compared thrombin generation in plasma from adult pedigree members and control plasma (National Institute for Biological Standards and Control standard plasma) as previously reported [373]. The TM-AC cases (II.2, III.2, and III.3) demonstrated a reduction in endogenous thrombin potential and reduced peak thrombin concentration (Table 8-3). These data with *THBD* p.Pro496Argfs*10 echo those of the previous descriptions of TM-AC associated with the p.Cys537* variant and are consistent with increased generation of APC and excessive suppression of thrombin generation [373–376]. The presence of the additional *CPB2* p.Arg114* variant in the TM-AC case II.2 had no discernible effect on thrombin generation.

8.4.4 The *CPB2* p.Arg114* variant downregulates fibrinolysis

The effect of the *THBD* and *CPB2* variants on tPA-mediated fibrinolysis was analyzed by monitoring the turbidity of plasma samples after clot formation with 0.1 U/mL thrombin and calcium. *In vitro* plasma clot lysis was significantly delayed in samples from TM-AC cases III.2 and III.3 harboring the *THBD* variant alone (223 ± 5.2 and 221 ± 5.9 min respectively versus 85 ± 1.9 min in control; $p < 0.0001$; Figure 8-5A), similar to previously reported cases with TM-AC [373]. In the TM-AC case II.2, which also harbors the *CPB2* p.Arg114* variant, fibrinolysis was delayed compared to control plasma, but to a lesser extent than in the TM-AC cases without *CPB2* p.Arg114* (CLT 127 ± 1.6 min, $p < 0.0001$). Clot lysis was enhanced in case III.4 who had the *CPB2* p.Arg114* variant but did not carry the *THBD* mutation (CLT 66 ± 0.4 versus 85 ± 1.9 min in control, $p < 0.001$; Figure 8-5 A-B).

To explore whether the modulatory effect of *CPB2* p.Arg114* on fibrinolysis was a consequence of a reduction in the proCPU level, CPU concentration was measured during *in vitro* clot lysis. This model enables the resolution of two peaks of CPU formation, generated first by thrombin-thrombomodulin (first CPU activity peak) and subsequently by plasmin (second peak; Figure 8-6). In the TM-AC cases III.2 and III.3

which had the *THBD* variant alone, the first CPU activity peak was dramatically elevated, almost 50-fold compared to the control. In pedigree members II.2 and II.3 that harbor both the *THBD* and *CPB2* p.Arg114* there was approximately a 50% reduction in the first CPU activity peak compared to those members of the pedigree with *THBD* only (Figure 8-6 and Table 8-4). The second CPU activity peak was diminished in all TM-AC cases, reflecting the consumption of plasma proCPU in the first peak by excessive thrombin-thrombomodulin-dependent activation. Both phases of CPU generation were significantly reduced in case III.4 with the *CPB2* p.Arg114* variant alone compared to the control, consistent with reduced plasma proCPU levels (Figure 8-6 and Table 8-4).

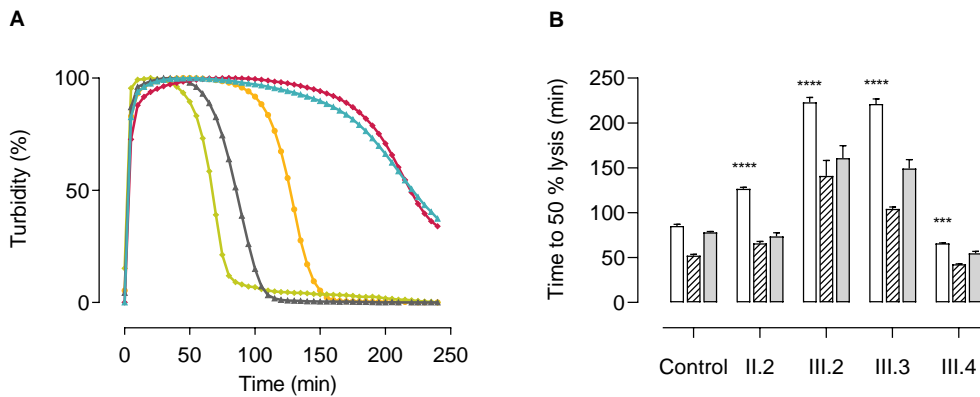


Figure 8-5. Delayed fibrinolysis in thrombomodulin-associated coagulopathy. A) Representative turbidity curves showing clot lysis in plasma from controls or thrombomodulin-associated coagulopathy (TM-AC) cases. Green: case III.4 *CPB2*; grey: control; yellow: case II.2 *THBD + CPB2*; pink: case III.2 *THBD*; blue: case III.3 *THBD*. **B) 50% lysis times** were calculated from triplicate plasma samples using Shiny App for calculating clot lysis times [380]. Experiments were performed with and without 75 $\mu\text{g}/\text{mL}$ potato tuber carboxypeptidase inhibitor (PTCI, Sigma Aldrich) or 65 $\mu\text{g}/\text{mL}$ MA-T12D11.11. Data shown represent the mean \pm standard error of the mean of the turbidity measurements. *** $p < 0.001$ **** $p < 0.0001$ case versus control in plasma without CPU inhibitors. Statistical significance was determined by one-way analysis of variance with Bonferroni's post hoc test.

Pharmacological inhibition of CPU activity with PTCI or direct inhibition of thrombin-thrombomodulin mediated proCPU activation with the specific antibody MA-T12D11 partially corrected the delayed fibrinolysis in the TM-AC cases III.2 and III.3 with the *THBD* variant (Figure 8-5B). The concentrations of inhibitors included here had

previously been used to overcome CPU activity in plasma [116,373,379]. However, in this study the exceptionally high concentrations of thrombomodulin in the plasma of the case studies precluded the complete correction of the CLT. Higher concentrations of inhibitor were able to reduce levels further (data not shown). In TM-AC case II.2, who also harbors *CPB2* p.Arg114*, the same concentrations of inhibitor permitted more complete correction of the fibrinolytic abnormalities, with CLTs similar to those of control plasma (Figure 8-5B). These data are the first to describe a genetic deficiency of proCPU and emphasize the key role of proCPU in attenuating fibrinolysis in TM-AC.

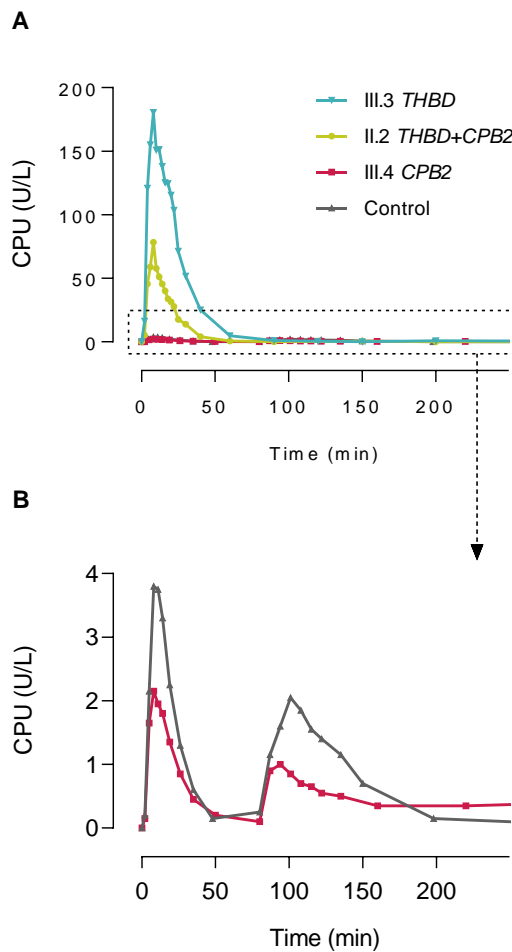


Figure 8-6. Representative profiles of biphasic CPU generation during *in vitro* clot lysis from controls or TM-AC cases. The first and second CPU activity peak correspond to thrombin-thrombomodulin-mediated and plasmin-mediated CPU generation respectively.

Table 8-4. CPU activity levels for the first and second peak of CPU generation during *in vitro* clot lysis for all adult pedigree members. Data represent mean \pm standard deviation (N = 6).

Case	Height first CPU activity peak (U/L)	Height second CPU activity peak (U/L)
Control	3.8 \pm 0.1	2.0 \pm 0.2
II.2 (<i>THBD</i> + <i>CPB2</i>)	78.0 \pm 11.0	0.4 \pm 0.2
II.3 (<i>THBD</i> + <i>CPB2</i>)	85.0 \pm 4.0	0.1 \pm 0.1
III.2 (<i>THBD</i>)	195.0 \pm 4.0	0.5 \pm 0.6
III.3 (<i>THBD</i>)	181.0 \pm 1.0	0.9 \pm 0.6
III.4 (<i>CPB2</i>)	2.2 \pm 0.1	1.0 \pm 0.4

8.5 Conclusion

The pedigree described herein harbors a variant in *THBD* that marks only the second worldwide reported genetic variant to result in the rare bleeding disorder TM-AC. The variant identified, *THBD* p.Pro496Argfs*10, predicts protein chain truncation close to the transmembrane domain, thereby promoting excessive shedding of the thrombomodulin extracellular domain. The marked elevation in plasma thrombomodulin attenuates thrombin generation and delays fibrinolysis. This is a similar consequence to the *THBD* p.Cys537* variant associated with all previously described cases of TM-AC [373–376]. The reported results suggest a common pathogenic mechanism in both *THBD* variants in which the chain truncation promotes shedding of a functionally active thrombomodulin extracellular domain into plasma [381].

Remarkably, some pedigree members also harbor a pathogenic variant in *CPB2* predicting p.Arg114* in proCPU, resulting in a partial deficiency of plasma proCPU levels. To our knowledge, this is the first known case of a genetic deficiency in proCPU to be described in humans. We show that proCPU deficiency is clinically asymptomatic, but that the reduction of proCPU activity in plasma accelerates fibrinolysis *in vitro*. Coinheritance of the *CPB2* p.Arg114* with *THBD* p.Pro496Argfs*10 partially ameliorates the delayed fibrinolytic profile associated with TM-AC, clearly demonstrating a crucial role for proCPU in this laboratory feature of TM-AC. The effect of this variant was similar

to pharmacological inhibition of CPU in members of the pedigree with TM-AC. Analysis of this pedigree, in which members have highly impactful variants affecting two interacting coagulation pathway genes, enhances our understanding of ultra-rare human hemostatic disorders. The different combinations of the variants in the pedigree family members is a unique platform to allow insights into the regulation of the thrombin-thrombomodulin system and proCPU activation that is highly relevant to a broad range of hemostatic disorders and therapies. The asymptomatic nature of genetic depletion of human proCPU underscores the potential to exploit inhibition of proCPU pharmacologically without bleeding complications.

Chapter 9

Activation of the CPU system in patients with SARS-CoV-2 infection could contribute to COVID-19 hypofibrinolytic state and disease severity prognosis

Based on:

Claesen K, Sim Y, Bracke A, De bruyn M, De Hert E, Vliegen G, Hotterbeekx A, Vujkovic, A, van Petersen L, De Winter FHR, Brosius I, Theunissen C, van Ierssel S, van Frankenhuijsen M, Vlieghe E, Vercauteren K, Kumar-Singh S, De Meester I, Hendriks D. Activation of the carboxypeptidase U (CPU, TAF1a, CPB2) system in patients with SARS-CoV-2 infection could contribute to COVID-19 hypofibrinolytic state and disease severity prognosis. *Journal of Clinical Medicine*. 2022; 11: 1489.

9 Activation of the CPU system in patients with SARS-CoV-2 infection could contribute to COVID-19 hypofibrinolytic state and disease severity prognosis

9.1 Abstract

Background

COVID-19 is a viral lower respiratory tract infection caused by the highly transmissible and pathogenic SARS-CoV-2. Besides respiratory failure, systemic thromboembolic complications are frequent in COVID-19 patients and suggested to be the result of a dysregulation of the hemostatic balance. Although several markers of coagulation and fibrinolysis have been studied extensively, little is known about the effect of SARS-CoV-2 infection on the potent antifibrinolytic enzyme CPU.

Methods

Blood was collected longitudinally from 56 hospitalized COVID-19 patients and 32 healthy controls. ProCPU levels and total active and inactivated CPU (CPU+CPUi) antigen levels were measured.

Results

At study inclusion (shortly after hospital admission) proCPU levels were significantly lower and CPU+CPUi antigen levels significantly higher in COVID-19 patients compared to controls. Both proCPU and CPU+CPUi antigen levels showed a subsequent progressive increase in these patients. Hereafter, proCPU levels decreased and were at discharge comparable to the controls. CPU+CPUi antigen levels at discharge were still higher compared to controls. Baseline CPU+CPUi antigen levels (shortly after hospital admission) correlated with disease severity and the duration of hospitalization.

Conclusion

In conclusion, CPU generation with concomitant proCPU consumption during early SARS-CoV-2 infection might (at least partly) contribute to the hypofibrinolytic state observed in COVID-19 patients, thus enlarging their risk for thrombosis. Moreover, given the association between CPU+CPUi antigen levels and both disease severity and duration of hospitalization, this parameter may be a potential biomarker with prognostic value in SARS-CoV-2 infection.

9.2 Introduction

COVID-19 is a viral lower respiratory tract infection caused by the highly transmissible and pathogenic SARS-CoV-2. The infection primarily affects the respiratory system with the majority of individuals with SARS-CoV-2 developing no or minimal symptoms (including fever, cough, myalgia, headache, and taste and smell dysfunction) [308,309]. About 15% of patients develop viral pneumonia with significant hypoxemia that requires oxygen support. In approximately 5% of patients, this hypoxemic respiratory failure leads to a rapidly evolving severe ARDS, sepsis and/or multiorgan failure [310–312].

Besides respiratory failure, systemic thromboembolic complications are frequent in COVID-19 patients and the result of a dysregulation of the hemostatic balance [309,313–316]. Abnormalities observed in most patients include a (minimally) prolonged prothrombin time, low antithrombin concentrations, elevated fibrinogen and mild (if any) thrombocytopenia [310,313,382,383]. Findings of elevated PAI-1 levels and substantially reduced clot lysis as measured by thromboelastography point towards hypofibrinolysis in COVID-19 patients [314,315,384,385]. Moreover, markedly increased plasma D-dimer concentrations are a hallmark of COVID-19 and strongly suggestive of plasmin-mediated fibrinolysis following activation of the coagulation cascade [313,383,386]. COVID-19 thus causes the hemostatic balance to tip towards an overall hypercoagulable and hypofibrinolytic state.

The enzyme CPU is a potent inhibitor of fibrinolysis. After activation of the zymogen proCPU by thrombin(-thrombomodulin) or plasmin, CPU delays efficient plasminogen activation by cleaving off C-terminal lysines from partially degraded fibrin [3,91,326]. As such, CPU counteracts the progression of fibrinolysis. The question arises whether CPU may play a role in the hypofibrinolytic state observed in COVID-19 patients and thus may contribute to the high prothrombotic status in these patients. Here, we explored the effect of SARS-CoV-2 infection on the CPU system by measuring both proCPU and CPU+CPUi over time.

9.3 Materials and methods

9.3.1 Study design and participants

This was a *post-hoc* analysis within the COVID-19 Immune Repertoire Sequencing (IMSEQ) study, a single-center prospective cohort study conducted at the Antwerp University Hospital (UZA) of which the study design was previously described (clinical trials.gov NCT04368143) [387]. The study was approved by the institutional Ethics Committee UZA/UAntwerp (20/12/135) and the Institute of Tropical Medicine Antwerp (ITM) institutional review board, and written informed consent was obtained from all participants or their legal representative at inclusion.

Patients (≥ 18 years of age) with SARS-CoV-2 infection (confirmed by SARS-CoV-2 PCR test) were included shortly after hospital admission. Clinical data and recorded interventions (e.g. routine laboratory parameters, use of antivirals, antibiotics, respiratory support...) were collected from the electronic patient medical file. Disease severity was assessed by the WHO COVID-19 disease severity categorization [308].

Clinically healthy individuals were recruited at the ITM as a control population for comparison of CPU-related parameters. Some of these individuals previously tested positive for SARS-CoV-2 (COVID-19 exposed controls), while others did not have evidence of SARS-CoV-2 exposure (COVID-19 non-exposed controls).

9.3.2 Sample collection and biochemical analysis

Blood samples were collected longitudinally from hospitalized COVID-19 patients: the inclusion time point was shortly after hospital admission, with follow-up time points until discharge. In control subjects, two blood collections were performed approximately four weeks apart. Blood was drawn in lithium heparin tubes (16 IU/mL blood, S-Monovette®, Germany). Plasma proCPU concentrations were determined as previously described [81,200]. Antigen levels of activated and inactivated CPU (CPU+CPUi) were measured by ELISA according to the manufacturer's instructions (Asserachrom TAFIa/TAFIai, Diagnostica Stago, France) and routine laboratory parameters of the COVID-19 cohort were determined at the hospital's clinical laboratory.

9.3.3 Statistical analysis

Results were expressed as mean \pm SD. GraphPad Prism version 9.3.1 (GraphPad Software, Inc., USA) was used for statistical analysis and data plotting. A Kolmogorov-Smirnov test showed that none of the continuous variables were normally distributed. A Mann-Whitney U test (unpaired data) or a Wilcoxon Matched-Pairs Signed Rank test (paired data) were performed to compare differences between continuous variables. Spearman correlation coefficients were computed to assess possible associations. A *p*-value < 0.05 was considered statistically significant.

9.4 Results and discussion

9.4.1 Patient characteristics

Patient enrollment took place at the Antwerp University Hospital between April 2020 and February 2021. During the study period, a total of 56 patients (38 male, 18 female) with laboratory-confirmed COVID-19 were recruited. Mean age was 58 ± 14 years (range 29–84 years). On average, patients with SARS-CoV-2 infection were hospitalized for 19 ± 6 days (range 3–61 days) in this study. Additional characteristics of the COVID-19 patients are summarized in Table 9-1.

Table 9-1. Clinical and biological characteristics of COVID-19 patients (N = 56).

Parameter	Result	Reference value
Demographics		
Age – years (range)	58 (29 – 84)	-
Sex		
Male – N (%)	38 (68%)	-
Female – N (%)	18 (32%)	-
Baseline Clinical Parameters		
Comorbidities		
Obesity	13 (22%)	-
Diabetes	9 (16%)	-
Chronic respiratory disease	10 (17%)	-
Cardiovascular disease	10 (17%)	-
Cancer	6 (10%)	-
SpO ₂ at admission (%)	96 ± 4	-
WHO severity classification		
Moderate	39 (70%)	-
Severe	5 (9%)	-
Critical	12 (21%)	-
Laboratory Parameters		
Platelet count (*10 ⁹ /L)	181 ± 79	166 – 396
WBC (*10 ⁹ /L)	8.6 ± 6.0	4.2 – 10.3
CRP (mg/L)	94 ± 125	< 10
Hospital Care		
Medication use		
Antibiotics	36 (62%)	-
Antivirals	4 (7%)	-
Antifungals	1 (2%)	-
Steroids	25 (43%)	-
Vasoactive medications	7 (12%)	-
Antiplatelet agent	2 (3%)	-
Anticoagulation	8 (14%)	-
Respiratory status		
Room air	6 (10%)	-
High-flow nasal oxygen	44 (76%)	-
Invasive ventilation	7 (12%)	-
Extracorporeal life support	1 (2%)	-
Outcome		
ICU stay	9 (16%)	-
Days in hospital	19 ± 6	-
In-hospital death	4 (7%)	-

Results are given as a number (N) with percentage in parentheses or as mean ± standard deviation (SD). COVID-19: coronavirus disease 19; CRP: C-reactive protein; ICU: intensive care unit; WBC: white blood cell.

For comparison of CPU-related parameters, 32 clinically healthy subjects were included (21 male, 11 female; mean age 45 ± 12 years [range 19–62 years]). Although the control group is younger on average, the age difference with the COVID-19 group was not statistically significant. Of those 32 individuals, 14 had a history of PCR-confirmed SARS-CoV-2 infection (at least 2 months before inclusion) or a positive serological test result (COVID-19 exposed controls; 11 male, 3 female; mean age 41 ± 15 years [range 19–62 years]), while the other 18 did not have indications of SARS-CoV-2 infection history (i.e. no known high-risk contact and absence of COVID-19 clinical symptoms, or a negative PCR test in the event of a high-risk contact or COVID-19 clinical symptoms [COVID-19 non-exposed controls; 10 male, 8 female; mean age 45 ± 11 years (range 24–59 years)]).

9.4.2 ProCPU and CPU+CPUi antigen levels do not differ between COVID-19 exposed and non-exposed controls

To evaluate whether there was a long-term effect of COVID-19 on CPU-related parameters in clinically healthy individuals that had previously experienced the disease, proCPU- and CPU+CPUi antigen levels of the COVID-19 exposed controls were compared with those of the COVID-19 non-exposed controls. Neither proCPU- ($p = 0.66$) (Figure 9-1A) nor CPU+CPUi antigen levels ($p = 0.96$) (Figure 9-1B) significantly differed between the two control groups. In further analysis, COVID-19 exposed and non-exposed controls were merged into a single control group.

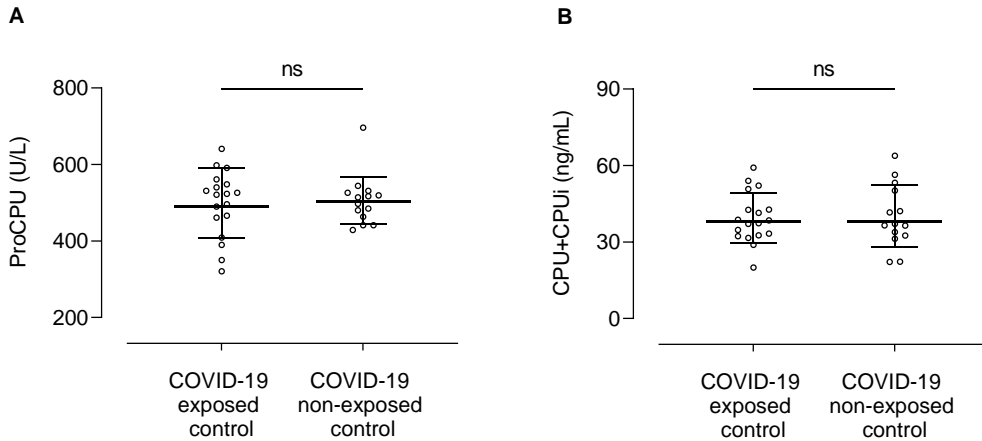


Figure 9-1. Plasma proCPU levels (A) and total active and inactivated carboxypeptidase U (CPU+CPUi) antigen levels (B) in COVID-19 exposed (N = 14) and COVID-19 non-exposed (N = 18) controls. COVID-19 exposed controls are individuals that previously tested positive for SARS-CoV-2 (PCR-confirmed SARS-CoV-2 infection (at least 2 months before inclusion) or a positive serological test result), while COVID-19 non-exposed controls are individuals without evidence of SARS-CoV-2 exposure. Data are presented as mean \pm SD. Mann Whitney U test; NS = not significant.

9.4.3 ProCPU consumption with concomitant CPU generation in COVID-19 patients upon hospital admission

ProCPU and CPU+CPUi antigen levels were measured in longitudinal COVID-19 patient samples. CPU+CPUi measurements are a good indicator of recent and ongoing CPU activation, representing the total amount of active CPU and thermally inactivated CPU (CPUi) present at a certain time point.

Shortly after hospital admission (inclusion time point), mean proCPU levels were significantly lower in COVID-19 patients (466 ± 130 U/L) compared to controls (501 ± 77 U/L; $p = 0.01$) (Figure 9-2A). Lower proCPU levels in COVID-19 patients (N = 14) compared to healthy controls (N = 14) were also reported by Juneja and co-workers [388]. Mean CPU+CPUi antigen levels on the other hand were significantly higher in COVID-19 patients shortly after hospital admission (54.9 ± 17.8 ng/mL vs 41.2 ± 23.6 ng/mL; $p < 0.0001$) (Figure 9-2B). These results reflect consumption of proCPU and thus ongoing cleavage of proCPU with concomitant CPU generation in the early phase of SARS-CoV-2

infection. An increase in active CPU is known to slow down fibrinolysis, and thus can contribute to the hypofibrinolytic status of COVID-19 patients and will likely enlarge the risk of thrombosis in these patients.

9.4.4 Time course of CPU-related parameters

To get a more complete picture of the effect of SARS-CoV-2 infection on the CPU system, proCPU and CPU+CPUi antigen levels were further measured during patient hospitalization.

9.4.4.1 Total study population

Following low proCPU concentrations early after admission (inclusion time point), a pronounced elevation of proCPU levels was observed in COVID-19 patients during the first weeks. Around day 14, proCPU levels were significantly higher compared to controls ($p < 0.001$) and to initial values ($p = 0.002$) (Figure 9-2A). Hereafter, proCPU levels declined, with levels at discharge that were comparable to those of the controls ($p = 0.99$) (Figure 9-2A). ProCPU levels in the control cohort remained stable over a period of 28 days ($p = 0.99$) (Figure 9-2A). In addition, measurement of CPU+CPUi antigen levels over time showed that these levels also progressively increased in COVID-19 patients up to approximately day 14. This period was followed by a clear and significant decrease in CPU+CPUi antigen levels, with CPU+CPUi antigen levels at discharge similar to those shortly after admission. Compared to controls CPU+CPUi antigen levels at discharge were still elevated in COVID-19 patients (Figure 9-2B). CPU+CPUi antigen levels of the control cohort remained stable over a period of 28 days ($p = 0.93$) (Figure 9-2B). The time course of these parameters sheds light on the changes in CPU-related parameters caused by COVID-19. Most likely, the hypercoagulable state in SARS-CoV-2 infection results in elevated concentrations of thrombin, which will cause increased proCPU consumption (evidenced by a decrease in proCPU levels shortly after admission) together with CPU generation, and explains the rise in CPU+CPUi antigen levels over time. Activation of the CPU system arising from an inflammation-driven increase in

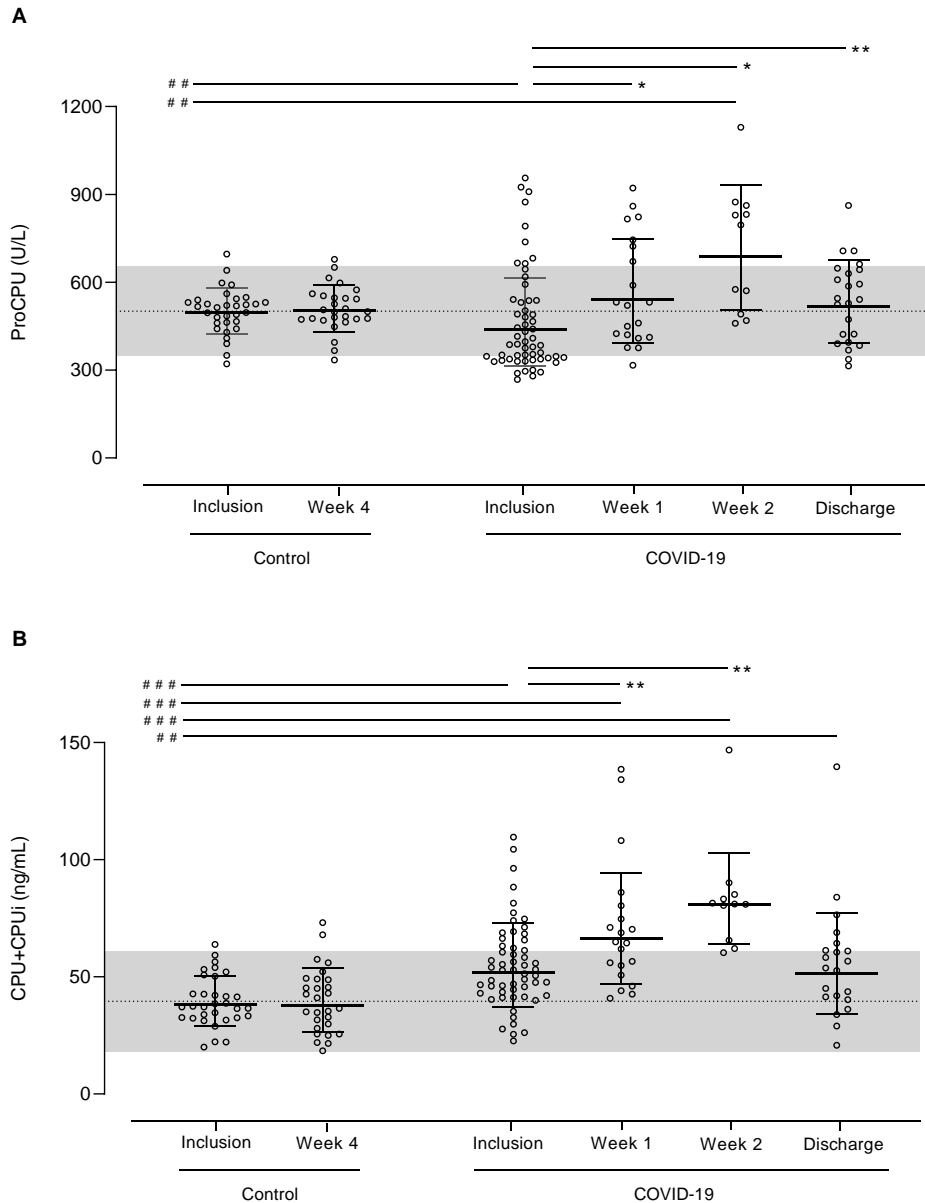


Figure 9-2. Time course of plasma proCPU levels (A) and total active and inactivated carboxypeptidase U (CPU+CPUi) antigen levels (B) in hospitalized COVID-19 patients (N = 12 - 56) at inclusion (ranging from 1 – 5 days after hospital admission), 1 week after inclusion (ranging from 5 – 8 days after inclusion), 2 weeks after inclusion (ranging from 12 – 15 days after inclusion) and at discharge (ranging from 17 – 61 days after inclusion) and in clinically healthy controls at inclusion and 28 days later (N = 32). Data are presented as mean \pm SD. Mann Whitney U test (unpaired data); # $p < 0.05$; ## $p < 0.01$ and ### $p < 0.001$. Wilcoxon Matched-Pairs Signed Rank test (paired data); * $p < 0.05$; ** $p < 0.01$; * $p < 0.001$. The horizontal dotted line represents the mean proCPU level or CPU+CPUi antigen level of the healthy controls with corresponding confidence interval ($2 \times \text{SD}$; grey area).**

thrombin concentration is not only seen in COVID-19, but also in other inflammatory disease states which is supported by several studies investigating the CPU system in sepsis. In these studies, admission proCPU levels were consistently decreased in septic patients compared to controls, while CPU+CPUi antigen levels were significantly higher at that time [389–394]. Moreover, CPU+CPUi antigen levels were significantly higher in non-survivors versus survivors and strongly correlated with severity scores of the disease [394–396]. The secondary increase in proCPU concentrations on the other hand is most likely the result of an increase in proCPU synthesis in the liver. Interestingly, Lustenberger and colleagues described a similar time course for proCPU in trauma-induced coagulopathy, including a secondary increment in proCPU levels as observed here in the setting of COVID-19 [21]. A possible explanation for this increased proCPU synthesis is that the inflammatory environment in COVID-19 causes a proCPU upregulation since it is known that plasma proCPU concentrations are subject to inflammation and that inflammatory cytokines are able to modulate the expression of *CPB2*, the gene encoding proCPU [17,21].

9.4.4.2 Critical versus non-critical disease

When comparing the time course of proCPU levels in COVID-19 patients with critical vs non-critical disease, the above-described pattern of low admission proCPU levels that markedly increased during the first weeks of hospitalization, and an overall normalization at discharge was clearly visible in both groups (Figure 9-3A). While the secondary rise in proCPU levels seems to be more pronounced in the critical disease cohort, no statistical significance was reached comparing patients with non-critical vs critical disease at any time point. Detailed individual proCPU profiles of six critically ill patients (patients with ≥ 4 sampling time points available) also showed a similar time course (Figure 9-3B).

The time courses of CPU+CPUi antigen levels in the critical- and non-critical disease cohort were also comparable and followed the earlier described trend of elevated admission levels that further increased up to approximately day 14 and normalized at discharge. However, the normalization of the CPU+CPUi antigen levels is slower in

patients with critical disease (Figure 9-4A). Moreover, the detailed individual CPU+CPUi antigen level profiles of the same six critically ill patients showed substantial interindividual variability in CPU+CPUi antigen levels (Figure 9-4B). While two out of six patients displayed only limited CPU activation (CPU+CPUi peak levels < 70 ng/mL), the other four displayed extensive CPU activation (> 130 ng/mL). In the latter patients, the extent of CPU+CPUi peak levels was similar, but the time when these peak levels were reached, was highly variable among patients and ranged between 5 and 22 days.

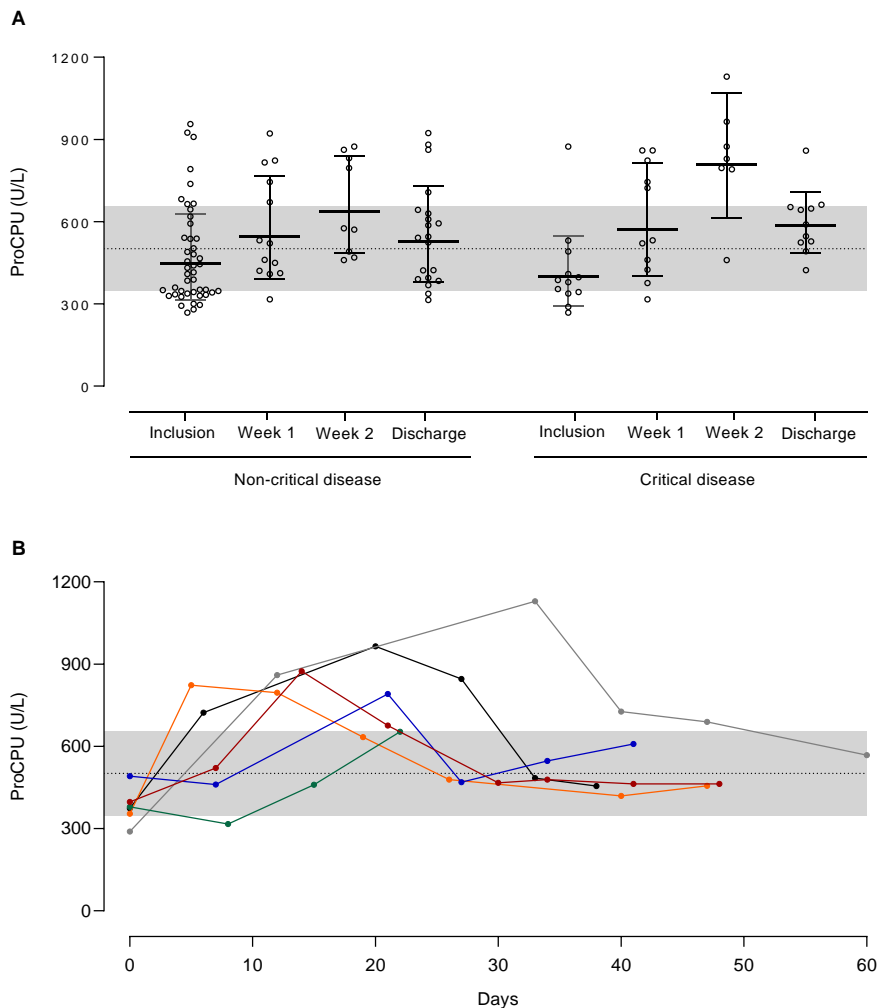


Figure 9-3. A) Time course of plasma proCPU levels at inclusion (ranging from 1 – 5 days after hospital admission), 1 week after inclusion (ranging from 5 – 8 days after inclusion), 2 weeks after inclusion (ranging from 12 – 15 days after inclusion) and at discharge (ranging from 17 to 61 days after inclusion) in COVID-19 patients with critical disease (right; N = 12) versus non-critical disease

(left; N = 44). Data are presented as mean \pm SD. The horizontal dotted line represents the mean proCPU level of the healthy controls with corresponding confidence interval ($2 \times$ SD; grey area). **Mann Whitney U test (unpaired data). Wilcoxon Matched-Pairs Signed Rank test (paired data).** **B) Individual proCPU profiles of six critically ill patients (samples at ≥ 4 time points available).** The horizontal dotted line represents the mean proCPU level of the healthy controls with corresponding confidence interval ($2 \times$ SD; grey area).

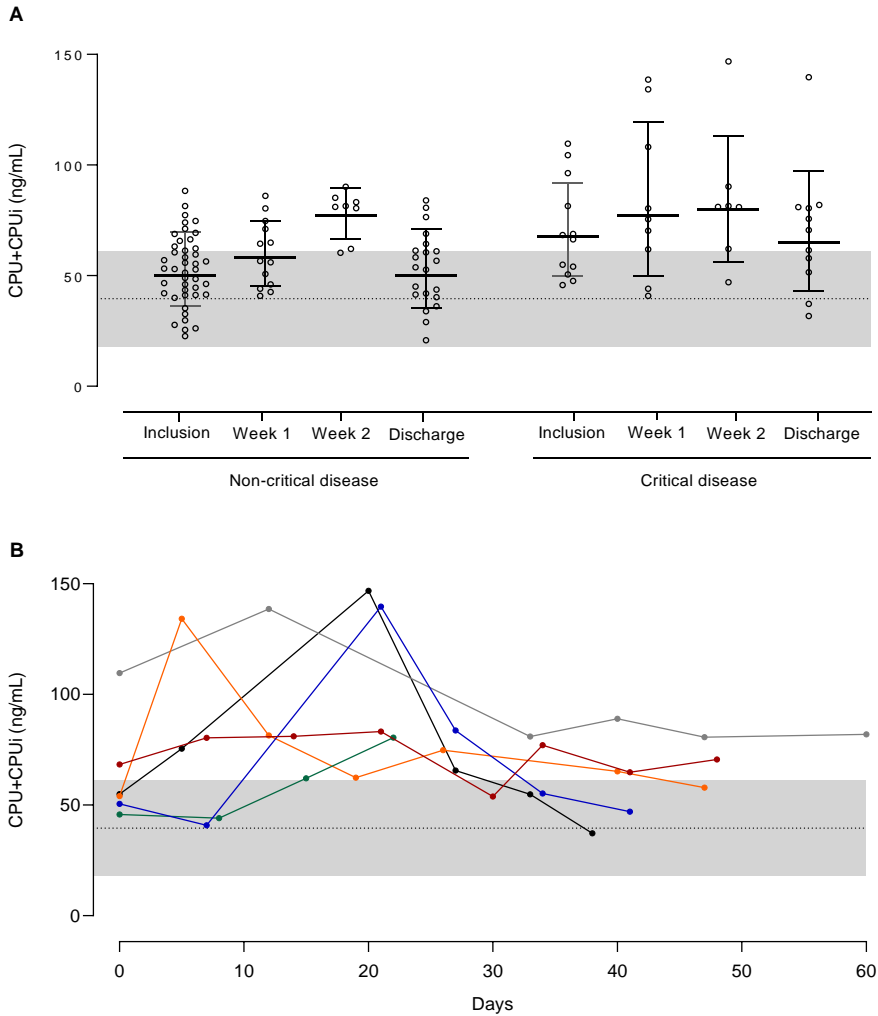


Figure 9-4. A) Time course of plasma CPU+CPUi antigen levels at inclusion (ranging from 1 – 5 days after hospital admission), 1 week after inclusion (ranging from 5 – 8 days after inclusion), 2 weeks after inclusion (ranging from 12 – 15 days after inclusion) and at discharge (ranging from 17 to 61 days after inclusion) in COVID-19 patients with critical disease (right; N = 12) versus non-critical disease (left; N = 44). Data are presented as mean \pm SD. The horizontal dotted line represents the mean CPU+CPUi antigen level of the healthy controls with corresponding confidence interval ($2 \times$ SD; grey area). **Mann Whitney U test (unpaired data). Wilcoxon Matched-Pairs Signed Rank test (paired data).** **B) Individual CPU+CPUi antigen level profiles of six critically ill patients (samples at ≥ 4 time points available).** The horizontal dotted line represents the mean CPU+CPUi antigen level of the healthy controls with corresponding confidence interval ($2 \times$ SD; grey area).

9.4.5 CRP levels correlate with the decrease in proCPU levels early after disease onset

To better understand the link between inflammation and CPU activation/proCPU consumption in SARS-CoV-2 infection, the relationship between the highest recorded CRP value and the corresponding proCPU concentration or CPU+CPUi antigen level was assessed. For the majority of patients, the highest CRP value was measured within one week after enrolment in the study. A negative correlation between the highest recorded CRP levels and the corresponding proCPU levels was observed ($r = -0.43$, $p = 0.015$) (Figure 9-5A): the highest CRP values were seen in patients with the largest initial proCPU reduction. CPU+CPUi antigen levels at the same time point did however not correlate with these CRP levels ($r = 0.14$, $p = 0.28$) (Figure 9-5B).

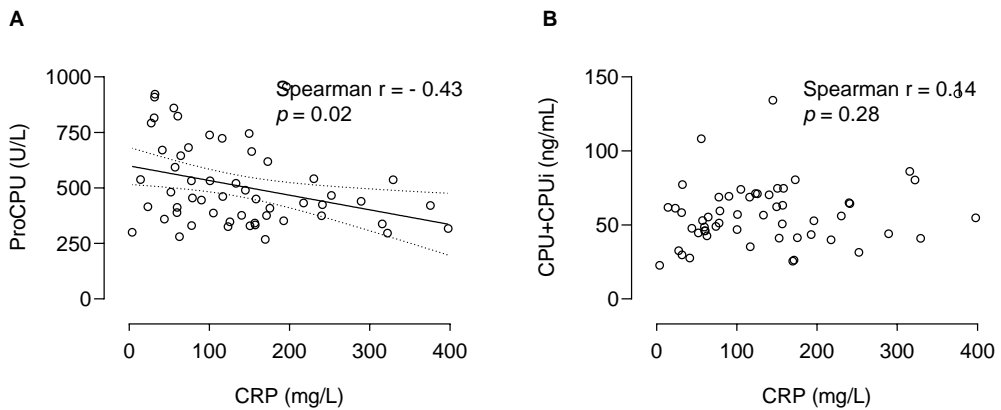


Figure 9-5. Relationship between the highest recorded CRP levels and corresponding proCPU levels (A) or CPU+CPUi antigen levels (B). For the majority of the patients, the highest CRP value was measured within one week after enrolment in the study. Spearman correlation coefficient r was determined for both correlations. In case of a significant correlation ($p > 0.05$), linear regression analysis was performed, and the best-fit line (solid line) with 95% confidence bands was plotted (dashed lines).

Thus, there is a correlation between the ongoing inflammation in SARS-CoV-2 infection and the decrease in proCPU early after onset of the disease. For CPU+CPUi antigen levels such correlation was not observed. This may be related to CPU+CPUi kinetics, but knowledge about this is limited, especially regarding CPUi kinetics.

9.4.6 Baseline CPU+CPUi antigen levels correlate with disease severity and the duration of hospitalization

Possible associations between CPU-related parameters and both disease severity and the duration of hospitalization were investigated. Baseline CPU+CPUi antigen, but not proCPU levels, were found to be positively correlated with the duration of a patient's hospital stay ($r = 0.53$; $p < 0.001$) (Figure 9-6A-B). Further, when plotting admission levels of these parameters stratified by disease severity (moderate, severe and critical), it is apparent that CPU+CPUi antigen levels shortly after admission are positively related to disease severity (sicker patients present with higher CPU+CPUi antigen levels), while no relationship with disease severity was observed for proCPU levels (Figure 9-6C-D). Accordingly, Nougier and co-workers described significantly higher CPU+CPUi antigen levels at admission in 48 intensive care unit (ICU) versus 30 non-ICU COVID-19 patients [313].

The association of CPU+CPUi antigen levels with both disease severity and the duration of hospitalization suggests that this parameter may be a potential biomarker with prognostic value and supports further studies on CPU+CPUi antigen levels, as well as CPU activity in the context of SARS-CoV-2 infection.

Because of the focus of this study on the CPU system and its related parameters, additional hemostasis parameters were not followed in detail over time. Moreover, no group of patients with asymptomatic SARS-CoV-2 infection was included here and therefore it is unclear how the current results will generalize in this type of patient population. Future research should profile the changes in CPU-related parameters to answer this. In addition, future work should also focus on possible correlations of fibrinolytic activity, and CPU-related parameters in particular, with thrombotic complications in patients with severe SARS-CoV-2 infection. This was not possible in the current study, given none of the COVID-19 patients enrolled in our study had clinical evidence for thrombosis, and systematic screening for thrombotic complications with ultrasound and computed tomography with pulmonary angiography (CTPA) is not

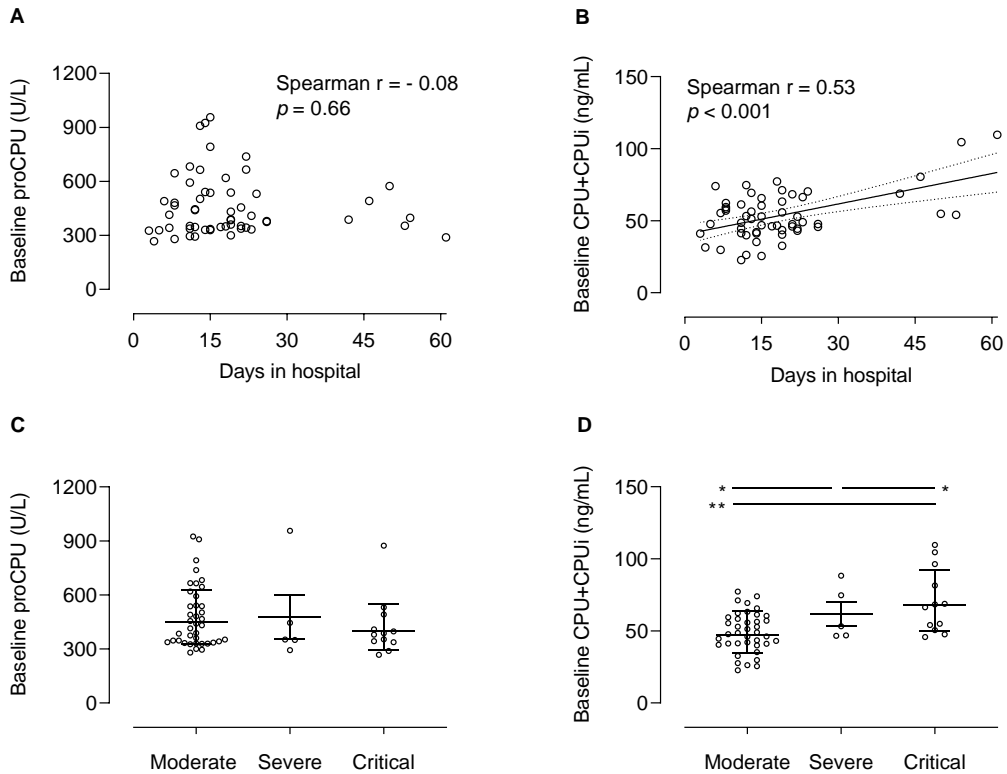


Figure 9-6. Correlation between the duration of hospitalization and both baseline (inclusion time point shortly after hospital admission) proCPU (A) and total active and inactivated carboxypeptidase U (CPU+CPUi) antigen levels (B) in hospitalized COVID-19 patients (N = 56). Spearman correlation coefficient r was determined. For statistically significant correlations ($p < 0.05$), linear regression analysis was performed and the best-fit line (solid line) with 95% confidence bands was plotted (dashed lines). **Baseline proCPU levels (C) and baseline CPU+CPUi antigen levels (D) of hospitalized COVID-19 patients grouped by disease severity (WHO COVID-19 disease severity categorization): moderate (N = 39), severe (N = 5) and critical (N = 12).** Mann Whitney U test (unpaired data); * $p < 0.05$; ** $p < 0.01$ and *** $p < 0.001$.

included in the standard care [397]. Moreover, the sample size of our study was not calculated to allow the evaluation of this correlation [398]. Finally, given the similar/parallel observations in COVID-19 and sepsis with regard to activation of the CPU system, future research examining the effect of COVID-19 and sepsis on this pathway side by side is of interest. This will not only advance our understanding of common and divergent aspects of this pathway during COVID-19 and sepsis, but also broaden our

knowledge on the activation and role of the CPU system in diseases with an inflammatory basis in general.

9.5 Conclusion

In conclusion, we showed an initial significant generation of CPU with concomitant proCPU consumption during the early phase of SARS-CoV-2 infection, with a subsequent progressive increase in both proCPU concentration and CPU+CPU_i antigen levels in hospitalized COVID-19 patients. These alterations in CPU-related parameters might (at least partly) contribute to the fibrinolysis shutdown observed in COVID-19 patients and are likely to enlarge their risk of thrombosis. These results point to the potential of CPU inhibitors to be used as therapeutic agents in COVID-19 patients in the future to enhance these patients' fibrinolytic capacity. However, further studies are needed on this topic. Moreover, CPU+CPU_i antigen levels around admission were related to disease severity and the duration of hospitalization, putting forward the hypothesis that high circulating CPU+CPU_i antigen levels may be a potential biomarker with prognostic value in SARS-CoV-2 infection.

Chapter 10

Conclusions and future perspectives

10 Conclusions and future perspectives

A proof-of-concept observational study was conducted to explore the influence of statin therapy on proCPU biology in a limited number of statin-eligible patients with hyperlipidemia. The results of this pilot study showed that increased proCPU levels are present in hyperlipidemic patients. Treatment of these patients with a statin led to a significant decrease in proCPU levels and lowered the proCPU concentration to the same level as in control subjects. Furthermore, both baseline proCPU levels and the decrease in proCPU showed high interindividual variation and on a functional level the largest improvement in fibrinolysis (as measured by the change in ΔCLT) was seen in those patients with the highest baseline proCPU levels. As a result, it is expected that this subset of patients will benefit to a larger extent from statin therapy. The latter needs to be examined further in a large cohort to identify the clinical relevance of this observation and to evaluate the hypothesis that it might be valuable to include proCPU measurement in risk assessment for starting statin therapy.

Studying the nature of the effect of HMG-CoA reductase inhibitors on the CPU system (lipid- or non-lipid related) in a mouse model of advanced atherosclerosis revealed that proCPU levels were significantly lowered under the influence of atorvastatin even though no lipid reduction was observed. Evidence was thus provided that the proCPU downregulation is a pleiotropic effect of atorvastatin treatment.

Furthermore, in a larger clinical study we further substantiated that it might be valuable to include a plasma proCPU measurement in risk assessment for starting statin therapy. Again, we showed that plasma proCPU concentrations and its expected effect on the fibrinolytic rate (as measured by ΔCLT) are increased in hyperlipidemic patients and these effects can be normalized (and even further reduced versus normolipidemic patients) by treatment with atorvastatin. High interindividual variation in proCPU levels was observed in hyperlipidemic individuals, with proCPU levels up to 80% higher compared to normolipidemic controls. In accordance, the longest ΔCLT was seen in those

patients with the highest proCPU levels, but these were not necessarily the individuals with the highest cholesterol levels. These observations support that plasma proCPU concentrations and/or Δ CLT may be valuable, novel biomarkers to help reclassify moderate-risk individuals as high or low risk and reassess the need for atorvastatin therapy in these individuals. Furthermore, given the dose-dependent decrease in proCPU and Δ CLT under influence of atorvastatin treatment, measurement of these parameters may also aid in choosing the appropriate atorvastatin start dosage (moderate- or high) or guide clinical decision-making on intensifying atorvastatin treatment. An important next step in positioning proCPU as such a marker will be prospectively studying the value of proCPU screening to help optimize statin therapy in cardiovascular risk prevention and to determine the impact of using proCPU as a cardiovascular risk prediction biomarker on patient outcomes (morbidity and mortality). In addition, repeating this study with other statins will allow to determine whether these effects on the proCPU system are class-mediated.

In the future, it will also be interesting to unravel the molecular mechanism by which atorvastatin modulates plasma proCPU levels. A possible mechanism for the observed proCPU downregulation by statin treatment is related to peroxisome proliferator-activated receptor α (PPAR α). PPAR α participates in the regulation of various aspects of lipid metabolism in the liver, finally resulting in hypolipidemic effects [330,331]. Kilicarslan *et al.* described that fenofibrate, a PPAR α agonist, decreased proCPU levels in patients with metabolic syndrome, suggesting that agonists of PPAR α possess anti-thrombotic properties through the decrease in circulating proCPU levels on top of their role as anti-lipidemic agents [180]. Moreover, Masuda *et al.* reported on the downregulation of the *CPB2* gene expression cells and leading to lowered *CPB2* mRNA and proCPU antigen levels in HepG2, mediated by the PPAR α signaling pathway upon treatment with the PPAR α agonist WY14643 [332]. Since it has been described that statins increase PPAR α expression (although they are not direct ligands for PPAR α), the hypothesis that statin therapy could increase PPAR α expression—which in turn could

lead to reduced *CPB2* gene expression and thus lower plasma proCPU levels—seems plausible and provides an interesting approach for further research [222,333–335].

In this thesis, we also studied the expression of proCPU in (primary) human monocytes and macrophages. *CPB2* mRNA was found to be expressed by the monocytic cell line THP-1 and THP-1 cells differentiated into a macrophage-like phenotype with PMA, as well as in primary human monocytes isolated from PBMCs and macrophages derived from these monocytes. On a protein level, proCPU activity was detected in lysate and conditioned medium of HepG2, THP-1, PMA stimulated THP-1 cells, primary human monocytes, primary human M-CSF macrophages, primary human IFN γ /LPS stimulated macrophages and primary human IL-4 stimulated macrophages. Moreover, CPU was detected in the conditioned media of all investigated cell types and it was demonstrated that proCPU can be activated into functionally active CPU in the *in vitro* cell culture environment. Comparison of both *CPB2* mRNA expression and proCPU concentrations in the cell medium between the different cell types provided evidence that *CPB2* mRNA expression and proCPU secretion in monocytes and (activated) macrophages are related to the degree to which these cells are differentiated and activated. This sheds new light on monocytes and macrophages as potential local proCPU sources within atherosclerotic plaques and extra-vascular inflammatory sites.

Monocyte/macrophage-derived CPU may play a number of roles in inflammatory environments: CPU is capable of inactivating a variety of pro-inflammatory substrates, but can also limit plasmin generation, thereby preventing fragmentation of a fibrin network for example in atherosclerotic plaques and contributing to keeping the plaque intact. The fact that monocyte/macrophage-derived CPU can have multiple roles within atherosclerotic plaques and extravascular inflammatory sites shows that the exact role of the CPU system in inflammation is very complex [302]. Elucidating the significance of these roles (and any additional roles) of proCPU expressed by monocytes and macrophages will serve as an exciting new avenue for CPU research in the future.

In the context of hyperlipidemia, enhanced monocyte production has been reported in patients with familial hypercholesterolemia [399–401]. Hence, it seems possible that monocyte/macrophage-derived proCPU could contribute to the increase in plasma proCPU concentration observed in hyperlipidemic patients. Following this reasoning, the reduction of inflammatory cytokines and circulating monocytes induced by atorvastatin therapy could also in part be attributed to the decrease in proCPU levels that is seen with this therapy.

A pedigree with co-inheritance of a loss-of-function rare variant in *CPB2* – the first genetic deficiency in proCPU to be described in humans – and the second worldwide reported *THBD* variant causing abnormal bleeding was identified in a genotypic inspection of cases with unexplained bleeding. Functional characterization revealed that the *THBD* mutation results in protein chain truncation close to the transmembrane domain, thereby shedding functionally active thrombomodulin extracellular domain into plasma. The marked elevation of plasma thrombomodulin in individuals with this *THBD* mutation attenuates thrombin generation (through the protein C pathway) and delays fibrinolysis (through the CPU pathway). The *CPB2* mutation gave rise to a clinically asymptomatic, partial deficiency of the plasma proCPU concentration and was to our knowledge the first genetic deficiency in proCPU described in humans. On a functional level, the reduction of proCPU activity in plasma accelerated fibrinolysis *in vitro*. Coinheritance of both mutations ameliorated the delayed *in vitro* fibrinolysis associated with the *THBD* mutation, clearly demonstrating a crucial role for proCPU herein. Analysis of the pedigree, in which members have highly impactful variants affecting two interacting coagulation pathway genes, enhanced our understanding of ultra-rare human hemostatic disorders. The different combinations of the variants in the pedigree family members offered a unique platform to allow insights into the regulation of the thrombin-thrombomodulin system and proCPU activation that is highly relevant to a broad range of hemostatic disorders and therapies. The asymptomatic nature of genetic

depletion of human proCPU underscores the potential to exploit CPU inhibitors – increasing fibrinolysis – without bleeding complications.

Infection with SARS-CoV-2 primarily affects the respiratory system, but also results in a dysregulated hemostatic balance [309–316]. Measurement of CPU-related parameters in hospitalized COVID-19 patients indicated that there is an initial significant generation of CPU with concomitant proCPU consumption during the early phase of SARS-CoV-2 infection, with a subsequent progressive increase in both proCPU concentration and CPU+CPUi antigen levels. The alterations in CPU-related parameters will (at least partly) contribute to the hypofibrinolytic state observed in COVID-19 patients and are likely to enlarge their risk of thrombosis. These results point to the potential of CPU inhibitors to be used as therapeutic agents in COVID-19 patients in the future to enhance these patients' fibrinolytic capacity. Moreover, CPU+CPUi antigen levels around admission were related to disease severity and the duration of hospitalization, putting forward the hypothesis that high circulating CPU+CPUi antigen levels may be a potential biomarker with prognostic value in SARS-CoV-2 infection. Future work should focus on possible correlations of fibrinolytic activity, and CPU-related parameters in particular, with thrombotic complications in patients with severe SARS-CoV-2 infection.

Activation of the CPU system arising from an inflammation-driven increase in thrombin concentration is not only seen in COVID-19 but also in other inflammatory disease states which is supported by several studies investigating the CPU system in sepsis [389–394]. Given this similarity between COVID-19 and sepsis, examining the effect of COVID-19 and sepsis on this pathway side by side is of interest. This will advance our understanding of common and divergent aspects of this pathway during COVID-19 and sepsis and will broaden our knowledge on the activation and role of the CPU system in diseases with an inflammatory basis in general.

In conclusion, the data presented in this doctoral research provide new insight into the potential of proCPU as a novel biomarker for identifying benefit from (atorva)statin

therapy and into monocytes and macrophages as a source of proCPU in inflammation. Moreover, a new *CPB2* mutation was functionally characterized. Finally, evidence was provided that the CPU system most likely contributes to the hypofibrinolytic state in COVID-19 patients.

References

References

- 1 Hendriks D, Scharpe S, Van Sande M, Lommaert MP. A labile enzyme in fresh human serum interferes with the assay of carboxypeptidase N. *Clin Chem Clin Chem*; 1989; **35**: 177.
- 2 Hendriks D, Scharpé S, van Sande M, Lommaert MP. Characterisation of a carboxypeptidase in human serum distinct from carboxypeptidase N. *J Clin Chem Clin Biochem* 1989; **27**: 277–85.
- 3 Hendriks D, Wang W, Scharpé S, Lommaert MP, van Sande M. Purification and characterization of a new arginine carboxypeptidase in human serum. *BBA - Gen Subj* 1990; **1034**: 86–92.
- 4 Campbell W, Okada H. An Arginine Specific Carboxypeptidase Generated in Blood During Coagulation or Inflammation which is Unrelated to Carboxypeptidase N or its Subunits. *Biochem Biophys Res Commun* 1989; **162**: 933–9.
- 5 Eaton DL, Malloy BE, Tsai SP, Henzel W, Drayna D. Isolation, molecular cloning, and partial characterization of a novel carboxypeptidase B from human plasma. *J Biol Chem* 1991; **266**: 21833–8.
- 6 Bajzar L, Manuel R, Nesheim ME. Purification and characterization of TAFI, a thrombin-activable fibrinolysis inhibitor. *Journal of Biological Chemistry* Jun 1995 p. 14477–84.
- 7 Vanhoof G, Wauters J, Schatteman K, Hendriks D, Goossens F, Bossuyt P, Scharpé S. The gene for human carboxypeptidase U (CPU) - A proposed novel regulator of plasminogen activation - Maps to 13q14.11. *Genomics* 1996; **38**: 454–5.
- 8 Yamaguchi Y, Shao Z, Sharif S, Du XY, Myles T, Merchant M, Harsh G, Glantz M, Recht L, Morser J, Leung LLK. Thrombin-cleaved fragments of osteopontin are overexpressed in malignant glial tumors and provide a molecular niche with survival advantage. *J Biol Chem* 2013; **288**: 3097–111.
- 9 Shao Z, Nishimura T, Leung LLK, Morser J. Carboxypeptidase B2 deficiency reveals opposite effects of complement C3a and C5a in a murine polymicrobial sepsis model. *J Thromb Haemost* 2015; **13**: 1090–102.
- 10 Foley JH, Kim PY, Hendriks D, Morser J, Gils A, Mutch NJ. Evaluation of and recommendation for the nomenclature of the CPB2 gene product (also known as TAFI and proCPU): Communication from the SSC of the ISTH. *J Thromb Haemost* 2015; **13**: 2277–8.
- 11 NC-IUBMB. Recommendations of the Nomenclature Committee of the International Union of Biochemistry and Molecular Biology on the Nomenclature and Classifications of enzymes. San Diego, California: Academic Press Inc.; 1992.
- 12 Rawlings ND, Barrett AJ. Evolutionary families of peptidases. *Biochem J* 1993; **290**:

- 205–18.
- 13 Rawlings N, Salvesen G. Handbook of Proteolytic Enzymes. 3th ed. San Diego, California: Academic Press Inc.; 2013.
 - 14 Boffa MB, Reid TS, Joo E, Nesheim ME, Koschinsky ML. Characterization of the gene encoding human TAFI (thrombin-activable fibrinolysis inhibitor; plasma procarboxypeptidase B). *Biochemistry* 1999; **38**: 6547–58.
 - 15 Boffa MB, Koschinsky ML. Curiouser and curiouser: Recent advances in measurement of thrombin-activatable fibrinolysis inhibitor (TAFI) and in understanding its molecular genetics, gene regulation, and biological roles. *Clin Biochem* 2007; **40**: 431–42.
 - 16 Boffa MB, Hamill JD, Bastajian N, Dillon R, Nesheim ME, Koschinsky ML. A role for CCAAT/enhancer-binding protein in hepatic expression of thrombin-activable fibrinolysis inhibitor. *J Biol Chem* 2002; **277**: 25329–36.
 - 17 Boffa MB, Hamill JD, Maret D, Brown D, Scott ML, Nesheim ME, Koschinsky ML. Acute phase mediators modulate thrombin-activable fibrinolysis inhibitor (TAFI) gene expression in HepG2 cells. *J Biol Chem* 2003; **278**: 9250–7.
 - 18 Garand M, Bastajian N, Nesheim ME, Boffa MB, Koschinsky ML. Molecular analysis of the human thrombin-activatable fibrinolysis inhibitor gene promoter. *Br J Haematol* 2007; **138**: 231–44.
 - 19 Maret D, Boffa MB, Brien DF, Nesheim ME, Koschinsky ML. Role of mRNA transcript stability in modulation of expression of the gene encoding thrombin activable fibrinolysis inhibitor. *J Thromb Haemost* 2004; **2**: 1969–79.
 - 20 Lin JHH, Novakovic D, Rizzo CM, Zagorac B, Garand M, Filipieva A, Koschinsky ML, Boffa MB. The mRNA encoding TAFI is alternatively spliced in different cell types and produces intracellular forms of the protein lacking TAFIa activity. *Thromb Haemost* 2013; **109**: 1033–44.
 - 21 Komnenov D, Scipione CA, Bazzi ZA, Garabon JJW, Koschinsky ML, Boffa MB. Pro-inflammatory cytokines reduce human TAFI expression via tristetraprolin-mediated mRNA destabilisation and decreased binding of HuR. *Thromb Haemost* 2015; **114**: 337–49.
 - 22 Novakovic D, Kuo ACY, Lin JH, Koschinsky ML, Boffa MB. Identification of tristetraprolin as a factor that modulates the stability of the TAFI transcript through binding to the 3'-untranslated region. *J Thromb Haemost* 2012; **10**: 887–94.
 - 23 NCBI. CPB2 carboxypeptidase B2 [Homo sapiens (human)]. https://www.ncbi.nlm.nih.gov/projects/SNP/snp_ref.cgi?rs=797014517.
 - 24 Tàssies D, Roqué M, Monteagudo J, Martorell T, Sionis A, Arzamendi D, Heras M, Reverter JC. Thrombin-activatable fibrinolysis inhibitor genetic polymorphisms as

- markers of the type of acute coronary syndrome. *Thromb Res* 2009; **124**: 614–8.
- 25 Kozian DH, Lorenz M, März W, Cousin E, Mace S, Deleuze JF. Association between the Thr325Ile polymorphism of the thrombin-activatable fibrinolysis inhibitor and stroke in the Ludwigshafen Risk and Cardiovascular Health Study. *Thromb Haemost* 2010; **103**: 976–83.
- 26 Schneider M, Boffa M, Stewart R, Rahman M, Koschinsky M, Nesheim M. Two naturally occurring variants of TAFI (Thr-325 and Ile-325) differ substantially with respect to thermal stability and antifibrinolytic activity of the enzyme. *J Biol Chem* 2002; **277**: 1021–30.
- 27 Brouwers G-J, Vos HL, Leebeek FWG, Bulk S, Schneider MM, Boffa MB, Koschinsky ML, Van Tilburg NH, Nesheim ME, Bertina RM, Gómez Garcia E. A novel, possibly functional, single nucleotide polymorphism in the coding region of the thrombin-activatable fibrinolysis inhibitor (TAFI) gene is also associated with TAFI levels. *Blood* 2001; **98**: 1992–3.
- 28 Westbury SK, Whyte CS, Stephens J, Downes K, Turro E, Claesen K, Mertens JC, Hendriks D, Latif AL, Leishman EJ, Mutch NJ, Tait RC, Mumford AD. A new pedigree with thrombomodulin-associated coagulopathy in which delayed fibrinolysis is partially attenuated by co-inherited TAFI deficiency. *J Thromb Haemost* 2020; **18**: 2209–14.
- 29 Frère C, Morange PE, Saut N, Tregouet DA, Grosley M, Beltran J, Juhan-Vague I, Alessi MC. Quantification of thrombin activatable fibrinolysis inhibitor (TAFI) gene polymorphism effects on plasma levels of TAFI measured with assays insensitive to isoform-dependent artefact. *Thromb Haemost* 2005; **94**: 373–9.
- 30 Van Tilburg NH, Rosendaal FR, Bertina RM. Thrombin activatable fibrinolysis inhibitor and the risk for deep vein thrombosis. *Blood* 2000; **95**: 2855–9.
- 31 Chetaille P, Alessi MC, Kouassi D, Morange PE, Juhan-Vague I. Plasma TAFI antigen variations in healthy subjects. *Thromb Haemost* 2000; **83**: 902–5.
- 32 Mousa HA, Downey C, Alfirevic Z, Toh CH. Thrombin activatable fibrinolysis inhibitor and its fibrinolytic effect in normal pregnancy. *Thromb Haemost* 2004; **92**: 1025–31.
- 33 Watanabe T, Minakami H, Sakata Y, Matsubara S, Sato I, Suzuki M. Changes in activity of plasma thrombin activatable fibrinolysis inhibitor in pregnancy. *Gynecol Obstet Invest* 2004; **58**: 19–21.
- 34 Chabloz P, Reber G, Boehlen F, Hohlfeld P, De Moerloose P. TAFI antigen and D-dimer levels during normal pregnancy and at delivery. *Br J Haematol* 2001; **115**: 150–2.
- 35 Boffa MB, Wang W, Bajzar L, Nesheim ME. Plasma and recombinant thrombin-activatable fibrinolysis inhibitor (TAFI) and activated TAFI compared with respect to

- glycosylation, thrombin/thrombomodulin-dependent activation, thermal stability, and enzymatic properties. *J Biol Chem* 1998; **273**: 2127–35.
- 36 Valnickova Z, Christensen T, Skottrup P, Thøgersen IB, Højrup P, Enghild JJ. Post-translational modifications of human thrombin-activatable fibrinolysis inhibitor (TAFI): Evidence for a large shift in the isoelectric point and reduced solubility upon activation. *Biochemistry* 2006; **45**: 1525–35.
- 37 Mosnier LO, Von Dem Borne PAK, Meijers JCM, Bouma BN. Plasma TAFI levels influence the clot lysis time in healthy individuals in the presence of an intact intrinsic pathway of coagulation. *Thromb Haemost* 1998; **80**: 829–35.
- 38 Strömquist M, Schatteman K, Leurs J, Verkerk R, Andersson JO, Johansson T, Scharpé S, Hendriks D. Immunological assay for the determination of procarboxypeptidase U antigen levels in human plasma. *Thromb Haemost* 2001; **85**: 12–7.
- 39 Guo X, Morioka A, Kaneko Y, Okada N, Obata K, Nomura T, Campbell W, Okada H. Arginine carboxypeptidase (CPR) in human plasma determined with sandwich ELISA. *Microbiol Immunol* 1999; **43**: 691–8.
- 40 Schatteman KA, Goossens FJ, Scharpé SS, Hendriks DF. Activation of plasma procarboxypeptidase U in different mammalian species points to a conserved pathway of inhibition of fibrinolysis. *Thromb Haemost* 1999; **82**: 1718–21.
- 41 Heylen E, Willemsse J, Hendriks D. An update on the role of carboxypeptidase U (TAFIa) in fibrinolysis. *Front Biosci* 2011; **16**: 2427.
- 42 Sillen M, Declerck PJ. Thrombin activatable fibrinolysis inhibitor (TAFI): An updated narrative review. *Int J Mol Sci* 2021; **22**.
- 43 Mosnier LO, Buijtenhuijs P, Marx PF, Meijers JCM, Bouma BN. Identification of thrombin activatable fibrinolysis inhibitor (TAFI) in human platelets. *Blood* 2003; **101**: 4844–6.
- 44 Schadinger SL, Lin JHH, Garand M, Boffa MB. Secretion and antifibrinolytic function of thrombin-activatable fibrinolysis inhibitor from human platelets. *J Thromb Haemost* 2010; **8**: 2523–9.
- 45 Carrieri C, Galasso R, Semeraro F, Ammollo CT, Semeraro N, Colucci M. The role of thrombin activatable fibrinolysis inhibitor and factor XI in platelet-mediated fibrinolysis resistance: A thromboelastographic study in whole blood. *J Thromb Haemost* 2011; **9**: 154–62.
- 46 Lin JHH, Garand M, Zagorac B, Schadinger SL, Scipione C, Koschinsky ML, Boffa MB. Identification of human thrombin-activatable fibrinolysis inhibitor in vascular and inflammatory cells. *Thromb Haemost* 2011; **105**: 999–1009.
- 47 Uszyński W, Uszyński M, Zekanowska E. Thrombin activatable fibrinolysis inhibitor (TAFI) in human amniotic fluid. A preliminary study. *Thromb Res* 2007;

- 119**: 241–5.
- 48 Hori Y, Gabazza EC, Yano Y, Katsuki A, Suzuki K, Adachi Y, Sumida Y. Insulin resistance is associated with increased circulating level of thrombin-activatable fibrinolysis inhibitor in type 2 diabetic patients. *J Clin Endocrinol Metab* 2002; **87**: 660–5.
- 49 Jönsson Rylander AC, Lindgren A, Deinum J, Bergström GML, Böttcher G, Kalies I, Wåhlander K. Fibrinolysis inhibitors in plaque stability: a morphological association of PAI-1 and TAFI in advanced carotid plaque. *J Thromb Haemost* 2017; **15**: 758–69.
- 50 Matsumoto A, Motozaki K, Seki T, Sasaki R, Kawabe T. Expression of human brain carboxypeptidase B, a possible cleaving enzyme for β -amyloid precursor protein, in peripheral fluids. *Neurosci Res* 2001; **39**: 313–7.
- 51 Hillmayer K, Macovei A, Pauwels D, Compennolle G, Declerck PJ, Gils A. Characterization of rat thrombin-activatable fibrinolysis inhibitor (TAFI) - A comparative study assessing the biological equivalence of rat, murine and human TAFI. *J Thromb Haemost* 2006; **4**: 2470–7.
- 52 Komura H, Shimomura Y, Yumoto M, Katsuya H, Okada N, Okada H. Heat stability of carboxypeptidase R of experimental animals. *Microbiol Immunol* 2002; **46**: 217–23.
- 53 Sato T, Miwa T, Akatsu H, Matsukawa N, Obata K, Okada N, Campbell W, Okada H. Pro-Carboxypeptidase R is an Acute Phase Protein in the Mouse, Whereas Carboxypeptidase N Is Not. *J Immunol* 2000; **165**: 1053–8.
- 54 Garand M, Lin JHH, Hill CE, Zagorac B, Koschinsky ML, Boffa MB. Regulation of the mouse gene encoding TAFI by TNF α : Role of NF κ B binding site. *Cytokine* 2012; **57**: 389–97.
- 55 Leung LLK, Morser J. Carboxypeptidase B2 and carboxypeptidase N in the crosstalk between coagulation, thrombosis, inflammation, and innate immunity. *J Thromb Haemost* 2018; **16**: 1474–86.
- 56 Wang W, Hendriks DF, Scharpé SS. Carboxypeptidase U, a plasma carboxypeptidase with high affinity for plasminogen. *J Biol Chem* 1994; **269**: 15937–44.
- 57 Tan AK, Eaton DL. Activation and Characterization of Procarboxypeptidase B from Human Plasma. *Biochemistry* 1995; **34**: 5811–6.
- 58 Marx PF, Havik SR, Marquart JA, Bouma BN, Meijers JCM. Generation and Characterization of a Highly Stable Form of Activated Thrombin-activatable Fibrinolysis Inhibitor. *J Biol Chem* 2004; **279**: 6620–8.
- 59 Foley JH, Cook PF, Nesheim ME. Kinetics of activated thrombin-activatable fibrinolysis inhibitor (TAFI α)-catalyzed cleavage of C-terminal lysine residues of

- fibrin degradation products and removal of plasminogen-binding sites. *J Biol Chem* 2011; **286**: 19280–6.
- 60 Valnickova Z, Thøgersen IB, Christensen S, Chu CT, Pizzo S V., Enghild JJ. Activated human plasma carboxypeptidase B is retained in the blood by binding to α 2-macroglobulin and pregnancy zone protein. *J Biol Chem* 1996; **271**: 12937–43.
- 61 Marx PF, Brondijk THC, Plug T, Romijn RA, Hemrika W, Meijers JCM, Huizinga EG. Crystal structures of TAFI elucidate the inactivation mechanism of activated TAFI: A novel mechanism for enzyme autoregulation. *Blood* 2008; **112**: 2803–9.
- 62 Foley JH, Kim PY, Mutch NJ, Gils A. Insights into thrombin activatable fibrinolysis inhibitor function and regulation. *J Thromb Haemost* 2013; **11**: 306–15.
- 63 Bajzar L, Morser J, Nesheim M. TAFI, or plasma procarboxypeptidase B, couples the coagulation and fibrinolytic cascades through the thrombin-thrombomodulin complex. *J Biol Chem* 1996; **271**: 16603–8.
- 64 Mao SS, Cooper CM, Wood T, Shafer JA, Gardell SJ. Characterization of plasmin-mediated activation of plasma procarboxypeptidase B. Modulation by glycosaminoglycans. *J Biol Chem* 1999; **274**: 35046–52.
- 65 Kawamura T, Okada N, Okada H. Elastase from activated human neutrophils activates procarboxypeptidase R. *Microbiol Immunol* 2002; **46**: 225–30.
- 66 Schatteman KA, Goossens FJ, Scharpé SS, Hendriks DF. Proteolytic activation of purified human procarboxypeptidase U. *Clin Chim Acta* 2000; **292**: 25–40.
- 67 Bajzar L, Nesheim M, Morser J, Tracy PB. Both cellular and soluble forms of thrombomodulin inhibit fibrinolysis by potentiating the activation of Thrombin-activable fibrinolysis inhibitor. *J Biol Chem* 1998; **273**: 2792–8.
- 68 Wang W, Nagashima M, Schneider M, Morser J, Nesheim M. Elements of the primary structure of thrombomodulin required for efficient thrombin-activable fibrinolysis inhibitor activation. *J Biol Chem* 2000; **275**: 22942–7.
- 69 Wu C, Kim PY, Swystun LL, Liaw PC, Weitz JI. Activation of protein C and thrombin activable fibrinolysis inhibitor on cultured human endothelial cells. *J Thromb Haemost* 2016; **14**: 366–74.
- 70 Kokame K, Zheng X, Sadler JE. Activation of thrombin-activable fibrinolysis inhibitor requires epidermal growth factor-like domain 3 of thrombomodulin and is inhibited competitively by protein C. *J Biol Chem* 1998; **273**: 12135–9.
- 71 Mosnier LO, Meijers JCM, Bouma BN. Regulation of fibrinolysis in plasma by TAFI and protein C is dependent on the concentration of thrombomodulin. *Thromb Haemost* 2001; **85**: 5–11.
- 72 Bajzar L, Nesheim M. The effect of activated protein C on fibrinolysis in cell-free plasma can be attributed specifically to attenuation of prothrombin activation. *J*

- Biol Chem* 1993; **268**: 8608–16.
- 73 Binette TM, Taylor FB, Peer G, Bajzar L. Thrombin-thrombomodulin connects coagulation and fibrinolysis: More than an in vitro phenomenon. *Blood* 2007; **110**: 3168–75.
- 74 Leurs J, Wissing BM, Nerme V, Schatteman K, Björquist P, Hendriks D. Different mechanisms contribute to the biphasic pattern of carboxypeptidase U (TAFIa) generation during in vitro clot lysis in human plasma. *Thromb Haemost* 2003; **89**: 264–71.
- 75 Mishra N, Vercauteren E, Develter J, Bammens R, Declerck PJ, Gils A. Identification and characterisation of monoclonal antibodies that impair the activation of human thrombin activatable fibrinolysis inhibitor through different mechanisms. *Thromb Haemost* 2011; **106**: 90–101.
- 76 Vercauteren E, Emmerechts J, Peeters M, Hoylaerts MF, Declerck PJ, Gils A. Evaluation of the profibrinolytic properties of an anti-TAFI monoclonal antibody in a mouse thromboembolism model. *Blood* 2011; **117**: 4615–22.
- 77 Gomis-Ruth FX. Structure and mechanism of metallo-carboxypeptidases. *Crit Rev Biochem Mol Biol* 2008; **43**: 319–45.
- 78 Wu S, Zhang C, Xu D, Guo H. Catalysis of carboxypeptidase A: Promoted-water versus nucleophilic pathways. *J Phys Chem B* 2010; **114**: 9259–67.
- 79 Willemse JL, Polla M, Olsson T, Hendriks DF. Comparative substrate specificity study of carboxypeptidase U (TAFIa) and carboxypeptidase N: Development of highly selective CPU substrates as useful tools for assay development. *Clin Chim Acta* 2008; **387**: 158–60.
- 80 Willemse JL, Hendriks DF. Measurement of procarboxypeptidase U (TAFI) in human plasma: A laboratory challenge. *Clin Chem* 2006; **52**: 30–6.
- 81 Heylen E, Van Goethem S, Willemse J, Olsson T, Augustyns K, Hendriks D. Development of a sensitive and selective assay for the determination of procarboxypeptidase U (thrombin-activatable fibrinolysis inhibitor) in plasma. *Anal Biochem* 2010; **396**: 152–4.
- 82 Hendriks D, Wang W, van Sande M, Scharpé S. Human serum carboxypeptidase U: a new kininase? *Agents Actions Suppl* 1992; **38**: 407–13.
- 83 Myles T, Nishimura T, Yun TH, Nagashima M, Morser J, Patterson AJ, Pearl RG, Leung LLK. Thrombin Activatable Fibrinolysis Inhibitor, a Potential Regulator of Vascular Inflammation. *J Biol Chem* 2003; **278**: 51059–67.
- 84 Campbell WD, Lazoura E, Okada N, Okada H. Inactivation of C3a and C5a octapeptides by carboxypeptidase R and carboxypeptidase N. *Microbiol Immunol* 2002; **46**: 131–4.

- 85 Wyseure T, Sinha R, Declerck P, Meijers J, von Drygalski A, Mosnier L. Modification of the VEGF165 C-terminus by Activated Thrombin-activatable Fibrinolysis Inhibitor (TAFIa) Inhibits Neuropilin-1 (Nrp1)-dependent Induction of Angiogenesis in vitro and in vivo [Abstract]. *Res Pract Thromb Haemost* 2017; **1**: 270.
- 86 Wyseure TL, Cooke EJ, Declerck PJ, Meijers JC, von Drygalski A, Mosnier LO. Defective TAFI Activation in Hemophilia Exacerbates Vascular Remodeling in Hemophilic Arthropathy. *Blood* 2016; **128**: 82–82.
- 87 Shinohara T, Sakurada C, Suzuki T, Takeuchi O, Campbell W, Ikeda S, Okada N, Okada H. Pro-Carboxypeptidase R Cleaves Bradykinin following Activation. *Int Arch Allergy Immunol* 1994; **103**: 400–4.
- 88 Marx PF, Hackeng TM, Dawson PE, Griffin JH, Meijers JCM, Bouma BN. Inactivation of active thrombin-activable fibrinolysis inhibitor takes place by a process that involves conformational instability rather than proteolytic cleavage. *J Biol Chem* 2000; **275**: 12410–5.
- 89 Walker JB, Hughes B, James I, Haddock P, Kluft C, Bajzar L. Stabilization versus inhibition of TAFIa by competitive inhibitors in vitro. *J Biol Chem* 2003; **278**: 8913–21.
- 90 Schneider M, Nesheim M. Reversible inhibitors of TAFIa can both promote and inhibit fibrinolysis. *J Thromb Haemost* 2003; **1**: 147–54.
- 91 Plug T, Meijers JCM. Structure-function relationships in thrombin-activatable fibrinolysis inhibitor. *J Thromb Haemost* 2016; **14**: 633–44.
- 92 Zhou X, Declerck PJ. Generation of a stable thrombin-activatable fibrinolysis inhibitor deletion mutant exerting full carboxypeptidase activity without activation. *J Thromb Haemost* 2015; **13**: 1084–9.
- 93 Knecht W, Willemsse J, Stenhamre H, Andersson M, Berntsson P, Furebring C, Harrysson A, Hager ACM, Wissing BM, Hendriks D, Cronet P. Limited mutagenesis increases the stability of human carboxypeptidase U (TAFIa) and demonstrates the importance of CPU stability over proCPU concentration in down-regulating fibrinolysis. *FEBS J* 2006; **273**: 778–92.
- 94 Marx PF, Dawson PE, Bouma BN, Meijers JCM. Plasmin-Mediated Activation and Inactivation of Thrombin-Activatable Fibrinolysis. *Biochem Pharmacol* 2002; **41**: 6688–96.
- 95 Gale AJ. Current Understanding of Hemostasis. *Toxicol pathol* 2011; **39**: 273–80.
- 96 Bhaskar A, Nair SC, Thomas TA. Cell based model of haemostasis. *Clin Microbiol Infect J* 2016; **6**: 53–8.
- 97 Hoffbrand A, Moss P. Platelets, blood coagulation and haemostasis. *Hoffbrand's Essent Haematology*. 7th ed. John Wiley & Sons Ltd; 2016. p. 265–77.

-
- 98 Pasi K. Hemostasis - Components and Processes. In: Perry D, Pasi K, editors. *Hemost Thromb Protoc Methods Mol Med*. New Jersey: Humana Press; 1999. p. 3–21.
- 99 Sira J, Eyre L. Physiology of haemostasis. *Anaesth Intensive Care Med* 2016; **17**: 79–82.
- 100 Yau JW, Teoh H, Verma S. Endothelial cell control of thrombosis. *BMC Cardiovasc Disord* 2015; **15**: 1–11.
- 101 Arble E, Arnetz BB. Anticoagulants and the hemostatic system: A primer for occupational stress researchers. *Int J Environ Res Public Health* 2021; **18**: 10626.
- 102 Linden M. Platelet Physiology. In: Monagle P, editor. *Haemost Methods Protoc*. New York: Springer Science and Business Media New York; 2013. p. 14–30.
- 103 White GC, Marden VJ, Schulmans S, Aird WC, Bennet JS. Overview of Basic Coagulation and Fibrinolysis. In: Marden VJ, Aird WC, Bennett JS, Schulman S, White GC, editors. *Haemost Thromb Basic Principles Clin Pract*. 6th ed. Philadelphia: Lippincott Williams and Wilkins; 2012.
- 104 Hoffman M, Monroe DM. A Cell-Based Model of Hemostasis. *Thromb Haemost* 2001; **85**: 958–65.
- 105 Lord ST. Molecular mechanisms affecting fibrin structure and stability. *Arterioscler Thromb Vasc Biol* 2011; **31**: 494–9.
- 106 Sillen M. Structural analysis of antibody-based and small molecule profibrinolytics. Doctoral thesis. KU Leuven; 2021.
- 107 Chapin JC, Hajjar KA. Fibrinolysis and the control of blood coagulation. *Blood Rev* 2015; **29**: 17–24.
- 108 Levin EG, Marzec U, Anderson J, Harker LA. Thrombin Stimulates Tissue Plasminogen Activator Release from Cultured Human Endothelial Cells of tissue plasminogen activator from endothelial cells Thrombin inactivated with diisopropylfluorophosphate or hirudin did not induce an increase in tissue plas. *J Clin Invest* 1984; **74**: 1988–95.
- 109 Oliver JJ, Webb DJ, Newby DE. Stimulated tissue plasminogen activator release as a marker of endothelial function in humans. *Arterioscler Thromb Vasc Biol* 2005; **25**: 2470–9.
- 110 Longstaff C, Kolev K. Basic mechanisms and regulation of fibrinolysis. *J Thromb Haemost* 2015; **13**: S98–105.
- 111 Cesarman-Maus G, Hajjar KA. Molecular mechanisms of fibrinolysis. *Br J Haematol* 2005; **129**: 307–21.
- 112 Rijken DC, Lijnen HR. New insights into the molecular mechanisms of the fibrinolytic system. *J Thromb Haemost* 2009; **7**: 4–13.
-

- 113 Silva MMCG, Thelwell C, Williams SC, Longstaff C. Regulation of fibrinolysis by C-terminal lysines operates through plasminogen and plasmin but not tissue-type plasminogen activator. *J Thromb Haemost* 2012; **10**: 2354–60.
- 114 Schneider M, Brufatto N, Neill E, Nesheim M. Activated Thrombin-activatable Fibrinolysis Inhibitor Reduces the Ability of High Molecular Weight Fibrin Degradation Products to Protect Plasmin from Antiplasmin. *J Biol Chem* 2004; **279**: 13340–5.
- 115 Wang W, Boffa MB, Bajzar L, Walker JB, Nesheim ME. A study of the mechanism of inhibition of fibrinolysis by activated thrombin-activable fibrinolysis inhibitor. *J Biol Chem* 1998; **273**: 27176–81.
- 116 Mutch NJ, Thomas L, Moore NR, Lisiak KM, Booth NA. TAFIa, PAI-1 and α 2-antiplasmin: Complementary roles in regulating lysis of thrombi and plasma clots. *J Thromb Haemost* *J Thromb Haemost*; 2007; **5**: 812–7.
- 117 Wiman B, Lijnen HR, Collen D. On the specific interaction between the lysine-binding sites in plasmin and complementary sites in α 2-antiplasmin and in fibrinogen. *BBA - Protein Struct* 1979; **579**: 142–54.
- 118 Leurs J, Nerme V, Sim Y, Hendriks D. Carboxypeptidase U (TAFIa) prevents lysis from proceeding into the propagation phase through a threshold-dependent mechanism. *J Thromb Haemost* 2004; **2**: 416–23.
- 119 Walker JB, Bajzar L. The intrinsic threshold of the fibrinolytic system is modulated by basic carboxypeptidases, but the magnitude of the antifibrinolytic effect of activated thrombin-activable fibrinolysis inhibitor is masked by its instability. *J Biol Chem* 2004; **279**: 27896–904.
- 120 Ceresa E, Brouwers E, Peeters M, Jern C, Declerck PJ, Gils A. Development of ELISAs measuring the extent of TAFI activation. *Arterioscler Thromb Vasc Biol* 2006; **26**: 423–8.
- 121 Hillmayer K, Brouwers E, León-Tamariz F, Meijers JCM, Marx PF, Declerck PJ, Gils A. Development of sandwich-type ELISAs for the quantification of rat and murine thrombin activatable fibrinolysis inhibitor in plasma. *J Thromb Haemost* 2008; **6**: 132–8.
- 122 Gils A, Alessi MC, Brouwers E, Peeters M, Marx P, Leurs J, Bouma B, Hendriks D, Juhan-Vague I, Declerck PJ. Development of a genotype 325-specific proCPU/TAFI ELISA. *Arterioscler Thromb Vasc Biol* 2003; **23**: 1122–7.
- 123 Guimarães AHC, Van Tilburg NH, Vos HL, Bertina RM, Rijken DC. Association between thrombin activatable fibrinolysis inhibitor genotype and levels in plasma: Comparison of different assays. *Br J Haematol* 2004; **124**: 659–65.
- 124 Heylen E, Willemse JL, Hendriks DF. Comparative study of commercially available procarboxypeptidase U (thrombin-activatable fibrinolysis inhibitor) assays. *J*

- Thromb Haemost* 2011; **9**: 1407–9.
- 125 Willemse J, Leurs J, Verkerk R, Hendriks D. Development of a fast kinetic method for the determination of carboxypeptidase U (TAFIa) using C-terminal arginine containing peptides as substrate. *Anal Biochem* 2005; **340**: 106–12.
- 126 Mock WL, Stanford DJ. Anisylazoformylarginine: A superior assay substrate for carboxypeptidase B type enzymes. *Bioorganic Med Chem Lett* 2002; **12**: 1193–4.
- 127 Foley JH, Kim P, Nesheim ME. Thrombin-activable fibrinolysis inhibitor zymogen does not play a significant role in the attenuation of fibrinolysis. *J Biol Chem* 2008; **283**: 8863–7.
- 128 Willemse JL, Polla M, Hendriks DF. The intrinsic enzymatic activity of plasma procarboxypeptidase U (TAFI) can interfere with plasma carboxypeptidase N assays. *Anal Biochem* 2006; **356**: 157–9.
- 129 Willemse JL, Matus V, Heylen E, Mezzano D, Hendriks DF. Influence of the Thr325Ile polymorphism on procarboxypeptidase U (thrombin-activable fibrinolysis inhibitor) activity-based assays. *J Thromb Haemost* 2007; **5**: 872–5.
- 130 Wheeler JX, Thelwell C, Rigsby P, Whiting G. Quantitation of thrombin-activatable fibrinolysis inhibitor in human plasma by isotope dilution mass spectrometry. *Anal Biochem* 2022; **638**: 114413.
- 131 Heylen E, Van Goethem S, Augustyns K, Hendriks D. Measurement of carboxypeptidase U (active thrombin-activatable fibrinolysis inhibitor) in plasma: Challenges overcome by a novel selective assay. *Anal Biochem* 2010; **403**: 114–6.
- 132 Kim PYG, Foley J, Hsu G, Kim PY, Nesheim ME. An assay for measuring functional activated thrombin-activatable fibrinolysis inhibitor in plasma. *Anal Biochem* 2008; **372**: 32–40.
- 133 Santamaría A, Borrell M, Oliver A, Ortín R, Forner R, Coll I, Mateo J, Souto JC, Fontcuberta J. Association of functional thrombin-activatable fibrinolysis inhibitor (TAFI) with conventional cardiovascular risk factors and its correlation with other hemostatic factors in a Spanish population. *Am J Hematol* 2004; **76**: 348–52.
- 134 Santamaría A, Oliver A, Borrell M, Mateo J, Belvis R, Martí-Fábregas J, Ortín R, Tirado I, Souto JC, Fontcuberta J. Risk of ischemic stroke associated with functional thrombin-activatable fibrinolysis inhibitor plasma levels. *Stroke* 2003; **34**: 2387–91.
- 135 Franco RF, Fagundes MG, Meijers JCM, Reitsma PH, Lourenço DM, Morelli VM, Maffei FH, Ferrari IC, Piccinato CE, Silva-Jr WA, Zago MA. Identification of polymorphisms in the 5'-untranslated region of the TAFI gene: relationship with plasma TAFI levels and risk of venous thrombosis. *Haematologica* 2001; **86**: 510–7.

- 136 Schatteman KA, Goossens FJ, Scharpé SS, Neels HM, Hendriks DF. Assay of procarboxypeptidase U, a novel determinant of the fibrinolytic cascade, in human plasma. *Clin Chem* 1999; **45**: 807–13.
- 137 Silveira A, Schatteman K, Goossens F, Moor E, Scharpe S, Stromqvist M, Hendriks D, Hamsten A. Plasma procarboxypeptidase U in men with symptomatic coronary artery disease. *Thromb Haemost* 2000; **84**: 364–8.
- 138 Puccetti L, Bruni F, Pasqui AL, Pastorelli M, Bova G, Cercignani M, Palazzuoli A, Auteri A. Dyslipidemias and fibrinolysis. *Ital Hear J* 2002; **3**: 579–86.
- 139 Brouns R, Heylen E, Sheorajpanday R, Willemse JL, Kunnen J, De Surgeloose D, Hendriks DF, De Deyn PP. Carboxypeptidase U (TAFIa) decreases the efficacy of thrombolytic therapy in ischemic stroke patients. *Clin Neurol Neurosurg* 2009; **111**: 165–70.
- 140 Schatteman KA, Goossens FJ, Leurs J, Kasahara Y, Scharpé SS, Hendriks DF. Fast homogeneous assay for plasma procarboxypeptidase U. *Clin Chem Lab Med* 2001; **39**: 806–10.
- 141 Brouns R, Heylen E, Willemse JL, Sheorajpanday R, De Surgeloose D, Verkerk R, De Deyn PP, Hendriks DF. The decrease in procarboxypeptidase U (TAFI) concentration in acute ischemic stroke correlates with stroke severity, evolution and outcome. *J Thromb Haemost* 2010; **8**: 75–80.
- 142 Mertens JC, Leenaerts D, Brouns R, Engelborghs S, Ieven M, De Deyn PP, Lambeir AM, Hendriks D. Procarboxypeptidase U (proCPU, TAFI, proCPB2) in cerebrospinal fluid during ischemic stroke is associated with stroke progression, outcome and blood–brain barrier dysfunction. *J Thromb Haemost* 2018; **16**: 342–8.
- 143 Alessi M, Gaudin C, Grosjean P, Martin V, Timsit S, Brouns R, Montaner J, Castellanos M, Donazzola Y, Cho T-H, Suissa L, Mechtouff L, Derex L, Suchon P, Mezzapesa A, Nigho. Changes in Activated Thrombin-Activatable Fibrinolysis Inhibitor Levels Following Thrombolytic Therapy in Ischemic Stroke Patients Correlate with Clinical Outcome. *Cerebrovasc Dis* 2016; **42**: 404–14.
- 144 Cruden NLM, Graham C, Harding SA, Ludlam CA, Fox KAA, Newby DE. Plasma TAFI and soluble CD40 ligand do not predict reperfusion following thrombolysis for acute myocardial infarction. *Thromb Res* 2006; **118**: 189–97.
- 145 Zorio E, Castelló R, Falcó C, España F, Osa A, Almenar L, Aznar J, Estellés A. Thrombin-activatable fibrinolysis inhibitor in young patients with myocardial infarction and its relationship with the fibrinolytic function and the protein C system. *Br J Haematol* 2003; **122**: 958–65.
- 146 Lisowski P, Małyszko J, Hirnle T, Lisowska A, Jackowski R, Małyszko JS, Buzun L, Myśliwiec M. Thrombin activatable fibrinolysis inhibitor (TAFI) in stable angina pectoris patients undergoing coronary artery bypass grafting (CABG). *Rocz Akad*

- Med w Białymstoku* 2005; **50**: 166–72.
- 147 Malyszko J, Malyszko JS, Hryszko T, Mysliwiec M. Thrombin-activatable fibrinolysis inhibitor in kidney transplant recipient with dyslipidemia. *Transplant Proc* 2003; **35**: 2219–21.
- 148 Malyszko J, Tymcio J. Thrombin activatable fibrinolysis inhibitor and other hemostatic parameters in patients with essential arterial hypertension. *Pol Arch Med Wewn* 2008; **118**: 36–40.
- 149 Antovic JP, Yngen M, Östenson CG, Antovic A, Wallen HN, Jorreskög G, Blombäck M. Thrombin activatable fibrinolysis inhibitor and hemostatic changes in patients with type I diabetes mellitus with and without microvascular complications. *Blood Coagul Fibrinolysis* 2003; **14**: 551–6.
- 150 Martí-Fàbregas J, Borrell M, Cocho D, Martínez-Ramírez S, Martínez-Corral M, Fontcuberta J, Martí-Vilalta JL. Change in hemostatic markers after recombinant tissue-type plasminogen activator is not associated with the chance of recanalization. *Stroke* 2008; **39**: 234–6.
- 151 Meltzer ME, Lisman T, De Groot PG, Meijers JCM, Le Cessie S, Doggen CJM, Rosendaal FR. Venous thrombosis risk associated with plasma hypofibrinolysis is explained by elevated plasma levels of TAFI and PAI-1. *Blood* 2010; **116**: 113–21.
- 152 Meltzer ME, Doggen CJM, De Groot PG, Meijers JCM, Rosendaal FR, Lisman T. Low thrombin activatable fibrinolysis inhibitor activity levels are associated with an increased risk of a first myocardial infarction in men. *Haematologica* 2009; **94**: 811–8.
- 153 Folkeringa N, Coppens M, Veeger NJGM, Bom VJJ, Middeldorp S, Hamulyak K, Prins MH, Büller HR, Van Der Meer J. Absolute risk of venous and arterial thromboembolism in thrombophilic families is not increased by high thrombin-activatable fibrinolysis inhibitor (TAFI) levels. *Thromb Haemost* 2008; **100**: 38–44.
- 154 Schroeder V, Wilmer M, Buehler B, Kohler HP. TAFI activity in coronary artery disease: A contribution to the current discussion on TAFI assays. *Thromb Haemost* 2006; **96**: 236–7.
- 155 Schol-gelok S, Maat D, Biedermann JS, Gelder T Van, Frank WG, Lijfering WM, Meer FJM Van Der, Dingeman C, Versmissen J, Kruijff JHA. Rosuvastatin use increases plasma fibrinolytic potential : a randomised clinical trial. *Br J Haematol* 2020; : 1–7.
- 156 Harmanci A, Kandemir N, Dagdelen S, Gonc N, Buyukasik Y, Alikasifoglu A, Kirazli S, Ozon A, Gurlek A. Thrombin-activatable fibrinolysis inhibitor activity and global fibrinolytic capacity in Type 1 diabetes: Evidence for normal fibrinolytic state. *J Diabetes Complications* 2006; **20**: 40–4.
- 157 Skeppholm M, Wallén NH, Malmqvist K, Kallner A, Antovic JP. Comparison of two

- immunochemical assays for measuring thrombin-activatable fibrinolysis inhibitor concentration with a functional assay in patients with acute coronary syndrome. *Thromb Res* 2007; **121**: 175–81.
- 158 Zhou J, Kochan J, Yin O, Warren V, Zamora C, Atiee G, Pav J, Orihashi Y, Vashi V, Dishy V. A first-in-human study of DS-1040, an inhibitor of the activated form of thrombin-activatable fibrinolysis inhibitor, in healthy subjects. *J Thromb Haemost* 2017; **15**: 961–71.
- 159 Zhou J, Limsakun T, Yin O, Warren V, Zamora C, Atiee G, Kochan J, Pav J, Kobayashi F, Vashi V, Dishy V. First-in-Human Study to Assess the Safety, Pharmacokinetics, and Pharmacodynamics of an Oral Formulation of DS-1040, an Inhibitor of the Activated Form of Thrombin-Activatable Fibrinolysis Inhibitor, in Healthy Subjects. *J Clin Pharmacol* 2019; **59**: 1669–77.
- 160 Verkleij CJN, Nieuwdorp M, Gerdes VEA, Mörgelin M, Meijers JCM, Marx PF. The effects of hyperglycaemia on thrombin-activatable fibrinolysis inhibitor. *Thromb Haemost* 2009; **102**: 460–8.
- 161 Verkleij CJN, De Bruijn RE, Meesters EW, Gerdes VEA, Meijers JCM, Marx PF. The hemostatic system in patients with type 2 diabetes with and without cardiovascular disease. *Clin Appl Thromb* 2011; **17**.
- 162 Meltzer ME, Doggen CJM, De Groot PG, Rosendaal FR, Lisman T. Plasma levels of fibrinolytic proteins and the risk of myocardial infarction in men. *Blood* 2010; **116**: 529–36.
- 163 de Bruijne ELE, Gils A, Guimarães AHC, Dippel DWJ, Deckers JW, van den Meiracker a H, Poldermans D, Rijken DC, Declerck PJ, de Maat MPM, Leebeek FWG. The role of thrombin activatable fibrinolysis inhibitor in arterial thrombosis at a young age: the ATTAC study. *J Thromb Haemost* 2009; **7**: 919–27.
- 164 De Bruijne ELE, Gils A, Rijken DC, De Maat MPM, Guimarães AHC, Poldermans D, Declerck PJ, Leebeek FWG. High thrombin activatable fibrinolysis inhibitor levels are associated with an increased risk of premature peripheral arterial disease. *Thromb Res* 2011; **127**: 254–8.
- 165 Martini CH, Brandts A, De Bruijne ELE, Van Hylckama Vlieg A, Leebeek FWG, Lisman T, Rosendaal FR. The effect of genetic variants in the thrombin activatable fibrinolysis inhibitor (TAFI) gene on TAFI-antigen levels, clot lysis time and the risk of venous thrombosis. *Br J Haematol* 2006; **134**: 92–4.
- 166 Jood K, Redfors P, Gils A, Blomstrand C, Declerck PJ, Jern C. Convalescent plasma levels of TAFI activation peptide predict death and recurrent vascular events in ischemic stroke survivors. *J Thromb Haemost* 2012; **10**: 725–7.
- 167 Ladenvall C, Gils A, Jood K, Blomstrand C, Declerck PJ, Jern C. Thrombin activatable fibrinolysis inhibitor activation peptide shows association with all major subtypes of ischemic stroke and with TAFI gene variation. *Arterioscler*

- Thromb Vasc Biol* 2007; **27**: 955–62.
- 168 Bridge KI, Bollen L, Zhong J, Hesketh M, Macrae FL, Johnson A, Philippou H, Scott DJ, Gils A, Ariëns RAS. Thrombin-activatable fibrinolysis inhibitor in human abdominal aortic aneurysm disease. *J Thromb Haemost* 2017; **15**: 2218–25.
- 169 Rooth E, Wallen H, Antovic A, von Arbin M, Kaponides G, Wahlgren N, Blombäck M, Antovic J. Thrombin activatable fibrinolysis inhibitor and its relationship to fibrinolysis and inflammation during the acute and convalescent phase of ischemic stroke. *Blood Coagul Fibrinolysis* 2007; **18**: 365–70.
- 170 Brouwers G-J, Leebeek FWG, Tanck MWT, Jukema JW, Klufft C, de Maat MPM. Association between thrombin-activatable fibrinolysis inhibitor (TAFI) and clinical outcome in patients with unstable angina pectoris. *Thromb Haemost* 2003; **90**: 92–100.
- 171 Schroeder V, Chatterjee T, Mehta H, Windecker S, Pham T, Devantay N, Meier B, Kohler HP. Thrombin activatable fibrinolysis inhibitor (TAFI) levels in patients with coronary artery disease investigated by angiography. *Thromb Haemost* 2002; **88**: 1020–5.
- 172 Juhan-Vague I, Morange PE. Very high TAFI antigen levels are associated with a lower risk of hard coronary events: the PRIME study. *J Thromb Haemost* 2003; **1**: 2243–4.
- 173 Juhan-Vague I, Morange PE, Aubert H, Henry M, Aillaud MF, Alessi MC, Samnegård A, Hawe E, Yudkin J, Margaglione M, Di Minno G, Hamsten A, Humphries SE, Boquist S, Ericsson CG, Lundman P, Samnegard A, Silveira A, Tornvall P, Mohamed-Ali V, et al. Plasma thrombin-activatable fibrinolysis inhibitor antigen concentration and genotype in relation to myocardial infarction in the North and South of Europe. *Arterioscler Thromb Vasc Biol* 2002; **22**: 867–73.
- 174 Malyszko J, Malyszko JS, Mysliwiec M. Fluvastatin therapy affects TAFI concentration in kidney transplant recipients. *Transpl Int* 2003; **16**: 53–7.
- 175 Schroeder V, Kucher N, Kohler HP. Role of thrombin activatable fibrinolysis inhibitor (TAFI) in patients with acute pulmonary embolism. *J Thromb Haemost* 2003; **1**: 492–3.
- 176 Lau HK, Segev A, Hegele R a., Sparkes JD, Teitel JM, Chisholm RJ, Strauss BH. Thrombin-activatable fibrinolysis inhibitor (TAFI): A novel predictor of angiographic coronary restenosis. *Thromb Haemost* 2003; **90**: 1187–91.
- 177 Segev A, Hegele RA, Lau HK, Sparkes JD, Teitel JM, Chisholm RJ, Strauss BH. Thr325Ile polymorphism of the TAFI gene is related to TAFI antigen plasma levels and angiographic restenosis after percutaneous coronary interventions. *Thromb Res* 2004; **114**: 137–41.

- 178 Ozkan G, Ulusoy S, Sönmez M, Caner Karahan S, Menteşe A, Kaynar K, Bektaş O. Thrombin activatable fibrinolysis inhibitor (TAFI) levels in hypertensive patients and a comparison of the effects of amlodipine and ramipril on TAFI levels. *Clin Exp Hypertens* 2013; **35**: 134–40.
- 179 Guven GS, Atalar E, Yavuz B, Beyazit Y, Kekilli M, Kilicarslan A, Sahiner L, Oz G, Ozer N, Aksoyek S, Haznedaroglu IC, Sozen T. Simvastatin treatment improves endothelial function and increases fibrinolysis in patients with hypercholesterolemia. *J Natl Med Assoc* 2006; **98**: 627–30.
- 180 Kilicarslan A, Yavuz B, Guven GS, Atalar E, Sahiner L, Beyazit Y, Kekilli M, Ozer N, Oz G, Haznedaroglu IC, Sozen T. Fenofibrate improves endothelial function and decreases thrombin-activatable fibrinolysis inhibitor concentration in metabolic syndrome. *Blood Coagul Fibrinolysis* 2008; **19**: 310–4.
- 181 Verdú J, Marco P, Benlloch S, Lucas J. Association between the Thr325Ile and Ala147Thr polymorphisms of the TAFI gene and the risk of venous thromboembolic disease. *Clin Appl Thromb* 2008; **14**: 494–5.
- 182 Eichinger S, Schönauer V, Weltermann A, Minar E, Bialonczyk C, Hirschl M, Schneider B, Quehenberger P, Kyrle PA. Thrombin-activatable fibrinolysis inhibitor and the risk for recurrent venous thromboembolism. *Blood* 2004; **103**: 3773–6.
- 183 Tregouet DA, Schnabel R, Alessi MC, Godefroy T, Declerck PJ, Nicaud V, Munzel T, Bickel C, Rupprecht HJ, Lubos E, Zeller T, Juhan-Vague I, Blankenberg S, Tiret L, Morange PE. Activated thrombin activatable fibrinolysis inhibitor levels are associated with the risk of cardiovascular death in patients with coronary artery disease: The Athero Gene study. *J Thromb Haemost* 2009; **7**: 49–57.
- 184 Biswas A, Tiwari AK, Ranjan R, Meena A, Akhter MS, Yadav BK, Behari M, Saxena R. Thrombin activatable fibrinolysis inhibitor gene polymorphisms are associated with antigenic levels in the Asian-Indian population but may not be a risk for stroke. *Br J Haematol* 2008; **143**: 581–8.
- 185 Morange PE, Tregouet DA, Frere C, Luc G, Arveiler D, Ferrieres J, Amouyel P, Evans A, Ducimetiere P, Cambien F, Tiret L, Juhan-Vague I. TAFI gene haplotypes, TAFI plasma levels and future risk of coronary heart disease: The PRIME Study. *J Thromb Haemost* 2005; **3**: 1503–10.
- 186 Yano Y, Kitagawa N, Gabazza EC, Morioka K, Urakawa H, Tanaka T, Katsuki A, Araki-Sasaki R, Hori Y, Nakatani K, Taguchi O, Sumida Y, Adachi Y. Increased plasma thrombin-activatable fibrinolysis inhibitor levels in normotensive type 2 diabetic patients with microalbuminuria. *J Clin Endocrinol Metab* 2003; **88**: 736–41.
- 187 Kitagawa N, Yano Y, Gabazza EC, Bruno NE, Araki R, Matsumoto K, Katsuki A, Hori Y, Nakatani K, Taguchi O, Sumida Y, Suzuki K, Adachi Y. Different metabolic

- correlations of thrombin-activatable fibrinolysis inhibitor and plasminogen activator inhibitor-1 in non-obese type 2 diabetic patients. *Diabetes Res Clin Pract* 2006; **73**: 150–7.
- 188 Morange PE, Juhan-Vague I, Scarabin PY, Alessi MC, Luc G, Arveiler D, Ferrieres J, Amouyel P, Evans A, Ducimetiere P. Association between TAFI antigen and Ala 147Thr polymorphism of the TAFI gene and the angina pectoris incidence: The PRIME Study. *Thromb Haemost* 2003; **89**: 554–60.
- 189 Kim SH, Han SW, Kim EH, Kim DJ, Lee KY, Kim DI, Heo JH. Plasma fibrinolysis inhibitor levels in acute stroke patients with thrombolysis failure. *J Clin Neurol* 2005; **1**: 142–7.
- 190 Montaner J, Ribo M, Monasterio J, Molina CA, Alvarez-Sabin J. Thrombin-activatable fibrinolysis inhibitor levels in the acute phase of ischemic stroke. *Stroke* 2003; **34**: 1038–40.
- 191 Shantsila E, Montoro-Garcia S, Tapp LD, Apostolakis S, Wrigley BJ, Lip GYH. Fibrinolytic status in acute coronary syndromes: Evidence of differences in relation to clinical features and pathophysiological pathways. *Thromb Haemost* 2012; **108**: 32–40.
- 192 Cellai AP, Antonucci E, Liotta AA, Fedi S, Marcucci R, Falciani M, Giglioli C, Abbate R, Prisco D. TAFI activity and antigen plasma levels are not increased in acute coronary artery disease patients admitted to a coronary care unit. *Thromb Res* 2006; **118**: 495–500.
- 193 Leenaerts D, Bosmans JM, van der Veken P, Sim Y, Lambeir AM, Hendriks D. Plasma levels of carboxypeptidase U (CPU, CPB2 or TAFIa) are elevated in patients with acute myocardial infarction. *J Thromb Haemost* 2015; **13**: 2227–32.
- 194 Leenaerts D, Loyau S, Mertens JC, Boisseau W, Michel JB, Lambeir AM, Jandrot-Perrus M, Hendriks D. Carboxypeptidase U (CPU, carboxypeptidase B2, activated thrombin-activatable fibrinolysis inhibitor) inhibition stimulates the fibrinolytic rate in different in vitro models. *J Thromb Haemost* 2018; **16**: 2057–69.
- 195 Petit Dop F, Latreille M, Guicherd L, Mertens J., Claesen K, Hendriks D, Arnaud E, Donazzolo Y. Favourable safety profile of S62798, a potent TAFIa (activated thrombin-activatable fibrinolysis inhibitor) inhibitor, in first-in-man study in healthy subjects. *Eur Heart J* 2020; **41**.
- 196 Rigla M, Wagner AM, Borrell M, Mateo J, Foncuberta J, de Leiva A, Ordonez-Llanos J, Perez A. Postprandial thrombin activatable fibrinolysis inhibitor and markers of endothelial dysfunction in type 2 diabetic patients. *Metabolism* 2006; **55**: 1437–42.
- 197 Ribo M, Montaner J, Molina C a., Arenillas JF, Santamarina E, Alvarez-Sabın J. Admission fibrinolytic profile predicts clot lysis resistance in stroke patients treated with tissue plasminogen activator. *Thromb Haemost* 2004; **91**: 1146–51.

- 198 Khalifa NM, Gad MZ, Hataba AA, Mahran LG. Changes in ADMA and TAFI levels after stenting in coronary artery disease patients. *Mol Med Rep* 2012; **6**: 855–9.
- 199 Willemse JL, Brouns R, Heylen E, De Deyn PP, Hendriks DF. Carboxypeptidase U (TAFIa) activity is induced in vivo in ischemic stroke patients receiving thrombolytic therapy. *J Thromb Haemost* 2008; **6**: 200–2.
- 200 Mertens JC, Claesen K, Leenaerts D, Sim Y, Lambeir AM, Hendriks D. Inhibition of the procarboxypeptidase U (proCPU, TAFI, proCPB2) system due to hemolysis. *J Thromb Haemost* 2019; **17**: 878–84.
- 201 Pedersen A, Redfors P, Lundberg L, Gils A, Declerck PJ, Nilsson S, Jood K, Jern C. Haemostatic biomarkers are associated with long-term recurrent vascular events after ischaemic stroke. *Thromb Haemost* 2016; **116**: 537–43.
- 202 Hulme JP, An SSA. Detecting activated thrombin activatable fibrinolysis inhibitor (TAFIa) and inactivated TAFIa (TAFIai) in normal and hemophilia a plasmas. *Bull Korean Chem Soc* 2009; **30**: 77–82.
- 203 Lisman T. Decreased Plasma Fibrinolytic Potential As a Risk for Venous and Arterial Thrombosis. *Semin Thromb Hemost* 2017; **43**: 178–84.
- 204 Pieters M, Philippou H, Undas A, de Lange Z, Rijken DC, Mutch NJ. An international study on the feasibility of a standardized combined plasma clot turbidity and lysis assay: communication from the SSC of the ISTH. *J Thromb Haemost* 2018; **16**: 1007–12.
- 205 Leenaerts D, Aernouts J, Van Der Veken P, Sim Y, Lambeir AM, Hendriks D. Plasma carboxypeptidase U (CPU, CPB2, TAFIa) generation during in vitro clot lysis and its interplay between coagulation and fibrinolysis. *Thromb Haemost* 2017; **117**: 1498–508.
- 206 Leenaerts D, Loyau S, Mertens JC, Boisseau W, Michel JB, Lambeir AM, Jandrot-Perrus M, Hendriks D. Carboxypeptidase U (CPU, carboxypeptidase B2, activated thrombin-activatable fibrinolysis inhibitor) inhibition stimulates the fibrinolytic rate in different in vitro models. *J Thromb Haemost* 2018; **16**: 2057–69.
- 207 Insull W. The Pathology of Atherosclerosis: Plaque Development and Plaque Responses to Medical Treatment. *Am J Med* 2009; **122**: 3–14.
- 208 Benjamin EJ, Virani SS, Callaway CW, Chamberlain AM, Chang AR, Cheng S, Chiuve SE, Cushman M, Dellings FN, Deo R, De Ferranti SD, Ferguson JF, Fornage M, Gillespie C, Isasi CR, Jiménez MC, Jordan LC, Judd SE, Lackland D, Lichtman JH, et al. Heart disease and stroke statistics - 2018 update: A report from the American Heart Association. *Circulation* 2018; **137**: 67–492.
- 209 Chinetti-Gbaguidi G, Colin S, Staels B. Macrophage subsets in atherosclerosis. *Nat Rev Cardiol* 2015; **12**: 10–7.
- 210 Libby P, Buring JE, Badimon L, Hansson GK, Deanfield J, Bittencourt MS,

- Tokgözoğlu L, Lewis EF. Atherosclerosis. *Nat Rev Dis Prim* 2019; **5**: 1–18.
- 211 Visseren FLJ, Mach F, Smulders YM, Carballo D, Koskinas KC, Böck M, Benetos A, Biffi A, Boavida JM, Capodanno D, Cosyns B, Crawford C, Davos CH, Desormais I, Di Angelantonio E, Franco OH, Halvorsen S, Hobbs FDR, Hollander M, Jankowska EA, et al. 2021 ESC Guidelines on cardiovascular disease prevention in clinical practice. *Eur Heart J* 2021; **42**: 3227–337.
- 212 Nordestgaard BG, Nicholls SJ, Langsted A, Ray KK, Tybjaerg-Hansen A. Advances in lipid-lowering therapy through gene-silencing technologies. *Nat Rev Cardiol* 2018; **15**: 261–72.
- 213 Cordon A, De Meester C, Gerkens S, Roberfroid D, De Laet C. Statins for the primary prevention of cardiovascular disease. Health Technology Assessment (HTA). KCE Reports 306. *Belgian Health Care Knowledge Centre (KCE)*. 2019.
- 214 Zhao X-Q. Pathogenesis of Atherosclerosis. *UpToDate*. www.uptodate.com/contents/pathogenesis-of-atherosclerosis. 2021.
- 215 Steinberg D, Witztum JL. History of discovery: Oxidized low-density lipoprotein and atherosclerosis. *Arterioscler Thromb Vasc Biol* 2010; **30**: 2311–6.
- 216 Lilly LS, Harvard Medical School. Pathophysiology of heart disease : a collaborative project of medical students and faculty. Wolters Kluwer/Lippincott Williams & Wilkins; 2011.
- 217 Reiner Ž. Hypertriglyceridaemia and risk of coronary artery disease. *Nat Rev Cardiol* 2017; **14**: 401–11.
- 218 Nelson RH. Hyperlipidemia as a Risk Factor for Cardiovascular Disease. *Prim Care* 2013; **40**: 195–211.
- 219 Silverthorn DU, Johnson BR, Ober WC, Garrison CW, Silverthorn AC. Human physiology : an integrated approach. Pearson Education; 2013.
- 220 BCFI. Ezetimibe. https://www.bcfi.be/nl/chapters/2?frag=1701&view=pvt&vm_p_group=12047.
- 221 Rang HP, Dale MM, Flower RJ, Henderson G. Rang and Dale's pharmacology. 8th ed. Elsevier Health Sciences; 2012.
- 222 Cappelletti RM. Statins Therapy: Effects on Plasma Fibrinogen Levels and Fibrinolysis. *J Nutr Disord Ther* 2013; **03**: 1–6.
- 223 RIZIV. Infospot - De TOP 25 van de werkzame bestanddelen in de uitgaven in de ambulante sector van de verzekering voor geneeskundige verzorging in 2019. 2020.
- 224 RIZIV. Infospot - De TOP 25 van de werkzame bestanddelen in de uitgaven in de ambulante sector van de verzekering voor geneeskundige verzorging in 2020. 2021.

- 225 Chong PH, Seeger JD, Franklin C. Clinically relevant differences between the statins: Implications for therapeutic selection. *Am J Med* 2001; **111**: 390–400.
- 226 Sirtori CR. The pharmacology of statins. *Pharmacol Res* 2014; **88**: 3–11.
- 227 Rosenson RS. Low-density lipoprotein cholesterol lowering with drugs other than statins and PCSK9 inhibitors. *UpToDate*. 2021.
- 228 De Costa G, Park A. Hyperlipidaemia. *Medicine (Baltimore)* 2017; **45**: 579–82.
- 229 Mach F, Baigent C, Catapano AL, Koskinas KC, Casula M, Badimon L, Chapman MJ, De Backer GG, Delgado V, Ference BA, Graham IM, Halliday A, Landmesser U, Mihaylova B, Pedersen TR, Riccardi G, Richter DJ, Sabatine MS, Taskinen MR, Tokgozoglu L, et al. 2019 ESC/EAS Guidelines for the management of dyslipidaemias: Lipid modification to reduce cardiovascular risk. *Eur Heart J* 2020; **41**: 111–88.
- 230 Stroes ESG, Stiekema LCA, Rosenson RS. PCSK9 inhibitors: Pharmacology, adverse effects, and use. *UpToDate*. 2021.
- 231 Wright RS, Ray KK, Raal FJ, Kallend DG, Jaros M, Koenig W, Leiter LA, Landmesser U, Schwartz GG, Friedman A, Wijngaard PLJ, Garcia Conde L, Kastelein JJP. Pooled Patient-Level Analysis of Inclisiran Trials in Patients With Familial Hypercholesterolemia or Atherosclerosis. *J Am Coll Cardiol* 2021; **77**: 1182–93.
- 232 Fitzgerald K, Frank-Kamenetsky M, Shulga-Morskaya S, Liebow A, Bettencourt BR, Sutherland JE, Hutabarat RM, Clausen VA, Karsten V, Cehelsky J, Nochur S V., Kotelianski V, Horton J, Mant T, Chiesa J, Ritter J, Munisamy M, Vaishnav AK, Gollob JA, Simon A. Effect of an RNA interference drug on the synthesis of proprotein convertase subtilisin/kexin type 9 (PCSK9) and the concentration of serum LDL cholesterol in healthy volunteers: A randomised, single-blind, placebo-controlled, phase 1 trial. *Lancet* 2014; **383**: 60–8.
- 233 Akinci B. Role of Thrombin Activatable Fibrinolysis Inhibitor in Endocrine and Cardiovascular Disorders: An Update. *Recent Pat Endocr Metab Immune Drug Discov* 2012; **6**: 210–7.
- 234 Meltzer ME, Doggen CJM, De Groot PG, Rosendaal FR, Lisman T. Fibrinolysis and the risk of venous and arterial thrombosis. *Curr Opin Hematol* 2007; **14**: 242–8.
- 235 Meltzer ME, Bol L, Rosendaal FR, Lisman T, Cannegieter SC. Hypofibrinolysis as a risk factor for recurrent venous thrombosis; results of the LETS follow-up study. *J Thromb Haemost* 2010; **8**: 605–7.
- 236 Libourel EJ, Bank I, Meinardi JR, Baljé-Volkers CP, Hamulyak K, Middeldorp S, Koopman MM, Van Pampus EC, Prins MH, Büller HR, Van Der Meer J. Co-segregation of thrombophilic disorders in factor V Leiden carriers; the contributions of factor VIII, factor XI, thrombin activatable fibrinolysis inhibitor and lipoprotein(a) to the absolute risk of venous thromboembolism.

- Haematologica* 2002; **87**: 1068–73.
- 237 Qian K, Xu J, Wan H, Fu F, Lu J, Lin Z, Liu Z, Liu H. Impact of genetic polymorphisms in thrombin activatable fibrinolysis inhibitor (TAFI) on venous thrombosis disease: A meta-analysis. *Gene* 2015; **569**: 173–81.
- 238 Wang W, Ma H, Lu L, Sun G, Liu D, Zhou Y, Tong Y, Lu Z. Association between thrombin-activatable fibrinolysis inhibitor gene polymorphisms and venous thrombosis risk: A meta-analysis. *Blood Coagul Fibrinolysis* 2016; **27**: 419–30.
- 239 Zwingerman N, Medina-Rivera A, Kassam I, Wilson MD, Morange PE, Trégouët DA, Gagnon F. Sex-specific effect of CPB2 Ala147Thr but not Thr325Ile variants on the risk of venous thrombosis: A comprehensive meta-Analysis. *PLoS One* 2017; **12**: 1–18.
- 240 Arauz A, Argüelles N, Jara A, Guerrero J, Barboza MA. Thrombin-Activatable Fibrinolysis Inhibitor Polymorphisms and Cerebral Venous Thrombosis in Mexican Mestizo Patients. *Clin Appl Thromb* 2018; **24**: 1291–6.
- 241 Orikaza CM, Morelli VM, Matos MF, Lourenço DM. Haplotypes of TAFI gene and the risk of cerebral venous thrombosis - A case-control study. *Thromb Res* 2014; **133**: 120–4.
- 242 Tokgoz S, Zamani AG, Durakbasi-Dursun HG, Yılmaz O, İlhan N, Demirel S, Tavli M, Sinan A. TAFI gene polymorphisms in patients with cerebral venous thrombosis. *Acta Neurol Belg* 2013; **113**: 291–7.
- 243 Verdú J, Marco P, Benlloch S, Sanchez J, Lucas J. Thrombin activatable fibrinolysis inhibitor (TAFI) polymorphisms and plasma TAFI levels measured with an ELISA insensitive to isoforms in patients with venous thromboembolic disease (VTD). *Thromb Haemost* 2006; **95**: 585–6.
- 244 Zee RYL, Hegener HH, Ridker PM. Carboxypeptidase B2 gene polymorphisms and the risk of venous thromboembolism. *J Thromb Haemost* 2005; **3**: 2819–21.
- 245 Isordia-Salas I, Martínez-Marino M, Alberti-Minutti P, Ricardo-Moreno MT, Castro-Calvo R, Santiago-Germán D, Alvarado-Moreno JA, Calleja-Carreño C, Hernández-Juárez J, Leños-Miranda A, Majluf-Cruz A. Genetic Polymorphisms Associated with Thrombotic Disease Comparison of Two Territories: Myocardial Infarction and Ischemic Stroke. *Dis Markers* 2019; **2019**.
- 246 Rattanawan C, Komanasin N, Settasatian N, Settasatian C, Kukongviriyapan U, Intharapetch P, Senthong V. Association of TAFI gene polymorphisms with severity of coronary stenosis in stable coronary artery disease. *Thromb Res* 2018; **171**: 171–6.
- 247 Guimarães AHC, Bertina RM, Rijken DC. A new functional assay of thrombin activatable fibrinolysis inhibitor. *J Thromb Haemost* 2005; **3**: 1284–92.
- 248 Kamal HM, Ahmed AS, Fawzy MS, Mohamed FA, Elbaz AA. Plasma thrombin-

- activatable fibrinolysis inhibitor levels and Thr325ile polymorphism as a risk marker of myocardial infarction in Egyptian patients. *Acta Cardiol* 2011; **66**: 483–8.
- 249 Fernandez-Cadenas I, Alvarez-Sabin J, Ribo M, Rubiera M, Mendioroz M, Molina CA, Rosell A, Montaner J. Influence of thrombin-activatable fibrinolysis inhibitor and plasminogen activator inhibitor-1 gene polymorphisms on tissue-type plasminogen activator-induced recanalization in ischemic stroke patients. *J Thromb Haemost* 2007; **5**: 1862–8.
- 250 Leebeek FWG, Van Goor MPJ, Guimaraes AHC, Brouwers GJ, De Maat MPM, Dippel DWJ, Rijken DC. High functional levels of thrombin-activatable fibrinolysis inhibitor are associated with an increased risk of first ischemic stroke. *J Thromb Haemost* 2005; **3**: 2211–8.
- 251 Santamaría A, Martínez-Rubio A, Borrell M, Mateo J, Ortín R, Foncuberta J. Risk of acute coronary artery disease associated with functional thrombin activatable fibrinolysis inhibitor plasma level. *Haematologica* 2004; **89**: 880–1.
- 252 Akatsu H, Yamagata H, Chen Y, Miki T, Kamino K, Takeda M, Campbell W, Kondo I, Kosaka K, Yamamoto T, Okada H. TAFI polymorphisms at amino 147 and 325 are not risk factors for cerebral infarction. *Br J Haematol* 2004; **127**: 440–7.
- 253 Morange PE, Henry M, Frere C, Juhan-Vague I. Thr325Ile polymorphism of the TAFI gene does not influence the risk of myocardial infarction. *Pacing Clin Electrophysiol* 2002; **99**: 1878–9.
- 254 Leurs J, Hendriks D. Carboxypeptidase U (TAFIa): A metallo-carboxypeptidase with a distinct role in haemostasis and a possible risk factor for thrombotic disease. *Thromb Haemost* 2005; **94**: 471–87.
- 255 Shi J, Zhi P, Chen J, Wu P, Tan S. Genetic variations in the thrombin-activatable fibrinolysis inhibitor gene and risk of cardiovascular disease: a systematic review and meta-analysis. *Thromb Res* 2014; **134**: 610–6.
- 256 Wang SW, Zhang HH, Dong CY, Sun HH. Meta-analysis of TAFI polymorphisms and risk of cardiovascular and cerebrovascular diseases. *Genet Mol Res* 2016; **15**: 1–13.
- 257 Santos IR, Fernandes AP, Carvalho MG, Sousa MO, Ferreira CN, Gomes KB. Thrombin-activatable fibrinolysis inhibitor (TAFI) levels and its polymorphism rs3742264 are associated with dyslipidemia in a cohort of Brazilian subjects. *Clin Chim Acta* 2014; **433**: 76–83.
- 258 Agirbasli M, Cincin A, Baykan OA. Short-term effects of angiotensin receptor blockers on blood pressure control, and plasma inflammatory and fibrinolytic parameters in patients taking angiotensin-converting enzyme inhibitors. *J Renin Angiotensin Aldosterone Syst* 2008; **9**: 22–6.

-
- 259 Mertens JC, Blanc-Guillemaud V, Claesen K, Cardona P, Hendriks D, Tyl B, Molina C a. Carboxypeptidase U (TAFIa) Is Rapidly Activated and Deactivated Following Thrombolysis and Thrombectomy in Stroke Patients. *Tranl Stroke Res* 2021; .
- 260 Mattsson C, Björkman JA, Abrahamsson T, Nerme V, Schatteman K, Leurs J, Scharpé S, Hendriks D. Local proCPU (TAFI) activation during thrombolytic treatment in a dog model of coronary artery thrombosis can be inhibited with a direct, small molecule thrombin inhibitor (melagatran). *Thromb Haemost* 2002; **87**: 557–62.
- 261 Pang H, Zhang C, Liu F, Gong X, Jin X, Su C. Reduced thrombin activatable fibrinolysis inhibitor and enhanced proinflammatory cytokines in acute coronary syndrome. *Med Intensiva* 2017; **41**: 475–82.
- 262 Mao SS, Colussi D, Bailey CM, Bosserman M, Burlein C, Gardell SJ, Carroll SS. Electrochemiluminescence assay for basic carboxypeptidases: Inhibition of basic carboxypeptidases and activation of thrombin-activatable fibrinolysis inhibitor. *Anal Biochem* 2003; **319**: 159–70.
- 263 Redlitz A, Tan AK, Eaton DL, Plow EF. Plasma carboxypeptidases as regulators of the plasminogen system. *J Clin Invest* 1995; **96**: 2534–8.
- 264 Reverter D, Fernández-Catalán C, Baumgartner R, Pfänder R, Huber R, Bode W, Vendrell J, Holak TA, Avilés FX. Structure of a novel leech carboxypeptidase inhibitor determined free in solution and in complex with human carboxypeptidase A2. *Nat Struct Biol* 2000; **7**: 322–8.
- 265 Arolas JL, Lorenzo J, Rovira A, Castellà J, Aviles FX, Sommerhoff CP. A carboxypeptidase inhibitor from the tick *Rhipicephalus bursa*: Isolation, cDNA cloning, recombinant expression, and characterization. *J Biol Chem* 2005; **280**: 3441–8.
- 266 Willemse JL, Heylen E, Nesheim ME, Hendriks DF. Carboxypeptidase U (TAFIa): A new drug target for fibrinolytic therapy? *J Thromb Haemost* 2009; **7**: 1962–71.
- 267 Gils A, Ceresa E, Macovei AM, Marx PF, Peeters M, Compennolle G, Declerck PJ. Modulation of TAFI function through different pathways - implications for the development of TAFI inhibitors. *J Thromb Haemost* 2005; **3**: 2745–53.
- 268 Hendrickx ML V, DE Winter A, Buelens K, Compennolle G, Hassanzadeh-Ghassabeh G, Muyldermans S, Gils A, Declerck PJ. TAFIa inhibiting nanobodies as profibrinolytic tools and discovery of a new TAFIa conformation. *J Thromb Haemost* 2011; **9**: 2268–77.
- 269 Buelens K, Hassanzadeh-Ghassabeh G, Muyldermans S, Gils A, Declerck PJ. Generation and characterization of inhibitory nanobodies towards thrombin activatable fibrinolysis inhibitor. *J Thromb Haemost* 2010; **8**: 1302–12.
- 270 Eriksson H, Sandset PM, Jensen E, Wall U, Andersson M, Nerme V, Eriksson-

- Lepkowska M, Wahlander K, Eriksson H, Jensen E, Sandset PM, Wall U, Andersson M, Nerme V, Eriksson-Lepkowska M, Wåhlander K, Day O. CPU inhibition with AZD9684: Profibrinolytic effects in acute pulmonary embolism patients [Abstract]. *J Thromb Haemost* 2007; **5**: P-S-367.
- 271 Brink M, Dahlén A, Olsson T, Polla M, Svensson T. Design and synthesis of conformationally restricted inhibitors of TAFIa. *Bioorganic Med Chem* 2014; **22**: 2261–8.
- 272 Davidsson P, Nerme VK. WO2009082340 - Method for monitoring the progression of fibrinolysis. International Patent Application No. PCT/SE2008/051487, 2 July 2009.
- 273 Mertens JC, Boisseau W, Leenaerts D, Di Meglio L, Loyau S, Lambeir A, Ducroux C, Jandrot-Perrus M, Michel J, Mazighi M, Hendriks D, Desilles J. Selective inhibition of carboxypeptidase U may reduce microvascular thrombosis in rat experimental stroke. *J Thromb Haemost* 2020; .
- 274 Zhang X-S, Xiang B-R. Discontinued drugs in 2007: cardiovascular drugs. *Expert Opin Investig Drugs* 2008; **17**: 1817–28.
- 275 Mertens JC, Leenaerts D, Brouns R, Engelborghs S, Ieven M, De Deyn PP, Lambeir A-M, Hendriks D. Procarboxypeptidase U (proCPU, TAFI, proCPB2) in cerebrospinal fluid during ischemic stroke is associated with stroke progression, outcome and blood-brain barrier dysfunction. *J Thromb Haemost* 2018; **16**: 342–8.
- 276 Bunnage ME, Blagg J, Steele J, Owen DR, Allerton C, McElroy AB, Miller D, Ringer T, Butcher K, Beaumont K, Evans K, Gray AJ, Holland SJ, Feeder N, Moore RS, Brown DG. Discovery of potent & selective inhibitors of activated thrombin-activatable fibrinolysis inhibitor for the treatment of thrombosis. *J Med Chem* 2007; **50**: 6095–103.
- 277 Atkinson JM, Pullen N, Johnson TS. An inhibitor of thrombin activated fibrinolysis inhibitor (TAFI) can reduce extracellular matrix accumulation in an in vitro model of glucose induced ECM expansion. *Matrix Biol* 2013; **32**: 277–87.
- 278 Atkinson JM, Pullen N, Da Silva-Lodge M, Williams L, Johnson TS. Inhibition of thrombin-activated fibrinolysis inhibitor increases survival in experimental kidney fibrosis. *J Am Soc Nephrol* 2015; **26**: 1925–37.
- 279 Pogačić Kramp V. List of drugs in development for neurodegenerative diseases: update October 2011. *Neurodegener Dis* 2012; **9**: 210–83.
- 280 Halland N, Czech J, Czechtizky W, Evers A, Follmann M, Kohlmann M, Schreuder HA, Kallus C. Sulfamide as Zinc Binding Motif in Small Molecule Inhibitors of Activated Thrombin Activatable Fibrinolysis Inhibitor (TAFIa). *J Med Chem* 2016; **59**: 9567–73.

-
- 281 Halland N, Brönstrup M, Czech J, Czechtizky W, Evers A, Follmann M, Kohlmann M, Schiell M, Kurz M, Schreuder HA, Kallus C. Novel Small Molecule Inhibitors of Activated Thrombin Activatable Fibrinolysis Inhibitor (TAFIa) from Natural Product Anabaenopeptin. *J Med Chem* 2015; **58**: 4839–44.
- 282 Durand A, Chauveau F, Cho T-H, Kallus C, Wagner M, Boutitie F, Maucort-Boulch D, Berthezène Y, Wiart M, Nighoghossian N. Effects of a TAFI-Inhibitor Combined with a Suboptimal Dose of rtPA in a Murine Thromboembolic Model of Stroke. *Cerebrovasc Dis* 2014; **38**: 268–75.
- 283 Björquist P, Buchanan M, Campitelli M, Carroll A, Hyde E, Neve J, Polla M, Quinn R. WO2005039617 - Use of cyclic anabaenopeptin-type peptides for the treatment of a condition wherein inhibition of carboxypeptidase U is beneficial, novel anabaenopeptin derivatives and intermediates thereof. International Patent Application No. PCT/SE2004/001568, 6 May 2005;
- 284 Sakai N, Takeuchi M, Imamura H, Shimamura N, Yoshimura S, Naito H, Kimura N, Masuo O, Hirotsune N, Morita K, Toyoda K, Yamagami H, Ishihara H, Nakatsu T, Miyoshi N, Suda M, Fujimoto S. Safety, Pharmacokinetics and Pharmacodynamics of DS-1040, in Combination with Thrombectomy, in Japanese Patients with Acute Ischemic Stroke. *Clin Drug Investig* 2022; **42**: 137–49.
- 285 Noguchi K, Edo N, Miyoshi N, Isobe A, Watanabe A, Ito Y, Morishima Y, Yamaguchi K. Fibrinolytic potential of DS-1040, a novel orally available inhibitor of activated thrombin-activatable fibrinolysis inhibitor (TAFIa). *Thromb Res* 2018; **168**: 96–101.
- 286 Sansilvestri-Morel P, Bertin F, Lapret I, Neau B, Blanc-Guillemaud V, Petit-Dop F, Tupinon-Mathieu I, Delerive P. S62798, a TAFIa inhibitor, accelerates endogenous thrombolysis in a murine model of pulmonary thromboembolism. *Eur Heart J* 2020; **41**.
- 287 Hendrickx MLV, Zatloukalova M, Hassanzadeh-Ghassabeh G, Muyltermans S, Gils A, Declerck PJ. Identification of a novel, nanobody-induced, mechanism of TAFI inactivation and its in vivo application. *J Thromb Haemost* 2014; **12**: 229–36.
- 288 Hendrickx ML V, Zatloukalova M, Hassanzadeh-Ghassabeh G, Muyltermans S, Gils A, Declerck PJ. In vitro and in vivo characterisation of the profibrinolytic effect of an inhibitory anti-rat TAFI nanobody. *Thromb Haemost* 2014; **111**: 824–32.
- 289 Semeraro F, Ammollo CT, Gils A, Declerck PJ, Colucci M. Monoclonal antibodies targeting the antifibrinolytic activity of activated thrombin-activatable fibrinolysis inhibitor but not the anti-inflammatory activity on osteopontin and C5a. *J Thromb Haemost* 2013; **11**: 2137–47.
- 290 Denorme F, Wyseure T, Peeters M, Vandeputte N, Gils A, Deckmyn H, Vanhoorelbeke K, Declerck PJ, De Meyer SF. Inhibition of Thrombin-Activatable Fibrinolysis Inhibitor and Plasminogen Activator Inhibitor-1 Reduces Ischemic

- Brain Damage in Mice. *Stroke* 2016; **47**: 2419–22.
- 291 Wyseure T, Rubio M, Denorme F, Lizarrondo SM De, Peeters M, Gils A, Meyer SF De, Vivien D, Declerck PJ. Innovative thrombolytic strategy using a heterodimer diabody against TAFI and PAI-1 in mouse models of thrombosis and stroke. *Blood* 2015; **125**: 1325–33.
- 292 Declerck PJ, De Meyer SF, Geukens N, Gils A, Rubio M, Vivien D, Wyseure TL. WO2015118147 - Dual targeting of TAF and PAI-1. Patent Application No. PCT/EP2015/052624, 13 August 2015;
- 293 Vercauteren E, Gils A. Is there any need for a TAFI(a) inhibitor as thrombolytic drug? *Thromb Res* 2012; **130**: 574–5.
- 294 Willemse JL, Hendriks DF. A role for carboxypeptidase U (TAFI) in thrombosis. *Front Biosci* 2007; **12**: 1973–87.
- 295 Muto Y, Suzuki K, Iida H, Sakakibara S, Kato E, Itoh F, Kakui N, Ishii H. EF6265, a novel inhibitor of activated thrombin-activatable fibrinolysis inhibitor, protects against sepsis-induced organ dysfunction in rats. *Crit Care Med* 2009; **37**: 1744–9.
- 296 Polla MO, Tottie L, Nordén C, Linschoten M, Müsil D, Trumpp-Kallmeyer S, Aukrust IR, Ringom R, Holm KH, Neset SM, Sandberg M, Thurmond J, Yu P, Hategan G, Anderson H. Design and synthesis of potent, orally active, inhibitors of carboxypeptidase U (TAFIa). *Bioorganic Med Chem* 2004; **12**: 1151–75.
- 297 Bird E, Tamura J, Bostwick JS, Steinbacher TE, Stewart A, Liu Y, Baumann J, Feyen J, Tamasi J, Schumacher WA. Is exogenous tissue plasminogen activator necessary for antithrombotic efficacy of an inhibitor of thrombin activatable fibrinolysis inhibitor (TAFI) in rats? *Thromb Res* 2007; **120**: 549–58.
- 298 Orbe J, Alexandru N, Roncal C, Belzunce M, Bibiot P, Rodriguez JA, Meijers JCM, Georgescu A, Paramo JA. Lack of TAFI increases brain damage and microparticle generation after thrombolytic therapy in ischemic stroke. *Thromb Res* 2015; **136**: 445–50.
- 299 Kraft P, Schwarz T, Meijers JCM, Stoll G, Kleinschnitz C. Thrombin-Activatable Fibrinolysis Inhibitor (TAFI) Deficient Mice Are Susceptible to Intracerebral Thrombosis and Ischemic Stroke. *PLoS One* 2010; **5**: 10–5.
- 300 Rehill AM, Preston RJS. A new thrombomodulin-related coagulopathy. *J Thromb Haemost* 2020; **18**: 2123–5.
- 301 Wang X, Smith PL, Hsu MY, Tamasi JA, Bird E, Schumacher WA. Deficiency in thrombin-activatable fibrinolysis inhibitor (TAFI) protected mice from ferric chloride-induced vena cava thrombosis. *J Thromb Thrombolysis* 2007; **23**: 41–9.
- 302 Morser J, Gabazza EC, Myles T, Leung LLK. What has been learnt from the thrombin-activatable fibrinolysis inhibitor-deficient mouse? *J Thromb Haemost*

- 2010; **8**: 868–76.
- 303 Koschinsky ML, Boffa MB, Nesheim ME, Zinman B, Hanley AJG, Harris SB, Cao H, Hegele RA. Association of a single nucleotide polymorphism in CPB2 encoding the thrombin-activable fibrinolysis inhibitor (TAFI) with blood pressure. *Clin Genet* 2001; **60**: 345–9.
- 304 Fujimoto H, Gabazza EC, Taguchi O, Nishii Y, Nakahara H, Bruno NE, D’Alessandro-Gabazza CN, Kasper M, Yano Y, Nagashima M, Morser J, Broze GJ, Suzuki K, Adachi Y. Thrombin-activatable fibrinolysis inhibitor deficiency attenuates bleomycin-induced lung fibrosis. *Am J Pathol* 2006; **168**: 1086–96.
- 305 Te Velde EA, Wagenaar GTM, Reijerkerk A, Roose-Girma M, Borel Rinkes IHM, Voest EE, Bouma BN, Gebbink MFBG, Meijers JCM. Impaired healing of cutaneous wounds and colonic anastomoses in mice lacking thrombin-activatable fibrinolysis inhibitor. *J Thromb Haemost* 2003; **1**: 2087–96.
- 306 Swaisgood CM, Schmitt D, Eaton D, Plow EF. In vivo regulation of plasminogen function by plasma carboxypeptidase B. *J Clin Invest* 2002; **110**: 1275–82.
- 307 Guimarães AHC, Laurens N, Weijers EM, Koolwijk P, Van Hinsbergh VWM, Rijken DC. TAFI and pancreatic carboxypeptidase B modulate in vitro capillary tube formation by human microvascular endothelial cells. *Arterioscler Thromb Vasc Biol* 2007; **27**: 2157–62.
- 308 World Health Organization (WHO). Coronavirus (COVID-19).
- 309 Wiersinga W, Rhodes A, Cheng A, Peacock S, Prescott H. Pathophysiology, Transmission, Diagnosis, and Treatment of Coronavirus Disease 2019 (COVID-19): A Review. *JAMA* 2020; **324**: 782–93.
- 310 Huang C, Wang Y, Li X, Ren L, Zhao J, Hu Y, Zhang L, Fan G, Xu J, Gu X, Cheng Z, Yu T, Xia J, Wei Y, Wu W, Xie X, Yin W, Li H, Liu M, Xiao Y, et al. Clinical features of patients infected with 2019 novel coronavirus in Wuhan, China. *Lancet* 2020; **395**: 497–506.
- 311 Wu Z, McGoogan J. Characteristics of and Important Lessons From the Coronavirus Disease 2019 (COVID-19) Outbreak in China: Summary of a Report of 72 314 Cases From the Chinese Center for Disease Control and Prevention. *JAMA* 2020; **323**: 1239–42.
- 312 Chen N, Zhou M, Dong X, Qu J, Gong F, Han Y, Qiu Y, Wang J, Liu Y, Wei Y, Xia J, Yu T, Zhang X, Zhang L. Epidemiological and clinical characteristics of 99 cases of 2019 novel coronavirus pneumonia in Wuhan, China: a descriptive study. *Lancet* 2020; **395**: 507–13.
- 313 Nougier C, Benoit R, Simon M, Desmurs-Clavel H, Marcotte G, Argaud L, David JS, Bonnet A, Negrier C, Dargaud Y. Hypofibrinolytic state and high thrombin generation may play a major role in SARS-COV2 associated thrombosis. *J Thromb*

- Haemost* 2020; **18**: 2215–9.
- 314 Seheult JN, Seshadri A, Neal MD. Fibrinolysis Shutdown and Thrombosis in Severe COVID-19. *J Am Coll Surg* 2020; **231**: 203–4.
- 315 Wright FL, Vogler TO, Moore EE, Moore HB, Wohlauser M V, Urban S, Nydam TL, Moore PK, McIntyre RC. Fibrinolysis Shutdown Correlation with Thromboembolic Events in Severe COVID-19 Infection. *J Am Coll Surg* 2020; **231**: 193–203.
- 316 Levi M, Thachil J, Iba T, Levy J. Coagulation abnormalities and thrombosis in patients with COVID-19. *Lancet Haematol* 2020; **7**: 438–40.
- 317 Oesterle A, Laufs U, Liao JK. Pleiotropic Effects of Statins on the Cardiovascular System. *Circ Res* 2017; **120**: 229–43.
- 318 Almeida SO, Budoff M. Effect of statins on atherosclerotic plaque. *Trends Cardiovasc Med* 2019; **29**: 451–5.
- 319 Krysiak R, Okopień B, Herman ZS. Effects of HMG-CoA reductase inhibitors on coagulation and fibrinolysis processes. *Drugs* 2003; **63**: 1821–54.
- 320 Roth L, Rombouts M, Schrijvers DM, Martinet W, De Meyer GRY. Cholesterol-independent effects of atorvastatin prevent cardiovascular morbidity and mortality in a mouse model of atherosclerotic plaque rupture. *Vascul Pharmacol* 2016; **80**: 50–8.
- 321 Barrett TJ. Macrophages in Atherosclerosis Regression. *Arterioscler Thromb Vasc Biol* 2020; **40**: 20–33.
- 322 Bruni F, Pasqui AL, Pastorelli M, Bova G, Di Renzo M, Cercigani M, Leo A, Auteri A, Puccetti L. Effect of atorvastatin on different fibrinolysis mechanisms in hypercholesterolemic subjects. *Int J Cardiol* 2004; **95**: 269–74.
- 323 BE71030031000; BioBank Antwerpen@UZA, BBMR-ERIC; No. Access: (4), Last: September, 03, 2020. [BIORESOURCE].
- 324 Asher J, Houston M. Statins and C-reactive protein levels. *J Clin Hypertens* 2007; **9**: 622–8.
- 325 Bardou M, Barkun A, Martel M. Effect of statin therapy on colorectal cancer. *Gut* 2010; **59**: 1572–85.
- 326 Claesen K, Mertens JC, Leenaerts D, Hendriks D. Carboxypeptidase U (CPU, TAF1a, CPB2) in thromboembolic disease: What do we know three decades after its discovery? *Int J Mol Sci* 2021; **22**: 1–32.
- 327 Claesen K, Mertens JC, Basir S, De Belder S, Maes J, Bosmans J, Stoffelen H, De Meester I, Hendriks D. Effect of Statin Therapy on the Carboxypeptidase U (CPU, TAF1a, CPB2) System in Patients With Hyperlipidemia: A Proof-of-Concept Observational Study. *Clin Ther* 2021; **43**: 908–16.

-
- 328 Emini Veseli B, Perrotta P, De Meyer GRA, Roth L, Van der Donckt C, Martinet W, De Meyer GRY. Animal models of atherosclerosis. *Eur J Pharmacol* 2017; **816**: 3–13.
- 329 Kahn SE, Watkins BF, Bermes EW. An evaluation of a spectrophotometric scanning technique for measurement of plasma hemoglobin. *Ann Clin Lab Sci* 1981; **11**: 126–31.
- 330 Bougarne N, Weyers B, Desmet SJ, Deckers J, Ray DW, Staels B, De Bosscher K. Molecular actions of PPAR α in lipid metabolism and inflammation. *Endocr Rev* 2018; **39**: 760–802.
- 331 Yoon M. The role of PPAR α in lipid metabolism and obesity: Focusing on the effects of estrogen on PPAR α actions. *Pharmacol Res* 2009; **60**: 151–9.
- 332 Masuda Y, Saotome D, Takada K, Sugimoto K, Sasaki T, Ishii H. Peroxisome proliferator-activated receptor-alpha agonists repress expression of thrombin-activatable fibrinolysis inhibitor by decreasing transcript stability. *Thromb Haemost* 2012; **108**: 74–85.
- 333 Paumelle R, Staels B. Cross-talk Between Statins and PPAR α in Cardiovascular Diseases: Clinical Evidence and Basic Mechanisms. *Trends Cardiovasc Med* 2008; **18**: 73–8.
- 334 Paumelle R, Staels B. Peroxisome proliferator-activated receptors mediate pleiotropic actions of statins. *Circ Res* 2007; **100**: 1394–5.
- 335 Pawlak K, Myśliwiec M, Pawlak D. Kynurenine pathway - A new link between endothelial dysfunction and carotid atherosclerosis in chronic kidney disease patients. *Adv Med Sci* 2010; **55**: 196–203.
- 336 Takemoto M, Liao J. Pleiotropic Effects of 3-Hydroxy-3-Methylglutaryl Coenzyme A Reductase Inhibitors. *Arterioscler Thromb Vasc Biol* 2001; **21**: 1712–9.
- 337 Claesen K, Roth L, Mertens JC, Hermans K, Sim Y, Hendriks D. Pleiotropic effects of atorvastatin result in a downregulation of the carboxypeptidase u system (Cpu, tafia, cpb2) in a mouse model of advanced atherosclerosis. *Pharmaceutics* 2021; **13**: 2–9.
- 338 Dhand NK, Khatkar MS. Statulator: An online statistical calculator. <http://statulator.com/SampleSize/ss2M.html>. 2014.
- 339 Claesen K, Sim Y, Bracke A, De M, Hert E De, Vliegen G, Hotterbeekx A, Vujkovic A, Petersen L Van, Winter FHR De, Brosius I, Theunissen C, Ierssel S Van, Frankenhuijsen M Van, Vlieghe E, Vercauteren K, Kumar-singh S, Meester I De, Hendriks D. Activation of the Carboxypeptidase U (CPU , TAF1a , CPB2) System in Patients with SARS-CoV-2 Infection Could Contribute to COVID-19 Hypofibrinolytic State and Disease Severity Prognosis. *J Clin Med* 2022; **11**: 1494.
- 340 Kinlay S. Role of c-reactive protein when prescribing a Statin. *Curr Atheroscler Rep*
-

- 2012; **14**: 26–32.
- 341 Lloyd-Jones DM, Braun LT, Ndumele CE, Smith SC, Sperling LS, Virani SS, Blumenthal RS. Use of Risk Assessment Tools to Guide Decision-Making in the Primary Prevention of Atherosclerotic Cardiovascular Disease: A Special Report from the American Heart Association and American College of Cardiology. *Circulation* 2019; **139**: 1162–77.
- 342 Liu PY, Liu YW, Lin LJ, Chen JH, Liao JK. Evidence for statin pleiotropy in humans: Differential effects of statins and ezetimibe on Rho-associated coiled-coil containing protein kinase activity, endothelial function, and inflammation. *Circulation* 2009; **119**: 131–8.
- 343 Landmesser U, Bahlmann F, Mueller M, Spiekermann S, Kirchhoff N, Schulz S, Manes C, Fischer D, De Groot K, Fliser D, Fauler G, März W, Drexler H. Simvastatin versus ezetimibe pleiotropic and lipid-lowering effects on endothelial function in humans. *Circulation* 2005; **111**: 2356–63.
- 344 Gagné C, Gaudet D, Bruckert E. Efficacy and safety of ezetimibe coadministered with atorvastatin or simvastatin in patients with homozygous familial hypercholesterolemia. *Circulation* 2002; **105**: 2469–75.
- 345 Niedzielski M, Broncel M, Gorzelak-Pabiś P, Woźniak E. A comparison of the effects of monotherapy with rosuvastatin, atorvastatin or ezetimibe versus combination treatment with rosuvastatin-ezetimibe and atorvastatin-ezetimibe on the integrity of vascular endothelial cells damaged by oxidized cholesterol. *PLoS One* 2021; **16**: 1–13.
- 346 Fujita M, Morimoto T, Ikemoto M, Takeda M, Ikai A, Miwa K. Dose-dependency in pleiotropic effects of atorvastatin. *Int J Angiol* 2007; **16**: 89–91.
- 347 Camnitz W, Burdick MD, Strieter RM, Mehrad B, Keeley EC. Dose-dependent Effect of Statin Therapy on Circulating CXCL12 Levels in Patients with Hyperlipidemia. *Clin Transl Med* 2012; **1**: 1.
- 348 Levi M, Van Der Poll T. Two-way interactions between inflammation and coagulation. *Trends Cardiovasc Med* 2005; **15**: 254–9.
- 349 Lek M, Karczewski K, Minikel E, Samocha K, Banks E, Fennell T, O'Donnell-Luria A, Ware J, Hill A, Cummings B, Tukiainen T, Birnbaum D, Kosmicki J, Duncan L, Estrada K, Zhao F, Zou J, Pierce-Hoffman E, Berghout J, Cooper D, et al. Analysis of protein-coding genetic variation in 60 706 humans. *Nature* 2016; **536**: 285–91.
- 350 Semeraro F, Ammollo CT, Semeraro N, Colucci M. Tissue factor-expressing monocytes inhibit fibrinolysis through a TAFI-mediated mechanism, and make clots resistant to heparins. *Haematologica* 2009; **94**: 819–26.
- 351 Depuydt MA, Prange KH, Slenders L, Örd T, Elbersen D, Boltjes A, de Jager SC, Asselbergs FW, de Borst GJ, Aavik E, Lönnberg T, Lutgens E, Glass CK, den Ruijter

- HM, Kaikkonen MU, Bot I, Slütter B, van der Laan SW, Yla-Herttuala S, Mokry M, et al. Microanatomy of the Human Atherosclerotic Plaque by Single-Cell Transcriptomics. *Circ Res* 2020; **127**: 1437.
- 352 Moore K, Sheedy F, Fisher E. Macrophages in atherosclerosis: a dynamic balance. *Nat Rev Immunol* 2013; **13**: 709–21.
- 353 Cochain C, Vafadarnejad E, Arampatzi P, Pelisek J, Winkels H, Ley K, Wolf D, Saliba AE, Zerneck A. Single-Cell RNA-Seq Reveals the Transcriptional Landscape and Heterogeneity of Aortic Macrophages in Murine Atherosclerosis. *Circ Res* 2018; **122**: 1661–74.
- 354 Martinet W, Coornaert I, Puylaert P, De Meyer GRY. Macrophage Death as a Pharmacological Target in Atherosclerosis. *Front Pharmacol* 2019; **0**: 306.
- 355 De Paoli F, Staels B, Chinetti-Gbaguidi G. Macrophage phenotypes and their modulation in atherosclerosis. *Circ J* 2014; **78**: 1775–81.
- 356 Gleissner CA. Macrophage phenotype modulation by CXCL4 in atherosclerosis. *Front Physiol* 2012; **3**: 1–7.
- 357 Song JJ, Hwang I, Cho KH, Garcia MA, Kim AJ, Wang TH, Lindstrom TM, Lee AT, Nishimura T, Zhao L, Morser J, Nesheim M, Goodman SB, Lee DM, Bridges SL, Gregersen PK, Leung LL, Robinson WH. Plasma carboxypeptidase B downregulates inflammatory responses in autoimmune arthritis. *J Clin Invest* 2011; **121**: 3517–27.
- 358 van der Kroef M, Carvalheiro T, Rossato M, de Wit F, Cossu M, Chouri E, Wichers CGK, Bekker CPJ, Beretta L, Vazirpanah N, Trombetta E, Radstake TRDJ, Angiolilli C. CXCL4 triggers monocytes and macrophages to produce PDGF-BB, culminating in fibroblast activation: Implications for systemic sclerosis. *J Autoimmun* 2020; **111**: 102444.
- 359 Matheeußen V, Waumans Y, Martinet W, Van Goethem S, Van Der Veken P, Scharpé S, Augustyns K, De Meyer GRY, De Meester I. Dipeptidyl peptidases in atherosclerosis: Expression and role in macrophage differentiation, activation and apoptosis. *Basic Res Cardiol* 2013; **108**.
- 360 Bradford M. Rapid and Sensitive Method for the Quantitation Microgram Quantities of Protein Utilizing the Principle of Protein-Dye Binding. *Anal Biochem* 1976; **254**: 248–54.
- 361 Spandidos A, Wang X, Wang H, Seed B. PrimerBank: a resource of human and mouse PCR primer pairs for gene expression detection and quantification. *Nucl Acid Res* 2010; **38**: 792–9.
- 362 Spandidos A, Wang X, Wang H, Dragnev S, Thurber T, Seed B. A comprehensive collection of experimentally validated primers for Polymerase Chain Reaction quantitation of murine transcript abundance. *BMC Genomics* 2008; **9**: 633.

- 363 Wang X, Seed B. A PCR primer bank for quantitative gene expression analysis. *Nucl Acids Res* 2003; **31**: 1–8.
- 364 Hellemans J, Mortier G, De Paepe A, Speleman F, Vandesompele J. qBase relative quantification framework and software for management and automated analysis of real-time quantitative PCR data. *Genome Biol* 2008; **8**.
- 365 Hellemans J, Vandesompele J. Selection of reliable reference genes for RT-qPCR analysis. *Methods Mol Biol* 2014; **1160**: 19–26.
- 366 Hossain MS, Ahmed R, Haque MS, Alam MM, Islam MS. Identification and validation of reference genes for real-time quantitative RT-PCR analysis in jute. *BMC Mol Biol* 2019; **20**: 1–13.
- 367 Cao X mei, Luo X guang, Liang J hong, Zhang C, Meng X ping, Guo D wei. Critical selection of internal control genes for quantitative real-time RT-PCR studies in lipopolysaccharide-stimulated human THP-1 and K562 cells. *Biochem Biophys Res Commun* 2012; **427**: 366–72.
- 368 Chanput W, Mes JJ, Wichers HJ. THP-1 cell line: An in vitro cell model for immune modulation approach. *Int Immunopharmacol* 2014; **23**: 37–45.
- 369 Mosser DM, Edwards JP. Exploring the full spectrum of macrophage activation. *Nat Rev Immunol* 2008; **8**: 958–69.
- 370 Liberale L, Dallegri F, Montecucco F, Carbone F. Pathophysiological relevance of macrophage subsets in atherogenesis. *Thromb Haemost* 2017; **117**: 7–18.
- 371 Zhao L, Morser J, Bajzar L, Nesheim ME, Nagashima M. Identification and characterization of two thrombin-activatable fibrinolysis inhibitor isoforms. *Thromb Haemost* 1998; **80**: 949–55.
- 372 Weiler H, Isermann B. Thrombomodulin. *J Thromb Haemost* 2003; **1**: 1515–24.
- 373 Burley K, Whyte C, Westbury S, Walker M, Stirrups KE, Turro E, Chapman OG, Reilly-stitt C, Mutch NJ, Mumford AD. Altered fibrinolysis in autosomal dominant thrombomodulin-associated coagulopathy. *Blood* 2016; **128**: 1879–83.
- 374 Dargaud Y, Scoazec JY, Wielders SJH, Trzeciak C, Hackeng TM, Négrier C, Hemker HC, Lindhout T, Castoldi E. Characterization of an autosomal dominant bleeding disorder caused by a thrombomodulin mutation. *Blood* 2015; **125**: 1497–501.
- 375 Langdown J, Luddington R, Huntington J, Baglin T. A hereditary bleeding disorder resulting from a premature stop codon in thrombomodulin (p.Cys537Stop). *Blood* 2014; **124**: 1951–6.
- 376 Maclachlan A, Dolan G, Grimley C, SP W, Morgan N. Whole exome sequencing identifies a mutation in thrombomodulin as the genetic cause of a suspected platelet disorder in a family with normal platelet function. *Platelets* 2017; **28**: 611–3.

- 377 Westbury S, Turro E, Greene D, Lentaigine C, Kelly A, Bariana T, Simeoni I, Pillois X, Attwood A, Austin S, Jansen S, Bakchoul T, Crisp-Hihn A, Erber W, Favier R, Foad N, Gattens M, Jolley J, Liesner R, Meacham S, et al. Human phenotype ontology annotation and cluster analysis to unravel genetic defects in 707 cases with unexplained bleeding and platelet disorders. *Genome Med* 2015; **7**.
- 378 Downes K, Megy K, Duarte D, Vries M, Gebhart J, Hofer S, Shamardina O, Deevi S, Stephens J, Mapeta R, Tuna S, Al Hasso N, Besser M, Cooper N, Daugherty L, Gleadall N, Greene D, Haimel M, Martin H, Papadia S, et al. Diagnostic high-throughput sequencing of 2396 patients with bleeding, thrombotic, and platelet disorders. *Blood* 2019; **134**: 2082–91.
- 379 Mutch NJ, Moore NR, Wang E, Booth NA. Thrombus lysis by uPA, scuPA and tPA is regulated by plasmaTAFI. *J Thromb Haemost* 2003; **1**: 2000–7.
- 380 Longstaff C. Development of Shiny app tools to simplify and standardize the analysis of hemostasis assay data: communication from the SSC of the ISTH. *J Thromb Haemost* 2017; **15**: 1044–6.
- 381 Jourdy Y, Enjolras N, Le Quellec S, Bordet J, Négrier C, Vinciguerra C, Dargaud Y. Why patients with THBD c.1611C>A (p.Cys537X) nonsense mutation have high levels of soluble thrombomodulin? *PLoS One* 2017; **12**: e0188213.
- 382 Han H, Yang L, Liu R, Liu F, Wu K, Li L, Liu X, Zhu C. Prominent changes in blood coagulation of patients with SARS-CoV-2 infection. *Clin Chem Lab Med* 2020; **58**: 1116–20.
- 383 Tang N, Li D, Wang X, Sun Z. Abnormal coagulation parameters are associated with poor prognosis in patients with novel coronavirus pneumonia. *J Thromb Haemost* 2020; **18**: 844–7.
- 384 Zuo Y, Warnock M, Harbaugh A, Yalavarthi S, Gockman K, Zuo M, Madison JA, Knight JS, Kanthi Y, Lawrence DA. Plasma tissue plasminogen activator and plasminogen activator inhibitor-1 in hospitalized COVID-19 patients. *Sci Rep* 2021; **11**: 1–9.
- 385 Della-Morte D, Pacifici F, Ricordi C, Massoud R, Rovella V, Proietti S, Iozzo M, Lauro D, Bernardini S, Bonassi S, Di Daniele N. Low level of plasminogen increases risk for mortality in COVID-19 patients. *Cell Death Dis* 2021; **12**.
- 386 Zhou F, Yu T, Du R, Fan G, Liu Y, Liu Z, Xiang J, Wang Y, Song B, Gu X, Guan L, Wei Y, Li H, Wu X, Xu J, Tu S, Zhang Y, Chen H, Cao B. Clinical course and risk factors for mortality of adult inpatients with COVID-19 in Wuhan, China: a retrospective cohort study. *Lancet* 2020; **395**: 1054–62.
- 387 COVID-19 Immune Repertoire Sequencing - NCT04368143 - ClinicalTrials.gov.
- 388 Juneja GK, Castelo M, Yeh CH, Cerroni SE, Hansen BE, Chessum JE, Abraham J, Cani E, Dwivedi DJ, Fraser DD, Slessarev M, Martin C, McGilvray S, Gross PL, Liaw

- PC, Weitz JI, Kim PY, Trigatti B, Fox-Robichaud A, Werstuck G, et al. Biomarkers of coagulation, endothelial function, and fibrinolysis in critically ill patients with COVID-19: A single-center prospective longitudinal study. *J Thromb Haemost* 2021; **19**: 1546–57.
- 389 Emonts M, De Bruijne ELE, Guimarães AHC, Declerck PJ, Leebeek FWG, De Maat MPM, Rijken DC, Hazelzet JA, Gils A. Thrombin activatable fibrinolysis inhibitor is associated with severity and outcome of severe meningococcal infection in children. *J Thromb Haemost* 2008; **6**: 268–76.
- 390 Vollrath JT, Marzi I, Herminghaus A, Lustenberger T, Relja B. Post-traumatic sepsis is associated with increased c5a and decreased TAFI levels. *J Clin Med* 2020; **9**.
- 391 Zeerleder S, Schroeder V, Hack CE, Kohler HP, Wuillemin WA. TAFI and PAI-1 levels in human sepsis. *Thromb Res* 2006; **118**: 205–12.
- 392 Relja B, Lustenberger T, Puttkammer B, Jakob H, Morser J, Gabazza EC, Takei Y, Marzi I. Thrombin-activatable fibrinolysis inhibitor (TAFI) is enhanced in major trauma patients without infectious complications. *Immunobiology* 2013; **218**: 470–6.
- 393 Bouck EG, Denorme F, Holle LA, Middelton EA, Blair AM, Laat B De, Schiffman JD, Yost CC, Rondina MT, Wolberg AS, Campbell RA. COVID-19 and Sepsis Are Associated with Different Abnormalities in Plasma Procoagulant and Fibrinolytic Activity. *Arterioscler Thromb Vasc Biol* 2021; **41**: 401–14.
- 394 Park R, Song J, An SSA. Elevated levels of activated and inactivated thrombin-activatable fibrinolysis inhibitor in patients with sepsis. *Korean J Hematol* 2010; **45**: 264.
- 395 Semeraro F, Colucci M, Caironi P, Masson S, Ammollo CT, Teli R, Semeraro N, Magnoli M, Salati G, Isetta M, Panigada M, Tonetti T, Tognoni G, Latini R, Pesenti A, Gattinoni L. Platelet drop and fibrinolytic shutdown in patients with sepsis. *Crit Care Med* 2018; **46**: 221–8.
- 396 Totoki T, Ito T, Kakuuchi M, Yashima N, Maruyama I, Kakihana Y. An evaluation of circulating activated TAFI in septic DIC : a case series and review of the literature. *Thromb J* 2022; **20**: 6–10.
- 397 Spyropoulos AC, Levy JH, Ageno W, Connors JM, Hunt BJ, Iba T, Levi M, Samama CM, Thachil J, Giannis D, Douketis JD. Scientific and Standardization Committee communication: Clinical guidance on the diagnosis, prevention, and treatment of venous thromboembolism in hospitalized patients with COVID-19. *J Thromb Haemost* 2020; **18**: 1859–65.
- 398 Jenner WJ, Gorog DA. Incidence of thrombotic complications in COVID-19: On behalf of ICODE: The International COVID-19 Thrombosis Biomarkers Colloquium. *J Thromb Thrombolysis* 2021; **52**: 999–1006.

- 399 Stiekema LCA, Willemsen L, Kaiser Y, Prange KHM, Wareham NJ, Boekholdt SM, Kuijk C, De Winther MPJ, Voermans C, Nahrendorf M, Stroes ESG, Kroon J. Impact of cholesterol on proinflammatory monocyte production by the bone marrow. *Eur Heart J* 2021; **42**: 4309–20.
- 400 Johnsen SH, Fosse E, Joakimsen O, Mathiesen EB, Stensland-Bugge E, Njølstad I, Arnesen E. Monocyte count is a predictor of novel plaque formation: A 7-year follow-up study of 2610 persons without carotid plaque at baseline the Tromsø study. *Stroke* 2005; **36**: 715–9.
- 401 Nasir K, Guallar E, Navas-Acien A, Criqui MH, Lima JAC. Relationship of monocyte count and peripheral arterial disease: Results from the National Health and Nutrition Examination Survey 1999-2002. *Arterioscler Thromb Vasc Biol* 2005; **25**: 1966–71.

Summary

Summary

The intrinsically unstable carboxypeptidase U (CPU, TAFIa, CPB2) circulates in plasma as the inactive zymogen procarboxypeptidase U (proCPU, TAFI, proCPB2) and is primarily seen as a potent attenuator of fibrinolysis through its action of cleaving C-terminal lysines on partially degraded fibrin. Additionally, there is increasing evidence that the function of CPU may not be restricted to fibrinolysis, but that it also may play a role as a modulator of inflammation.

In **Chapter 1** a general introduction to the CPU system is provided, focusing on the characteristics of CPU and the methods available for measuring proCPU, CPU and CPUi (inactivated CPU).

The current literature on the pathophysiological role of the CPU system is summarized in **Chapter 2**.

Chapter 3 defines the main objectives of this doctoral research project with the overall aim to contribute to a better understanding of the clinical context and expression of CPU, mainly focusing on hyperlipidemia & atherosclerosis.

In **Chapter 4**, a proof-of-concept observational study was conducted to explore the influence of statin therapy on proCPU biology in statin-eligible patients with hyperlipidemia. The results of this pilot study showed that increased plasma proCPU concentrations are present in hyperlipidemic patients. Treatment of these patients with a statin led to a significant decrease in proCPU levels and brought the proCPU concentration to the same level as in control subjects. Furthermore, both baseline proCPU levels and the decrease in proCPU showed high interindividual variation and interestingly the largest improvement in fibrinolysis (as measured by the change in Δ CLT) was seen in those patients with the highest baseline proCPU levels. As a result, these individuals are likely to benefit most from statin therapy. No association between the reduction in LDL-C and the reduction in plasma proCPU concentrations was observed,

suggesting that the downregulation of plasma proCPU levels may be a non-lipid related pleiotropic effect of statin therapy.

A study to gain more insight into the nature of the effect of statin treatment on the CPU system (lipid- or non-lipid related) is described in **Chapter 5**. Since it is challenging to discriminate between lipid- and non-lipid related pleiotropic effects in humans, this was investigated in a mouse model of advanced atherosclerosis (apolipoprotein E-deficient mice with a heterozygous mutation in the fibrillin-1 gene: ApoE^{-/-}Fbn1^{C1039G^{+/+}}) in which statins do not predominantly lower cholesterol. ProCPU levels were found to be significantly lowered under the influence of atorvastatin even though no lipid reduction was observed. Evidence is thus provided that the proCPU downregulation is a pleiotropic effect of atorvastatin treatment.

The above pilot study provided the hypothesis that it might be valuable to include proCPU measurement in risk assessment for starting statin therapy. Therefore, a larger clinical study was conducted (**Chapter 6**) in which we aimed to further substantiate this hypothesis. Consistent with the pilot study results, this larger study clearly showed that plasma proCPU concentrations and its expected effect on the fibrinolytic rate (as measured by Δ CLT) are increased in hyperlipidemic patients and these effects can be normalized (and even further reduced versus normolipidemic patients) by treatment with atorvastatin. High interindividual variation in proCPU levels was again observed in hyperlipidemic individuals, with proCPU levels up to 80% higher compared to normolipidemic controls. In accordance, the longest Δ CLT was seen in those patients with the highest proCPU levels, but these were not necessarily the individuals with the highest cholesterol levels. The proCPU downregulation and the improvement of the plasma fibrinolytic potential by atorvastatin are dose-dependent. The current results support the hypothesis that including measurement of proCPU and/or Δ CLT in risk assessment for starting statin therapy might be valuable, in particular for those patients where there are doubts about starting statin therapy based on conventional risk factors or for choosing the proper dosing of atorvastatin.

In **Chapter 7**, the expression of proCPU (on mRNA, protein and activity level) in (primary) human monocytes and different (primary) human macrophage subsets is described to gain more insight into these cells as potential sources of proCPU within atherosclerotic plaques and extra-vascular inflammatory sites. *CPB2* mRNA was expressed in the monocytic cell line THP-1 and in THP-1 cells stimulated into a macrophage-like phenotype with PMA, as well as in primary human monocytes isolated from PBMCs and macrophages derived from these monocytes. On a protein level, proCPU was detected in lysate and conditioned medium of HepG2, THP-1, PMA-stimulated THP-1 cells, primary human monocytes, primary human M-CSF macrophages, primary human IFN- γ /LPS-stimulated macrophages and primary human IL-4-stimulated macrophages. Moreover, CPU was detected in the conditioned media of all investigated cell types and it was demonstrated that proCPU can be activated into functionally active CPU in the *in vitro* cell culture environment. Comparison of both relative *CPB2* mRNA expression and proCPU concentrations in the cell medium between the different cell types provided evidence that *CPB2* mRNA expression and proCPU secretion in monocytes and (activated) macrophages are related to the degree to which these cells are differentiated and activated.

During the time course of my PhD research, some very interesting and unexpected CPU-related research questions/opportunities came into the spotlight that we eagerly explored further.

A first one was the functional characterization of a new mutation in the *CPB2* gene of proCPU – the first known case of a genetic proCPU deficiency described in humans (**Chapter 8**). The case was particularly interesting because of the co-inheritance of a new mutation in the *THBD* gene of thrombomodulin, which – in complex with thrombin – is one of the activators of proCPU. The single nucleotide deletion in the *THBD* gene resulted in protein chain truncation, promoting excessive shedding of a functionally active TM extracellular domain. The marked elevation in plasma TM levels resulted in a bleeding phenotype and delayed fibrinolysis *in vitro*. Premature truncation of the proCPU protein

was observed when the *CPB2* mutation was present, thereby preventing functional proCPU expression from this allele. The deficiency in proCPU was clinically asymptomatic, but the reduction of proCPU activity in plasma accelerated fibrinolysis *in vitro*. Co-inheritance of both mutations partially ameliorated the delayed fibrinolytic profile associated with the *THBD* mutation.

In the final chapter of this thesis (**Chapter 9**), the effect of SARS-CoV-2 infection on CPU-related parameters was evaluated. Measurement of these parameters in hospitalized COVID-19 patients showed that there is an initial significant generation of CPU with concomitant proCPU consumption during the early phase of SARS-CoV-2 infection, with a subsequent progressive increase in both proCPU concentration and CPU+CPUi antigen levels. The alterations in CPU-related parameters might (at least partly) contribute to the hypofibrinolytic state observed in COVID-19 patients and are likely to enlarge their risk of thrombosis. Moreover, CPU+CPUi antigen levels around admission were related to disease severity and the duration of hospitalization, putting forward the hypothesis that high circulating CPU+CPUi antigen levels may be a potential biomarker with prognostic value in SARS-CoV-2 infection.

Samenvatting

Samenvatting

Het intrinsiek onstabiele carboxypeptidase U (CPU, TAFIa, CPB2) circuleert in plasma onder de vorm van zijn inactieve zymogeen procarboxypeptidase U (proCPU, TAFI, proCPB2) en wordt voornamelijk gezien als een krachtige remmer van de fibrinolyse doordat het C-terminale lysines verwijdert van gedeeltelijk gedegradieerd fibrine. Daarnaast is er steeds meer bewijs dat de functie van CPU naar alle waarschijnlijkheid niet beperkt is tot de fibrinolyse, maar dat CPU ook een rol kan spelen als een modulator van inflammatie.

In **Hoofdstuk 1** werd een algemene introductie over het CPU systeem gegeven, met focus op methoden die beschikbaar zijn voor het meten van proCPU, CPU en CPUi (geïnactiveerd CPU).

De huidige literatuur over de pathofysiologische rol van het CPU systeem werd samengevat in **Hoofdstuk 2**.

In **Hoofdstuk 3** werden de belangrijkste doelstellingen van dit doctoraatsonderzoek weergegeven, met als algemeen doel bij te dragen tot een beter begrip van de klinische context en expressie van CPU, waarbij de focus ligt op hyperlipidemie en atherosclerose.

In **Hoofdstuk 4** werd een *proof-of-concept* observationele studie uitgevoerd om het effect van statinetherapie op de proCPU biologie te onderzoeken bij patiënten met hyperlipidemie waarbij de opstart van statinetherapie noodzakelijk is. De resultaten van deze pilotstudie toonden aan dat verhoogde plasma proCPU concentraties aanwezig zijn bij hyperlipidemische patiënten. Behandeling van deze patiënten met een statine zorgde voor een significante verlaging van de proCPU spiegels en bracht de proCPU concentratie tot op hetzelfde niveau als bij gezonde controle individuen. Bovendien vertoonden zowel de proCPU concentratie voor de start van statinetherapie, als de daling in proCPU spiegels een hoge interindividuele variatie, en werd de grootste verbetering in fibrinolyse (gemeten als de verandering in Δ CLT) gezien bij de patiënten met de hoogste

proCPU concentratie voor de start van de statine behandeling. Als gevolg hiervan hebben deze personen waarschijnlijk het meeste baat van statinetherapie. Ten slotte werd er geen verband gevonden tussen de verlaging van LDL-C en de verlaging van de plasma proCPU concentraties, wat doet vermoeden dat de downregulatie van de plasma proCPU concentratie een niet-lipide-gerelateerd pleiotroop effect van statinetherapie kan zijn.

Een studie om meer inzicht te krijgen in de aard van het effect van statinebehandeling op het CPU-systeem (lipide- of niet-lipide-gerelateerd) werd beschreven in **Hoofdstuk 5**. Aangezien het een uitdaging is om bij mensen een onderscheid te maken tussen lipide- en niet-lipide-gerelateerde pleiotrope effecten van statines, werd dit onderzocht in een muismodel van gevorderde atherosclerose (apolipoproteïne E-deficiënte muizen met een heterozygote mutatie in het fibrilline-1-gen: ApoE^{-/-}Fbn1^{C1039G^{+/-}}) waarbij statines cholesterol niet verlagen. ProCPU concentraties waren significant verlaagd onder invloed van atorvastatine, hoewel er geen daling in cholesterol werd waargenomen. Dit levert dus bewijs dat de proCPU downregulatie een pleiotroop effect is van behandeling met atorvastatine.

De bovenvermelde pilotstudie leverde de hypothese op dat het waardevol zou kunnen zijn om het meten van proCPU op te nemen in de risicobeoordeling voor het starten van statinetherapie. Om deze hypothese verder te onderbouwen, werd een grotere klinische studie uitgevoerd (**Chapter 6**). Net als de piloot studie toonde deze grotere studie duidelijk aan dat plasma proCPU concentraties en het verwachte effect op de fibrinolyse (gemeten als Δ CLT) verhoogd zijn bij hyperlipidemische patiënten en dat deze effecten genormaliseerd kunnen worden (en dat zelfs nog lagere proCPU concentraties bereikt kunnen worden in vergelijking met normolipidemische patiënten) door behandeling met atorvastatine. Hoge interindividuele variatie in proCPU concentratie werd opnieuw waargenomen bij hyperlipidemische individuen, met proCPU waarden die tot 80% hoger waren in vergelijking met normolipidemische controles. In overeenstemming hiermee werd de grootste Δ CLT gezien bij patiënten met de hoogste proCPU waarden, maar deze

personen hadden niet noodzakelijk ook de hoogste cholesterolwaarden. De proCPU downregulatie en de verbetering van het plasma fibrinolytisch potentieel onder invloed van atorvastatine zijn dosisafhankelijk. De huidige resultaten ondersteunen de hypothese dat het opnemen van een meting van proCPU en/of Δ CLT in de risicobeoordeling voor het starten van statinetherapie waardevol kan zijn, in het bijzonder voor patiënten waarbij er twijfels zijn over het starten van statinetherapie op basis van conventionele risicofactoren of voor het kiezen van de juiste dosering van atorvastatine.

In **Hoofdstuk 7** werd de expressie van proCPU (zowel op mRNA-, eiwit- als activiteitsniveau) in (primaire) humane monocyten en verschillende (primaire) humane macrofaag-subsets bestudeerd om meer inzicht te krijgen in deze cellen als een potentiële bron van proCPU in atherosclerotische plaques en extravasculaire ontstekingsplaatsen. *CPB2* mRNA expressie werd gezien in de monocyt cellijn THP-1 en in THP-1-cellen die met PMA gestimuleerd werden tot een macrofaag-*like* fenotype, evenals in primaire humane monocyten geïsoleerd uit PBMC's en macrofagen afgeleid van deze monocyten. Op eiwitniveau werd proCPU gedetecteerd in lysaat en geconditioneerd medium van HepG2, THP-1, PMA-gestimuleerde THP-1-cellen, primaire humane monocyten, primaire humane M-CSF macrofagen, primaire humane IFN- γ /LPS-gestimuleerde macrofagen en primaire humane IL-4-gestimuleerde macrofagen. Bovendien werd CPU gedetecteerd in de geconditioneerde media van alle onderzochte celtypen en werd er aangetoond dat proCPU kan worden geactiveerd tot functioneel actief CPU in de *in vitro* celcultuuromgeving. Vergelijking van zowel relatieve *CPB2* mRNA expressie als proCPU concentraties in het celmedium tussen de verschillende celtypen leverde bewijs dat *CPB2* mRNA expressie en proCPU secretie in monocyten en (geactiveerde) macrofagen gerelateerd is aan de mate waarin deze cellen zijn gedifferentieerd en geactiveerd.

Tijdens het uitvoeren van dit doctoraatsonderzoek kruisten een aantal zeer interessante CPU-gerelateerde onderzoeksvragen ons pad die niet onmiddellijk verband hielden met

hyperlipidemie en atherosclerose, maar die we toch graag verder wilden onderzoeken.

Een eerste was de functionele karakterisatie van een nieuwe mutatie in het *CPB2* gen van proCPU (het eerste beschreven geval van een genetische proCPU deficiëntie bij mensen) (**Hoofdstuk 8**). De casus was bijzonder interessant omwille de co-overerving van een nieuwe mutatie in het *THBD* gen van trombomoduline, dat – in complex met trombine – één van de activatoren van proCPU is. De deletie van één enkel nucleotide in het *THBD* gen resulteerde in verkorting van de eiwitketen, wat overmatige uitscheiding van functioneel actief extracellulair TM-domein bevorderde. De duidelijke verhoging van de plasma TM-spiegels resulteerde in een bloedingsfenotype en vertraagde de fibrinolyse *in vitro*. Wanneer de *CPB2* mutatie aanwezig was, werd enkel het activatie peptide van het proCPU eiwit aangemaakt, waardoor er geen functionele proCPU expressie was van het allel met de mutatie. De deficiëntie in proCPU was klinisch asymptomatisch, maar de lager plasma proCPU concentraties resulteerden in versnelde fibrinolyse *in vitro*. Co-overerving van beide mutaties verbeterde gedeeltelijk het vertraagde fibrinolytische profiel dat geassocieerd was met de *THBD* mutatie.

In het laatste hoofdstuk van dit doctoraatsonderzoek (**Hoofdstuk 9**) werd het effect van SARS-CoV-2 infectie op CPU-gerelateerde parameters geëvalueerd. Meting van deze parameters bij gehospitaliseerde COVID-19-patiënten toonde aan dat er een initiële significante generatie is van CPU met gelijktijdig proCPU verbruik tijdens de vroege fase van een SARS-CoV-2-infectie, met een daaropvolgende progressieve toename van zowel de proCPU concentratie als de CPU+CPUi antigeen spiegels. De veranderingen in CPU-gerelateerde parameters zal (op zijn minst gedeeltelijk) bijdragen tot de hypofibrinolytische toestand die wordt waargenomen bij COVID-19-patiënten en zal naar alle waarschijnlijkheid hun thrombose risico vergroten. Bovendien werd een correlatie waargenomen tussen de CPU+CPUi-antigeen levels bij opname en zowel de ernst van de ziekte als de duur van de ziekenhuisopname, wat de hypothese naar voren brengt dat hoge circulerende CPU+CPUi-antigeen levels een potentiële biomarker met prognostische waarde kunnen bij SARS-CoV-2-infectie zijn.

Scientific curriculum vitae

Scientific curriculum vitae

Personalia

Name	Karen Claesen
Date of birth	April 30, 1995
Place of birth	Duffel
Nationality	Belgian

Education

2018 – Present	Advanced Master in Clinical Biology University of Antwerp, Belgium
2018 – 2022	PhD student in Pharmaceutical Sciences Laboratory of Medical Biochemistry Title of doctoral dissertation: The carboxypeptidase U system in atherosclerosis: Insights in carboxypeptidase U mediated pleiotropic effects of statins Supervisor: prof. dr. D. Hendriks & prof. dr. I. De Meester
2016 – 2018	Master in Pharmaceutical Sciences, option Drug Development: Magna Cum Laude University of Antwerp, Belgium Master thesis: The CPU system: time-dependent variability and method validation in the presence of statins Supervisor: prof. dr. D. Hendriks
2014 – 2016	Honours Program of the Faculty of Pharmaceutical, Biomedical and Veterinary Sciences University of Antwerp, Belgium
2013 – 2016	Bachelor in Pharmaceutical Sciences: Summa Cum Laude University of Antwerp, Belgium
2007 - 2013	Humaniora, option Mathematics-Sciences Sint-Jozefinstituut, Kontich Belgium

Extracurricular activities

2019 – 2022 President of Farmant, the alumni association of the pharmacists graduated at the University of Antwerp

Scientific publications

PAPERS IN PEER-REVIEWED JOURNALS

2022 Bracke A, De Hert E, De bruyn, **Claesen K**, Vliegen G, Vujkovic A, van Petersen L, De Winter FHR, Hotterbeekx A, Brosius I, Theunissen C, Van Ierssele S, van Frankenhuijsen M, Vlieghe A, Vercauteren K, Van der Veken P, Hendriks D, Kumar-Singh S, De Meester I. Proline-specific peptidase activities (DPP4, PRCP, FAP and PREP) in plasma of hospitalized COVID-19 patients. *Clin Chim Acta* (2022); 531: 4-11.

Claesen K, Sim Y, Bracke A, De bruyn M, De Hert E, Vliegen G, Hotterbeekx A, Vujkovic A, van Petersen L, De Winter F.H.R, Brosius I, Theunissen C, van Ierssel S, van Frankenhuijsen M, Vlieghe E, Vercauteren K, Kumar-Singh S, De Meester I, Hendriks D. Activation of the carboxypeptidase U (CPU, TAF1a, CPB2) system in patients with SARS-CoV-2 infection could contribute to COVID-19 hypofibrinolytic state and disease severity prognosis. *J Clin Med* (2022); 11: 1494.

2021 Mertens JC, Blanc-Guillemaud V, **Claesen K**, Cardona P, Hendriks D, Tyl B, Molina CA. Carboxypeptidase U (TAF1a) Is Rapidly Activated and Deactivated Following Thrombolysis and Thrombectomy in Stroke Patients. *Transl Stroke Res.* (2021).

Claesen K, Roth L, Mertens JC, Hermans K, Sim Y, Hendriks D. Pleiotropic effect of atorvastatin result in a downregulation of the carboxypeptidase U system (CPU, TAF1a, CPB2) in a mouse model of advanced atherosclerosis. *Pharmaceutics.* (2021); 13: 1731.

Claesen K, Mertens JC, Basir S, De Belder S, Maes J, Bosmans J, Stoffelen H, De Meester I, Hendriks D. Effect of statin therapy on the carboxypeptidase U (CPU, TAF1a, CPB2) system in hyperlipidemic patients: a proof-of-concept observational study. *Clinical Therapeutics.* (2021); 43:908–916.

Claesen K, Mertens JC, Leenaerts D, Hendriks D. Carboxypeptidase U (CPU, TAFIa, CPB2) in Thromboembolic Disease: What Do We Know Three Decades after Its Discovery? *Int J Mol Sci.* (2021); 22(2):883.

2020 Westbury SK, Whyte CS, Stephens J, Downes K, Turro E, **Claesen K**, Mertens JC, Hendriks D, Latif A-L, Leishman EJ, NIHR BioResource, Mutch NJ, Tait RC, Mumford AD. Partial thrombin-activatable fibrinolysis inhibitor deficiency modulates fibrinolysis in a new pedigree with thrombomodulin-associated coagulopathy. *J Thromb Haemost.* (2020); 18(9):2209-2214.

2019 Mertens JC, **Claesen K**, Leenaerts D, Sim Y, Lambeir A.-M., Hendriks D. Inhibition of the procarboxypeptidase U (proCPU, TAFI, proCPB2) system due to hemolysis. *J Thromb Haemost.* (2019); 17: 878–884.

Submitted or in preparation **Claesen K**, Sim Y, De Belder S, van den Keybus T, Van Edom G, Stoffelen H, De Keulenaer G, Bosmans J, Bringmans T, De Meester I, Hendriks D. Procarboxypeptidase U (proCPU, TAFI, CPB2) as a novel marker for identifying benefit from atorvastatin therapy. Manuscript submitted.

Claesen K, De Loose J, Van Wielendaele P, De bruyn E, Sim Y, Thys S, Pintelon I, De Meester I, Hendriks D. Procarboxypeptidase U (proCPU, TAFI, CPB2) is expressed by (primary) human monocytes and macrophages and expression differs between states of differentiation and activation. Manuscript submitted.

Mertens JC, **Claesen K**, Hendriks D. Carboxypeptidase U. *Handbook of proteolytic enzymes*, 4th Ed. Handbook in preparation.

ABSTRACTS (Presenting author)

2022 **Claesen K**, Sim Y, De Belder S, van den Keybus T, Van Edom G, Stoffelen H, De Keulenaer G, Bosmans J, Bringmans T, De Meester I, Hendriks D. Procarboxypeptidase U (proCPU, TAFI, CPB2) as a novel marker for identifying benefit from atorvastatin therapy. 3th Joint Meeting of the International Society of Fibrinolysis and Proteolysis and the Plasminogen Activation Workshop (2022), Caen, France. Oral presentation

Claesen K, De Loose J, Van Wielendaele P, De bruyn E, Sim Y, Thys S, Pintelon I, De Meester I, Hendriks D. Procarboxypeptidase U (proCPU, TAFI, CPB2) is expressed by (primary) human monocytes and macrophages and expression differs between states of differentiation and activation. 3th Joint Meeting of the International Society of Fibrinolysis and Proteolysis and the Plasminogen Activation Workshop (2022), Caen, France. Poster presentation

Claesen K, Sim Y, De Belder S, van den Keybus T, Van Edom G, Stoffelen H, De Keulenaer G, Bosmans J, Bringmans T, De Meester I, Hendriks D. Procarboxypeptidase U (proCPU, TAFI, CPB2) as a novel marker for identifying benefit from atorvastatin therapy. Departmental Research Day of Pharmaceutical Sciences (2022), University of Antwerp, Antwerp, Belgium. Oral presentation

2021 **Claesen K**, Sim Y, Bracke A, De bruyn M, De Hert E, Vliegen G, Hotterbeeckx A, Kumar-Singh S, Vercauteren K, De Meester I, Hendriks D. Evaluation of the carboxypeptidase U (CPU, TAFIa, CPB2) system in patients with SARS-CoV-2 infection. European Congress on Thrombosis and Haemostasis (2021), Ghent, Belgium. Poster presentation

2020 **Petit Dop F**, Latreille M, Guicherd L, Mertens JC, **Claesen K**, Hendriks D, Arnaud E, Donazollo Y. S62798, a potent TAFIa (activated thrombin-activatable fibrinolysis inhibitor) inhibitor demonstrated a good safety profile in first-in-man study. Annual Congress of the European Society of Cardiology (2020), Amsterdam, The Netherlands. Oral presentation

Claesen K, Hermans K, Roth L, Mertens JC, De Meyer G, Hendriks D. Downregulation of the procarboxypeptidase U (proCPU, TAFI, proCPB2) system in *ApoE^{-/-} Fbn1^{C1039G+/-}* mice is a non-lipid related pleiotropic effect of statin therapy. XXVIII Congress of the International Society on Thrombosis and Haemostasis (2020), Milan, Italy. Poster presentation

Mertens JC, Blanc-Guillemaud V, **Claesen K**, Cardona P, Leenaerts D, Tyl B, Hendriks D, Molina CA. Carboxypeptidase U (CPU, TAFIa, CPB2) generation in acute ischemic stroke patients undergoing thrombolysis and endovascular thrombectomy. XXVIII Congress of the International Society on Thrombosis and Haemostasis (2020), Milan, Italy. Poster presentation

Whyte CS, Westbury S, Tait RT, Mutch NJ, Downes K, Mertens JC, **Claesen K**, Hendriks D, Leishman E, Mumford A, NIHR BioResource. Fibrinolytic alternations in a thrombomodulin-associated coagulopathy are diminished by coinheritance of a TAFI mutation. XXVIII Congress of the International Society on Thrombosis and Haemostasis (2020), Milan, Italy. Poster presentation

Claesen K, Whyte CS, Mertens JC, Hendriks D, Mutch NJ. Comparison of the time course of generation of CPU (TAFIa, CPB2) activity in two in vitro clot lysis systems. Plasminogen Activation and Extracellular Proteolysis GRS/GRC (2020), Ventura, USA. Poster presentation

Mertens JC, Boisseau W, Leenaerts D, Di Meglio L, **Claesen K**, Loyau S, Lambeir AM, Ducroux C, Jandrot-Perrus M, Michel JB, Mazighi M, Hendriks D, Desilles JP. Selective inhibition of CPU reduces microvascular thrombosis in experimental rat stroke model. Plasminogen Activation and Extracellular Proteolysis GRS and GRC (2020), Ventura, USA. Oral and poster presentation

Claesen K, Mertens JC, Basir S, De Belder S, Maes J, Bosmans J, Stoffelen H, De Meester I, Hendriks D. The influence of statin therapy on procarboxypeptidase U (proCPU, TAFI, proCBP2) biology in patients eligible for statin therapy: a proof of concept observational study. 39th Annual Congress of the Belgian Society of Cardiology (2020), Brussels, Belgium. Poster presentation

Whyte CS, Westbury S, Tait RT, Mutch NJ, Downes K, Mertens JC, **Claesen K**, Hendriks D, Leishman E, Mumford A, NIHR BioResource. Coinheritance of TAFI variant ameliorates fibrinolytic alternations induced by thrombomodulin-associated coagulopathy. Annual Scientific Meeting of the British Society for Thrombosis and Haemostasis (2020), Birmingham, United Kingdom. Oral presentation

2019

Claesen K, Mertens JC, De Belder S, Maes J, Bosmans J, Stoffelen H, De Meester I, Hendriks D. Evaluation of the influence of statin therapy on procarboxypeptidase U (proCPU, TAFI, proCBP2) system in patients eligible for statin therapy. 27th Annual Meeting of the Belgian Society on Thrombosis and Haemostasis (2019), Mechelen, Belgium. Oral presentation

Mertens JC, Claesen K, Leenaerts D, Sim Y, Lambeir A.-M., Hendriks D. Inhibition of the procarboxypeptidase U (proCPU, TAFI, proCPB2) system due to hemolysis. XXVII Congress of the International Society on Thrombosis and Haemostasis (2019), Melbourne, Australia. Poster presentation

Honors and awards

- 2022 **Travel Grant for 3th Joint Meeting of the International Society of Fibrinolysis and Proteolysis and the Plasminogen Activation Workshop, Caen, France**
Belgian Society on Thrombosis and Haemostasis
- 2021 **ECTH 2021 Best poster award**
European Congress on Thrombosis and Haemostasis
- 2020 **Travel Grant for Plasminogen Activation and Extracellular Proteolysis GRS/GRC, Ventura, USA**
Belgian Society on Thrombosis and Haemostasis
- 2018 **Price “Pharmacien et Doctoresse Nedeljkovitch” for academic achievements**
Graduation Ceremony Pharmaceutical Sciences, University of Antwerp, Belgium

Dankwoord

Bedankt!

Vier intense jaren en een bijna 300 pagina's later is het moment daar om terug te blikken en het onderdeel van dit boekje te schrijven dat naar alle waarschijnlijkheid het eerst en meest gelezen zal worden: het dankwoord. Mijn naam mag dan wel op de voorkant van dit boekje staan, een doctoraat behalen doe je niet alleen. Vanuit verschillende hoeken werd ik ondersteund en graag wil ik dan ook iedereen die, op welke manier dan ook, bijgedragen heeft aan deze thesis hartelijk bedanken.

Allereerst wil ik mijn promotor prof. dr. Dirk Hendriks bedanken. Dirk, dankjewel om me de kans te geven dit doctoraat uit te voeren en mij zo mee te laten schrijven aan een volgend hoofdstuk in het CPU onderzoek. Het is een onderwerp dat je nauw aan het hart ligt en het enthousiasme waarmee je vertelt over CPU werkte steeds aanstekelijk en inspirerend! Voor mij was dit doctoraat een enorme verrijking, zowel op persoonlijk als professioneel vlak en dat is mede te danken aan de zelfstandigheid die je me liet om dit onderzoek uit te voeren en de kansen die ik kreeg. Wanneer nodig werd er, ondanks je drukke agenda, steeds tijd gevonden voor een meeting, de nodige wetenschappelijke input of het kritisch nalezen van mijn schrijfwerk. Daarnaast ben ik je enorm dankbaar om me de kans te geven congressen bij te wonen over zowat heel de wereld. Dit waren voor mij stuk voor stuk fantastische ervaringen die me nog lang zullen bij blijven. Bedankt Dirk voor het in mij gestelde vertrouwen en de fijne samenwerking!

Daarnaast wil ik ook mijn co-promotor prof. dr. Ingrid De Meester uitdrukkelijk bedanken. Ingrid, jouw deur stond altijd open voor vragen, motiverende (na)besprekingen of gewoon een fijn gesprek. Bedankt voor je hulp bij het uitwerken van de verschillende aanvragen bij het Ethisch Comité en voor de begeleiding bij het celkweek-werk. Je was ook steeds bereid tijd vrij te maken om mijn manuscripten en deze thesis zorgvuldig na te lezen en waakte er over dat ik op tijd en stond mijn resultaten vanop de nodige afstand bekeek, zodat ik niet uit het oog verloor dat termen

Thank you!

zoals 'de Δ CLT' niet zo vanzelfsprekend zijn voor niet-CPU'ers. Bedankt voor alles! Jouw passie voor de wetenschap is iets om naar op te kijken.

Verder wil ik graag em. prof. dr. Anne-Marie Lambeir en prof. dr. Yann Sterckx bedanken. Bedankt voor de inzichten en ervaringen die jullie me hebben bijgebracht vanuit jullie onderzoeksdomein, voor het geboeid luisteren naar de presentaties die ik gaf en om een fijne werkomgeving te maken van het labo. Yann, bedankt ook voor je luisterend oor en voor de frisse wind die je met je komst door het labo liet waaien.

Yani, wat had ik zonder jou gedaan... dit boekje had nog niet eens half zo dik geweest. Jouw praktische hulp betekende heel veel voor mij en je enthousiasme en spontaniteit zorgde dat het steeds een plezier was om samen aan de *bench* te staan. Ook de vele uren stalen sorteren in de kou waren altijd fijner met z'n twee. Verder was geen wandeling of fietstochtje om stalen op te halen je te veel en wist je als geen ander wanneer het tijd was voor "pauze?" 😊. Geslaagde experimenten en gepubliceerde manuscripten werden op gepaste wijze gevierd, maar ook bij mindere momenten kon ik altijd op jou terugvallen en zorgde je voor de nodige zoetigheden om deze te overwinnen. Ik ben oprecht blij dat ik dit alles met jou mocht delen! Dankjewel voor alles!

Joachim, bedankt om mij onder je hoede te nemen en wegwijs te maken in de wondere, maar soms verdomd lastige, wereld van CPU! Ik heb heel wat van jou geleerd en kon altijd bij jou terecht met al mijn vragen. En ook nu je onze CPU *bench* al enkele jaren hebt in geruild voor het klinisch labo blijft jouw deur steeds voor me open staan, dat apprecieer ik enorm. Samen op congres gaan was steeds een hoogtepunt! Bedankt voor de leuke samenwerking!

Gwendolyn, ons onderzoek lag wat verder van elkaar verwijderd, toch stond je steeds klaar om te helpen en ook na je doctoraat bleef je bereikbaar voor vragen. Het was fijn om jou te leren kennen tijdens mijn eerste jaren op het labo. Bedankt!

An, corona zorgde er voor dat de wegen van ons onderzoek plots heel wat dichterbij elkaar lagen. Onze COVID-samenwerking had wel wat voeten in de aarde en ik ben dan ook trots dat we er in geslaagd zijn hieruit twee mooie artikels te laten voortkomen. Bedankt ook voor de leuke tijd samen in het bureau tijdens jouw laatste maanden op het labo.

Emilie en Michelle, mijn tijd op LMB was niet hetzelfde geweest zonder jullie. Emilie, bedankt om mij op weg te helpen in de celkweek. Michelle, onze dansbenen kunnen los gooien op jou trouwfeest was toch wel een hoogtepunt na corona! Bedankt allebei voor de gedeelde frustraties en vele gezellige babbels de afgelopen jaren. Het was voor mij dan ook wennen toen jullie vorig jaar kort na elkaar het labo verlieten. Gelukkig komen we elkaar regelmatig nog tegen tijdens een avondje casuïstiek en ... voor een babybezoekje binnenkort? 😊 Ik wil jullie heel veel succes toewensen met jullie nieuwe kleine “projectjes”, jullie gaan ongetwijfeld fantastische mama’s zijn!

Yentl, het was een plezier om het afgelopen jaar met jou het bureau te delen. We hebben samen heel wat afgelachen, maar er werd ook hard gewerkt en de nodige frustraties gedeeld. Je bent een enorm gedreven onderzoeker met een ongelooflijk talent voor planning en *multitasking*. Veel succes tijdens het laatste jaar van je doctoraat, ik kom graag supporteren tijdens jou verdediging. En 3 december 2022 staat in mijn agenda!
😊

Joni, ondanks de veel pogingen eindigde ons CXCL4-verhaal in mineur, gelukkig werd de ‘make-over’ van ons protocol voor monocyt isolatie uit *buffy coats* dankzij jou wel een succes! Bedankt voor alle hulp. Je bent een harde werker die steeds bereid is om anderen te helpen. Veel succes met je doctoraat en ga voor je dromen!

Lien, ik ken jou als een doorzetter die ondertussen helemaal haar plaats in het labo gevonden heeft en goed weet wat ze wil. Veel succes met alles wat je doet en dat daar niet te veel mieren in moeten voor komen! 😊

Thank you!

Natalia, jij bent een gedreven onderzoeker met het nodige relativiseringsvermogen en nuchtere kijk op dingen. Koffie- en middagpauzes waren altijd leuker met jou er bij. Ik kijk al uit naar feesten met de Polen. 😊 Veel succes met je verdere carrière en geniet met volle teugen van jullie mooie dag!

Rob, hoe jij al je labowerk weet te managen is ongezien. Ik hoop dat mijn presentatie over het afronden van een doctoraat je niet te veel heeft afgeschrikt... ik heb er alle vertrouwen in dat ook jou doctoraat een succesvol einde zal kennen. Veel succes!

Sam, Ellen en Emile, de nieuwe garde. In volle coronacrisis starten aan je doctoraat is niet evident, maar jullie hebben je weg gevonden en zijn helemaal open gebloeid. Ik wens jullie heel veel succes en vooral plezier tijdens de komende jaren, met af en toe een kleine portie geluk die elke doctoraatsstudent zou mogen ervaren.

Pieter, bedankt voor al je hulp bij de qPCR experimenten, zonder was dit niet goed gekomen. Trihn, bedankt voor al jouw administratieve hulp.

Tijdens mijn doctoraatsonderzoek heb ik het voorrecht gehad samen te werken met vele mensen binnen en buiten de muren van de UA.

Prof. dr. Johan Bosmans (Cardiologie, UZA), hartelijk dank voor uw interesse in het CPU onderzoek, om me in contact te brengen met de juiste mensen en het zorgvuldig nalezen van manuscripten. Prof. dr. Gilles De Keulenaer, Soraya Ahouari, Conny Vermeulen (Cardiologie, ZNA Middelheim), dr. Tijs Bringmans, Nathalie Brosens (Cardiologie, UZA), dr. Simon De Belder, dr. Jeroen Maes, dr. Glenn Van Edom, dr. Tinne van den Keybus (Huisartsenpraktijk Epione, Edegem) en in het bijzonder dr. Hilde Stoffelen (Huisartsenpraktijk Epione, Edegem), bedankt voor de fijne samenwerking. Het verzamelen van de bloedstalen van hyperlipidemische en statine patiënten heeft heel wat tijd en moeite gekost, maar het is gelukt en dat heb ik te danken aan jullie allemaal! Bedankt ook voor het zorgvuldig nalezen van de manuscripten.

Prof. dr. Guido De Meyer en prof. dr. Lynn Roth van het labo Fysiofarmacologie wil ik bedanken voor het ter beschikken stellen van de zeer waardevolle stalen van atorvastatine-behandelde muizen. Lynn, bedankt ook voor de kleine brainstorm sessies, voor de antwoorden op mijn vragen en je hulp bij het manuscript.

Verder wil ik dr. Sofie Thys en dr. Isabel Pintelon bedanken voor hun hulp bij de confocale microscoop en het nalezen van mijn manuscript.

Prof. dr. Nicola Mutch and dr. Claire Whyte, thank you for letting us take part in the study of the characterization of a new mutation in the *THBD* and *CPB2* gene. It was an interesting project and I enjoyed our meetings.

I also want to thank prof. dr. Koen Vercauteren, Alexandra Vujkovic, Lida van Petersen, Isabel Brosius, Caroline Theunissen, Maartje van Frankenhuijsen (ITG, Antwerpen), prof. dr. Samir Kumar-Singh, Ann Hotterbeeckx, Fine De Winter, Kumar-Singh (Molecular Pathology Group, UA), prof. dr. Erika Vlieghe and dr. Sabrina van Ierssel (Department of General Internal Medicine, Infectious Diseases and Tropical Medicine, UZA) for the use of the very valuable blood samples of COVID-19 patients, for their contribution to the manuscript and the pleasant collaboration.

Nina Jansoone (Labo Studies, UZA) wil ik bedanken voor haar hulp bij de bepalingen van de cholesterol panels. Kim Claes (Clinical Trial Center, UZA) verdient een woord van dank om me wegwijs te maken in REDCap. Pieter Moons en Sofie Goethals (Biobank, UZA/UA), bedankt dat ik gebruik kon maken van de Biobank Antwerpen. Voor *buffy coats* kon ik rekenen op de Dienst voor het Bloed van Rode Kruis Vlaanderen. Dorien Leenaerts (AZ Turnhout) wil ik bedanken voor het verzamelen van controle plasma.

Wie zeker niet mogen ontbreken in dit dankwoord zijn de vele patiënten en vrijwilligers die bereid waren om mee te werken en zich letterlijk met bloed, zweet en tranen, maar vooral met véél bloed, hebben ingezet voor dit onderzoek. Bedankt allemaal!

Thank you!

De leden van mijn interne doctoraatscommissie, prof. dr. Guido De Meyer en prof. dr. Gilles De Keulenaer wil ik graag bedanken voor het zorgvuldig nalezen van mijn thesis, de constructieve opmerkingen en stimulerende discussie. Equally, I would like to thank prof. dr. Joost Meijers and prof. dr. Nicola Mutch for accepting to be a member of my jury and for the evaluation of my thesis.

Graag wil ik ook Eva Sterckx van het secretariaat farmacie bedanken voor de administratieve hulp en het werk dat zij achter de schermen heeft gedaan. Ook bedankt Natacha Hoevenaegel voor de hulp bij de grafische vormgeving van deze thesis.

Ik heb ook enkele jaren de eer gehad om voorzitter te mogen zijn van Farmant en ik wil alle Farmant leden bedanken voor hun inzet en de leuke momenten samen.

Verder wil ik ook de masterstudenten die ik mocht begeleiden bedanken voor de hulp bij mijn onderzoek. Karlijn en Emilie, bedankt en ik wens jullie veel succes in jullie verdere carrière!

Charlotte, Lore, Lieze, Margaux, Wouter en Andrea, bedankt voor de vele welgekomen momenten van afleiding en van vriendschap. Jullie deden me al het werk rond het doctoraat even vergeten. Ann, Lise, Dorien, Selina, Katrien, Caro, Katleen en Katrientje, *'de visjes', zaterdag is krapuulekes dag en dan zwemmen we in bacardi lemon (of een wijntje)!* 😊 Bedankt voor alle zaterdagavonden en andere momenten samen. Lise, jou motivatie en doorzettingsvermogen zijn iets om een voorbeeld aan te nemen!

Bomma, bompa, moeke, vake en tante Roos, bedankt om er altijd voor mij te zijn en met veel enthousiasme te luisteren naar mijn wetenschappelijke verhalen (die voor jullie vaak toch wel wat 'chinees' waren). Jullie zijn mijn grootste supporters! Ook bedankt aan de rest van mijn familie en schoonfamilie voor alle warme momenten en jullie interesse in mijn onderzoek.

Katrien en Katleen, bedankt om jullie grote, kleine zus door dik en dun te steunen en altijd in mij te geloven. Ik kan me geen betere zussen wensen! Weet dat ik ook ongelooflijk trots ben op jullie! Niels, ook jij bedankt voor alle steun en lachmomenten.

Mama en papa, bedankt voor de onvoorwaardelijke steun en liefde, om ons te laten opgroeien in een warm en liefdevol nest en voor alle kansen die ik heb gekregen. De afgelopen jaren hebben jullie steeds enthousiast mijn doctoraatsverhalen aangehoord en me aangemoedigd, ook al was het niet altijd helemaal duidelijk wat ik nu weer met dat eiwit aan het doen was. Ik hoop dat ik jullie trots heb gemaakt. Bedankt voor alles. Wat zou ik zonder jullie doen!

En dan als laatste, Shahir. Zonder jou geduld en relativeringsvermogen was dit boekje er niet geweest. Bedankt om mijn steun en toeverlaat te zijn en telkens mijn frustraties te aan horen. Daarnaast kon ik tijdens mijn doctoraat ook handig gebruik maken van je bloedprik-skills. Bedankt om dit voor mij te doen. 😊 Toen we samen elf jaar geleden aan ons avontuur begonnen, had ik nooit kunnen dromen waar het ons zou brengen. De afgelopen jaren zijn intens geweest, zeker toen corona langs kwam en jij daarna aan de andere kant van het land in het mooie Limburg mocht gaan werken, maar het is ons toch maar gelukt. Bedankt om altijd een lach op mijn gezicht te toveren, jij bent steeds het hoogste punt van mijn dag! Op naar ons volgend avontuur.

Karen,

Augustus 2022

